Mario Leypold, BSc MSc

Mechanistic Investigation of the PhzF-Catalyzed Proton Transfer in the Biosynthesis of Phenazines

DISSERTATION

zur Erlangung des akademischen Grades

Doktor der technischen Wissenschaften

eingereicht an der

Technischen Universität Graz

Betreuer

Univ.-Prof. Dipl.-Ing. Dr. rer. nat. Rolf Breinbauer

Institut für Organische Chemie

Graz, August 2015

Die vorliegende Doktorarbeit wurde in der Zeit von Oktober 2011 bis August 2015 im Fachbereich Chemie unter der Betreuung von Univ.-Prof. Dipl.-Ing. Dr. rer. nat. Rolf BREINBAUER am Institut für Organische Chemie der Technischen Universität Graz angefertigt.

Eidesstattliche Erklärung

Ich erkläre an Eides statt, dass ich die vorliegende Arbeit selbstständig verfasst, andere als die angegebenen Quellen/Hilfsmittel nicht benutzt, und die den benutzten Quellen wörtlich und inhaltlich entnommenen Stellen als solche kenntlich gemacht habe. Das in TUGrazonline hochgeladene Textdokument ist mit der vorliegenden Dissertation identisch.

Graz, 24. 8. 2015

Datum

Unterschrift

Affidavit

I declare that I have authored this thesis independently, that I have not used other than the declared sources/resources, and that I have explicitly indicated all material which has been quoted either literally or by content from the sources used. The text document uploaded to TUGRAZonline is identical to the present doctoral thesis.

Graz, 24. 8. 2015

Date

Signature

Danksagung

An dieser Stelle gilt mein ganz besonderer Dank Prof. Rolf BREINBAUER für die Bereitstellung dieser interessanten und zugleich herausfordernden Themenstellung. Mit seinen zahlreichen Ideen und ausführlichen Diskussionen konnte er nicht nur zu einem guten Gelingen meiner Dissertation beigetragen, sondern beherrschte es auch, all meine primären Interessensgebiete in einem Projekt zu vereinigen. Danke für das in mich gesteckte Vertrauen, die Möglichkeit Verantwortung am Institut sowie Lehrtätigkeiten zu übernehmen und die unbezahlbare Unterstützung im Hinblick auf meinen kommenden Forschungsaufenthalt in den Vereinigten Staaten von Amerika. Herzlichen Dank für die schönen und arbeitsintensiven Jahre in deiner Forschungsgruppe, die ich stets positiv in Erinnerung behalten werde.

Ein weiterer Dank gebührt Prof. Michaela FLOCK für die Anfertigung eines Zweitgutachtens, ihre zuverlässige Unterstützung hinsichtlich quantenmechanischer Berechnungen und die Bereitstellung hilfreicher Vorschläge zur Lösung komplexer Aufgabenstellungen. Äußerst unterhaltsame Diskussionen begeisterten mich für die Theoretische Chemie und zeigten mir das aufstrebende Potential in diesem Gebiet.

Großer und aufrichtigster Dank gilt unseren Kooperationspartnern Prof. Wulf BLANKENFELDT und Christina DIEDERICH (Helmholtz-Zentrum für Infektionsforschung, Braunschweig, Deutschland) für die Durchführung essentieller biochemischer Studien und für die zahlreichen informativen Diskussionen, die maßgeblich zum Fortschritt dieser Arbeit beigesteuert haben. Dadurch wurde mir eine weitere Sichtweise zugänglich, welche mein Interesse bezüglich biochemischer Sachverhalte gestärkt hat. Weiters möchte ich mich bei Prof. G. Matthias ULLMANN und seiner Arbeitsgruppe für die Verwirklichung von QM/MM Rechnungen bedanken, die in naher Zukunft tiefere Einblicke in die enzymkatalysierte Isomerisierung liefern sollen, sowie bei Prof. Michael MÜLLER für die Bereitstellung von DHHS.

Besonders bedanken möchte ich mich bei Prof. Hansjörg WEBER für die Durchführung wichtiger NMR-Experimente und anregenden Diskussionen zur Aufklärung diffiziler spektroskopischer Problemstellungen. Im gleichen Zuge gilt mein Dank Carina ILLASZEWICZ-TRATTNER für die Aufzeichnung einzelner NMR-Spektren und Gernot STROHMEIER für seine Hilfestellung bezüglich chromatografischer Fragen.

Vielen Dank an Prof. Harald PICHLER (IMB, TU Graz) für die Bereitstellung der Schweineleberesterase (PLE), mit deren Hilfe die kinetischen Racemattrennungen erfolgreich durchgeführt werden konnten, an Prof. Roland C. FISCHER für die Lösung

Meiner Familie

"Nothing can be more incorrect than the assumption one sometimes meets with, that physics has one method, chemistry another, and biology a third."

Thomas Huxley

Kurzfassung

Phenazine repräsentieren überlebensnotwendige Sekundär-Metabolite von Bakterien mit ausgeprägtem redox-aktiven Charakter, die an entscheidenden biologischen Prozessen beteiligt sind. Neben der Bildung von toxischen, hoch reaktiven Sauerstoff-Intermediaten, fungieren sie sowohl als höchst effiziente Atmungspigmente, als auch als wichtige Botenstoffe. Die Bedeutung von Phenazinen wird zudem anhand der Beteiligung an Krankheiten dargelegt, z. B. in Studien mit *Pseudomonas aeruginosa*. Dieser Mikroorganismus befällt immungeschwächte Patienten und führt bei „zystischer Fibrose" in Folge dessen zu einer erhöhten Sterblichkeit.

Trotz einer generellen Kenntnis über die biosynthetische Bildung von Phenazinen sind wichtige mechanistische Details weiterhin unerforscht, was auf die erhöhte Anzahl an reaktiven Intermediaten zurückzuführen ist. Der Einsatz von synthetischen Methoden in Kombination mit biochemischen und quantenmechanischen Studien soll zum einen zur Verbesserung des allgemeinen Verständnisses beitragen, zum anderen einen wichtigen Schlüsselschritt in der Biosynthese von Phenazinen erforschen: Die PhzF-katalysierte Isomerisierung von DHHA. Voruntersuchungen deuten auf eine weitgehend unbekannte Enzym-katalysierte perizyklische Reaktion hin, eine [1,5]-prototrope Umlagerung.

In diesem Zusammenhang wurden in der vorliegenden Arbeit zentrale enantiomerenreine mechanistische Sonden, wie Deuterium-markiertes DHHA (d-DHHA) als auch strukturell verwandte Intermediate des natürlichen Substrates, synthetisiert, deren stufen- und redox-ökonomische Synthese im Folgenden ausführlich beschrieben wird. Diese Verbindungen dienen nicht nur der Aufklärung eines noch unbekannten Enzym-Mechanismus mit modernen physikochemischen Methoden, sondern zielen vielmehr auf die Erkenntnis, inwiefern die bakterielle Biosynthese von Phenazinen beeinflusst bzw. unterdrückt werden kann. Damit sollen molekulare Sonden bereitgestellt werden, die zur gezielten Behandlung von Infektionen dienen, hervorgerufen durch Phenazin-produzierende Bakterien Stämme.

Phenazin-1-carbonsäure
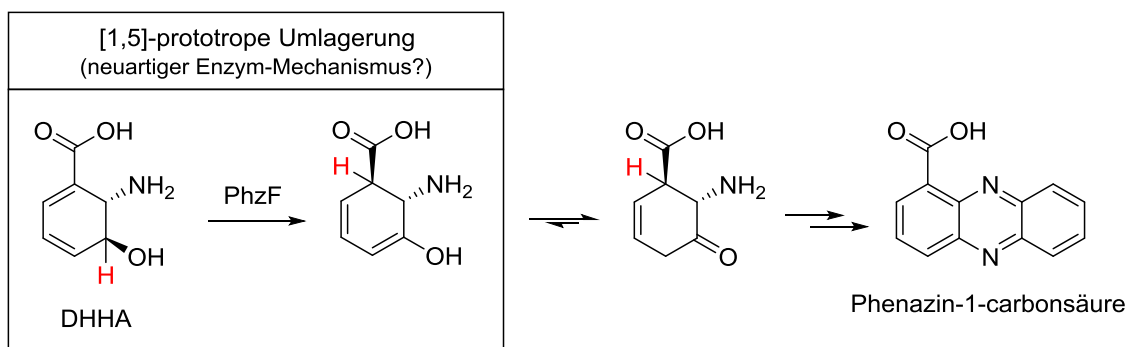
Abstract

Phenazines represent essential bacterial secondary metabolites that participate in various biological processes. Acting primarily as important signaling molecules and effective respiratory pigments, phenazines are able to generate highly reactive, toxic oxygen species, which explain their broad spectrum of antibiotic activity. In the case of lung infections, *Pseudomonas aeruginosa*, a potent pathogen, provokes a pronounced inflammatory response and hence is the leading cause for the premature mortality of people suffering from cystic fibrosis.

In spite of a general overview of the phenazine biosynthesis, important mechanistic details were still unexplored – a consequence of the high number of unstable intermediates. Modern physicochemical techniques should help to achieve a more comprehensive understanding of important key transformations within this pathway. In this context, the PhzF catalyzed isomerization of *trans*-2,3-dihydro-3-hydroxyanthranilic acid (DHHA) was explored, which generates the main precursor for the formation of the tricyclic core structure of phenazines. Resembling a formal non-enzymatic pericyclic reaction, the results of our studies do not rule out a so far undescribed [1,5]-prototropic rearrangement in nature.

The present thesis provides detailed description in the step- and redox-economical synthesis of enantiomerically pure mechanistic probes, e.g. deuterium labeled DHHA (d-DHHA) as well as related derivatives of the natural substrate. All of these compounds were further utilized for the clarification of the existing enzyme mechanism aiming chemical control over the biosynthesis of these secondary metabolites. Primarily, this should serve for one purpose: Providing tool compounds that can be employed as lead structures for the targeted pharmaceutical intervention of infectious disease evoked by phenazine producing bacteria strains.

Table of Contents

X

1.   Introduction

The emergence of terrestrial life is the result of a chemical evolution process that started approximately 4.5 billion years ago.[1] Today, more than 10 million – perhaps 100 million – different species are living on Earth and reproducing themselves faithfully. Most of these are unicellular organisms, others are complex structures, "molecular societies", in which groups of compartments are performing specialized functions linked together by an intricate system of communication. However, both of them have one thing in common: They consist of single cells, whether of only one or a well-regulated assembly of many.[2]

Proteins together with functional RNA are the vital components of life, primarily responsible for several biological activities in the organism, e.g. regulate gene expression or are involved in signal transduction.[3] Among them, enzymes fulfill essential tasks as catalysts by directing, controlling and enhancing chemical transformations. They evolved to mainly accomplish two contradictory assignments: On the one hand, to catalyze biochemical transformations at certain reaction rates that are most suitable for maintaining organism function, on the other hand to prevent alternative side reactions, which commonly occur in non-enzymatic processes. In other words, enzymes do explicitly catalyze the reaction of interest and also prevent the organism from undesired, toxic side product formation. Generally, the first effect is denoted as catalysis, the second as specificity. In this connection, rate enhancement in enzymatic transformations is usually several orders of magnitude higher than in solution.[4]

Catalysis, or colloquially "catalytic power", is defined as the ratio between reaction rates of the catalyzed and uncatalyzed transformation.[4] In an enzymatic process, mainly four phases within the catalytic cycle have to be distinguished: 1. Binding of the substrate to the enzyme, 2. Overcoming the activation barrier of the transition state (TS), 3. Formation of the product, and 4. Release of the product from the binding pocket of the enzyme.[5] It is widely accepted that many enzymes function in lowering the free energy barrier by preferentially binding to the transition state (TS) of the reaction, a concept, which is credited to PAULING.[6] This is the origin of the extraordinary potency of TS inhibitors,[7–10] but it has been recently recognized that internal enzyme motions additionally contribute to enhance catalytic activity.[4,11]

Understanding enzymatic reactions in living organisms and further realizing, which intrinsic effects make them so efficient, is one of the biggest challenges in biochemistry today. Many experimental as well as theoretical studies have attempted to assess specific contributions of physical phenomena to enzymatic rate enhancement. However, the effort to break catalysis down into additive contributions is always an artificial process that basically serves for the description of the existing entirety.[4]

2.   Theoretical Part

2.1.   General Aspects about Phenazines

The medicinal literature of the 19th century reports numerous publications concerning the topic "blue pus", which is normally associated with drastic surgical procedures requiring long periods of wound care. Even older are reports about "blue milk", a coloration of fresh milk that sometimes develops after several days.[12–14]

In 1859, FORDES was the first researcher, who investigated these phenomena and provided key insights into it describing the use of chloroform for the extraction of the blue pigment, which he named "pyocyanin" (Greek: πύο (pus) and κυανό (cyan)).[15] In this context, pyocyanin (**A**) was the first isolated example of the phenazine class that has been grown to over 150 members in the last 100 years (Figure 1).[16] The French pharmacist GESSARD was able to demonstrate that the blue coloration in pus was due to the presence of a microorganism nowadays known as *Pseudomonas aeruginosa*,[17] but it is still not clear if the color in milk is likewise a consequence of phenazine production. Nevertheless, *P. aeruginosa* is an important human opportunistic pathogen, which is responsible for a large number of nosocomial infections and additionally is the main cause for low life expectancy of patients suffering from cystic fibrosis, a chronic infection of the lungs.[12–14,18]

GESSARD's discovery of *P. aeruginosa* was resonated well in many of those mentioned medicinal publications,[17] but it required more than 50 years before the chemical structure of pyocyanin (**A**) was established by HILLEMANN as 5-*N*-methyl-1-hydroxophenazinium betaine (**A**) in 1938.[19] In the course of these and additional studies, it became clear that pyocyanin (**A**) is a strong redox-active compound, which changes its color depending on the oxidation state as well as the pH value of the solvent, in which it is dissolved.[20] Additionally, this explains the "chameleon phenomenon" of *P. aeruginosa* describing a temporary color change on solid media after exposure to air by the disturbance with a platinum needle.[12–14,21]

In general, strains of *Pseudomonas* and *Streptomyces* are the most prolific phenazine producers in nature and the latter tend to generate more complex structures in terms of side chain variety and annulated ring systems (Figure 1). While some of the biological effects of phenazine derivatives are tightly associated with their capacity in intercalating to DNA, most of their actions are directly linked to the redox potential of this substance class. For example, phenazines can reduce molecular oxygen to toxic reactive oxygen species explaining why they are broad-specificity antibiotics and virulence factors in infectious disease.[22] It has been long believed that the resulting competitive advantage is the physiological rationale for the production of phenazines. However, the field is currently experiencing a paradigm shift since

new data indicate the role of phenazines in the primary metabolism of their producers. In this connection, pyocyanin (**A**) can directly oxidize NADH, which may be required for sustaining glycolysis in anoxic regions of biofilms.[12–14,23]
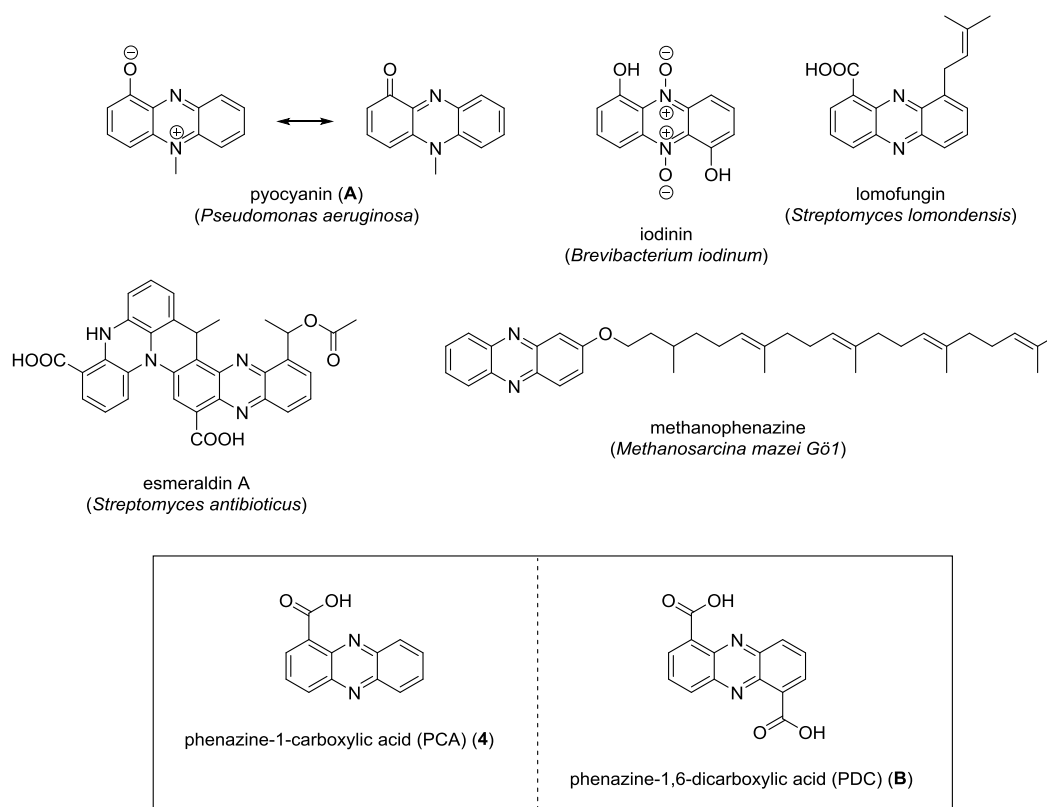
Figure 1: Collection of naturally occurring phenazine derivatives; Phenazine-1-carboxylic acid (PCA) (**4**) and phenazine-1,6-dicarboxylic acid (PDC) (**B**) are precursor for many bacterial phenazines; Methanophenazine is the only archaeal phenazine known to date,[24] which could arise through a different biosynthetic route.[12–14]

In all phenazine producing bacteria strains, a conserved set of phenazine biosynthesis genes has been identified, which have been subject of numerous research studies in recent years.[25] These genes are normally clustered in an operon, which encodes five enzymes required for the formation of two core building blocks in the strain specific phenazine synthesis, phenazine-1-carboxylic acid (PCA) (**4**) and phenazine-1,6-dicarboxylic acid (PDC) (**B**). Interestingly, the sequence of the *phz*-operon does not allow to distinguish between PCA- and PDC-producing bacteria strains, an observation, which is under further exploration. However, the *phz*-operon is usually extended by genes needed for the conversion of PCA (**4**) and PDC (**B**) into downstream products, genes involved in phenazine autoresistance and in delivery of precursors or regulation of the biosynthesis pathway.[12–14]

2.2. Phenazine Biosynthesis

Before enzymes were discovered, which are required for the biosynthesis of phenazines, most efforts towards an understanding of this biosynthetic pathway were put into the identification of precursor molecules.[26] Early studies concentrated on the influence of nutrients in the cultural media for the microbial production of pyocyanin (**A**), which was the only known phenazine derivative by that time. However, none of them provided direct insight into the immediate precursors of the phenazine moiety.[27] This situation improved after the development of a new methodology in the late 1940s that enabled the selection of growth-arrested mutants of *Escherichia coli* with penicillin leading to the discovery of shikimic acid and its secondary product chorismic acid (**53**) as precursor for many microbial aromatic compounds.[12–14,28]
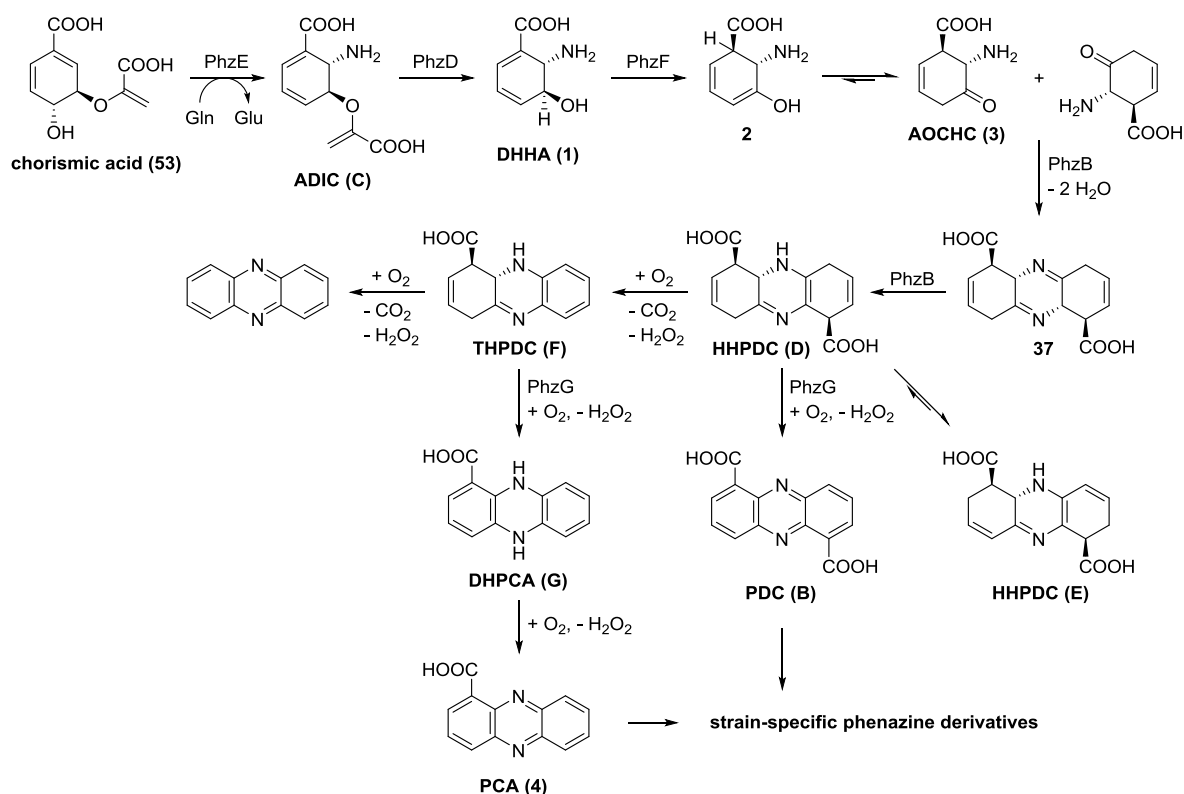
Scheme 1: Current understanding of phenazine biosynthesis; Phenazine-1-carboxylic acid (PCA) (**4**) and phenazine-1,6-dicarboxylic acid (PDC) (**B**) as precursors for strain-specific phenazine derivatives.[12–14]

Experiments in the early 1970s demonstrated that phenazines derive from two identical molecules of chorismic acid (**53**) (Scheme 1).[29] However, it was for a long time not understood, which catalytic transformation chorismic acid (**53**) undergoes before a tricyclic ring system is formed. Anthranilic acid was investigated in this context, but no significant

incorporation into phenazines was observed in any case.[30] FLOSS confirmed that 2-amino-2-desoxyisochorismic acid (ADIC) (**C**) is the branching point between anthranilic acid and the phenazine biosynthesis by a complete incorporation of ADIC (**C**) into PCA (**4**).[12–14]
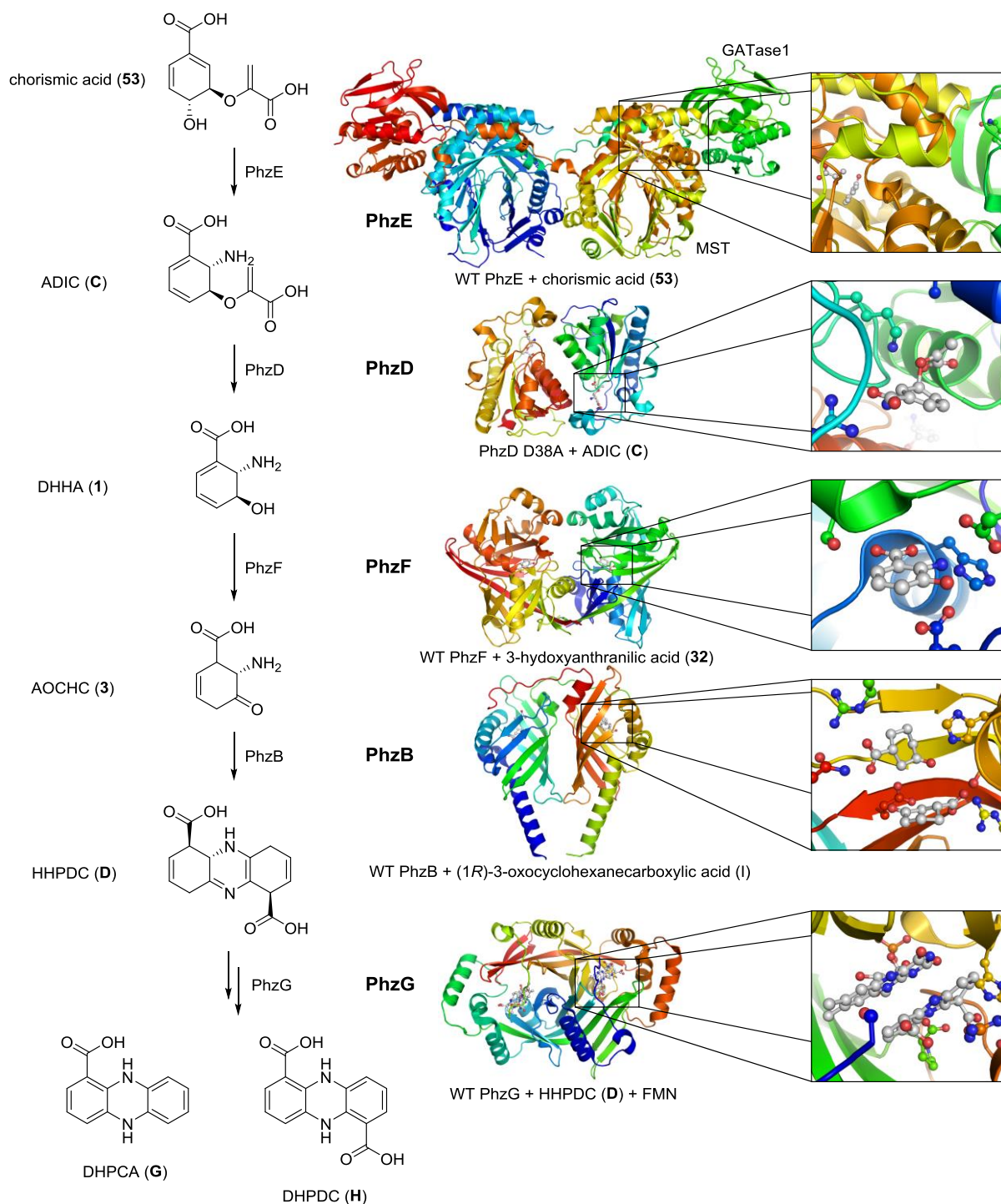
Figure 2: Structural view of the phenazine biosynthesis; Following Protein Data Bank entries have been used:[31] PhzE, 3R75;[32] PhzD, 1NF8;[33] PhzF, 1U1W;[34] PhzB, 3DZL[35] and PhzG, 4HMT;[36] Figures were generated with PyMOL.[12,37]

In phenazine producing bacteria strains, ADIC (**C**) formation is catalyzed by PhzE, a homodimeric enzyme that is closely related to anthranilate synthase (AS),[38] using chorismic acid (**53**) as well as glutamine. However, PhzE is incapable of invoking pyruvate elimination to yield anthranilic acid. It differs from previously characterized AS enzymes[39] in fusing its *N*-terminal chorismic acid (**53**) converting menaquinone, siderophore, tryptophan (MST) domain covalently to the type-1 glutamine amidotransferase (GATase1) domain by a 45 residues containing peptide linker. Even more surprisingly is that PhzE is an intertwined dimer in which the GATase1 domain of one chain provides ammonia to the MST domain of the other. It is believed that glutamine hydrolysis by GATase1 is only initiated once chorismic acid (**53**) has bound. Consequently, ammonia is delivered through a tunnel to the chorismic acid (**53**) binding site to avoid its loss to the solvent. The channel ends at the *Si*-face of prochiral chorismic acid (**53**), which explains the stereochemistry of ADIC (**C**). Interestingly, the active site of PhzE's MST domain is very similar to that of AS and reveals no further indication why PhzE does not convert chorismic acid (**53**) to anthranilic acid. Mutation experiments on PhzE yielded only inactive enzyme leaving questions regarding differences between these two enzymes open (Figure 2).[12,13,32]

In the following step, ADIC (**C**) is hydrolyzed to *trans*-2,3-dihydro-3-hydroxyanthranilic acid (DHHA) (**1**) and pyruvate by PhzD,[40] an α/β-hydrolase related to the isochorismatase domain of EntB in the biosynthesis of the siderophore enterobacticin.[41] Unlike structurally similar enzymes, PhzD is not metal-dependent, nor is a covalent intermediate formed in the ADIC (**C**) hydrolysis. Instead, the enzyme employs an acid-base catalyzed mechanism, which involves an aspartic acid side chain to protonate the vinyl ether and probably a lysine for the release of DHHA (**1**) (Figure 2).[12,13,33,42]

First described by HERBERT as a potential precursor for phenazines in 1979,[43] DHHA (**1**) is the last stable intermediate in the biosynthetic pathway leading to PCA (**4**) and PDC (**B**). It is the natural substrate of PhzF, an enzyme that possesses high structural similarity to diaminopimelate epimerase,[44] proline racemase[45] and 2-methylaconitate isomerase,[46] but does not require one or two cysteines as classical catalytic acid-base residues as the mentioned enzymes. The catalytic activity of PhzF relies on an active site glutamate to isomerize DHHA (**1**) into 6-amino-5-oxocyclohex-2-ene-1-carboxylic acid (AOCHC) (**3**) (Figure 2). Since ^{1}H-NMR spectroscopy revealed full conservation of the transferred hydrogen/proton in D_2O, this observation suggests that PhzF might be one of the few enzymes in nature, which catalyzes a pericyclic reaction, classified as a suprafacial [1,5]-prototropic rearrangement, rather than acid-base catalysis.[12,13,34,47,48]

Intriguingly, turnover of DHHA (**1**) by PhzF does not stop at the stage of ketamine **3**. AOCHC (**3**) is highly reactive and undergoes spontaneous two-fold self-condensation with a second

molecule of its structure forming the tricyclic phenazine ring precursor **37**.[34] Such a diagonal symmetrical pairing as one of the central steps in the phenazine biosynthesis has already been established in the 1970s, albeit not knowing the structure of the pairing intermediates.[49] The structure of PhzF, a homodimeric isomerase with two independent active sites facing each other, initially suggested that the dimerization of DHHA (**1**) occurs at the monomer-monomer interface.[34] The probability for self-condensation would be even increased, if one assumes that PhzF releases two molecules of ketamine **3** simultaneously from both active sites. However, the kinetic properties of PhzF have not been studied in sufficient detail to determine to what extent PhzF facilitates AOCHC (**3**) condensation.[12,13]

Since tricyclic precursor formation in a bimolecular reaction is even accelerated by high concentrations of DHHA (**1**), ketamine **3** probably reacts with other present amines, e.g. lysine residues in proteins. Hence, AOCHC (**3**) is likely toxic to cells such that its accumulation must be prevented. This hypothesis was proven by the perception that PhzB significantly improves the condensation reaction between two molecules of AOCHO (**3**). It is a dimeric enzyme of the ketosteroid isomerase nuclear transport factor 2 family that provides a large binding cavity for two molecules of ketamine **3** in each monomer. The crystal structure of PhzB reveals that the relative orientation in opposite direction of two AOCHO (**3**) is secured through interaction of their carboxylates with two arginine residues, one from the *C*-terminus of the other monomer. Acid-base catalysis of the first condensation reaction involves protonation of the tetrahedral intermediate by a glutamate emerging during the attack of the amino moiety. Similar to related enzymes,[50] protonation of the glutamate will occur at the onset of the reaction caused by the hydrophobic environment, which increases the pK_a value of this active site residue. However, it is believed that the second condensation is catalyzed by a combination of a histidine and serine, similarly protonating the second oxyanion intermediate (Figure 2).[12,13,35]

Interestingly, pseudomonads carry a second copy of the *phzB* gene termed as *phzA*, which is immediately located upstream in their *phz*-operons. This fact would explain, why these strains are among the most proficient phenazine producers in nature. Although PhzA is approximately 70 % equivalent to PhzB, it was found to be completely inactive in the dimerization of AOCHC (**3**) possibly attributed to mutations of both active site residues histidine and serine to leucines. Nevertheless, PhzA plays an important role in the phenazine biosynthesis of pseudomonads. MCDONALD demonstrated that the deletion of the *phzA/B* genes only decreases, but not abolishes the phenazine biosynthesis and that PCA (**4**) production is reduced to 25 % of the wildtype level, when PhzA was absent.[41] However, the molecular basis for this observation is presently not understood.[12,13,35]

Hexahydrophenazine-1,6-dicarboxylic acid (HHPDC) (**E**) was identified as product in the condensation reaction of AOCHC (**3**) catalyzed by PhzB using HPLC-coupled NMR spectroscopy.[35] This compound likely arises through spontaneous rearrangement of HHPDC isomer (**D**) containing four conjugated double bonds, instead, and possibly stabilizes the condensation product against back-hydrolysis. However, HHPDC (**D**) is not stable and hence undergoes rapid oxidative decarboxylation to tetrahydrophenazine-1-carboxylic acid (THPCA) (**F**). Besides, this decarboxylation was also observed, when PhzA/B was not present in the reaction mixture.[34] Since this reaction proceeds uncatalyzed, but consumes one equivalent oxygen, asymmetric PCA (**4**) is always observed as the major product, even several strains utilize PDC (**B**) as strain-specific precursor for the biosynthesis of phenazines (Figure 2).[12,13,35,51]

Finally, THPCA (**F**) needs to pass two additional two-electron oxidation processes to become fully aromatized, but the *phz* operon contains only one oxidase, namely PhzG. This protein is similarly a homodimeric enzyme, which employs FMN as cofactor for oxidation, and is related to PdxH, a pyridoxine-5'-phosphate oxidase. Interestingly, amino acid residues from both chains are involved in forming the binding site for the substrate and the cofactor, however, the flexible *N*-terminus seems to act as a lid for substrate fixation.[36,52] Trapping experiments in combination with diffraction analyses indicated that PhzG acts on different tricyclic intermediates contributing to the formation of both PCA (**4**) and PDC (**B**). Together, these observations suggest that the final oxidation steps in the phenazine biosynthesis may follow distinctive routes. Therefore, the difference between PCA (**4**) and PDC (**B**) producing bacteria strains is definitely not a consequence of enzyme modification, but rather based on altered activities of PhzF, PhzB as well as PhzG and the availability of molecular oxygen, as corroborated in recent studies of Rui.[12,13,53]

Since FMN is a two-electron acceptor, the reduced forms of PCA (**4**) and PDC (**B**), namely, DHPCA (**G**) and DHPDC (**H**), are most likely the end products of the phenazine biosynthesis explaining, why the *phz*-operon contains only one oxidase (Figure 2). This hypothesis is further supported by the results that enzymes, which convert PCA (**4**) and PDC (**B**) to strain-specific phenazine derivatives, possess significantly higher activity towards these reduced substrates.[12,13,54]

2.3. Enzyme Catalyzed Pericyclic Reactions

Despite their broad utility in laboratory and the general concept of orbital symmetry conservation,[55,56] only few examples have been reported for enzymes that catalyze pericyclic reactions.[57] These include chorismate mutase (CM),[5,58–62] isochorismate pyruvate lyase (IPL),[5,57,59] precorrin-8x methyl mutase (CobH),[63,64] dimethylallyltryptophan synthase (DMATS) [65,66] as well as one promising example for a DIELS-ALDERase.[67–74]

2.3.1. Chorismate Mutase (CM) Catalyzed CLAISEN Rearrangement

Chorismate Mutase (CM) catalyzes the transformation of chorismate (**53**) to prephenate (**J**) in a formally [3,3]-sigmatropic CLAISEN rearrangement located at the branching point in the shikimate pathway (Scheme 2).[58,62] Leading to the biosynthesis of aromatic amino acids in plants, fungi and bacteria,[75] CM accelerates the concerted asynchronous rearrangement by a factor of more than 10^6 compared to the uncatalyzed reaction, which also proceeds in aqueous solution quite rapidly.[58,60,62]

chorismate (**53**)   prephenate (**J**)   TS analogue **K**
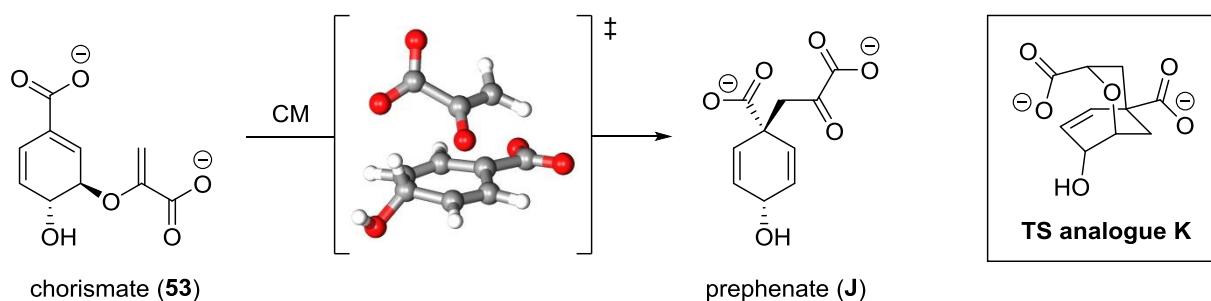
Scheme 2: [3,3]-Sigmatropic rearrangement of chorismate (**53**) to prephenate (**J**) catalyzed by chorismate mutase (CM); Transition state (TS) calculated at the B3LYP/6-31G* level of theory;[76–79] TS inhibitor **K** for the pericyclic reaction synthesized by BARTLETT.[8–10,58,60,62]

In this context, TS analogues, as compound **K**, were able to support the concerted [3,3]-sigmatropic rearrangement as the mechanism of action by a strong rate deceleration in the form of increased affinity towards inhibitor **K** in comparison to chorismate (**53**) as natural substrate.[8–10] Both reactions, the catalyzed and uncatalyzed rearrangement, proceed via a chair-like geometry in the TS.[80] However, in contrast to the chorismate mutase catalyzed transformation, the rate of the non-enzymatic reaction is highly sensitive to isotope labeling suggesting a TS before the pericyclic reaction.[81] Consequently, chorismate (**53**) must be available in its pseudo-diaxial conformation for the pericyclic rearrangement.[82] This

singularity reflects the unique nature of chorismate (**53**) bound to the active site supporting the possibility that the correct binding of the ligand is effectively synonymous with catalysis in the CLAISEN rearrangement.[58,60,62,83]

Heavy atom primary kinetic isotope effects (1° KIE) indicated that the enzymatic reaction proceeds via a concerted, but asynchronous and highly polarized TS with carbon-carbon bond formation lagging considerably behind carbon-oxygen bond cleavage.[84] The very large 1° KIE in experiments with ^{18}O-labeling ruled out protonation of the vinyl ether oxygen in the TS of chorismate (**53**), although hydrogen bonding cannot be totally excluded.[58,62,85]

2.3.2. Isochorismate Pyruvate Lyase (IPL) Catalyzed [1,5]-Prototropic Fragmentation

Isochorismate pyruvate lyase (IPL) catalyzes the elimination of the enolpyruvyl side chain from isochorismate (**L**) to salicylate (**N**) and pyruvate (**O**) (Scheme 3). A significant 1° KIE with deuterium labeled isochorismate (**M**) and the quantitative transfer of the label to pyruvate (**Nr**) are both consistent with a pericyclic reaction.[86–89]

isochorismate (**L**)
d-isochorismate (**M**)

salicylate (**N**)

pyruvate (**O**)
d-pyruvate (**P**)
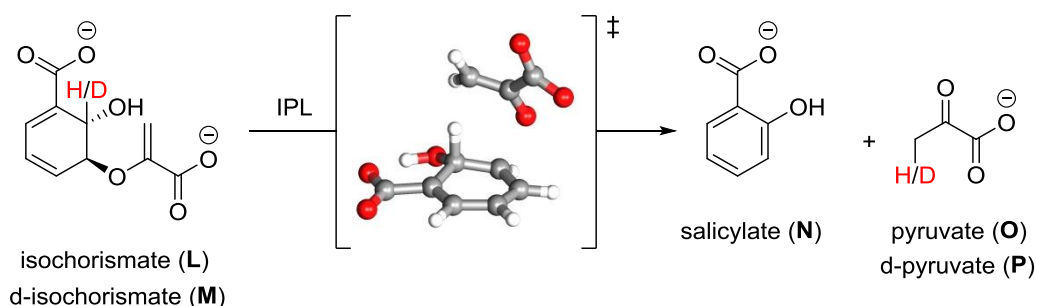
Scheme 3: [1,5]-Prototropic rearrangement of isochorismate (**L**) to salicylate (**N**) and pyruvate (**O**) catalyzed by isochorismate pyruvate lyase (IPL); Transition state (TS) calculated at the B3LYP/D95+(2d,p) level of theory.[76,86]

Table 1: Kinetic parameters for *Pseudomonas aeruginosa* isochorismate pyruvate lyase (IPL) determined by HILVERT; Conditions: 50 mM NaH$_2$PO$_4$/Na$_2$HPO$_4$, pH 7.5, 30 °C.[86]

Entry	Substrate	k_{cat} / s^{-1}	K_M / µM	k_{cat}/K_M / µM^{-1}.s^{-1}	1° KIE
1	isochorismate (**L**)	1.01 ± 0.02	1.05 ± 0.08	0.96 ± 0.07	2.35 ± 0.05
2	d-isochorismate (**M**)	0.43 ± 0.01	0.79 ± 0.05	0.55 ± 0.04	

Hybrid DFT computations at the B3LYP/D95+(2d,p) level of theory[76,90] pointed out a low energy TS for a concerted, but asynchronous [1,5]-prototropic shift (ΔG_{AE} = 107 kJ.mol^{-1}), in which the carbon-oxygen bond cleavage is more advanced than hydrogen atom transfer between both carbon atoms. This TS can be directly accessed from the predominant pseudo-diequatorial substrate conformer and predicts a 1° KIE_{calc} = 2.22, which is in good agreement with the observed of 1° KIE_{exp} = 2.35 ± 0.05. Interestingly, the decreased MICHAELIS-MENTEN constant of d-isochorismate (**M**) indicates a higher affinity of the labeled compound to the enzyme compared to its natural substrate **L**. Unfortunately, this exciting observation is not further discussed by HILVERT.[86–89]

2.3.3. Precorrin-8x Methyl Mutase (CobH) Catalyzed [1,5]-Sigmatropic Methyl Rearrangement

The transfer of a methyl group within the biosynthesis of vitamin B$_{12}$ was determined as a concerted [1,5]-sigmatropic rearrangement occurring on a 5,5-disubstituted 2*H*-pyrrole moiety by general acid catalyzes (Scheme 4). Structural analysis identified a strictly conserved histidine residue in the catalytic active site, which serves as an essential donor for the protonation of the ring nitrogen atom. Biomimetic model substrates highlighted that this type of pericyclic reaction proceeded in these compounds even at ambient temperatures, when acidic conditions were employed instead of thermal heating. Moreover, the specificity of CobH for a single tautomer of precorrin-8x (**Q**) and its quantitative conversion to hydrogenobyrinic acid (HBA) (**R**) lend strong evidence for the concerted mechanism against a stepwise process.[63,64]
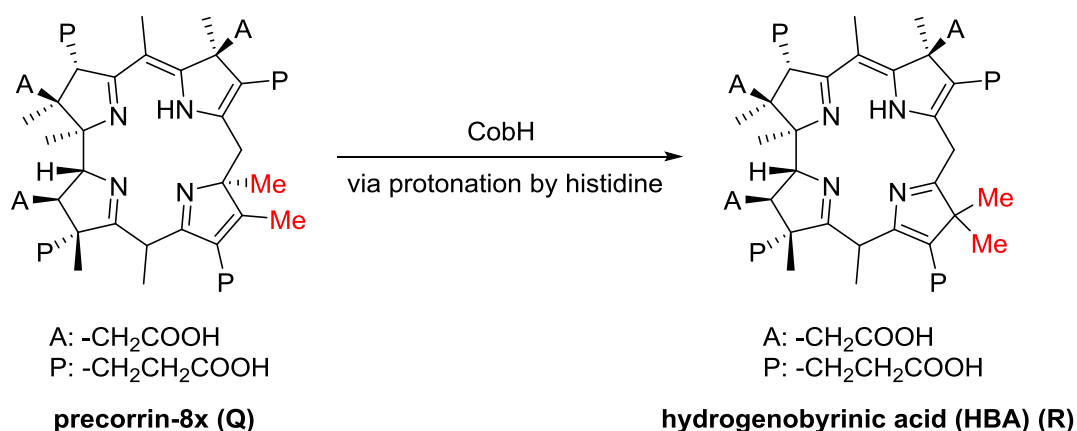
Scheme 4: CobH catalyzed concerted [1,5]-sigmatropic rearrangement of precorrin-8x (**Q**) to hydrogenobyrinic acid (HBA) (**R**) via protonation of the 2*H*-pyrrole moiety by an active site histidine.[63,64]

2.3.4. Dimethylallyltryptophan Synthase (DMATS) Catalyzed COPE Rearrangement

Dimethylallyltryptophan synthase (DMATS) catalyzes the prenylation of tryptophan (**S**) in the first step of the ergot alkaloid biosynthesis (Scheme 5). Interestingly, this enzyme belongs to a recently discovered family of fungal indole prenyltransferases that do not require metal ions for catalytic activity.[91] However, DMATS directs alkylation to the poorly nucleophilic C-4 position of indoles instead of the more highly nucleophilic C-2 and C-3 positions.[65,66,92]

The formation of a reversed-prenylated compound **V** suggested a COPE rearrangement as operating mechanism for DMATS, albeit TANNER could not exclude that intermediate **V** was an artefact during mutation studies with DMATS. Within these experiments, mutations of an active site glutamate to either glutamine or alanine caused a tremendous decrease of activity, which is consistent with the notion that glutamate plays a significant role in increasing the nucleophilicity of the indole moiety.[65,66,92]
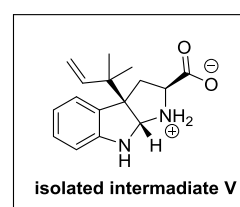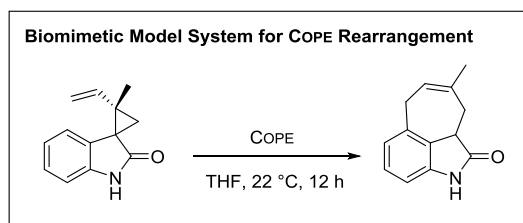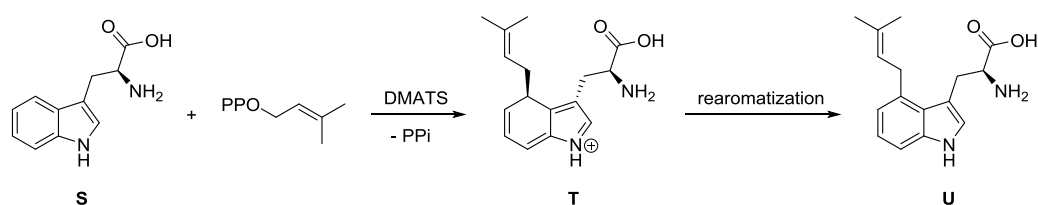
Scheme 5: Dimethylallyltryptophan synthase (DMATS) catalyzed prenylation of tryptophane (**S**); Isolation of reversed prenylated compound **V** by TANNER together with COPE rearrangements in biomimetic model systems performed by GAICH indicate a [3,3]-sigmatropic rearrangement catalyzed by an enzyme.[65,66,92]

GAICH reported the first experimental evidence for an enzyme catalyzed [3,3]-sigmatropic rearrangement by the synthesis of bioinspired model compounds. The reaction with these probes proceeded even at room temperature and did not depend on solvent effects. Consequently, these observations led to the conclusion that DMATS might catalyze a COPE rearrangement by forcing the substrate into the right conformation, when preorientation in the active site occurs.[66,92]

2.3.5. SpnF Catalyzed Cyclization as a Promising Example for a DIELS-ALDERase

Enzymes that catalyze [4+2]-cycloadditions were controversially discussed in recent years, however, only five purified enzymes have thus far be implicated in biotransformations, which are in an agreement with a DIELS-ALDER reaction: Solanapyrone synthase,[93] LovB,[94] macrophomate synthase,[67,71,95–99] riboflavin synthase[100] as well as SpnF.[67,72–74] Although the stereochemical outcome of these transformations is consistent with a pericyclic mechanism, the first four mentioned enzymes typically demonstrate more than one catalytic activity leaving their specific influence on the cyclization step uncertain.[67,73]

Macrophomate synthase (MS) was believed to be the first example for a DIELS-ALDERase, but two decarboxylation events, which happen during the catalytic cyclization, indicated a stepwise reaction involving a MICHAEL addition followed by an addition to afford the final product (Scheme 6).[71,96,97,101] Such a stepwise mechanism was later computationally confirmed by JORGENSEN to be energetically more reasonable in the MS active site compared to the pericyclic alternative.[95] Furthermore, HILVERT demonstrated experimentally that MS can operate as a promiscuous aldolase, which is consistent with the second half of the stepwise mechanistic hypothesis.[67,98] Consequently, these observations suggest that MS is not a true DIELS-ALDERase.[67]
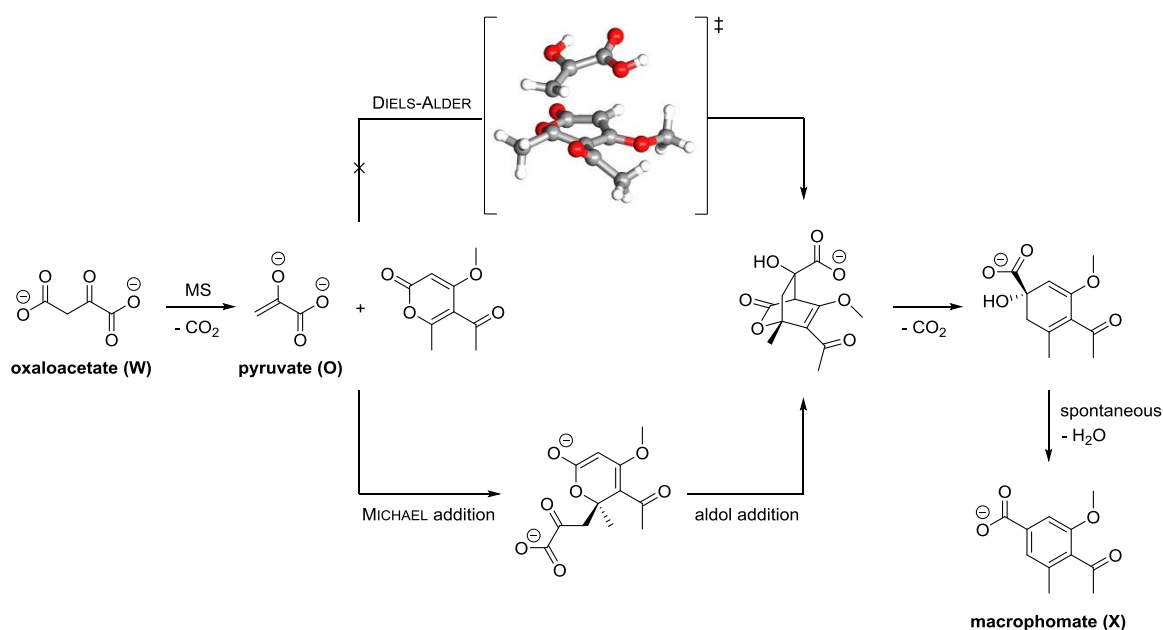
Scheme 6: Biosynthetic pathway for the formation of macrophomate (**X**) catalyzed by macrophomate synthase (MS); Stepwise process computationally and experimentally determined by JORGENSEN and HILVERT;[67,95,98] Neutral form of pyruvate (**O**) utilized to calculate TS of the DIELS-ALDER reaction at the B3LYP/6-31G* level of theory.[76–79]

In 2011, LIU published mechanistic studies about the biosynthesis of the spinosyn insecticides and identified SpnF, which represents the first enzyme for the specific acceleration of a [4+2]-cycloaddition reaction (Scheme 7). It has been experimentally confirmed that the mentioned cyclization process is the only known function of SpnF so far and accelerates the formation of aglycone (**Z**) by a 500-fold.[73,74]
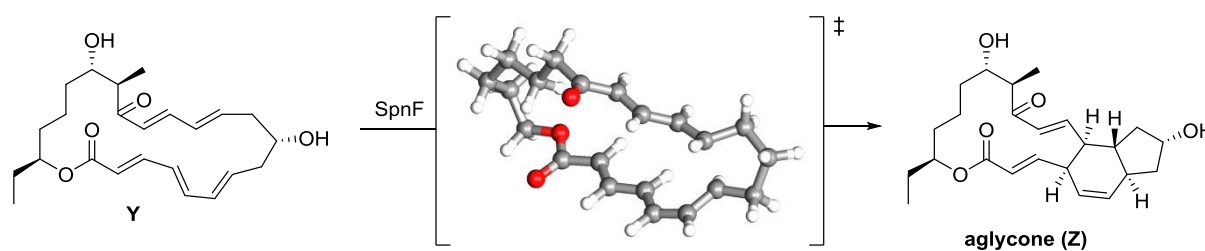
Scheme 7: SpnF catalyzed cyclization of compound **Y** as the most promising example for a naturally occurring DIELS-ALDER reaction; TS calculated at the B3LYP/6-31G* level of theory.[72–74]

Computational studies of HESS suggested a concerted, but highly asynchronous DIELS-ALDER reaction with a significant charge transfer in the TS. Activation energies at the B3LYP/6-31G* level of theory predicted ΔG_{AE} = 109 kJ.mol^{-1}.[72,76–79] However, it is known that hybrid DFT methods overestimate experimental DIELS-ALDER activation energies.[102] Hence, in comparison with *ab initio* MP2 methods, HESS estimated $\Delta G_{AE} \approx$ 65 kJ.mol^{-1} for the SpnF catalyzed cyclization of substrate **Y**. Additionally, it was proposed that SpnF possibly plays a dual role of not only folding the substrate into the proper conformation for the DIELS-ALDER reaction to occur, but also lowering its activation energy by a stabilization of the highly polarized transition structure.[72]

Although these computational studies suggest a pericyclic mechanism for SpnF, non-DIELS-ALDER routes, as dipolar or biradical mechanisms, are not easily disproven.[73,74] The recently resolved crystal structure of SpnF by KEATINGE-CLAY sets the stage for advanced experimental as well as computational studies to determine the precise mechanism of the SpnF mediated cyclization.[74]

3.   Aim of Scientific Research

The investigation of biochemical transformations is essential for a deeper understanding in the formation of essential molecules of life, e.g. high energy intermediates, as ATP,[2,103] neurotransmitter[104] etc., and supplies important information about the regulation of metabolic pathways impacting health and disease.[105,106] Infections are always associated with the occurrence of pathogens, which are in the broadest sense infectious agents, including bacteria, viruses and parasites, influencing the health status of its host tremendously. Evolving specific mechanisms to access nutrients from the host, distinctive interactions result in the production and delivery of particular virulence factors that manipulate cellular processes. In bacteria, replication is the most crucial factor for pathogen colonization and transmission.[107]

Pseudomonas aeruginosa is the most common bacterial pathogen connected to airway infections in cystic fibrosis. Since the lungs of patients are chronically colonized by these microorganisms, this infection contributes significantly to the low life expectancy of people suffering from this disease.[13,23,34,35,47,108] It has been demonstrated that pyocyanin producing bacteria strains provoked distinctive inflammatory response and in addition amplify their virulence with this factor. In this context, pyocyanin (**A**) is one well-known representative of the huge class of phenazines, which are fundamental redox-active pigments and signaling molecules in bacteria (Scheme 8). Securing the survival of these organisms by their broad antibiotic activity, an intervention in the biosynthesis of phenazines would mandatorily result in a targeted manipulation of the respiratory system of bacteria. This could on the one hand lead to the annihilation of these pathogens, on the other hand could make a new compound class of antibiotics accessible, which can support the treatment of infections caused by phenazine producing bacteria strains.
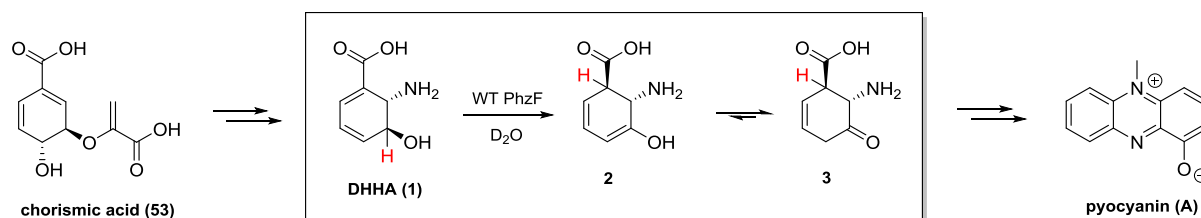
Scheme 8: Conservation of the migrating hydrogen atom in the WT PhzF catalyzed isomerization of DHHA (**1**) published by BLANKENFELDT in 2004.[34]

Based on publications of BLANKENFELDT and others,[34,35,47] this thesis should contribute to a better understanding of the biosynthesis of phenazines and hence should ultimately lead to the development of a new subclass of antibiotics. Although several important facts of this biosynthetical pathway are known,[13,34,35] the key transformation within this sequence, an isomerization reaction of DHHA (1) catalyzed by WT PhzF, is still not well understood. ^{1}H-NMR experiments of DHHA (1) performed in D_2O together with an observed hydrogen conservation suggest the possibility of a rare and by the time unknown pericyclic reaction in nature (Scheme 8).[34] It would be the first example for a concerted suprafacial [1,5]-prototropic rearrangement catalyzed by a native enzyme, which proceeds without the fragmentation of the natural substrate.

The experimental synthesis of tool compounds, e.g. mechanistic probes and substrate related derivatives, in combination with detailed biochemical studies for receiving enzyme characteristic parameters should deepen insight into this isomerization process. Especially, labeling experiments are commonly used and widely accepted techniques for the exploration of unknown mechanisms delivering so called primary and secondary kinetic isotope effects (1° KIE and 2° KIE).[4,109–111] Accompanied by the synthesis of deuterium labeled material, this value might prove a crucial factor for the differentiation of alternative mechanistic options. Additionally, quantum-mechanical calculations should afford valuable simulations in the gas phase as well as in aqueous media for the proposed pericyclic isomerization of DHHA (1) and should support considerations in this investigational process.

4. Results and Discussion

4.1. General Remarks and Mechanistic Proposal for the Exploration of the Isomerization Reaction of DHHA (1) Catalyzed by PhzF

The investigation of reaction mechanisms in biochemical pathways usually requires the help of diverse fields of Chemistry, including theoretical and experimental investigations. In addition to the synthesis of mechanistic probes, e.g. isotope labeled compounds,[4,109–117] inhibitors,[118,119] transition state analogues[8–10,120] and derivatives related to naturally occurring intermediates,[118,121] also the support with quantum-mechanical calculations[122–131] as well as biochemical studies are necessary.[131,132] However, validity evaluations of computations are often difficult, especially when there is not enough experimental data on the free energy profile from enzymatic assays.[127] As it is impossible to prove a reaction mechanism to its correctness, it is more convenient to exclude one type of mechanism by a concrete experimental proof.

Isotope effects are a powerful tool for the investigation of enzyme mechanisms, since they are directly connected to the chemical transformation and additionally give information on the transition state structure. Herein, lighter atoms are substituted by their heavier isotopes in the substrate of the enzyme, as hydrogen (H) by deuterium (D) or tritium (T). This isotopic substitution can affect either the equilibrium constant of a reaction (equilibrium isotope effect, EIE) or the rate of a reaction (kinetic isotope effect, KIE).[4,117] The last mentioned effect is caused by the difference in vibrational frequencies between the light and the heavy isotope and their associated zero point energies (ZPE) at ground and transition state (TS).[116] Moreover, it can be classified into two sub-categories. In primary KIEs (1° KIEs) the bond to the labeled atom is cleaved or formed in the rate determining reaction step (r.d.s.). In contrast, in secondary KIEs (2° KIEs) only the bonding to this isotope is influenced, e.g. by hybridization.[4,113,117,118] In other words, KIEs involve comparison in the bond stiffness of isotopic atoms in the TS relative to the substrate, while EIEs compare bond stiffness between product and substrate. In each case, stretching, bending and torsional vibrations contribute to the observed isotope effect. In conclusion, they are very useful in determining transitions state structures, since the motion of the isotopic atom is coupled to the reaction coordinate reporting about the bonding in the TS.[4,117]

In the PhzF catalyzed isomerization of DHHA (**1**) the nature of the hydrogen migration was investigated using the above mentioned techniques. Based on preliminary ^{1}H-NMR experiments with genuine DHHA (**1**) and wildtype PhzF (WT PhzF) in D_2O, BLANKENFELDT

made a remarkable observation detecting a full conservation of the migrating hydrogen atom/proton (no measurable exchange with deuterons of the surrounding media).[34] This result was the initiating factor for the formulation of two different reaction mechanisms, which could explain this preservation (Figure 3).
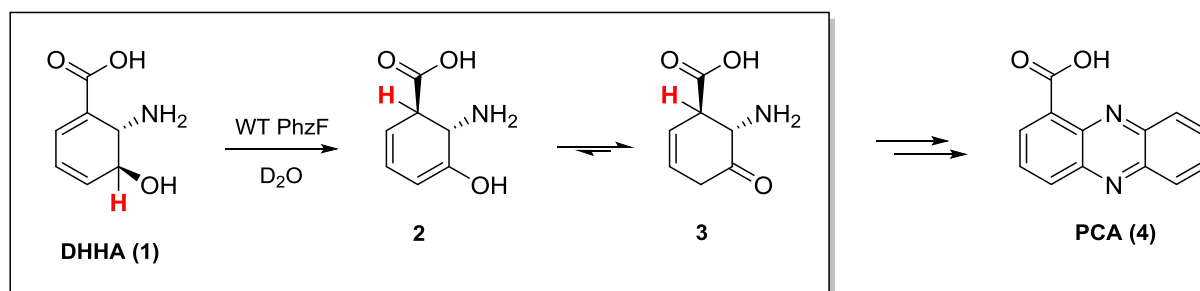
Figure 3: Observed conservation of migrating hydrogen atom by BLANKENFELDT in the enzymatic isomerization reaction of DHHA (**1**) in D_2O catalyzed by WT PhzF.

On the one hand, this transformation can follow a unique pericyclic reaction mechanism, namely an intramolecular suprafacial [1,5]-prototropic rearrangement, which includes the conjugated π-system and the involved carbon-hydrogen σ-bond of DHHA (**1**).[55,56,133–137] Perfectly in accordance with the WOODWARD-HOFFMANN rules for a thermal, sigmatropic isomerization,[55,56] it would be one of the rarely found pericyclic reactions in nature,[57–71,86] including e.g. chorismate mutase[58,60–62] and isochorismate pyruvate lyase,[57,86] and up to date the first example for a [1,5]-prototropic rearrangement in living organisms, which happens without the fragmentation of the substrate molecule. On the other hand, the isomerization can happen via an ordinary and usually in nature found acid-base catalyzed reaction pathway, where the proton is abstracted by a base in the first step and later returned to the anionic system after a conformational rearrangement of the enzyme-substrate complex (Figure 4).

In order to elucidate the mechanism of action in the isomerization of DHHA (**1**) by WT PhzF, all main differences between the pericyclic rearrangement and the acid-base catalyzed process have to be stated. Based on that proposal, an experimental proof should exclude one type of mechanism from the other.

Suprafacial [1,5]-Prototropic Rearrangement
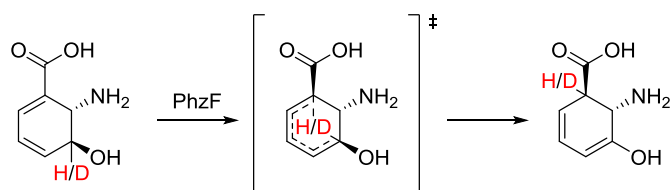
quantitative migration of H/D

high primary kinetic isotope effect possible
(1° KIE > 7)

Acid-Base Catalyzed Isomerization
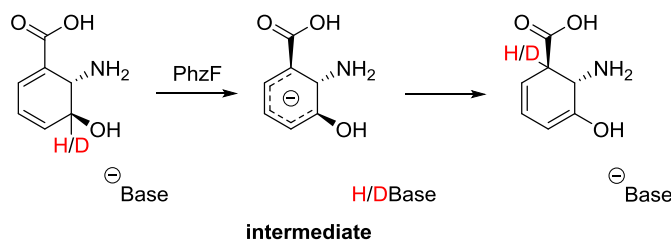
exchange of H/D possible

moderate primary kinetic isotope effect
(1° KIE < 7 (semiclassical limit))

rather strong base or efficient stabilization

Figure 4: Comparison between the concerted suprafacial [1,5]-prototropic rearrangement and the acid-base catalyzed isomerization together with main characteristics for both reaction types.

The complete acid-base transformation is defined by the quantitative abstraction of the rather non-acidic ε-proton within this vinylogous system of DHHA (**1**) by either a fairly strong basic amino acid, efficient stabilization by an excellent conformational fitting in the enzyme cavity or both. This would immediately lead to the formation of at least one anionic intermediate. Afterwards, the same or another proton is reattached to the α-position of the carboxylic acid destroying the formerly conjugated π-system of DHHA (**1**). In contrast, in a concerted suprafacial [1,5]-prototropic rearrangement the hydrogen atom efficiently migrates within the mentioned π-system of the cyclohexadiene core structure via only a single six-membered TS,[55,56] which excludes the necessity of the formation of an intermediate. Simultaneously, one carbon-hydrogen bond is synchronously broken and formed within this particular reaction step. This mechanism must exclusively result in the conservation of the migrating hydrogen atom. However, in the protic mechanism a conservation of the proton may be able to happen, but must not mandatorily be observed, if scrambling with protons of the surrounding media or protic amino acid side chain residues occurs.

Apart from that, the PhzF catalyzed isomerization of DHHA (**1**) is predestined for its elucidation via a 1° KIE, which should be characteristic for its underlying isomerization process. Associated with the synthesis of deuterium labeled DHHA (d-DHHA (**5**)), discrimination between both proposed mechanisms can be addressed by a 1° KIE of different magnitude (1° KIE = k_H/k_D; k_H, k_D: rate constant of unlabeled (H) and labeled (D) compound). In conventional transformations, e.g. acid-base catalyzed reactions, the 1° KIE

can reach the semiclassical limit of 1° KIE = 7 assuming that no unexpected quantum-mechanical effect, e.g. hydrogen tunneling etc., superimposes the r.d.s..[138] However, under special constellations, as in prototropic rearrangements, where a bond is simultaneously broken and formed to the labeled atom, higher 1° KIEs are published.[133,135,137] In 1966, ROTH reported a surprisingly large, experimental 1° KIE for the [1,5]-prototropic rearrangement of penta-1,3-diene (1° KIE = 5.2 at 473 K). Extrapolation, using the observed activation parameters, led moreover to a 1° KIE = 12.2 at 298 K.[137] Although normal ground state tunneling can be ruled out by the required large change in geometry,[133] vibrational assisted tunneling (VAT) was computationally demonstrated[133,139] and later on proved in many enzyme catalyzed hydrogen transfer reactions.[140–145] Herein, temperature dependent measurements of the 1° KIE have emerged as a powerful tool in the diagnosis of hydrogen tunneling,[138,140–145,146] however, the complexity of biological systems makes a demonstration of such correlations very challenging.[147] Besides that, SCRUTTON warned against the assumption that 1° KIE < 7 are indicative for classical reactions and, moreover, emphasized that VAT could also occur in cases with low 1° KIEs.[140,148]

Indispensable for the assignment of a 1° KIE, d-DHHA (**5**) may act as a key mechanistic probe in a second sense. Cross experiments in H_2O have to confirm the possibility of the suprafacial [1,5]-prototropic rearrangement by the conservation of the deuterium/deuteron in that molecule, as published for DHHA (**1**).[34] Its synthesis will be discussed in the following sections.

Nevertheless, in both cases, the acid-base catalyzed as well as the pericyclic mechanism, the same enolic structure **2** is formed with DHHA (**1**) as substrate. Spontaneous and stereoselective tautomerization to its kinetically instable ketamine **3** is also integral part of this research (see chapter: Stereoselective Tautomerization), which was preliminarily investigated by BLANKENFELDT. Acting energetically downstream, ketamine **3** accomplishes PhzA/B catalyzed self-condensation to the characteristic core structure of all known phanazine derivatives and in combination with PhzG, phenazine monocarboxylic acid (PCA) (**4**) is efficiently formed perhaps in a multienzyme complex.[34] However, before any synthetic work was performed, quantum-mechanical calculations should explore, if the concerted suprafacial pericyclic isomerization of DHHA (**1**) is a possible option for this WT PhzF catalyzed transformation.

4.2. Quantum-Mechanical Calculations for a Suprafacial [1,5]-Prototropic Rearrangement in DHHA (1)

Hybrid DFT methods in combination with well-selected basis sets represent powerful tools for the calculation and investigation of energetic minimum structures of molecules, molecular properties or even reaction pathways. Especially for molecules with an increased number of atoms or basis functions, respectively, this strategy achieves a given level of accuracy by means of acceptable costs in computation.[149] Although these calculations are often in suitable agreement with experimental results, experimental proofs are still aspired to exclude all possibilities of doubt.

In addition to the synthetic work described below for the investigation of the isomerization of DHHA (1) by WT PhzF, this transformation was analyzed with quantum-mechanical hybrid DFT methods at the mPW1PW91/6-31+G* level of theory.[77–79,150] This method was formerly validated by a comparison with post HARTREE-FOCK methods, e.g. MP2 method (perturbation theory),[151] and by the use of bigger POPLE type basis sets, e.g. 6-311+G*.[77–79] Cyclohexadiene (6), the core structure of DHHA (1), as well as the uncharged form of DHHA (1a) by itself served as model substrates for this mentioned validation process. In conclusion, it could be demonstrated that mPW1PW91/6-31+G* provided acceptable results for the analyzed sigmatropic rearrangements compared to methods with a higher effort in computation (Figure 5).[152]

Computational Studies of DHHA (1) at the mPW1PW91/6-31+G* level of theory
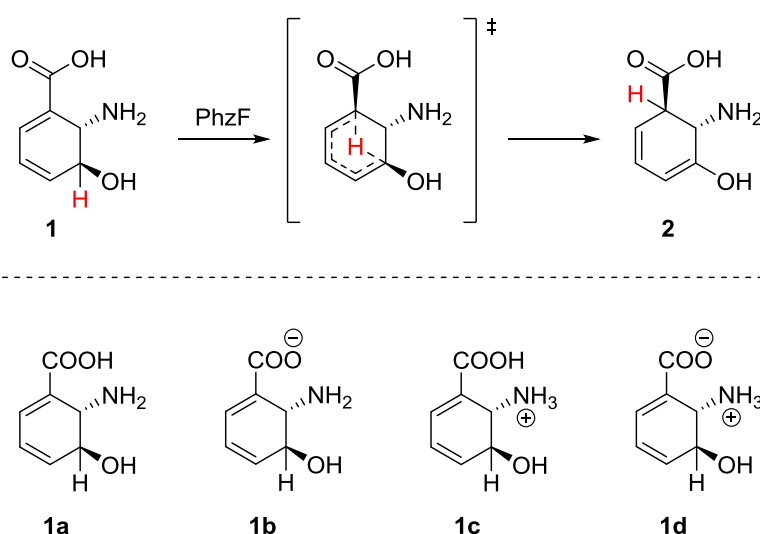
Figure 5: Simulation of the suprafacial [1,5]-prototropic rearrangement in DHHA (1) at the mPW1PW91/6-31+G* level of theory highlighted with the neutral form of DHHA (1a); Considered ionization states of DHHA (1): Neutral 1a, anionic 1b, cationic 1c and zwitter ionic 1d.[152]

All possible ionization states of DHHA (**1**), the neutral **1a**, anionic **1b**, cationic **1c** as well as zwitter ionic form **1d**, were taken into consideration and activation energies for the suprafacial [1,5]-prototropic rearrangement of DHHA (**1**) calculated at the mPW1PW91/6-31+G* level of theory. Hereby, computations were either performed in the gas phase or in H_2O simulating the solvent by surrounding five H_2O molecules around the active site (Figure 6 and Figure 7). Unfortunately, the commonly used polarized continuum model (PCM)[153] failed in finding correct transition states for the pericyclic reaction due to misplacing the migrating hydrogen atom within the considered molecules.

neutral E_n ($\Delta G = 0.0$ kJ.mol^{-1})　　　neutral TS_n ($\Delta G = 145$ kJ.mol^{-1})　　　neutral P_n ($\Delta G = -21$ kJ.mol^{-1})
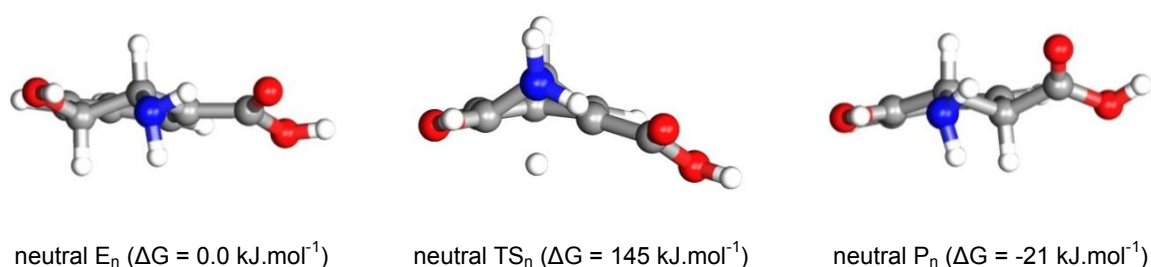
Figure 6: Energetically most stable conformers of the neutral form of DHHA (**1a**) as representative for geometries in starting material, TS and product; Free enthalpies (ΔG) calculated at the mPW1PW91/6-31+G* level of theory.[77–79,150,152]

neutral $E_{n,aq}$ ($\Delta G = 0.0$ kJ.mol^{-1})　　　neutral $TS_{n,aq}$ ($\Delta G = 150$ kJ.mol^{-1})　　　neutral $P_{n,aq}$ ($\Delta G = -26$ kJ.mol^{-1})
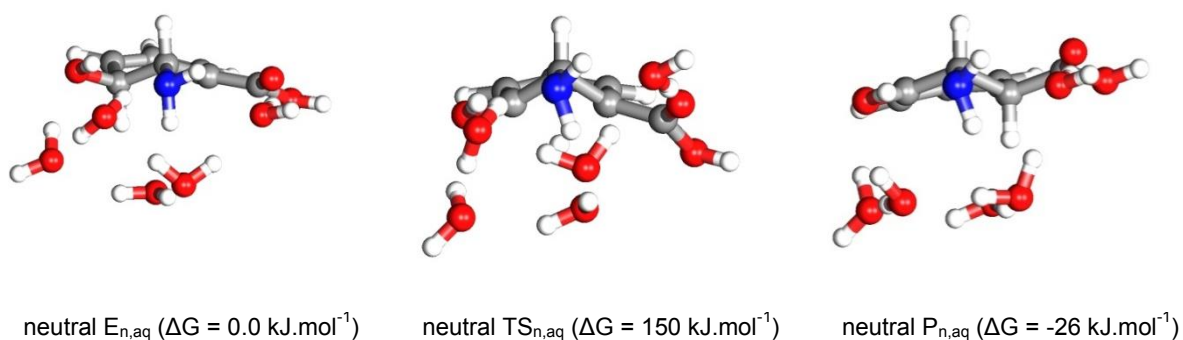
Figure 7: Solvent effect calculation by surrounding five H_2O molecules for the energetically most stable conformers of the neutral form of DHHA (**1a**) as representative for geometries in starting material, TS and product; Free enthalpies (ΔG) calculated at the mPW1PW91/6-31+G* level of theory.[77–79,150,152]

Details of previously performed quantum-mechanical calculations for a suprafacial [1,5]-prototropic rearrangement in DHHA (**1**) are illustrated and discussed below.[152]

1. Calculated activation energies for all considered ionization states of DHHA (**1**), except one cationic form simulated in H_2O, feature a reduced activation energy compared to cyclohexadiene (**6**),[154] the core structure of DHHA (**1**). This observation is explained

by tight hydrogen bond interactions within the TS of the neutral, anionic and zwitter ionic forms. Additionally, electron-donating groups, as the free amine as well as the hydroxy moiety, lower the activation barrier by enhancing electron density to the aromatic character of the six-membered TS.[152,155]

2. Calculations in solvent systems can be generally substituted by gas phase simulations featuring similar results in drastically shortened computation times. Nevertheless, depicted H_2O molecules in solvent simulations demonstrated the dynamic process during the considered pericyclic isomerization reaction.[152]

3. The lower the calculated activation energy of the [1,5]-prototropic rearrangement is, the more exergonic the isomerization process is found indicating a more starting material like character of the TS in the considered ionization form of DHHA (**1**). This observation perfectly agrees with the HAMMOND postulate referring to reaction coordinate diagrams.[152,156]

4. Conformational analyses assign different educt rotamers to the same TS. Depending on the symmetry of the considered functional group, the more symmetric it is, e.g. ammonium vs. amine, the lower the number of educt rotamers referring to one TS (neutral form of DHHA (**1a**) with highest number of energetically similar educt rotamers referring to one TS).[152]

5. Regarding all calculated activation energies for the suprafacial [1,5]-prototropic rearrangement in every ionization state of DHHA (**1**), the following trend was determined: Only the net charge of the entire system showed strong influence on the activation energy. Charge separation, however, as found in the zwitter ionic form, did not significantly contribute to an alteration of the activation barrier.[152]

ΔG_{AE}: anionic **1b** < neutral **1a** ≈ zwitter ionic **1d** < cationic **1c** ≈ cyclohexadiene (**6**)

131-141 kJ.mol^{-1} 145-151 kJ.mol^{-1} 161-175 kJ.mol^{-1} 172 kJ.mol^{-1}[152,154]

In conclusion, the suprafacial [1,5]-prototropic rearrangement is a possible option for the isomerization of DHHA (**1**). Although computationally low costing hybrid DFT methods were used for these simulations, they were judged to perform well in diverse hydrocarbon pericyclic processes.[134] Distinctive stabilization of diverse TS demonstrated that this type of transformation is favored in DHHA (**1**) compared to unsubstituted cyclohexadiene (**6**).[152,154] However, the lowest found activation energy of 131-140 kJ.mol^{-1} for the anionic DHHA (**1b**) is too high for a spontaneous isomerization. The enzymatic environment may cause an additional lowering of this energy barrier or facilitates a VAT by fluctuations in the protein, as proposed by BRUNO.[141,143,157] This hypothesis needs to be tested by achieving either concrete experimental results with mechanistic probes or by quantum-mechanical

calculations with the natural substrate in the enzyme cavity, abbreviated with the synonym of QM/MM calculations.[122–131,158]

4.3. Retrosynthetic Analysis for the Synthesis of Deuterium Labeled DHHA (d-DHHA) (5)

Mechanistic probes, especially isotope labeled molecules, gained immense attention in the last few decades for the investigation of proposed reaction pathways. Not only the migration of this isotope within the chemical transformation and later on its position in the formed product permit conclusions about the mechanism of action, but also kinetic measurements are often significant for reaction pathways as long as the labeled atom is involved in the r.d.s.. In the particular case of a 1° KIE, this effect is even higher, the larger the mass difference of the considered isotopes is. Depending on the related vibrational frequencies of the affected bonds, substitution of a hydrogen atom (H) by deuterium (D), results in a higher 1° KIE compared to the replacement of ^{12}C to ^{13}C.[4,109–117]

The isomerization of DHHA (**1**) catalyzed by PhzF is an illustrative example for the requirement of isotope labeled mechanistic probes. Due to the fact that only one hydrogen atom migrates within this reaction, deuterium labeled DHHA (d-DHHA) (**5**) should be synthesized based on previous arguments.

In principle, the "ideal synthesis" of a complex molecular structure assumes the compliance of several retrosynthetic rationales. Aside from the practicability of the reaction sequence, efficiency and economy are important parameters for reaching the intended target molecule. In the particular case of drug development, process chemists are especially aware of overall costs and the potential for scale-up. But even before the ideas of atom, step and redox economy were formally galvanized, HENDRICKSON addressed the definition of "the ideal synthesis" in 1975:[159–171]

> "*The ideal synthesis creates a complex skeleton from simpler starting materials … in a sequence of only successive construction reactions involving no intermediary refunctionalizations, and leading directly to the structure of the target, not only its skeleton but also its correctly placed functionality. If available, such a synthesis would be the most economical, and it would contain only construction reactions.*"[164]

Based on the mentioned concepts, the main elements for an efficient total synthesis of enantiomerically pure d-DHHA (**5**) are explicitly listed below:

1. Convergent route to minimize reaction steps in series for the synthesis of molecule fragments with comparable complexity (step economy).[163,167–169]

2. Minimal amount of reaction steps including the avoidance of not necessarily required protecting groups in chemoselective reactions for gaining a high percentage of overall yield (step and atom economy).[163,165–169]

3. High yielding transformations for preventing side product formation and a more convenient purification of intermediates or final product with respect to chemo-, regio-, diastereo- and enantioselective control (atom economy).[163,165,166]

4. Minimization of non-strategic redox manipulations in order to achieve an isohypsic synthesis (redox economy).[163,170,171]

5. Efficient insertion of the deuterium atom in the late stages of the synthesis using inexpensive labeling reagents and established methods for lowering total costs of the synthetic route.

6. Enantioselective synthesis or efficient kinetic resolution in the early stages of the reaction sequence to reduce costs of reagents in subsequent transformations. The wrong enantiomer is considered as a contamination, which consumes reagents and finally has to be separated.

Gratifyingly, the synthesis of unlabeled DHHA (**1**) published by STEEL in 2003[172–175] fulfilled most of our suggested requirements regarding the use of established methodologies, effectiveness, stereochemical reaction control and high yielding intermediates. Adopting this reaction sequence for the synthesis of enantiomerically pure d-DHHA (**5**), we proposed a retrosynthetic approach for the chemoselective insertion of the deuterium atom (Figure 8).[152]
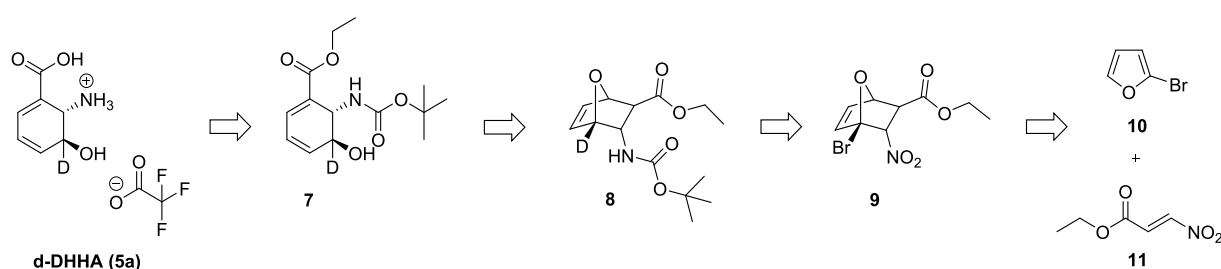
Figure 8: Retrosynthetic approach for the synthesis of enantiomerically pure d-DHHA (**5**) in analogy to DHHA (**1**) published by STEEL.[152,172–174]

Herein, both stereogenic centers in d-DHHA (**5**) should be correctly placed in a stereospecific DIELS-ALDER reaction between 2-bromofuran (**10**) and ethyl (*E*)-3-nitroacrylate (**11**) as starting materials.[55,56] The targeted use of dienophile **11** in its *trans*-configuration specifically results in reducing the number of all possible stereoisomers. After the isolation of the desired

bicyclic, racemic intermediate **9**, the insertion of the deuterium atom should be achieved in a single electron transfer reaction (SET) by a replacement of the tertiary bound bromide atom. If this reaction sequence succeeds, it would be possible to proceed with the optimized reaction protocol published by STEEL.[152,172–175] A subsequent kinetic resolution with pig liver esterase (PLE) on the stage of the bicyclic compound should lead to the separation of both enantiomers,[172–178] which would be followed by a base mediated, ring opening to the core structure of d-DHHA (**5**).[172–175,179] Finally, after saponification and cleavage of the Boc-protected amine under acidic conditions with trifluoroacetic acid (TFA), the enantiomerically pure, deuterium labeled compound, namely d-DHHA (**5**), should be isolated in the form of a TFA salt **5a**.[152,172–175]

The most challenging parts of this route were expected to be the separation of all four diastereomers after stereospecific DIELS-ALDER reaction, the chemoselective insertion of the deuterium atom in a SET reaction as well as the base mediated ring opening to the desired diene **7**. Although most of these transformations are well-known in literature, the exciting task would be the adaption of this reaction sequence for the synthesis of d-DHHA (**5**).[152,172–175]

4.4. Synthesis of d-DHHA (5)

4.4.1. Preliminary Achievements for the Synthesis of d-DHHA (5)

Previous investigations in the MSc thesis of Mario LEYPOLD on the synthesis of d-DHHA (**5**) succeeded in the isolation of diastereomerically pure brominated bicyclus **9** (Scheme 9). Within this reaction sequence, furan (**12**) was initially brominated using a combination of *N*-bromosuccinimide (NBS) (**13**) in DMF as effective brominating reagent. Interestingly, in contrast to the behavior of Br_2, the addition of NBS (**13**) to DMF was found to be not exothermic, as this allowed the controlled addition of this reagent to a solution of furan (**12**) at room temperature. 2-Bromofuran (**10**) could be straightforwardly isolated and purified in a yield of 55 % applying water steam distillation to the concentrated reaction mixture.[180] Due to the fairly neutral conditions during the bromination, 2-bromofuran (**10**) could be stored over anhydrous K_2CO_3 for several days without the risk of degradation.[152]

In parallel, dienophile **11** was synthesized starting from commercially available ethyl glyoxalate solution (~50 % (w/w) in toluene) via HENRY addition with $MeNO_2$ and neutral Al_2O_3 as heterogeneous catalyst. In contrast to optimized reaction protocols from literature,[181] reflux conditions were established to achieve quantitative conversion of aldehyde **14**. Subsequently, the resulting HENRY adduct was stereoselectively dehydrated to dienophile **11** in an E_{1cB}-elimination on the stage of its *in situ* prepared mesylated

intermediate.[181,182] Herein, this two-step reaction sequence was performed on a multigram scale isolating ethyl (*E*)-3-nitroacrylate (**11**) after distillation in form of an aggressively smelling, yellow liquid in a total yield of 41 %. Noteworthy, impurities of methanesulfonyl chloride (MsCl) in distilled dienophile **11** were quantitatively removed by drying it at 1.0 mbar for several hours at room temperature.[152]
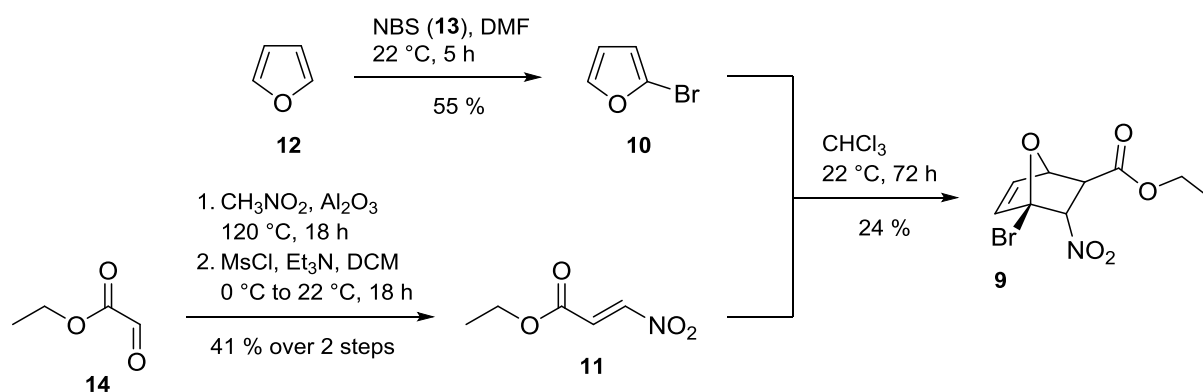
Scheme 9: Performed reaction sequence for the preparation of diastereomerically pure bicyclic ester **9**.[152]

Screening experiments for the stereospecific DIELS-ALDER reaction between 2-bromofuran (**10**) and dienophile **11** resulted in optimized reaction conditions. These were applied to the synthesis of bicyclic ester **9**, which reduced unwanted MICHAEL-type side product formation to a minimal amount. Semiempirical simulations of ITOH demonstrated that orbital energy differences between the $HOMO_{diene}$ and $LUMO_{dienophile}$ act as appropriate factor for estimating DIELS-ALDER product formation with furan (**12**) as reaction partner. The higher the energy gap is, the more favored the cycloaddition compared to MICHAEL-type addition is.[183] Fortunately, the required diastereomer **9** was formed as main product within this cycloaddition and could be perfectly separated from the remaining three others applying normal phase flash column chromatography. Full characterization and identification of bicyclic ester **9** was accomplished by NMR spectroscopy. Additionally, chemical shifts were supported by quantum-mechanical calculations and coupling constants were simulated at the mPW1PW91/IGLO-II//mPW1PW91/6-31+G* level of theory,[77–79,150,184] which are characteristic for each diastereomer.[152,172–175] Based on these results, the synthesis of d-DHHA (**5**) was pursued on this stage investigating chemoselective methods for the insertion of the deuterium atom at the tertiary carbon center.

4.4.2. One Pot Reaction Sequence: Bromide-Deuterium Exchange together with the Reduction of the Nitro Functionality and *in situ* Boc-Protection of the Free Amine

In general, many strategies for hydrodehalogenation reactions are known in literature depending on the nature of the substrate.[185,186] However, in the case of tertiary carbon centers, a large number of transformations is based on radical processes, e.g. with TBTH/AIBN[187–191] or TBTH/Et$_3$B/O$_2$[192–194] as reagent cocktails.[186] These conditions preferentially lead to the formation of tertiary carbon radical species, which can be captured by the use of radical hydrogen transfer reagents, mainly toxic stannane derivatives, as TBTH.[186–194] Although the deuterated form of TBTH, namely TBTD,[195–200] is widely found in the case of chemoselective labeling experiments, the application of this reagent on multigram scale is a high-priced issue. Besides, the existing nitro moiety in bicyclic ester **9** is well-known to consume a non-negligible amount of radical hydrogen/deuterium transfer reagent due to the radical scavenging character of highly oxidized nitrogen containing groups, e.g. nitroso, nitro and nitrite functionalities.[201] This difficulty was indeed observed in preliminary hydrodehalogenation reactions with bicyclic ester **9** resulting in the formation of uncharacterized side products.[152]

To overcome this issue of chemoselectivity, a reduction of the nitro group to the amine, followed by *in situ* Boc-protection, emerged as the most evident way for the subsequent hydrodehalogenation. Proceeding in the reaction sequence published by STEEL for DHHA (**1**),[172–175] the treatment of bicyclic ester **9** with activated Zn$_{act}$/HCl interestingly led to a partial bromide-hydrogen exchange during reduction of the nitro moiety. Compared to reactions with non-activated Zn/HCl, a loss of activity concerning the hydrodebromination was detected, after Zn was washed with 1 M HCl for activating purpose. It was assumed, that important impurities, e.g. metallic contaminants, were removed during activation, which were crucial for highly efficient SET processes (Scheme 10).
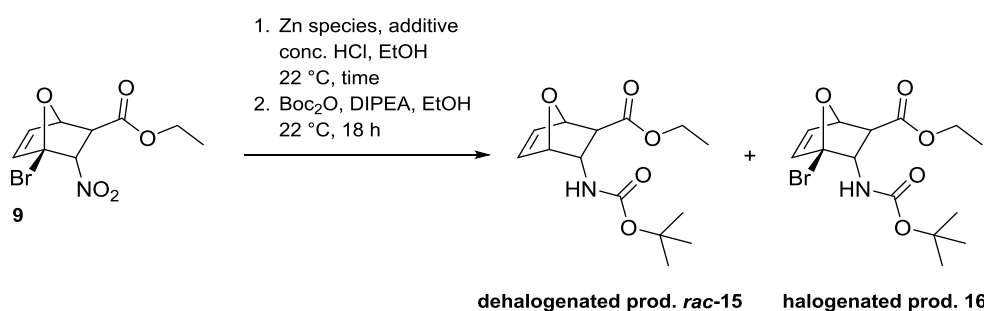
Scheme 10: Screening experiments for the chemoselective hydrodebromination during the reduction of the nitro moiety with Zn/HCl in combination with different additives.

Table 2: Screening experiments for the bromide-hydrogen exchange in combination with the reduction of the nitro functionality; Reaction conditions: 22 mg (75 µmol, 1.0 eq) ester **9**, 1.50 mmol (20 eq) Zn species, 103 µL (1.20 mmol, 16 eq) HCl (~36 % (w/w) in H_2O), 225 µmol (3.0 eq) ZnO or $ZnCl_2$ resp. 3.75 µmol (5 mol%) $NiCl_2$ or CuBr, 700 µL EtOH, 22 °C; Filtration through a pad of Celite®, washing with additional 150 µL EtOH and Boc-protection with: 210 µL (1.20 mmol, 16 eq) DIPEA, 29 mg (135 µmol, 1.8 eq) Boc_2O, 22 °C, 18 h.

Entry	Zn species	Additive	Time / h	Dehalo. prod. *rac*-15 / %	Halo. prod. 16 / %
1	Zn_{act}	-	3	15	85
2	Zn	-	3	35	65
3	Zn	ZnO	3	5	95
4	Zn	$ZnCl_2$	3	40	60
5[1]	Zn	$NiCl_2$	3	16	84
6	Zn	CuBr	3	94	6
7	Zn/Cu	-	3	90	10
8[1]	Zn/Cu	$NiCl_2$	3	24	76
9	Zn/Cu	CuBr	3	92	8
10[2]	**Zn/Cu**	**-**	**8**	**>99**	**<1**

1 Only hydrogenated product due to reduction of olefin detected via HPLC-MS.

2 Reaction conditions: 2.25 mmol (30 eq) Zn/Cu couple, 155 µL (1.80 mmol, 24 eq) HCl (~36 % (w/w) in H_2O), EtOH, 22 °C.

Screening experiments with different salt additives, as ZnO, $ZnCl_2$ and $NiCl_2$ (Table 2: Entries 3-5), did not further improve the amount of dehalogenated product *rac*-**15**. However, $NiCl_2$ induced the formation of derivatives, in which the isolated olefinic double bond in the backbone of the bicyclic structure was completely reduced. Indicating the generation of elementary Ni under these strongly reductive conditions (Entries 5 and 8),[202] this observation suggested the use of CuBr as additive (Entry 6). Herein, after HPLC-MS analysis a remarkable increase of the desired dehalogenated compound *rac*-**15** was detected referring to the formation of metallic Cu, which supported the SET substitution process.[203] Gratifyingly, commercially available Zn/Cu couple (Zn doped with max. 3 % Cu) met all of our demands in the reduction of the nitro group accompanying with a SET mediated bromide-hydrogen exchange (Entry 10).[204] Although a large excess of reducing reagent was needed for the quantitative transformation of both functional groups, the deuterium source with deuterated hydrochloric acid (DCl) in deuterated solvents is rather inexpensive compared to toxic TBTD.[195–200]

Under these optimized reaction conditions, bicyclic ester **9** was quantitatively converted with 30 eq Zn/Cu couple and 24 eq DCl (38 % (w/w) in D_2O) in EtOD at room temperature for

11 h. All solid materials were removed via filtration through a small pad of Celite® and the *in situ* formed amine intermediate was Boc-protected at room temperature for 18 h using 24 eq DIPEA as well as 1.8 eq Boc₂O. Summing up the whole process, brominated bicyclic ester **9** was converted in a three-step one pot synthesis to deuterium-labeled compound ***rac*-8**, which was finally purified via flash column chromatography and isolated in a total yield of 88 %. HPLC-MS analysis in SIM mode (ESI+) in combination with the purity of starting material **9** confirmed a deuterium content at the desired carbon atom of >97 % (atom% D) (Scheme 11).

atom% D at carbon: >97 %

Scheme 11: Synthesis of deuterium-labeled bicyclic ester ***rac*-8** by parallel reduction of the nitro moiety and bromide-deuterium exchange followed by Boc-protection of the *in situ* formed amine.

4.4.3. Kinetic Resolution of Deuterium-Labeled Bicyclus *rac*-8 by Utilization of Pig Liver Esterase (PLE)

Hydrolases, such as esterases, lipases and proteases, are well established enzymatic systems for the separation of enantiomers in saponification reactions of carboxylic esters. In contrast to the large number of already available microbial lipases, only a small amount of esterases have been used to perform highly stereoselective hydrolysis reactions. Pig liver as well as horse liver esterase (PLE and HLE)[205] are the most prominent representatives of this subclass of hydrolases. Among all others, PLE is characterized by its general versatility. Consisting of at least five isoenzymes, however, this crude mixture can be regarded as a single enzyme since it possesses similar, but not identical stereospecificities.[176,206–208]

Depending on the optimal agreement of bicyclus ***rac*-8** with preferred substrates of pig liver esterase (PLE),[172–177,209] it was employed as the enzyme of choice achieving excellent values in kinetic resolution experiments. Herein, a biphasic system consisting of Et₂O for the dissolution of starting material ***rac*-8** as well as 100 mM NaH₂PO₄/Na₂HPO₄ with pH 7.6 was chosen. 2.0 eq of buffer with respect to the amount of substrate were used in order to

maintain the pH value of the reaction mixture for the whole period of transformation.[172,173,175,177] As in biphasic systems the enzymatic transformation proceeds only in the aqueous layer, a sufficient mass transfer between catalyst and substrate is necessary. Obviously, mixing is a crucial factor for accelerating the whole enzymatic conversion and driving the reaction towards completion by removing the product from the enzyme surface.[176,210] The faster the mixing is, the larger the surface between the two chemically different layers. In order to ensure a high reproducibility in this kinetic resolution, a moderate mixing rate of 150 rpm was chosen that guaranteed mass transport at the interface, but avoided uncontrolled formation of turbulent flows (Scheme 12). Unfortunately, the inhomogeneous, two-phasic system in combination with the heterogeneous PLE suspension (in half-saturated $(NH_4)_2SO_4$) did not allow reproducibility in terms of reaction times. Steady reaction controls had to be performed for quenching the preparations at the desired *e.e.* value just in time to yield high optical purity of the saponified product.
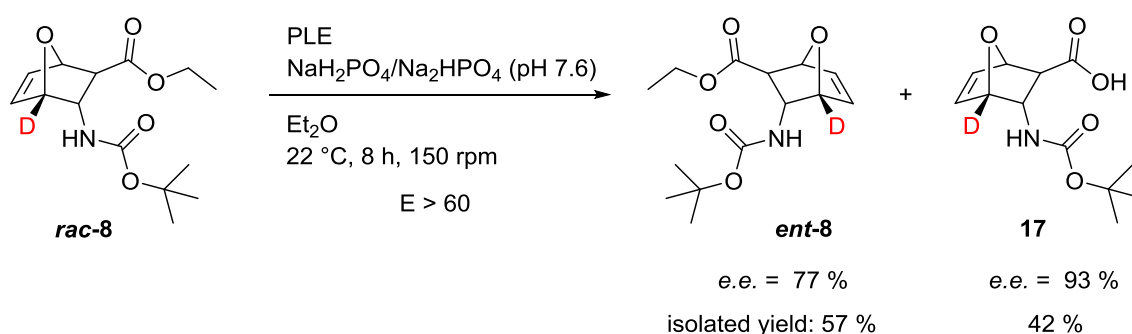
Scheme 12: Kinetic resolution of deuterated bicyclic ester *rac*-8 with PLE in a two-phase system.

PLE delivered superb results in the kinetic resolution of compound *rac*-8 without the need for further optimization, whereas these initial conditions were retained for onward enantioselective hydrolyses.[172,173,175,177] As hydrolytic reactions in aqueous systems can be regarded as completely irreversible due to the high concentration of H_2O (55.5 $mol.L^{-1}$) present, the enantioselectivity (E) can be mathematically linked to the conversion (ζ) and the optical purities of substrate (*e.e.$_s$*) as well as product (*e.e.$_p$*). In general, E, the ratio of the initial reaction rates for both substrate enantiomers, was determined by performing reaction control experiments at conversions between 40 % and 60 %.[176] Herein, the enantiomeric excess (*e.e.*) of the starting material (*e.e.$_s$*) along with the product (*e.e.$_p$*) for the hydrolysis with PLE towards bicyclus **17** and other related substrates was assigned via chiral HPLC separations. Conversion as well as E were calculated applying the formulas below (Figure 9).

$$E = \frac{\ln \dfrac{[e.e._P (1 - e.e._S)]}{(e.e._P + e.e._S)}}{\ln \dfrac{[e.e._P (1 + e.e._S)]}{(e.e._P + e.e._S)}} \qquad (1)$$

$$E = \frac{\ln[(1 - \zeta)(1 - e.e._S)]}{\ln[(1 - \zeta)(1 + e.e._S)]} \qquad (2)$$
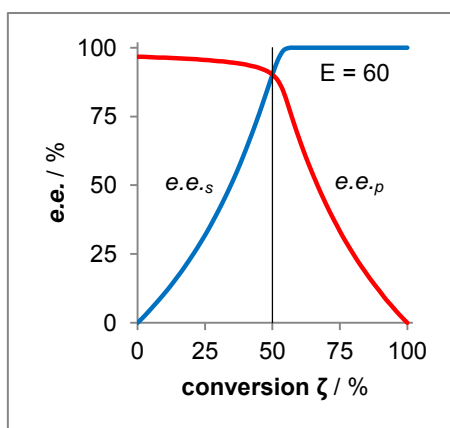
Figure 9: Mathematical relationship between enantioselectivity E, conversion ζ and enantiomeric excess (*e.e.*) of substrate (*e.e._s*) as well as product (*e.e._p*) (Formulas 1 and 2);[176] Representative diagram for the calculated *e.e.*'s in dependence on ζ for E = 60.

As a rule of thumb, enantioselectivities of E < 15 are inacceptable for practical purpose, however, values of E > 30 can be regarded as very good.[176] Caused by the high enantioselectivity for all tested and below mentioned bicyclic substrates with PLE, all reactions were stopped at conversions around 45 % by the simple separation of both layers. Regrettably, the inhomogeneous PLE precipitate prohibited an exact determination of E, nevertheless, in the worst case an excellent value of E = 60 was determined (Figure 9). After the acidifying denaturation of PLE by addition of saturated $KHSO_4$ to reach pH 1-2, the enzyme could be effortlessly separated by centrifugation. Herein, the protonated bicyclic carboxylic acid **17** was extracted with DCM into the organic phase and the concentrated crude material was finally purified by trituration in cyclohexane:EtOAc = 2:1 (v/v) achieving quantitative yields referred to the determined conversion.

Single crystal X-ray crystallography analysis of an optically pure, non-labeled ester of bicyclus **17** (see chapter: Synthesis of DHHA (**1**)) allowed the determination of the absolute configuration and furthermore demonstrated that the desired enantiomer of ester *rac*-**8** was hydrolyzed by PLE.[172,175] Generally, an attractive optical purity of the non-hydrolyzed enantiomer can be realized in a more convenient way by running the deracemization reaction to a conversion of slightly over 50 % depending on the E value of the system. In order to achieve excellent *e.e.* > 99 % for carboxylic acid **17**, repeated kinetic resolution appears less than ideal and lacks synthetic elegance, but in practice displays a great potential to synthesize optically pure molecules.[176] Consequently, reesterification with EtOH under 4-DMAP catalysis[211,212] using EDC.HCl as coupling reagent and repeated kinetic resolution with optically enriched ester **8** gave not only bicyclic acid **17** in excellent *e.e.* > 99 %, but also all other tested bicyclic esters mentioned in the following sections (Scheme 13).[172,173,175,176]
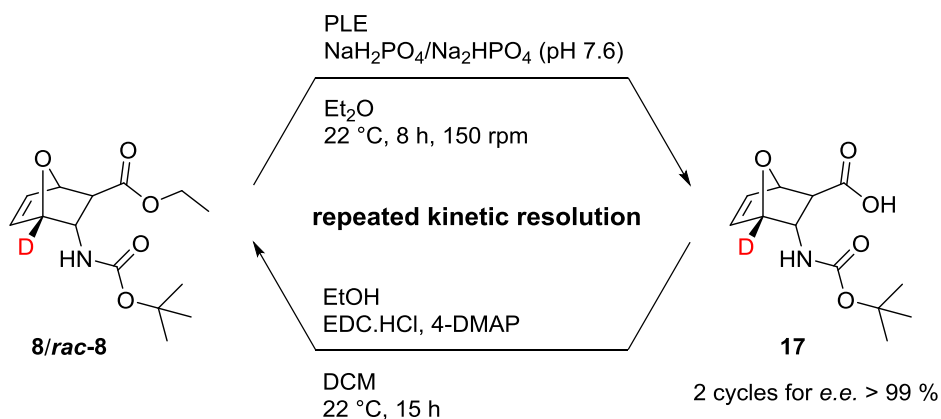
Scheme 13: Repeated kinetic resolution with PLE and subsequent reesterification with EtOH under 4-DMAP catalysis affording optically pure carboxylic acid **17**.[172,173,175,176,211,212]

4.4.4. KHMDS-Mediated Ring Opening of Deuterated Bicyclic Ester 8

One of the most challenging steps in the synthesis of d-DHHA (**5**) and its derivatives was the base-mediated ring opening of the bicyclic carboxylic esters to the cyclohexadiene core structure. BRION reported the first lithium hexamethyldisilazide (LHMDS) induced fragmentation for the oxygen bridge in oxanorbornene systems.[175,179] However, following the published procedure of STEEL from 2003, all preceding experiments with potassium hexamethyldisilazide (KHMDS) (**18**) as a base preferentially resulted in the formation of benzoic acid derivatives **19** and **20** in an elimination reaction after warming the reaction mixture from -78 °C to room temperature (Table 3: Entries 1-5). Although the ring opening reaction with racemic ester **rac-15** proceeded very rapidly at temperatures between -40 °C and -20 °C to structure **rac-21**, elevated temperatures preferred the formation of the two mentioned elimination products **19** and **20**. Noteworthy, well coordinating counter ions, as Li$^+$, were shown to accelerate the elimination process even at lower temperatures.[152,172–175]

Due to the rather high degree of hydrolysis of commercially available, solid KHMDS (**18**), this reagent was prepared freshly and synthesized according to a procedure published by SOMFAI.[213] Under ultrasonication, hexamethyldisilazane (HMDS) (**22**) was deprotonated with KH in THF achieving a clear solution of this base after filtration. In order to determine the exact concentration, the yellowish solution was titrated with 2-BuOH in toluene together with acid-base indicator **23**, according to a procedure of IRELAND. He could prove that none of the other standard protocols for the titration of alkyllithium base solutions are applicable for amide bases, as KHMDS (**18**).[214] Although the titer of KHMDS (**18**) was found to be in the correct range, the equivalence point was fairly hard to notice due to a non-distinctive color change of indicator **23** from red to pale orange. Importantly, KHMDS (**18**) prepared according

to this procedure could be stored in solution under argon atmosphere in a freezer at -24 °C for several days without a significant amount of degradation, as determined by repeated acid-base titration (Scheme 14).
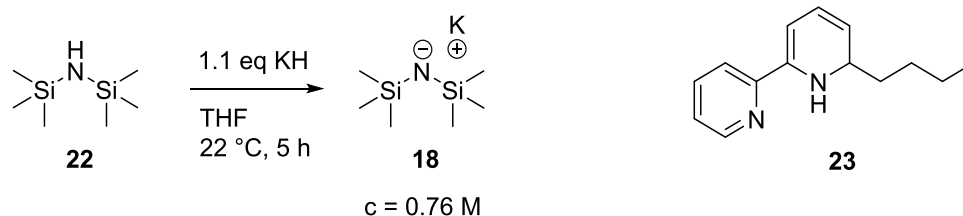
Scheme 14: Synthesis of KHMDS (**18**) in THF and acid-base titration with indicator **23**.[213,214]

Screening experiments for the KHMDS-mediated ring opening of bicyclic ester ***rac*-15** revealed that this transformation is very sensitive to reaction temperature and reaction time. Even at a temperature of -40 °C, a significant amount of elimination products **19** and **20** was detected, although the starting material was not quantitatively consumed. To find a satisfying compromise between reaction rate and amount of side product formation, an exact temperature of -45 °C during the whole time of isomerization had to be established. Essentially, all mentioned percentages in Table 3 have to be handled with care as they have been determined with HPLC-MS and were not corrected for the different absorption maxima of starting material, desired product and benzoic acid derivatives (λ_{max}(**15**): no maximum >200 nm, λ_{min}(**19**) = 224 nm, λ_{max}(**19**) = 209 nm and λ_{max}(**20**) = 223 nm). The reported values were recorded in single HPLC-MS runs at λ = 210 nm (Scheme 15).
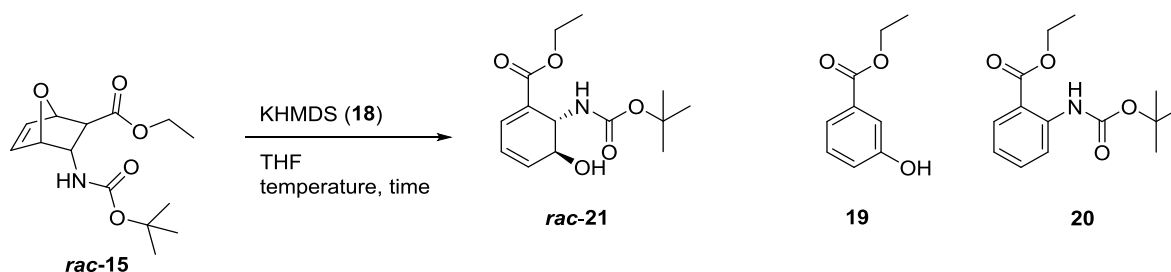
Scheme 15: KHMDS-mediated ring opening of bicyclic ester ***rac*-15**; formation of elimination products **19** and **20** at temperatures higher than -45 °C.[175]

Table 3: Screening results for the KHMDS-mediated ring opening of bicyclic ester **rac-15**; Reaction conditions: 99 mg (350 µmol, 1.0 eq) bicyclic ester **rac-15**, 1.38 mL (1.05 mmol, 3.0 eq) KHMDS (**18**) (c = 0.76 M in THF), 3.0 mL THF, KHMDS (**18**) addition to a solution of bicyclic ester **rac-15** at -78 °C, warmed to given temperatures; Conversion measured via HPLC-MS at λ = 210 nm after quenching with saturated NH_4Cl-solution and extraction with EtOAc.

Entry	Temp. / °C	Time / min	Ed. *rac*-15 / %	Prod. *rac*-21 / %	El. prod. 19 / %	El. prod. 20 / %
1	22	5	1	20	74	5
2	22	10	1	10	86	3
3	22	15	1	3	93	3
4	22	20	<1	2	94	3
5	22	25	<1	<1	95	3
6	-30	10	3	75	19	3
7	-30	20	1	73	23	3
8	-30	30	1	64	32	3
9	-30	40	<1	54	41	4
10	-30	50	<1	48	47	4
11	-40	10	30	64	4	2
12	-40	20	14	76	8	2
13	-40	30	12	76	9	3
14	-40	40	6	78	12	4
15	-40	50	4	76	15	5
16	-50	10	63	35	1	1
17	-50	20	59	39	1	1
18	-50	30	49	49	1	1
19	-50	40	37	60	1	2
20	-50	50	36	59	1	4
21	-45	20	33	65	1	1
22	-45	40	16	82	1	1
23	-45	60	10	85	2	3
24	-45	80	8	86	2	4
25	**-45**	**100**	**5**	**87**	**2**	**6**

Under optimized conditions with 3.0 eq KHMDS (**18**) at -45 °C over a period of 100 min, the KHMDS-mediated ring opening of bicyclic ester **8** processed smoothly and without significant amount of side product formation (Table 3: Entry 25). Gratifyingly, under these conditions

followed by a rapid quenching of the reaction mixture with saturated NH$_4$Cl solution at -45 °C, the desired product **7** could be isolated and purified via flash column chromatography in a total yield of 89 % (Scheme 16).
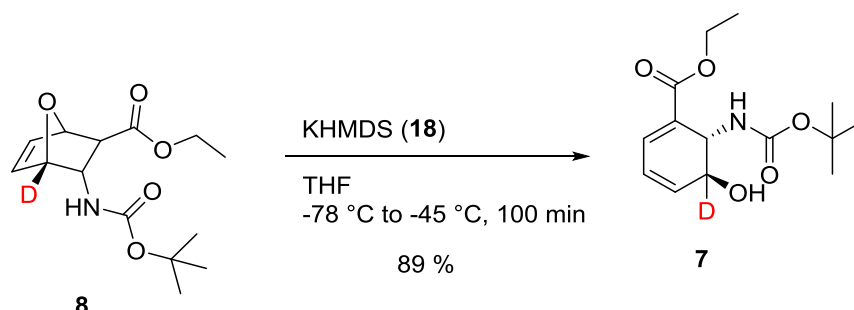
Scheme 16: Stereoselective KHMDS-mediated ring opening of bicyclic ester **8** to compound **7** under optimized conditions.

4.4.5.   Final Steps: Saponification and Deprotection to d-DHHA (5)

Compound **7** was saponified applying standard protocols with aqueous KOH in THF at room temperature.[172,175] Although rather basic conditions for this sensitive intermediate **7** in combination with a non-coordinating counter ion were used, the *trans*-configuration of the hydroxy group to the protected amine functionality avoided an E$_2$-elimination in the cyclohexadiene core structure and thus the facile formation of previously mentioned benzoic acid derivatives. Therefore, kinetically inert product **24** could be straightforwardly purified using established extraction protocols as well as flash column chromatography in satisfying isolated yields of 79 % (Scheme 17).
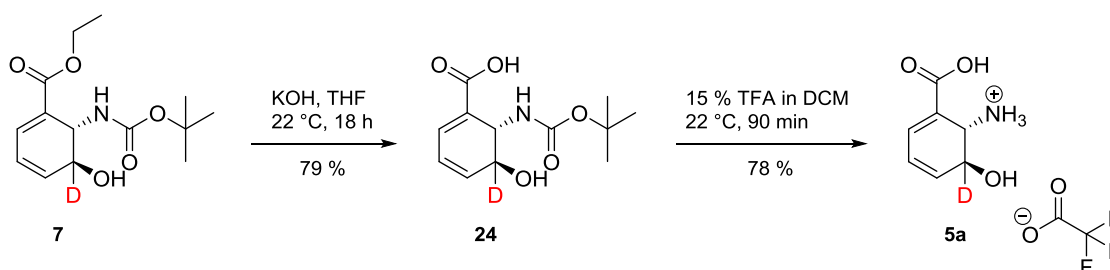
Scheme 17: Saponification of ester **7** followed by Boc-deprotection for the formation of d-DHHA in form of a TFA salt **5a**.

In the final reaction step, the Boc-protecting group was smoothly cleaved by stirring the brownish reaction mixture at room temperature under acidic conditions consisting of 15 % TFA in DCM (v/v).[172,175] Fortunately, the product precipitated from the reaction mixture as a brownish solid, which could be easily collected by filtration and was subsequently purified by trituration in DCM:MeCN = 2:1 (v/v) yielding optically pure d-DHHA in form of a TFA salt **5a** in 78 % yield (Scheme 17). Finally, d-DHHA (**5**) was fully analyzed by a combination of NMR experiments as well as HPLC-MS analyses after derivatization with MARFEY's reagent[215–217] to determine the optical purity of this final compound. Herein, both formed diastereomers **26a** and **26b** were separated on a reversed phase HPLC-MS system and the diastereomeric excess (*d.e.*) (correlated with the *e.e.* value of product **5**) was calculated by integration of the separated signals (Scheme 18, Figure 10).
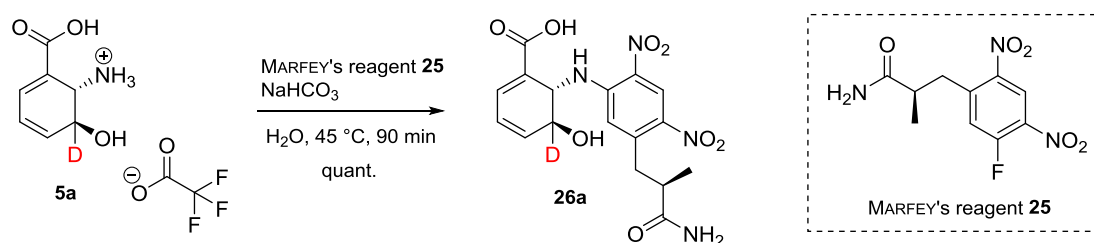
Scheme 18: Derivatization of d-DHHA (**5**) with MARFEY'S reagent[215–217] in order to determine the *e.e.* of mechanistic probe **5a** at the final stage.
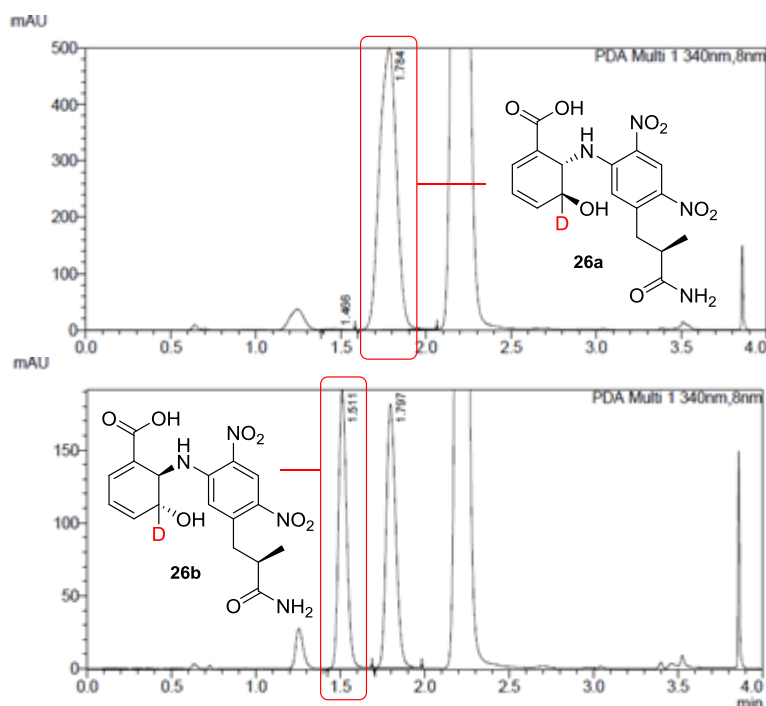
Figure 10: Reversed phase HPLC-MS chromatograms after derivatization of d-DHHA (**5**) with MARFEY's reagent **25** for the determination of the diastereomeric ratio (*d.e.*).

To conclude, enantiomerically pure d-DHHA (**5**) was produced in a 11 step synthesis (13 steps with reesterification and repeated kinetic resolution with PLE) for the longest linear sequence in an overall yield of ~2 %. Based on the published synthesis for genuine DHHA (**1**) by STEEL,[172–175] this labeling protocol fulfills several requirements for an "ideal synthesis" in terms of efficiency, practicability, scalability as well as step- and redox-economy.[159–164,167–171] Concerning the issue of overall purity, which includes the purity of this compound by itself (*e.e.* and deuterium content at the desired carbon atom (atom% D at carbon)), this value was determined to >96 % using a combination of established HPLC-MS and NMR techniques (Scheme 19).
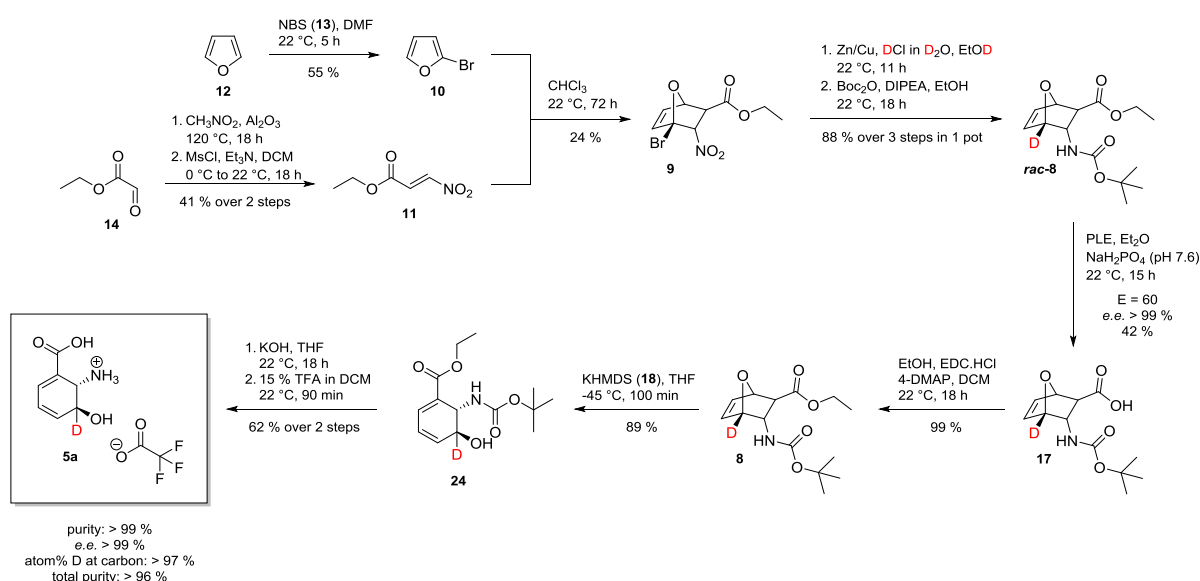
Scheme 19: Synthesis of d-DHHA in form of a TFA salt **5a** in analogy to the published synthesis of DHHA (**1**) by STEEL.[172–175]

4.5.   Synthesis of DHHA (1)

1° KIE measurements require the same quality of unlabeled and labeled starting materials for comparable results.[4,110] Although naturally occurring DHHA (**1**) can be produced in a biotechnological L-tyrosine-limited fed-batch process using *phzDE* expressed genes in *E. coli* cells on a kilogram scale,[41,218,219] it is not guaranteed that this engineered product features the same characteristics in terms of ionization state and minor impurities as synthetically prepared d-DHHA (**5**). As the available batch of biotechnological prepared DHHA (**1**) was grey colored instead of colorless, the chemical synthesis of DHHA (**1**) represented an indispensable goal in this thesis.

Again using the formerly published reaction sequence by STEEL[172–175] in combination with our improved approach for the preparation of d-DHHA (**5**), we could synthesize optically pure DHHA (**1**) in a total yield of ~4 % (Scheme 20). Omitting the chemoselective deuteration step within this sequence, the total synthesis of DHHA (**1**) was reduced to 10 reaction steps (12 steps with reesterification and repeated kinetic resolution with PLE). Starting with furan (**12**) and dienophile **11**, bicyclic ester **rac-15** could be isolated in a stereospecific DIELS-ALDER reaction yielding 51 % of this diastereomer as a chromatographically pure material. In analogy, the reduction of the nitro group together with *in situ* Boc-protection was achieved in the same pot, followed by the kinetic resolution with PLE, as described before. Noteworthy, an E > 180 was determined for the enantioselectivity in the enzymatic hydrolysis of bicyclic ester **rac-15** in the poorest case. However, different affinities (K_M values) for the labeled and unlabeled substrates were also determined by HILVERT,[57] but no information about this effect was further given. In addition it can be assumed that the heterogeneous PLE suspension is also a decisive parameter due to a mixture of several isoenzymes.[176,206–208] After reesterification,[211,212] the KHDMS-mediated ring opening and deprotection of both functional groups, synthetic DHHA (**1**) could be isolated in a total purity of >99 %.[172–175]
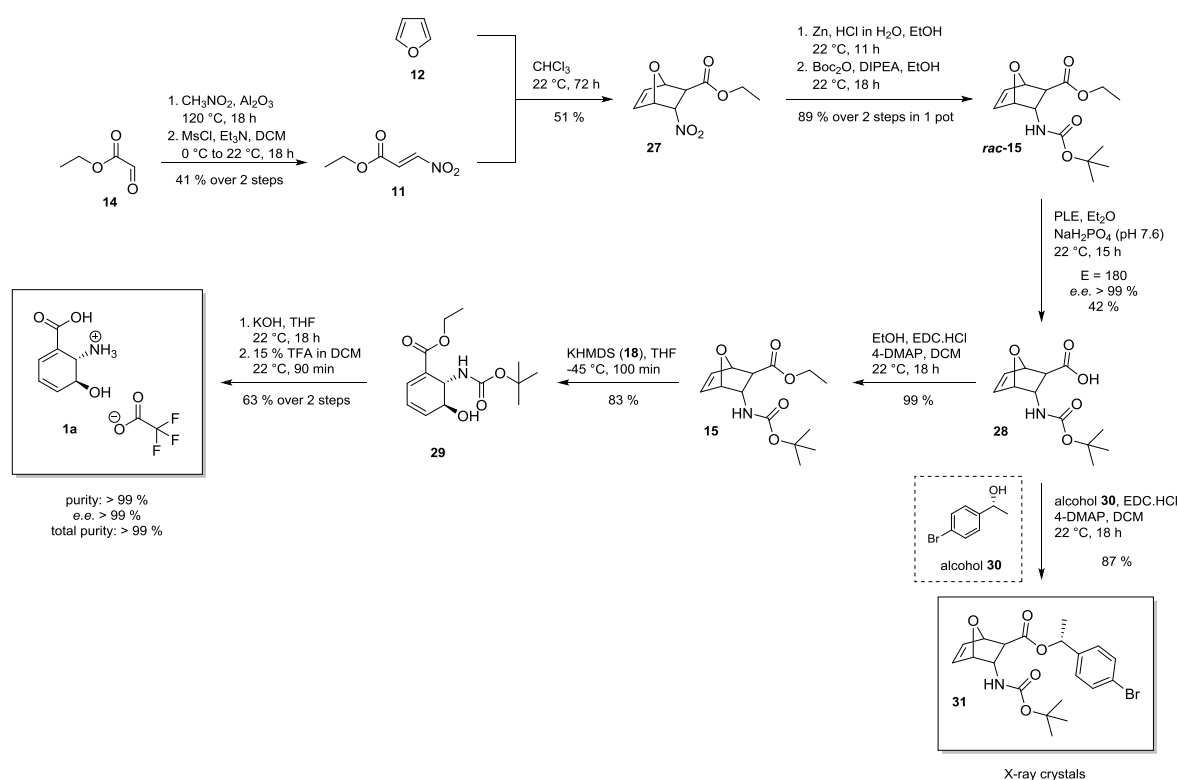
Scheme 20: Enantioselective synthesis of DHHA in form of a TFA salt **1a** in analogy to the published synthesis of STEEL.[172–175]

The optically pure bicyclic carboxylic acid **28** acted as precursor for the determination of the absolute configuration by single crystal X-ray crystallography (Scheme 20). Compound **28** was esterified with optically pure alcohol **30** to provide the following features: On the one hand, the inserted stereochemical information in alcohol **30** leads to an uncomplicated determination all other stereogenic centers in bicyclic ester **31**, on the other hand the bromide is necessary for the computation of the FLACK parameter in X-ray crystallography, a factor used to estimate the absolute configuration of a molecule.[220] After purification of bicyclic ester **31** via flash column chromatography, X-ray crystals were grown from MTBE as solvent. The structure was determined by Prof. Roland C. FISCHER from the Institute of Inorganic Chemistry at the TU Graz. The depicted ORTEP diagram confirmed that the desired enantiomer of bicyclic ester *rac*-**15** was saponified by PLE (Figure 11), which consequently required the higher effort in the purification process gaining optically pure ester **15** with *e.e.* > 99 %.[172,175,177]
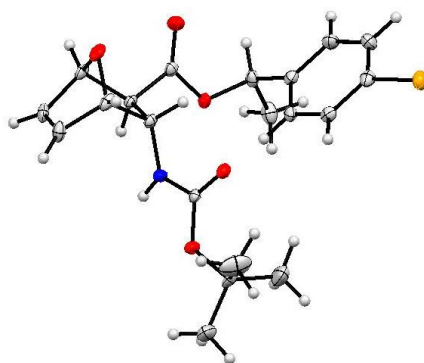
Figure 11: ORTEP diagram of bicyclic ester **31** for the determination of its absolute stereochemistry; Thermal ellipsoids are depicted at the 50 % probability level.

With these two compounds, namely DHHA (**1**) and d-DHHA (**5**), in hand, parallel experiments with PhzF have to demonstrate the migration behavior of the hydrogen and deuterium atom, respectively, and additionally should lead to the determination of a 1° KIE in NMR experiments as well as enzymatic assays.

4.6.   X-Ray Crystal Structure of WT PhzF

In a fruitful collaboration with the research group of Prof. Wulf BLANKENFELDT, we gained deeper insight as well as better understanding in the structure and reactivity of WT PhzF under the aid of important bioanalytical techniques, as X-ray crystallography and enzymatic assays. This tight cooperation was indispensable for an efficient and successful process in the investigation of the isomerization reaction catalyzed by PhzF. In the following section general aspects of PhzF, including crystal structure, characteristics of the enzyme/active site as well as mutation experiments, are discussed in detail, which provided ideas for the synthesis of mechanistic probes.

In general, WT PhzF consists of a homodimeric structure in an up/up configuration with two independent active sites facing each other. Structurally related to the lysine biosynthetic enzyme diaminopimelate epimerase DapF, gel filtration of WT PhzF assumed a calculated monomeric molecular mass of 32 kDa. The dimer in its "open" form interacts mainly through the α1-helices and the β16-strands in the *N*-terminal domains with a contact area of 1316 Å^2, which corresponds to 10.9 % of the monomer surface. Although the *C*-terminal domains are relatively close, there is no direct contact between them. Ligand binding studies with 3-hydroxyanthranilic acid (**32**) as a formally competitive inhibitor allowed the localization of the active site as well as the orientation of the inhibitor within this cavity, which can be adapted to DHHA (**1**) as natural substrate. However, in this "closed" conformation, the secluded surface area is increased to 12.2 % caused by newly established direct and H$_2$O mediated hydrogen bonds as well as hydrophobic contacts between residues in the α5-helices of the *C*-terminal domains (Figure 12).[34,47,48]
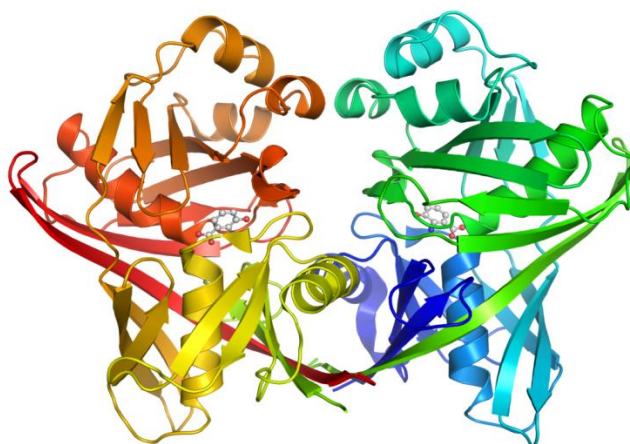
Figure 12: X-ray crystal structure of the "closed" configuration of WT PhzF with 3-hydroxyanthranilic acid (**32**) to the active site as competitive inhibitor; Homodimer with two independent active sites.[34,48]

41

At the junction of both domains, a narrow cleft with the dimensions of approximately 14 Å deep, 8 Å in length and just under 4 Å wide leads directly to the active site of WT PhzF.[47] This catalytically active region is mainly surrounded by four amino acids: Serine S213, aspartate D208, histidine H74 and glutamate E45. In contrast D208, H74 and E45 are entirely conserved among PhzF and related members of this enzyme family. These amino acids are substituted in DapF indicating a possible functional divergence between these two proteins. For DapF, which catalyzes the epimerization of L,L-diaminopimelate, an acid-base catalyzed mechanism has been attributed to two conserved cysteines, but none of them is present in PhzF.[34,44,47,221]

Soaking of co-crystals of WT PhzF and inhibitor **32** with DHHA (**1**) resulted in the formal substitution between both ligands. Although an acceptable resolution limit of 1.88 Å was achieved via X-ray crystallography, a small possibility remains in a retro-perspective view that DHHA (**1**) is quantitatively bound to the active site due to almost identical electronic properties between inhibitor **32** and the natural substrate (Figure 13).[34]
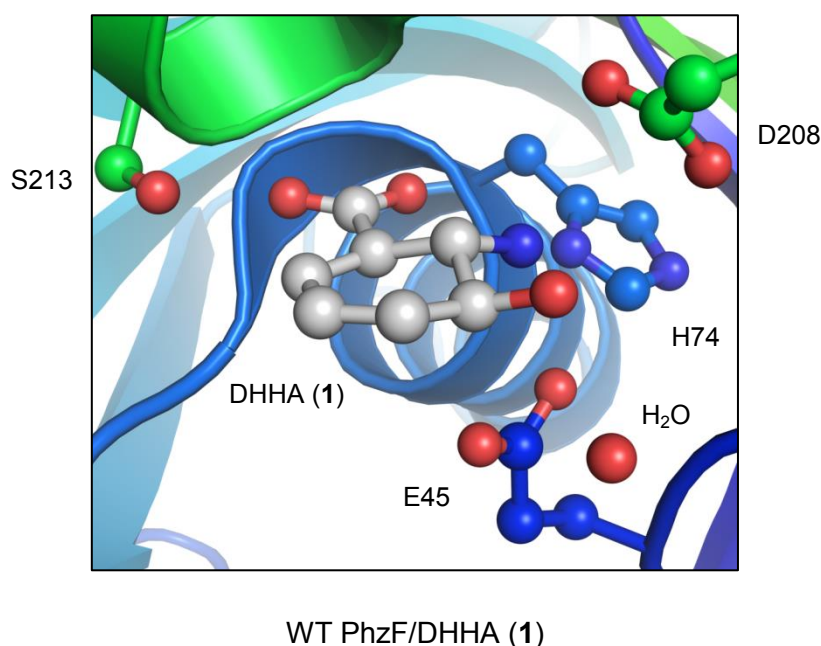
WT PhzF/DHHA (**1**)

Figure 13: X-ray crystal structure of WT PhzF; 3-Hydroxyanthranilic acid (**32**) replaced by DHHA (**1**), the natural substrate of PhzF.

Nevertheless, Figure 13 depicts the active site of WT PhzF with its natural ligand, DHHA (**1**). Interestingly, glutamate E45 is directly located beneath the carbon atom in a pretty linear fashion, at which the migrating hydrogen atom is bound and is additionally able to interact with the amino group of the ligand. In the "open" form, E45 is solvent accessible, but

42

becomes secluded in the "closed", ligand-bound conformation. However, most striking about this fact is the distance between the carbon atom of DHHA (**1**) and the oxygen atom of the linear orientated glutamate E45. It is with only 2.7 Å noticeably shortened.[34] Do these findings indicate a facile proton abstraction in an acid-base catalyzed mechanism by distinctive hydrogen bond interactions and excellent orientation of the substrate? Is VAT involved in the hydrogen transfer reaction? We hypothesize that the pK_a value of this desired proton will play a key role in the investigation of the PhzF catalyzed reaction mechanism.

4.7. pK_a Estimation of the ε-Proton in DHHA (1) and Insights into the Acid-Base Catalyzed Racemization of Mandelic Acid (33) by WT MR

Estimations of the pK_a value for the desired proton in DHHA (**1**) could be achieved by a comparison with wildtype mandelate racemase (WT MR), a highly efficient enzyme for the fast racemization of mandelic acid (**33**) in bacteria. KRESGE successfully measured the pK_a value of the α-proton in mandelic acid to pK_a = 22 (protonated form).[222,223] The rather high difference between the pK_a of the substrate (α-proton of mandelic acid (**33**)) to the active site base catalyst, an arrangement of lysine and histidine with an estimated pK_a = 6, is definitely too large to explain the measured k_{cat} = 500 s^{-1} for WT MR. The pK_a difference is even larger, when the mandelate anion is taken into account with an estimated pK_a = 29 (deprotonated form).[223,224] GERLT and GASSMANN proposed, how WT MR resolves this issue of unreactiveness. The high reaction rates in the considered proton transfer can be understood by electrophilic active site catalysis, in which a general acid, here glutamate E317, is properly positioned for the proton transfer. In this concerted general acid-general base catalyzed transformation of a stabilized enolic intermediate, k_{cat} can be maximized, if the pK_a of the acid catalyst and the enol tautomer of the substrate are matched. This matching allows significant stabilization of the enol relative to the more weakly basic keto tautomer of the substrate by the formation of a short, strong hydrogen bond in the solvent excluded environment of the active site (Scheme 21).[222–224,225,226–229]

For a bound mandelate anion to the active site of WT MR, strong interactions of one carboxylate oxygen with essential Mg^{2+} as well as with the ammonium functionality of lysine K164 insinuate a reduction of the considered pK_a from pK_a = 29 to pK_a = 22 resembling mandelic acid (**33**) electronically.[226,228,229] In the limiting case of a complete protonation of the carboxylic group in mandelic acid (**33**) by E317 to its cationic form, the pK_a will get reduced by additional 15 units to pK_a = 7.[224] If the pK_a of E317 matches exactly the value of

the enol, then the abstracted proton can be equally shared between E317 and mandelic acid (**33**) assuming a $pK_a = 15$ for the considered α-proton.[223,227–229]

Structural studies on WT MR suggested that E317 is protonated when mandelic acid (**33**) binds in its anionic form to the active site. However, the pK_a of the enol tautomer of mandelic acid (**33**) was determined to $pK_a = 6.6$ by CHIANG in 1990.[222] Expecting the pK_a of E317 in the same range ($pK_a \approx 6$), both, the components as well as the geometry of the active site are appropriate for maximizing k_{cat} in the racemization of mandelic acid (**33**) by WT MR via a general acid-general base catalyzed mechanism.[223,228,229]
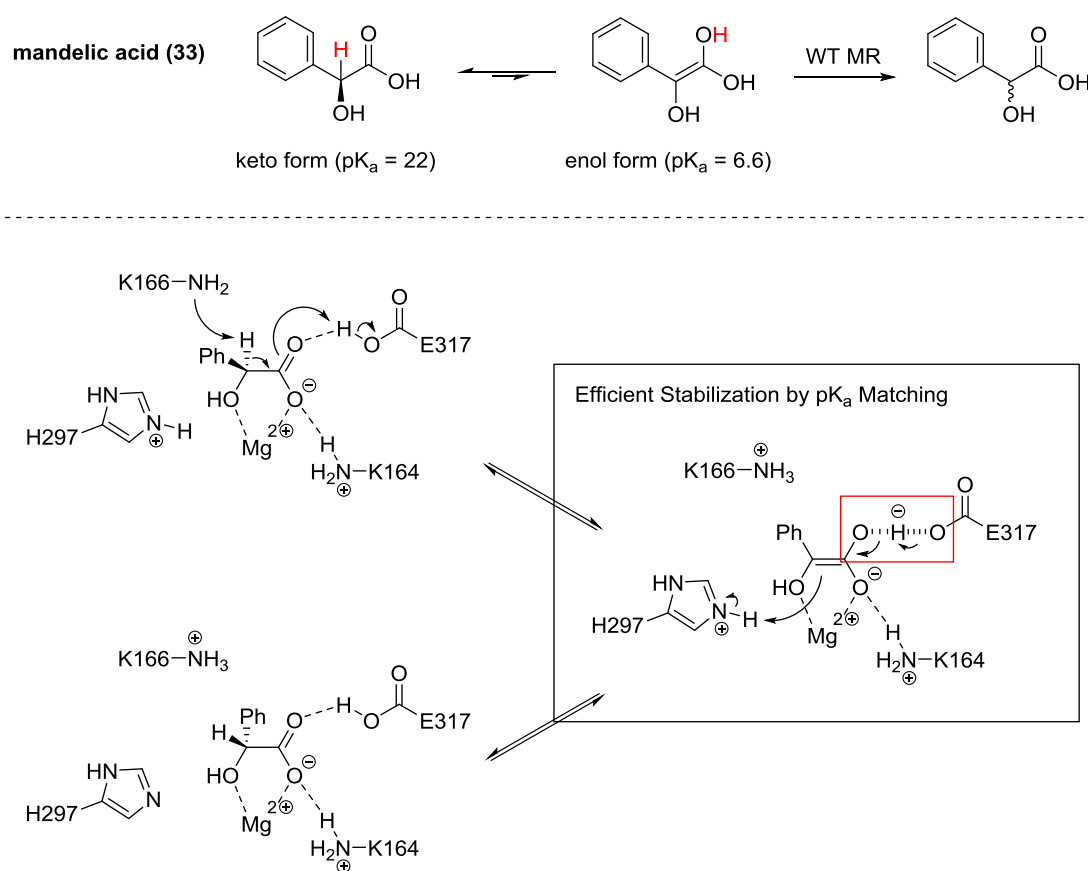
Scheme 21: Racemization reaction of mandelic acid (**33**) catalyzed by wildtype mandelate racemase (WT MR); Proposed mechanism for WT MR via a concerted general acid-general base formation; Enolic intermediate stabilized by a short, strong hydrogen bond with E317; Negative charge dispersed in the hydrogen bond and not localized on the heteroatom or the bridging proton.[223,228,229]

In comparison to the related model system of the α-proton in mandelic acid (**33**), we hypothesize that the pK_a of the migrating ε-proton in neutral DHHA (**1**) has a comparable, but even slightly higher pK_a value. Caused by the elongated vinylogous system in DHHA (**1**) and the absence of the polarizing hydroxy group in mandelic acid (**33**), a pK_a in the range of pK_a

= 24-30 is estimated for DHHA (**1**). As this is at the upper limit, which enzymes can handle under acid-base catalyzed conditions, WT PhzF needs to overcome this big difference in pK_as to deliver reasonable reaction rates in a potential protic mechanism.[223,228,229]

The side chain of aspartate D208 is part of an extended hydrogen bonding network, which includes asparagine N18, serine S44, alanine A210, threonine T211 as well as the amino group of DHHA (**1**). Since it is suggested that D208 is not directly involved in the chemical conversion of DHHA (**1**), its function possibly resides in positioning a negative charge in the vicinity of the amino moiety. This fact may ensure that DHHA (**1**) stays protonated during the isomerization, thereby decreasing the pK_a of the migrating proton by charge neutralization in an advantaged deprotonation step. A positively charged histidine H74 would furthermore assist the protonation of DHHA (**1**) in the active site. Unfortunately, it was by the time not possible to classify the orientation of H74 in WT PhzF due to insufficient resolution of single X-ray crystals, which is crucial for differentiation between similar electron densities of carbon and nitrogen atoms.[34]

In strong contrast to WT MR, the less basic glutamate E45 in WT PhzF compared to lysine K166 in WT MR would be responsible for the deprotonation of DHHA (**1**). Additionally, missing of strongly coordinating and hence stabilizing metal ions, e.g. Mg^{2+}, Zn^{2+}, in the active site of WT PhzF, the concerted general acid-general base mechanism, described by GERLT and GASSMANN in 1993,[228,229] is rather implausible for the isomerization of DHHA (**1**) by WT PhzF. Although serine S213 may adopt the role of glutamate E317 in WT MR, perfect pK_a matching of all participating active site residues in WT PhzF is definitely not given, as it is the case in the racemization of mandelic acid (**33**) by WT MR.[34,223,228,229]

4.8.   Mutation Experiments on PhzF Exploring the Importance of Active Site Residues

Mutation experiments on WT PhzF should provide evidence, which active site mutant maintained catalytic active concerning the isomerization of DHHA (**1**). Performed in the research group of Prof. Wulf BLANKENFELDT, remarkably, only one tested out of eight enzyme variants was able to convert DHHA (**1**) with moderate turnover efficiencies compared to WT PhzF. Herein, histidine H74 was mutated to the smaller and apolar amino acid alanine, further named as H74A. Although the enzyme activity was reduced by a factor of 4, the dissociation constant K_d for 3-hydroxyanthranilic acid (**32**) was surprisingly increased by 20-fold (K_d(WT PhzF) = 1.4 µM, K_d(H74A) = 69 nM).[34]

The crystal structure of H74A demonstrated that certainly more H_2O molecules fit into the active site, which occupy the space of the former histidine residue. Suggesting that the function of H74 lies in providing hydrogen bonds, these stabilizing interactions can be emulated to some extent by H_2O, although the basicity of the imidazole moiety was lost.[34] H74A could possibly play a key role for supporting a protic mechanism: The more H_2O molecules are located in the active site, the higher the possibility for the observation of a proton-deuteron exchange in an acid-base catalyzed mechanism.

Nevertheless, the crystal structures of WT PhzF in conjunction with H74A revealed other two interesting features of the active site. Two adjacent α-helices surround the catalytic active centers, respectively, and both positively polarized ends of the helical dipolar moments are pointing straight into the direction of the substrate. This observation led to the assumption that DHHA (**1**) possibly binds in its anionic form, which is in strong contradiction to the hypothesis for lowering the pK_a of the ε-proton in an acid-base catalyzed mechanism. However, the anionic ionization state of DHHA (**1**) would support the postulate for decreasing the activation energy in a pericyclic reaction due to better stabilization of the TS by mainly hydrogen bond interactions within the substrate (see quantum-mechanical section). Furthermore, the co-crystallized sulfate (SO_4^{2-}) in WT PhzF as well as H74A indicates the favored binding of an anionic species within this cavity (Figure 14).[47]

WT PhzF/SO_4^{2-} H74A/SO_4^{2-}
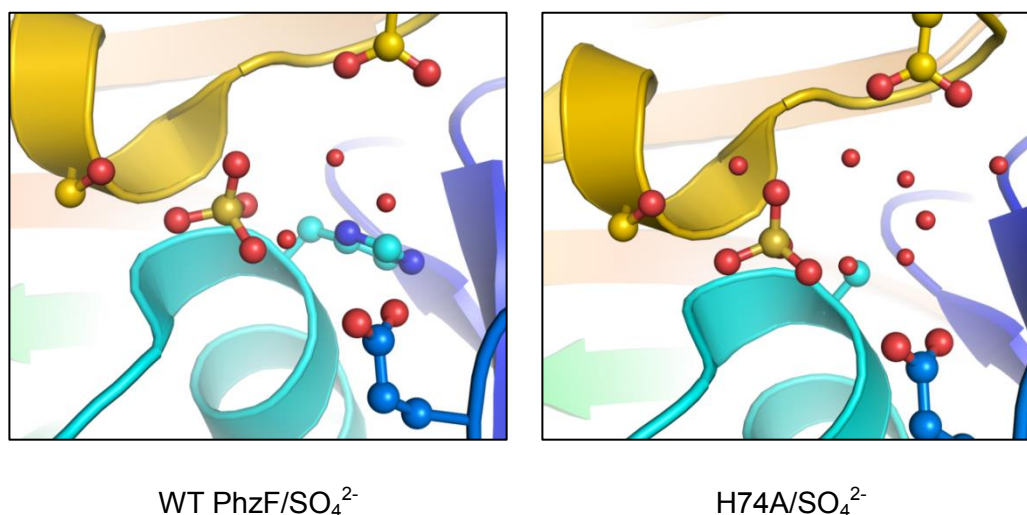
Figure 14: X-ray crystal structures of: Left: WT PhzF; Right: H74A mutant; Sulfate (SO_4^{2-}) bound to WT PhzF without co-crystallization of an inhibitor.

Glutamate E45 seemed indispensable for the efficient isomerization of DHHA (**1**). Each mutation on E45 led to the complete loss of enzyme activity, even in the mutants E45Q and

E45D. Herein, glutamate E45 is substituted by the in terms of bond length or polarity correlated amino acids glutamine and aspartate. However, fluorescence spectroscopy suggested that the affinity towards 3-hydroxyanthranilic acid (**32**) is again not altered significantly, although the alanine mutant E45A featured once more the lowest dissociation constant (K_d(WT PhzF) = 1.4 µM, K_d(E45D) = 4.0 µM, K_d(E45A) = 110 nM). It is believed that E45 is deprotonated, when DHHA (**1**) enters the active site in WT PhzF.[34] In parallel, replacement of E317 in WT MR to E317Q likewise prevented a sufficient hydrogen transfer in the racemization of mandelic acid (**33**) by at least a 4500-fold supposing that the geometry of the active site was not disrupted by this substitution. Consequently, glutamine Q317 behaves too little acidic in the conversion of mandelic acid (**33**) compared to glutamic acid in WT MR,[223] however, Q45 too little basic for the isomerization of DHHA (**11**) in a possible protic mechanism compared to glutamate E45 in WT PhzF.[34]

4.9. Synthesis of H₂-DHHA (34) and Co-Crystallization Experiments with WT PhzF

Although a putative crystal structure of DHHA (**1**) with WT PhzF might exist as discussed before,[34] we decided to synthesize H₂-DHHA (**34**) in order to enhance our understanding about the exact positioning of DHHA (**1**) in the active site of WT PhzF. Serving additionally as a potential competitive inhibitor, compound **34** would lead to an estimation of conformational changes during the binding of DHHA (**1**) by interpolating distances as well as angles in crystal structures with co-crystallized 3-hydroxyanthranilic acid (**32**) and H₂-DHHA (**34**) (Figure 15).

Applying the formerly published reaction sequence for the preparation of DHHA (**1**) by STEEL[172–175] together with our improved protocol to the synthesis of H₂-DHHA (**34**), we were able to isolate compound **34** in excellent purities likewise in form of a TFA salt **34a** (overall yield over 11 steps (13 steps with reesterification and repeated kinetic resolution with PLE): ~3 %). After a stereospecific DIELS-ALDER reaction between furan (**12**) and dienophile **11**, catalytic amounts of PdCl₂ (5 mol% PdCl₂)[175] were added to the reaction mixture with Zn and HCl leading to a reduction of the nitro moiety together with hydrogenation of the olefin in the bicyclic ring system. *In situ* Boc-protection of the free amine resulted in the formation of bicyclic ester ***rac*-35** in a three-step one-pot synthesis in 81 % isolated yield and a repeated kinetic resolution on this compound with PLE achieved ester **35** with an *e.e.* > 99 %.[172–175] Surprisingly, the KHMDS-mediated ring opening mainly led to the generation of two constitutional isomers **37** and **38** approximately in the same ratio.[172–175,179] We hypothesize that originally formed isomer **37** was converted to the thermodynamically more stable

47

compound **38** under proceeding reaction times by the abstraction of the γ-proton in compound **37** and subsequent isomerization. Although the absolute configuration of the freshly formed stereocenter in isomer **38** was not determined, it can be assumed that an all *trans*-configuration is existent within that molecule. This preferential arrangement of substituents must hereby lead to a decrease of repulsion energy compared to isomer **37** forming an enhanced amount of compound **38** over the time. Nevertheless, both isomers **37** and **38** could be converted to the same product in the saponification reaction with KOH and, finally, after deprotection of the Boc-protecting group, H_2-DHHA (**34**) was purified by trituration in DCM:MeCN = 2:1 (v/v) yielding 60 % of product **34a** over these two steps (Scheme 22).[172–175]

crystal structure for an enhanced understanding of the binding site

3-hydroxyanthranilic acid (**32**)   DHHA (**1**) H_2-DHHA (**34**)
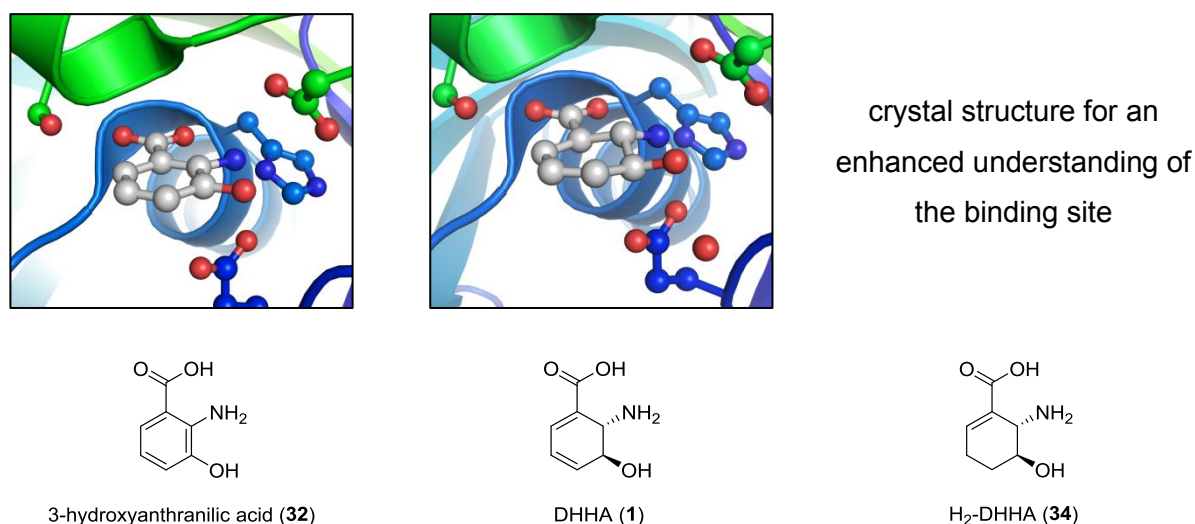
Figure 15: Co-crystallization experiments for an enhanced understanding about positioning and binding of DHHA (**1**) in WT PhzF.[34]

With enantiomerically pure H_2-DHHA (**34**) in hands, Christina DIEDERICH (research group of Prof. Wulf BLANKENFELDT) performed co-crystallization as well as soaking experiments over several days with suitable crystals of WT PhzF and 3-hydroxyanthranilic acid (**32**). Pursuing our goal for a better understanding in the binding mode of WT PhzF, however, her efforts did not succeed in the formation of a crystalline enzyme-inhibitor adduct in any case. This unexpected observation can primarily be explained by the fact that the cyclohexene core structure of H_2-DHHA (**34**) is not entirely planar anymore. Maybe either structural afflicted clashes through the narrow cleft of just 4 Å[47] prohibit inhibitor **34** in entering the active site or unfavorable conformational arrangements of the three substituents in H_2-DHHA (**34**) the formation of stabilizing hydrogen bond interactions to active site residues.
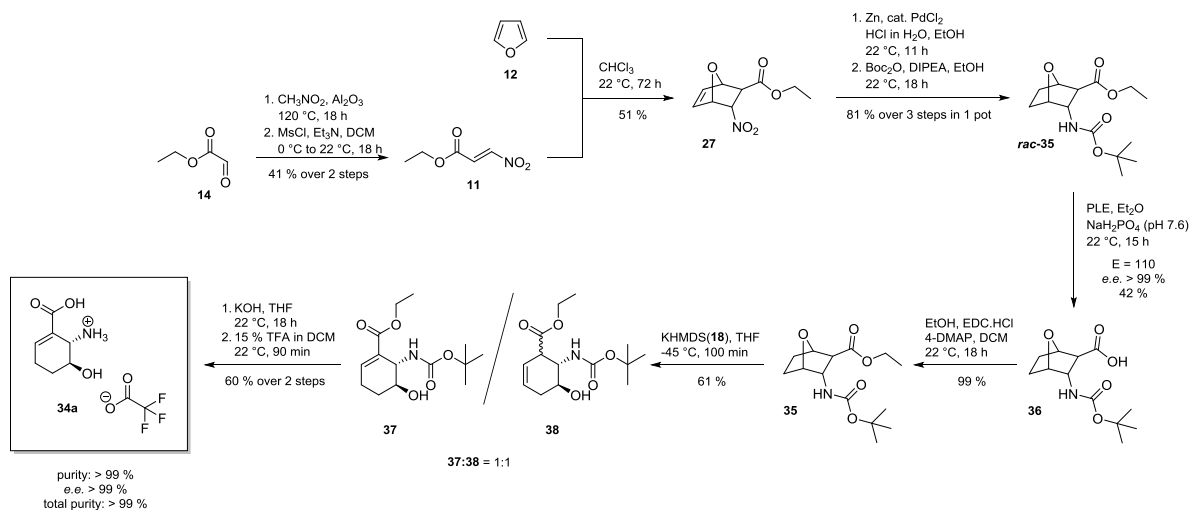
Scheme 22: Synthesis of H$_2$-DHHA in form of a TFA salt **34a** in analogy to DHHA (**1**) published by STEEL.[172–175]

Table 4: Calculated molecular volumes (mol. vol.) as well as dihedral angles (dih. angle) of 3-hydroxyanthranilic acid (**32**), DHHA (**1**) and H$_2$-DHHA (**34**) in its anionic forms at the mPW1PW91/6-31+G* level of theory[77–79,150] for the energetically most stable conformers.

Entry	Species		Mol. vol. / Å^3	Dih. angle / °	
				HO-C-C-NH$_2$	H$_2$N-C-C-COO$^-$
1		**32**	200	0.0	1.7
2		**1**	202	56.8	34.5
3		**34**	231	58.5	43.1

This assumption was tested by quantum-mechanical computations of the molecular volume at the mPW1PW91/6-31+G* level of theory.[77–79,150] Caused by the persistent neutral conditions of pH 7.6 in all buffer solutions, only the anionic and energetically most stable conformers of 3-hydroxyanthranilic acid (**32**), DHHA (**1**) and H$_2$-DHHA (**34**), respectively, were considered. Based on the contours of constant electron density around these molecules,[230] compounds **32** and **1** feature almost identical molecular volumes (200 Å^3 *vs.* 202 Å^3). In contrast, for the calculated molecular volume of the anionic form of H$_2$-DHHA (**34**)

49

a value of 231 $Å^3$ was determined indicating a ~15 % higher space requirement for this derivative compared to anions **1** and **32** (Table 4). Although the dihedral angles of all substituents attached to the ring moiety in compound **1** and **34** are in approximately the similar range (56.8° *vs.* 58.5° and 34.5° *vs.* 43.1°), which are crucial for stabilizing hydrogen bond interactions to active site residues, the ring conformation and consequently the molecular volume of the ring itself highly influences the binding of DHHA (**1**) to PhzF. According to these calculations, it is most likely that H_2-DHHA (**34**) does not fit into the active site only by its size, or even through the active site channel.

4.10. Results of ^{1}H-NMR Experiments for the Migration of Hydrogen/Deuterium in DHHA (1)/d-DHHA (5)

^{1}H-NMR experiments with DHHA (**1**) in D_2O, previously described by BLANKENFELDT,[34] were repeated in order to illustrate the quantitative migration of the hydrogen in the isomerization process with WT PhzF. Additionally, the identical transformation was explored with d-DHHA (**5**) in H_2O within cross experiments. All enzymatic transformations were performed either with WT PhzF or with H74A to provide evidence for the preliminary found results (Figure 16).[34] In the case that an exchange of the migrating hydrogen/deuterium with deuterons/protons of the surrounding solvent would be found in any single experiment, this result would be definitely the strong evidence for an acid-base catalyzed mechanism.

In general, all reactions were carried out in standard NMR tubes at a temperature of 15 °C in a 500 MHz NMR spectrometer, which was sufficient for a satisfying separation of the signals in the ^{1}H-NMR spectra. The progress was pursued via time-resolved NMR analysis. Every reaction was executed in 100 mM NaH_2PO_4/Na_2HPO_4 buffer solution either in H_2O or D_2O at pH 7.6. DHHA (**1**) in combination with WT PhzF was converted in the fastest reaction highlighting the optimized environment for the conversion of DHHA (**1**) in nature.[34]

Remarkably, but not unexpectedly, a quantitative migration of the hydrogen in DHHA (**1**) as well as deuterium in d-DHHA (**5**) was observed in every single experiment with WT PhzF and H74A retaining the high possibility of an [1,5]-prototropic rearrangement catalyzed by an enzyme. This conservation is indicated in the case of DHHA (**1**) by two doublet signals of neighboring protons in the appropriate product as well as by only one singlet signal in d-DHHA (**5**) due to the absence of a hydrogen atom as coupling partner (Figure 16, Figure 17 and Figure 18).

Isomerization of DHHA (1) catalyzed by WT PhzF or H74A:
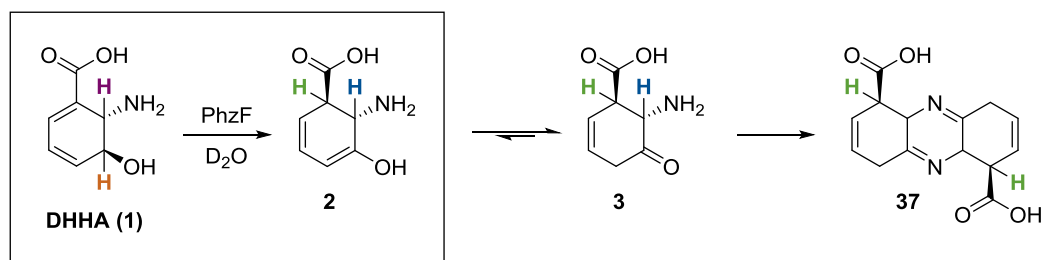
Isomerization of d-DHHA (5) catalyzed by WT PhzF or H74A:
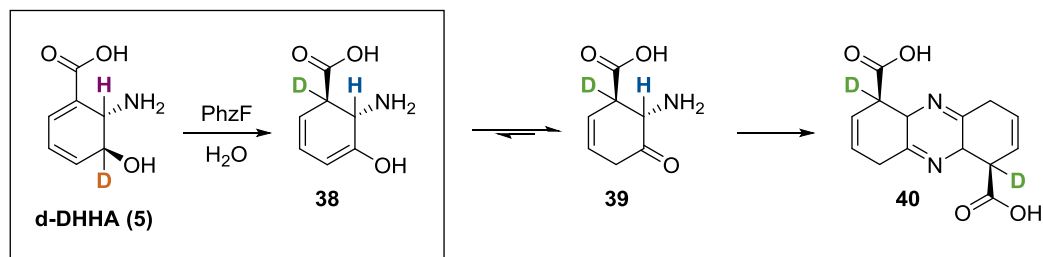
Figure 16: ^{1}H-NMR experiments for the isomerization of DHHA (**1**) or d-DHHA (**5**) catalyzed by WT PhzF or H74A, respectively.
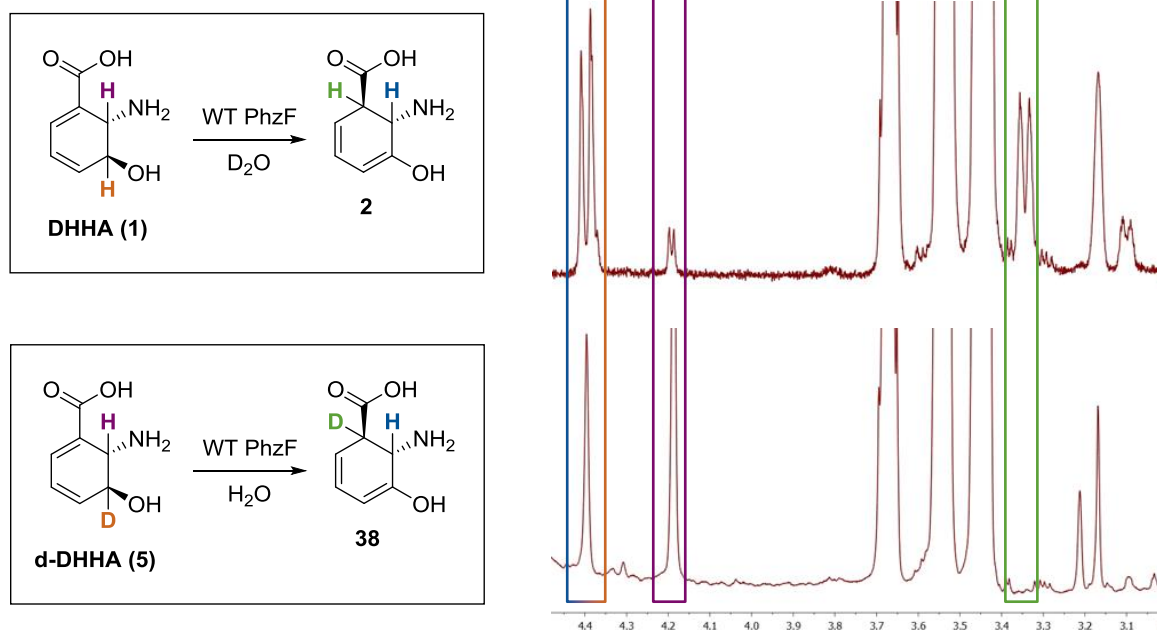
Figure 17: ^{1}H-NMR experiments for the isomerization of DHHA (**1**) and d-DHHA (**5**) catalyzed by WT PhzF indicating the quantitative migration of the hydrogen/proton and deuterium/deuteron, respectively.
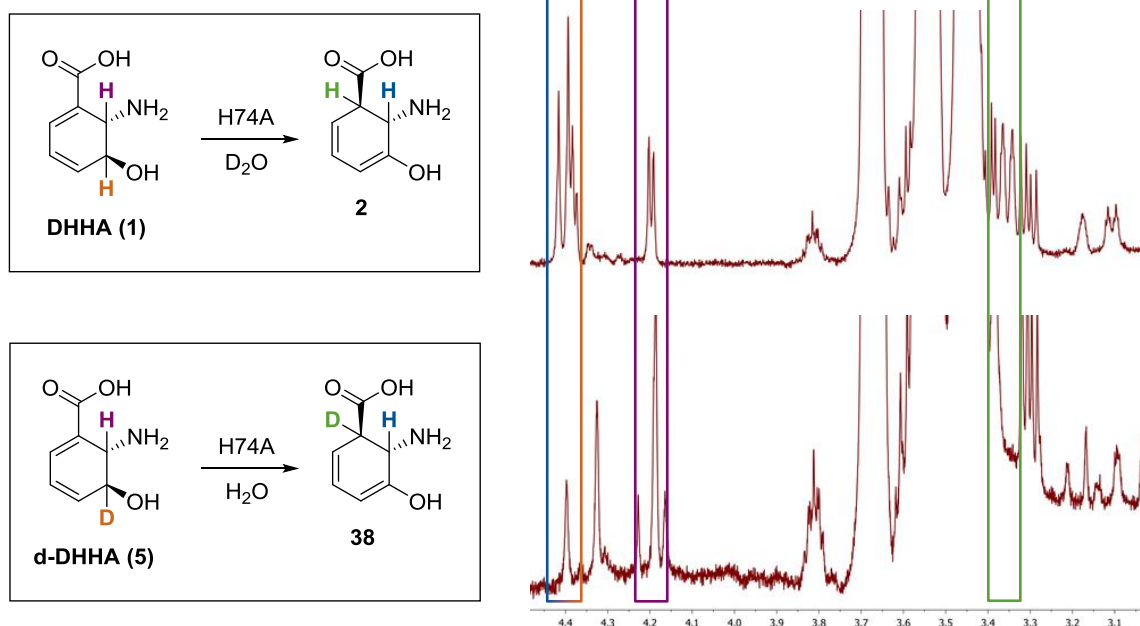
Figure 18: ^{1}H-NMR experiments for the isomerization of DHHA (**1**) and d-DHHA (**5**) catalyzed by H74A indicating the quantitative migration of the hydrogen/proton and deuterium/deuteron, respectively.

The high reactivity of the *in situ* formed intermediate **3/39** guarantees spontaneous self-condensation to the tricyclic ring system *in vitro*, however, this condensation is in bateria supplementary catalyzed by PhzB. It acts as an efficient acid-base catalyst and significantly increases the reaction rate even at low substrate concentrations, which are expected in bacterial cells.[13,34,35] Although the main product of this isomerization was not isolated from these reaction mixtures yet, it is pretty much likely that the monomeric form **3/39** and not the dimeric tricyclic ring structure **37/40** was primarily observed during these NMR experiments (δ = 5.81-5.76 ppm). Gradually arising and high field shifted signals in relation to monomer **3/39** (δ = 5.69-5.59 ppm) indicated self-condensation to the tricyclic ring system. Moreover, spontaneous oxidation as well as tautomerization, which manifested in the deep color change, provoked the formation of additional impurities indicating the high sensitivity of these compounds towards the surrounding environment (Figure 19). All attempts, which should lead to the suppression of side product formation, e.g. utilizing degassed solvents and operating under argon atmosphere, did not succeed.[34] This rather high instability of product intermediates turned out to be a matter of high importance affecting further analytical techniques for the investigation of this isomerization reaction. These will be discussed in the following chapters.
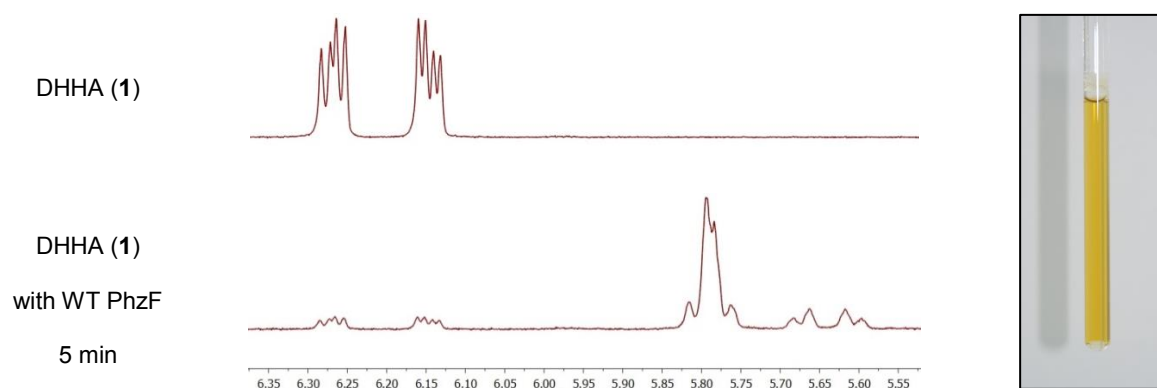
Figure 19: Fast side product formation in the isomerization of DHHA (**1**) with WT PhzF after 5 min reaction time indicated by the color change in the NMR tube.

Although several H_2O molecules are located in the active site of H74A (see chapter of mutation experiments), the migrating hydrogen or deuterium could by chance also be conserved in the case of an acid-base catalyzed mechanism. This proclamation is true, when reprotonation occurs with the same proton or deuteron abstracted previously by glutamate E45. However, all observations on the one hand demonstrate that nature developed an efficient isomerization process with certainly a high degree of hydrogen conservation, on the other hand do at this stage not allow an exclusion of one reaction mechanism from the other postulated.

By comparing initial reaction rates for the conversion of DHHA (**1**) and d-DHHA (**5**) with WT PhzF and H74A, respectively, a rough estimation with insufficient validity about the 1° KIE was made. Since it was so far not proven that those NMR experiments were performed under substrate saturation at least at starting conditions, a predicted 1° KIE = 7-12 from NMR data has to be handled with extreme care. Enzymatic assays must provide enzyme characteristic parameters for the isomerization of DHHA (**1**) as well as d-DHHA (**5**) and should give rise for the determination of reliable 1° KIEs.

4.11. Enzymatic Assays for the Determination of Enzyme Parameters and 1° KIEs

Christina DIEDERICH, our collaboration partner in the research group of Prof. Wulf BLANKENFELDT, put a lot of efforts into the realization of reliable enzymatic assays. As mentioned before, the significant amount of side product formation, resulting from the spontaneous condensation and subsequent oxidation of ketamine **3**,[13,34,35] showed tremendous impact on the results of these kinetic studies. Herein, similar absorption maxima

of diverse side products compared to DHHA (**1**) and ketamine **3** prohibit a quantitative analysis of individual compounds in solution. Even though only starting material and desired product show comparable absorption curves, an accurate determination of substrate concentrations is often difficult, sometimes impossible.

Due to the high instability of ketamine **3**,[34] we decided to monitor the consumption of the starting material, either DHHA (**1**) or d-DHHA (**5**), by photometric analysis. Fortunately, the main chromophore in these compounds, the double-conjugated olefinic π-system to the carboxylic moiety (douple MICHEAL acceptor), is lost during the isomerization, whereby the absorption maxima λ_{max}(DHHA (**1**), d-DHHA (**5**)) = 275 nm are shifted to smaller wavelengths. In general, the increase of product should be preferentially measured in enzymatic assays. However, the indirect determination of product formation, which is in these experiments identical to substrate depletion, normally allows the assignment of important enzymatic parameters, like v_{max}, K_M and k_{cat}. They are crucial for the exact determination of 1° KIEs in enzymatic transformations.

In the present case, product formation did not disturb the photometrical measurement of substrate consumption at λ = 275 nm due to sufficiently different absorption maxima, but side products, which absorb in this important range similar to the starting material **1**, did not allow quantitative analysis. Again, as mentioned in the chapter before, all attempts, which should lead to the minimization of side product formation regrettably failed.[34] High error bars indicate this impreciseness in every single data point, which led to inaccurate estimations of 1° KIEs in both enzymes.

Basically, two different 1° KIEs can be calculated for enzymatic transformations. The first value (1° KIE (k_{cat})) compares catalytic turnover numbers k_{cat} in reactions between the unlabeled and the labeled substrate, whereas the second value (1° KIE (k_{cat}/K_M)) encompasses also diffusion and binding differences of both substrates to the enzyme (Formula 1).[4] Based on MICHAELIS-MENTEN kinetics[231–234] for the considered isomerization of DHHA (**1**) and d-DHHA (**5**), respectively, data points were collected in experiments with three repetitions and enzymatic parameters as well as 1° KIEs calculated from reactions with WT PhzF in different buffer systems (Figure 20).

$$1° \text{ KIE } (k_{cat}) = \frac{k_{cat,H}}{k_{cat,D}} \qquad (1) \qquad\qquad 1° \text{ KIE } (k_{cat}/K_M) = \frac{\dfrac{k_{cat,H}}{K_{M,H}}}{\dfrac{k_{cat,D}}{K_{M,D}}} \qquad (2)$$

Formula 1: Formulas for the calculation of 1° KIEs: 1° KIE(k_{cat}) and 1° KIE(k_{cat}/K_M).
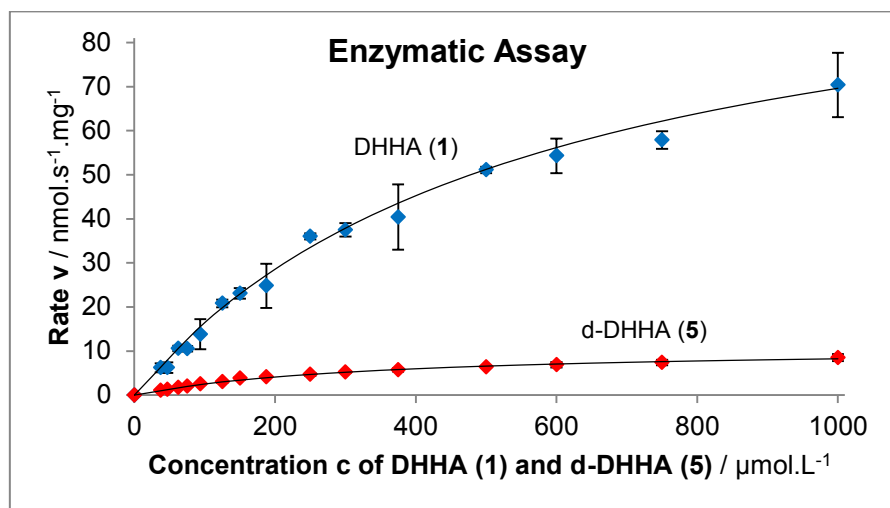
Figure 20: Enzymatic assay for WT PhzF catalyzed isomerization of DHHA (**1**) and d-DHHA (**5**), respectively, demonstrating challenges in collecting trustworthy enzymatic parameters; Conditions: 50 mM NaH$_2$PO$_4$/Na$_2$HPO$_4$ in H$_2$O, pH 7.5, 25 °C; Data measured by Christina DIEDERICH.

Table 5: Enzymatic parameters as well as 1° KIEs in the isomerization of DHHA (**1**) and d-DHHA (**5**) by WT PhzF; Buffer: H$_2$PO$_4^-$/HPO$_4^{2-}$: 50 mM NaH$_2$PO$_4$/Na$_2$HPO$_4$ in H$_2$O at pH 7.5; D$_2$PO$_4^-$/DPO$_4^{2-}$: 50 mM NaH$_2$PO$_4$/Na$_2$HPO$_4$ in D$_2$O:H$_2$O = 9:1 (v/v) at pD 7.5; TRIS: 20 mM TRIS/HCl in H$_2$O at pH 7.5, 150 mM NaCl and 10 % (v/v) glycerol added; TRIS w/o: 50 mM TRIS/HCl in H$_2$O at pH 7.5; 25 °C; Data measured by Christina DIEDERICH.

Entry	Buffer	Substrate	k_{cat} / s^{-1}	K_M / μM	1° KIE (k_{cat})	1° KIE (k_{cat}/K_M)
1	H$_2$PO$_4^-$/HPO$_4^{2-}$	DHHA (**1**)	3.50 ± 0.27	561 ± 68	9.9 ± 0.8	5.9 ± 0.9
2		d-DHHA (**5**)	0.36 ± 0.01	338 ± 17		
3	D$_2$PO$_4^-$/DPO$_4^{2-}$	DHHA (**1**)	6.60 ± 0.80	1133 ± 172	14.2 ± 1.9	4.9 ± 1.0
4		d-DHHA (**5**)	0.46 ± 0.02	390 ± 29		
5	TRIS	DHHA (**1**)	1.56 ± 0.06	409 ± 26	5.1 ± 0.2	3.7 ± 0.4
6		d-DHHA (**5**)	0.31 ± 0.01	300 ± 17		
7	TRIS w/o	DHHA (**1**)	2.50 ± 0.18	746 ± 77	6.4 ± 0.6	3.4 ± 0.5
8		d-DHHA (**5**)	0.39 ± 0.02	397 ± 28		

The determined kinetic values have to be treated very carefully and should not be over-interpreted. Since many data points are afflicted with high standard deviations, it was repeatedly found that all performed enzymatic assays were very sensitive towards any kind of external influence, e.g. oxygen, temperature, etc., ranging from rather low 1° KIEs (1° KIE = 3.4 ± 0.5) to pretty high values (1° KIE = 14.2 ± 1.9) (Table 5). Nevertheless, two trends are possibly apparent: As HILVERT demonstrated, MICHAELIS-MENTEN constants K_M can be influenced by the small alteration of exchanging one hydrogen with one deuterium atom.[57,231–234] However, computations of ITOU suggest that the carbon-hydrogen bond (C-H) is approximately 7 mÅ longer than its equivalent carbon-deuterium bond (C-D).[135] It seemed that d-DHHA (**5**) binds stronger to WT PhzF than DHHA (**1**) in every single experiment, which is indicated by a smaller MICHAELIS-MENTEN constant of compound **5**. Consequently, this led to the circumstance that every 1° KIE (k_{cat}) was calculated to a higher value than its corresponding 1° KIE (k_{cat}/K_M), in which binding properties are included. Secondly, all performed enzymatic assays proceeded faster in phosphate buffer than in organic systems possibly indicating an inhibiting effect of organic additives. This unexpected observation and its influence on the PhzF catalyzed isomerization of DHHA (**1**) will be investigated in upcoming experiments, which are executed by Christina DIEDERICH (research group of Prof. Wulf BLANKENFELDT).

4.12. How to Overcome Side Product Formation in the Isomerization of DHHA (1) by WT PhzF

There is no doubt that current enzymatic assays have to be improved for the generation of trustworthy kinetic data in the isomerization of DHHA (**1**) by WT PhzF. The major difficulty in such experiments is the side product formation caused by the high reactivity of ketamine **3**. In general, two approaches are conceivable, how to overcome this exhausting issue of reactiveness. On the one hand, the scavenging of the reactive keto moiety in compound **3** would be one simple option, but assumes several properties from the scavenging reagent:

1. In order to get a single defined product, the scavenging reagent must react with ketamine **3** at least one order of magnitude faster than intermediate **3** would perform spontaneous self-condensation forming the tricyclic ring structure.
2. The absorption maxima of the scavenging reagent as well as of all formed products should be located in an absorption region, which do not affect the measurement of the substrate consumption.
3. The scavenging reagent is not allowed to have an impact on the enzymatic isomerization reaction in any case, e.g. reacting with the enzyme.

4. The scavenging reagent must prevent ketamine **3** from decomposition, e.g. aromatization, tautomerization, fragmentation.

If the enzymatic transformation is measured in a direct way by the increase of formed product, two additional criteria have to be fulfilled by this reagent.

5. The trapping reagent should bathochromically shift the absorption maxima of the desired product to wavelengths $\lambda > 300$ nm avoiding interference with other compounds in solution.

6. Most importantly in this case of reaction control, the scavenging reaction itself has to occur faster than the enzymatic transformation in order to get kinetic insight into the rate determining step, the enzyme catalyzed isomerization.

Various organic hydrazines have been used as scavenging reagents for carbonyls, as aldehydes or ketones, which result in the fast formation of organic hydrazones[235] due to the kinetically favorable α-effect of this substance class.[236] On the other hand it seems much easier to simply avoid the tautomerization reaction, which is crucial for the formation of reactive ketamine **3** (Scheme 23).
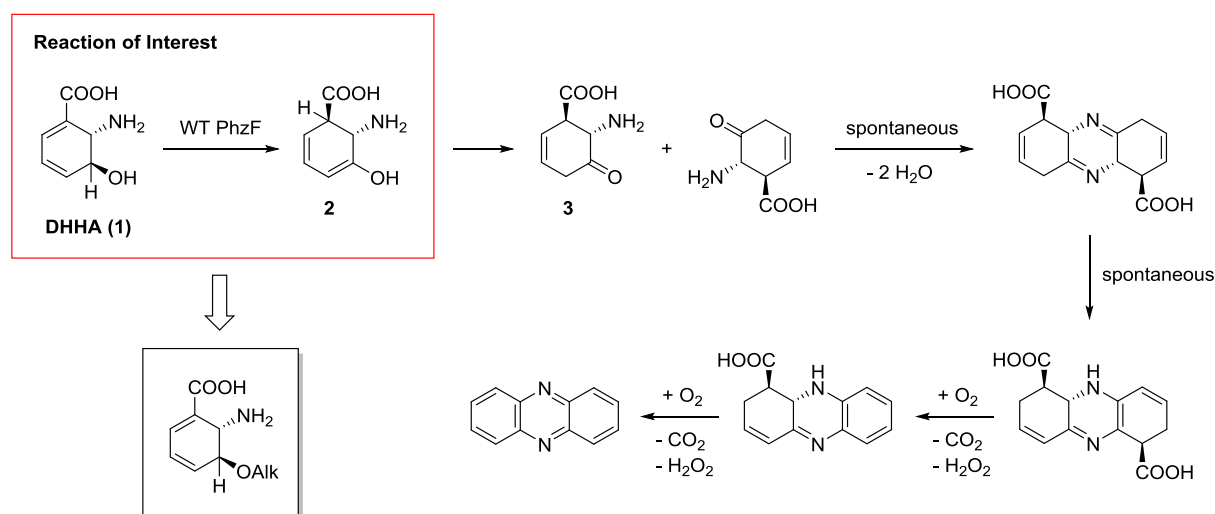
Scheme 23: Side product formation in the conversion of DHHA (**1**) by WT PhzF causing complications in enzymatic assays; Synthesis of *O*-alkylated DHHA derivatives for overcoming issue of tautomerization after enzyme catalyzed isomerization.[34]

This assumption can be achieved for instance by the synthesis of *O*-alkylated DHHA derivatives. Herein, the enzyme catalyzed isomerization would lead to the formation of diverse enol ethers, which are not able to tautomerize anymore. With these molecules in

hands, it would be explicitly possible to investigate in particular the isomerization step in PhzF provided that these derivatives will be recognized and transformed by the enzyme. However, these experiments would only provide kinetic parameters for the isomerization of *O*-alkylated DHHA derivatives with hopefully less uncertainties, but cannot substitute the real experiments with DHHA (**1**), the natural substrate of WT PhzF (Scheme 23).

4.13. Synthesis of *O*-Alkylated DHHA Derivatives

Once again our well-established synthesis for DHHA (**1**), initially published by STEEL,[172–175] was modified to primarily achieve diverse *O*-alkylated DHHA derivatives as racemic mixtures. In the absence of the kinetic resolution with PLE, racemic bicyclic ester **rac-15** underwent KHMDS-mediated ring opening and compound **rac-21** was modified by the use of different alkylating reagents, mainly alkyl halides and alkyl triflates. All of these reactions were performed in Et_2O under the addition of Ag_2O for activating non-reactive alkylating reagents.[237] Due to rather long reaction times in the alkylation of Et-DHHA (**rac-42**) and *n*Pr-DHHA (**rac-43**) between 70 h and 120 h, unfortunately, a significant amount of the corresponding intermediates was degraded caused by the acidic conditions after the formation of trifluoromethanesulfonic acid as side product. Nevertheless, under these non-further optimized conditions, all *O*-alkylated intermediates could be isolated as pure materials after flash column chromatography in yields between 11 % and 94 %. Interestingly, the alkylation reaction of ester **rac-21** with allyl bromide was accompanied by an intramolecular DIELS-ALDER reaction, which resulted in the formation of a highly complex tricyclic ring intermediate. All subsequent saponification reactions proceeded smoother and faster under the use of $LiOH.H_2O$ instead of KOH as a base and after Boc-deprotection as well as purification by trituration in different solvent mixtures, three *O*-alkylated DHHA derivatives plus one tricyclic compound could be isolated in form of TFA salts **rac-41a**, **rac-42a**, **rac-43a** and **rac-44a** (Scheme 24).[172–175]

Optically pure *O*-alkylated DHHA derivatives can be achieved in a 11 reaction sequence (13 steps with reesterification and repeated kinetic resolution with PLE), as it is demonstrated for Me-DHHA (**41**). Herein, compound **41a** was isolated in an overall yield of ~4 % (Scheme 25).[172–175]
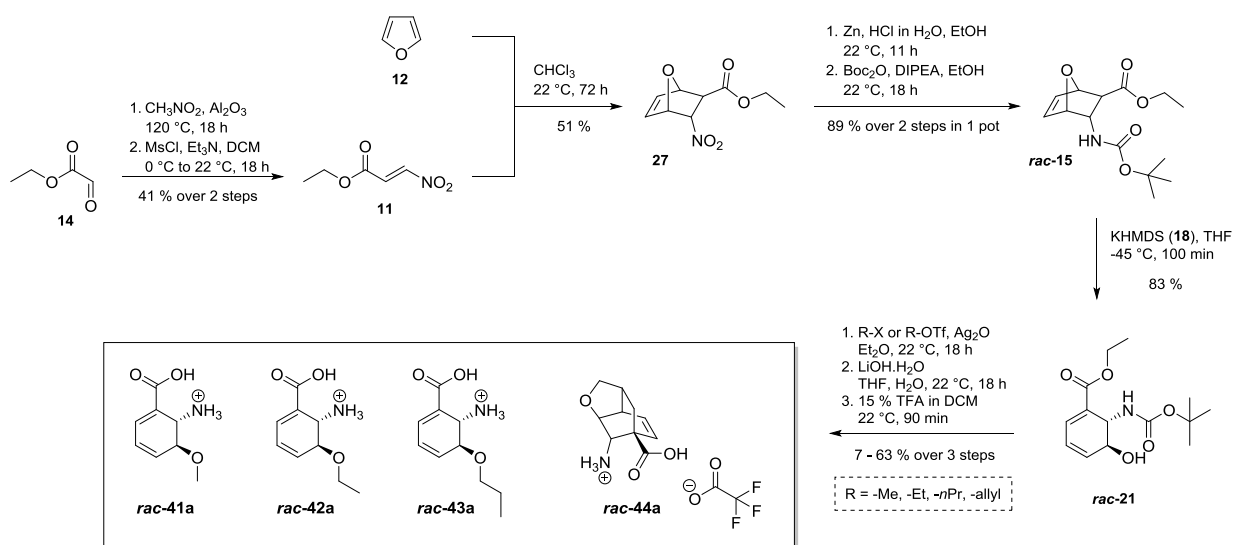
Scheme 24: Synthesis of *O*-alkylated DHHA derivatives in form of TFA salts in analogy to the synthesis of DHHA (**1**) published by STEEL.[172–175]
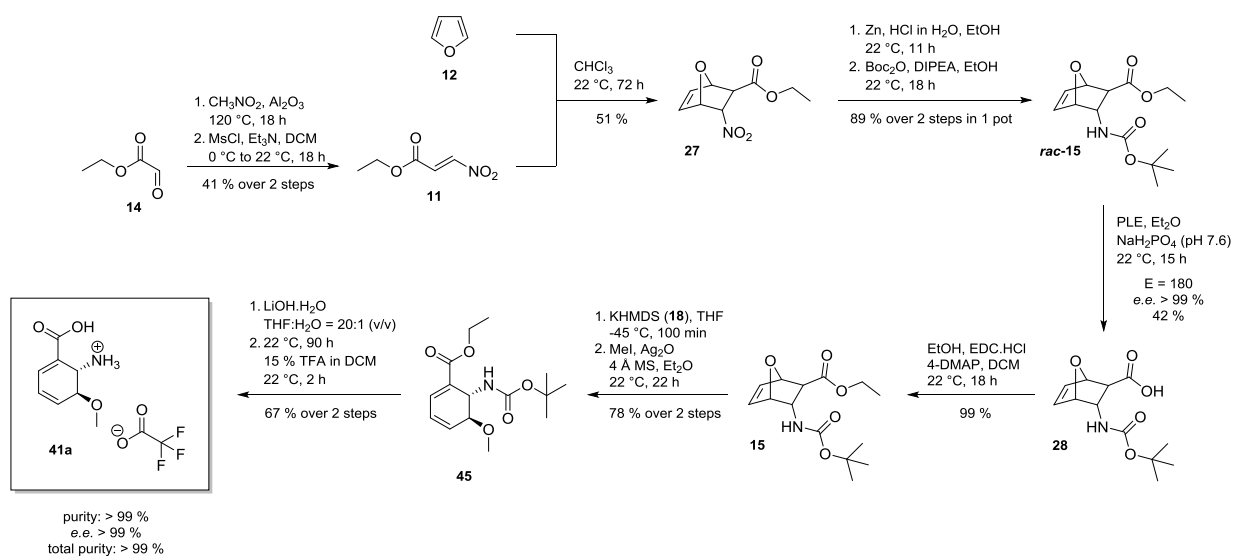
Scheme 25: Synthesis of enantiomerically pure Me-DHHA (**41**) in analogy to the synthesis of DHHA (**1**) by STEEL.[172–175]

4.14. ¹H-NMR Experiments for the Hydrogen Migration in *O*-Alkylated DHHA Derivatives

Exactly the same ¹H-NMR experiments,[34] as described in previous chapters, were performed in order to investigate the recognition and isomerization behavior of WT PhzF regarding *O*-alkylated DHHA derivatives. Primarily, only racemic mixtures of Me-DHHA

(*rac*-**41**), Et-DHHA (*rac*-**42**) and *n*Pr-DHHA (*rac*-**43**) were tested, whereas also racemic DHHA (*rac*-**1**) was used as reference compound. All experiments were performed with degassed, deuterated NaH$_2$PO$_4$/Na$_2$HPO$_4$ buffer at pD 7.6 and 15 °C was again selected as reaction temperature to guarantee a perfect separation of all substrate and product signals for a clear assignment and accurate integration.

Isomerization of DHHA (*rac*-1) Catalyzed by WT PhzF:
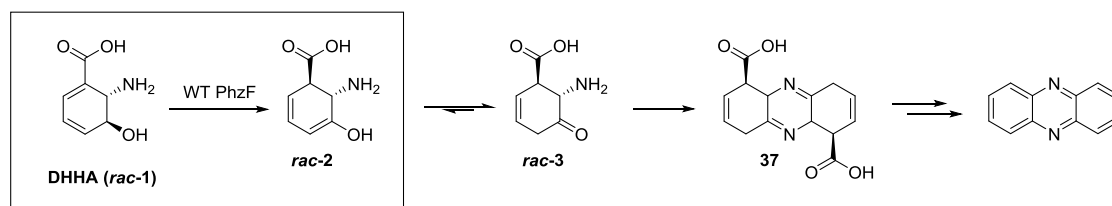
Isomerization of Me-DHHA (*rac*-41) Catalyzed by WT PhzF:
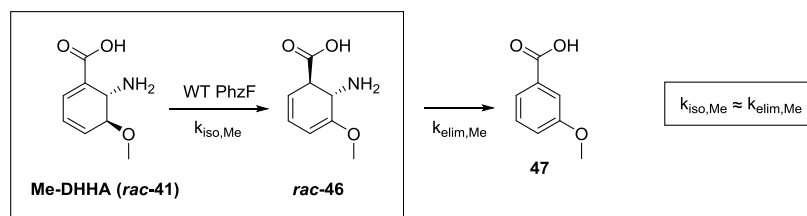
Isomerization of Et-DHHA (*rac*-42) Catalyzed by WT PhzF:
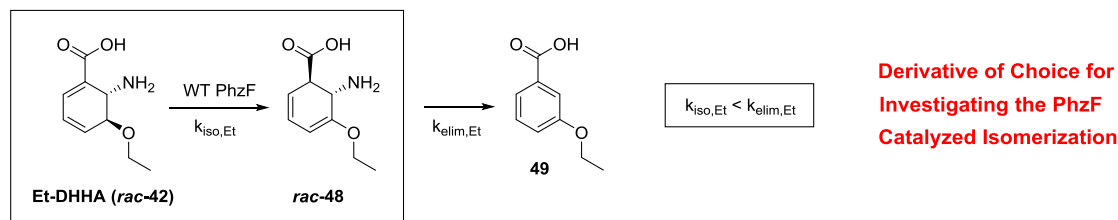
Isomerization of *n*Pr-DHHA (*rac*-43) Catalyzed by WT PhzF:
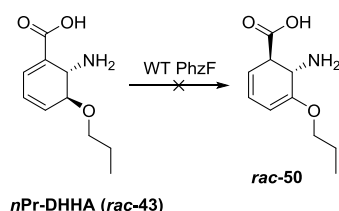
Scheme 26: WT PhzF catalyzed isomerization of different *O*-alkylated derivatives of DHHA; Racemic mixtures of substrates tested.

Gratifyingly, two out of four *O*-alkylated DHHA derivatives, namely Me-DHHA (*rac*-**41**) and Et-DHHA (*rac*-**42**), were successfully converted by WT PhzF. After the comparison of all

initial reaction rates, racemic Me-DHHA (*rac-41*) was isomerized with similar reaction rates as DHHA (*rac-1*), within NMR accuracy. However, Et-DHHA (*rac-42*) reacted at least one order of magnitude slower and no reaction was detected at all, when *n*Pr-DHHA (*rac-43*) was tested as starting material (Scheme 26).

Related to the co-crystallization experiments with H_2-DHHA (**34**), a small substituent, such as a methyl group, attached to the hydroxy moiety of DHHA (**1**) seemed to have minor influence on binding compared to ring conformation and space requirements of the cyclohexene moiety in H_2-DHHA (**34**). The alkyl residue can be oriented pointing in direction of free space by pushing one single H_2O molecule positioned in the active site of WT PhzF aside, whereas the ring itself must be located in the deep cavity of the active enzyme (see chapter X-ray structure of WT PhzF).[34] Obviously, too large substituents prevent proper binding to the catalytic active center, maybe caused by steric clashes between those residues and active site side chains, as is the case in *n*Pr-DHHA (*rac-43*).

Although tautomerization could be effectively prevented in the isomerization reaction of Me-DHHA (*rac-41*) and Et-DHHA (*rac-42*), yet one unexpected side reaction occurred. Both intermediates *rac-46* and *rac-48* spontaneously eliminated ammonia, which resulted in the rapid formation of the corresponding benzoic acid derivatives **47** and **49**. In the case of Me-DHHA (*rac-41*), however, the isomerization and elimination step mostly seemed to happen within similar reaction rates, demonstrated by *in situ* detection of intermediate *rac-46* in time resolved ^{1}H-NMR spectroscopy (Figure 21 and Figure 22). Despite the fact that isomerization and spontaneous elimination follow different kinetics, MICHEALIS-MENTEN[232,233] in the simplest case for the enzyme catalyzed part and a reaction of first order for an E_1-elimination, it would be impossible to measure only the enzyme catalyzed isomerization as the rate determining step photometrically. One simple way to overcome this issue of reactivity in general is to decelerate the enzymatic transformation that this reaction part becomes rate determining in any way.

Et-DHHA (*rac-42*) perfectly fulfilled this task of deceleration, whereas intermediate *rac-48* could not be detected at any time. Of course, it has to be proven, if the enzymatic isomerization or the diffusion of the substrate to the active site is rate determining within this transformation. However, in comparison to the natural substrate, the specificity constant for the isomerization of DHHA (**1**) catalyzed by WT PhzF was estimated with $k_{cat}/K_M = 6240 \pm 760$ $M^{-1}.s^{-1}$ and comparably lies several orders of magnitude below the value for diffusion controlled enzymatic reactions ($k_{cat}/K_M \approx 10^8$-10^9 $M^{-1}.s^{-1}$).[238]
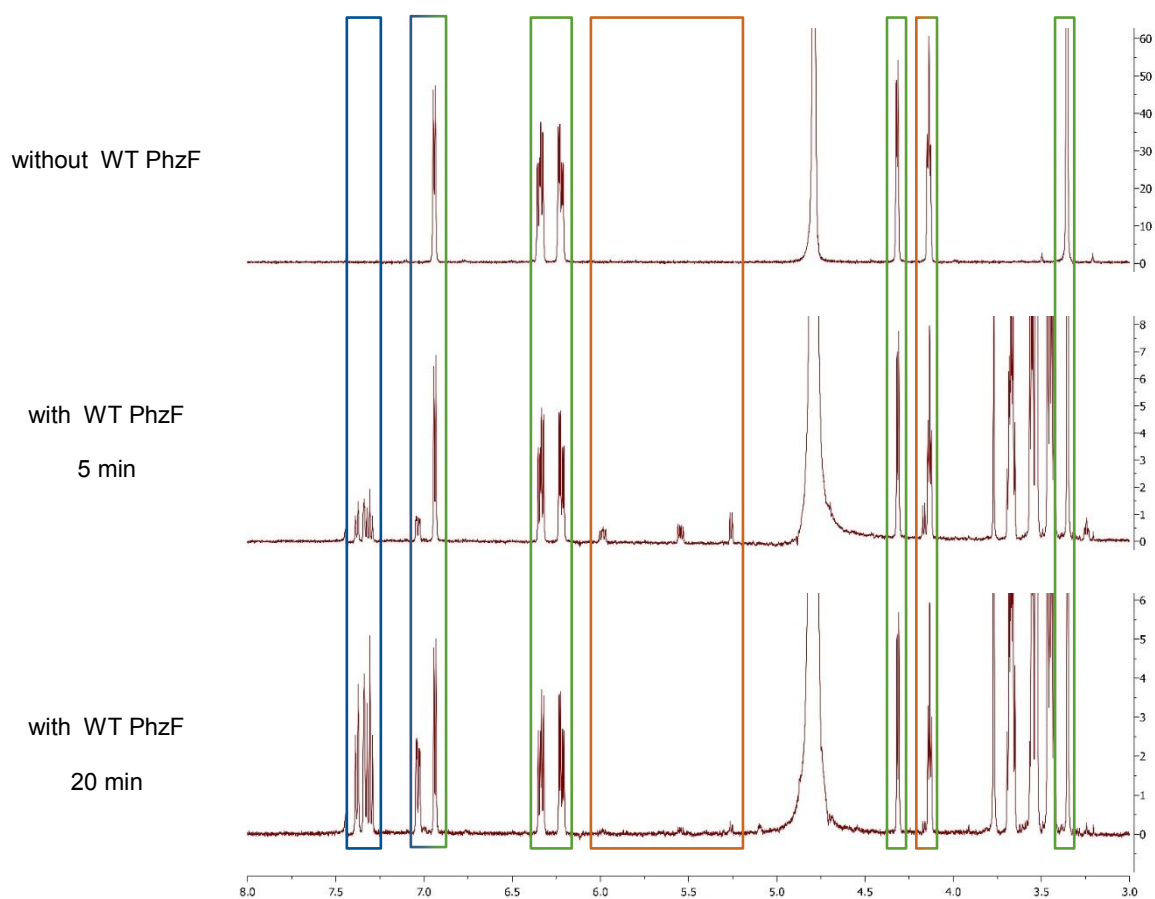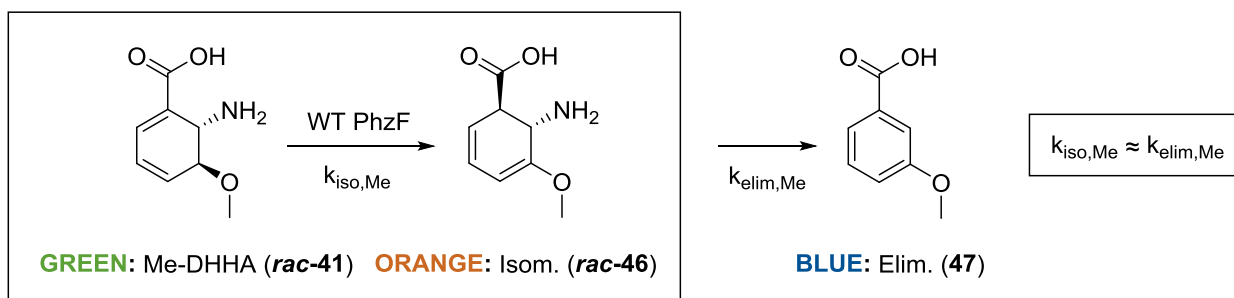
Figure 21: Time-resolved ^{1}H-NMR analyses of the WT PhzF catalyzed isomerization of Me-DHHA (***rac*-41**) followed by a spontaneous elimination of NH_3; Isomerization and elimination rate in the same range indicated by the observation of intermediate ***rac*-46**.

Absorption maxima for both *O*-alkylated substrates ***rac*-41** and ***rac*-42** (λ_{max} = 275 nm) as well as their elimination products **46** and **47** (λ_{max} = 286 nm) indicate that photometric measurements may cause problems in determining the correct concentration due to overlapping absorption maxima. Enzymatic assays must reveal, if Et-DHHA (***rac*-42**) is a suitable and promising candidate for the investigation of the PhzF catalyzed isomerization and if reliable kinetic values can be determined in experiments with this derivative. Then enantiomerically pure Et-DHHA (**42**) as well its deuterated analogue have to be synthesized

for the determination of 1° KIEs. However, it could be shown that against all odds additional substrates were converted by the highly specialized enzyme WT PhzF under standard conditions.[34] This observation led to the following, highly interesting question: Does WT PhzF convert further derivatives, which possess only minor differences compared to the natural substrate DHHA (**1**)? This important question was clarified in the following section.
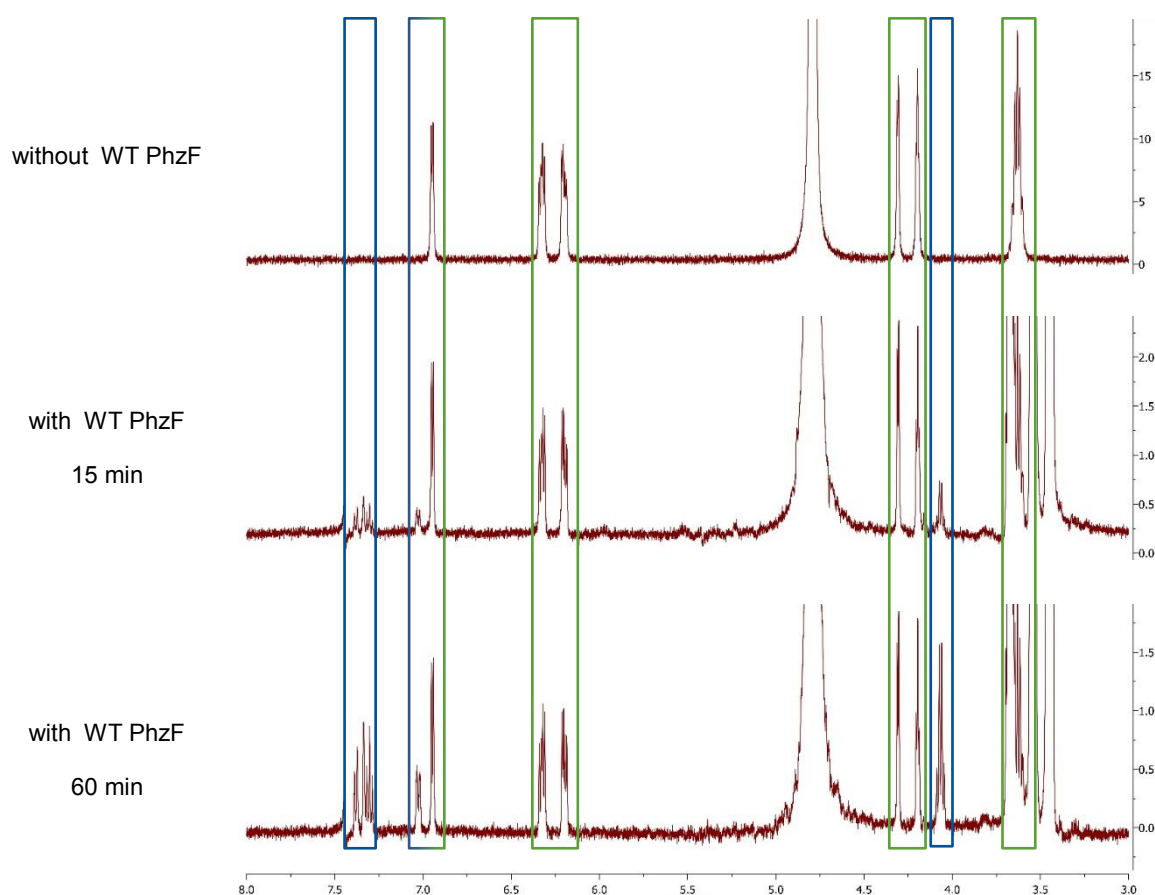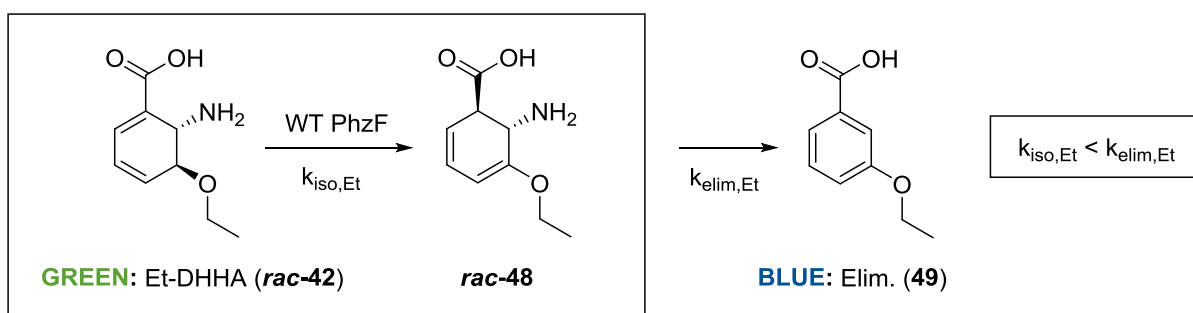
Figure 22: Time-resolved ^{1}H-NMR analyses of the WT PhzF catalyzed isomerization of Et-DHHA (*rac-42*) followed by a spontaneous elimination of NH$_3$; Isomerization step rate determining reaction in the formation of elimination product **49**.

4.15. Substrate Scope Investigations of the WT PhzF Catalyzed Isomerization

Results from experiments with Me-DHHA (*rac*-**41**) and Et-DHHA (*rac*-**42**) led to the assumption that WT PhzF is able to convert further derivatives with minor differences relative to DHHA (**1**), its natural substrate. Primarily, the influence of the amine moiety in DHHA (**1**) should be investigated as this functional group may affect the pK_a of the migrating ε-proton in an acid-base catalyzed mechanism. Apart from that, H74A was the only mutant, which was able to isomerize DHHA (**1**), however, in comparably low reaction rates, but formed hydrogen bond interactions as well to the amine moiety with additional H_2O molecules in its active site. Herein, this eminent substitution of the histidine to alanine, a non-polar aliphatic amino acid, led to the conclusion that an alteration at this position of DHHA (**1**) would certainly result in promising compounds, which might be recognized and converted by WT PhzF.
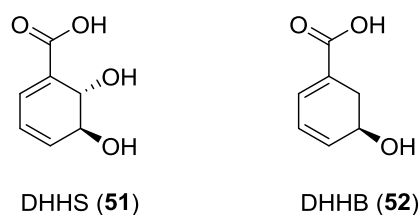
DHHS (**51**)   DHHB (**52**)

Figure 23: Selected derivatives of DHHA (**1**) for substrate scope investigations with WT PhzF.

DHHS (**51**) and DHHB (**52**) were predominantly selected for exploring the influence of the amine moiety on the isomerization reaction with WT PhzF (Figure 23). In compound **51**, the amino residue is substituted by a second hydroxyl functionality, which should manifest in a similar character regarding polarity and hydrogen bond interaction, but without the intrinsic basicity of the amine. Compound **52**, instead, is missing the amine moiety that is by so far crucial for binding the substrate to the active site and also for maintaining the cationic ionization state in a possible acid-base catalyzed isomerization.

Derivative **51** has already been synthesized using a biotechnological route published by LEISTNER in 1996,[239] but was further improved and translated to recombinant *Escherichia coli* strains by MÜLLER in 2001.[218,240] Starting from ubiquitous chorismate (**53**), DHHS (**51**) is an intermediate on the pathway of the iron chelator enterobactin and is produced in a two-step catalytic process involving isochorismate synthase and isochorismatase as key enzymes. Improvement in the genetic construction as well as fermentation process ultimately resulted in a high final concentration of more than 15 g.L^{-1}. By means of a 300 L fed-batch

approach, compound **51** was produced in a kilogram scale and could be separated using reactive extraction (Scheme 27).[218,219,240] Prof. Michael MÜLLER kindly sent us a small amount of enantiomerically pure DHHS (**51**) (*e.e.* > 99 %) for performing mentioned substrate scope experiments and later on enzymatic assays.
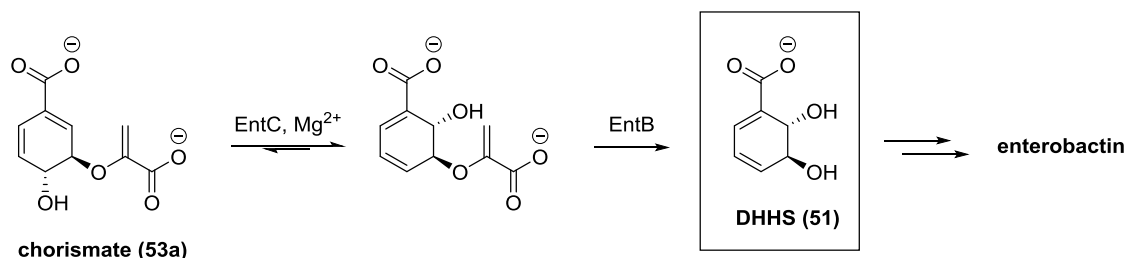
Scheme 27: Enterobactin pathway for the synthesis of enantiomerically pure DHHS (**51**); Participating enzymes: Isochorismate synthase (EntC) and isochorismatase (EntB).[218,219,240]

In contrast, DHHB (**52**) has not been synthesized before, but related structures are known in literature, which could be enantioselectively prepared.[179,218,241,242–244] In analogy to the synthesis of *ent*-shikimic acid, initially published by EVANS in 1997, we adopted this chemical route for the preparation of derivative **52** featuring an enantioselective DIELS-ALDER cycloaddition as key transformation.[242,243]

Herein, copper-catalyst **60** was needed for effectively lowering the LUMO energy of compound **62** in a compelling bidentate interaction with both carbonyl moieties, as described by EVANS.[242,243] It was prepared in a convergent reaction sequence starting from commercially available L-phenylglycine (**54**), which was quantitatively reduced with *in situ* generated borane achieving enantiomerically pure amino alcohol **55**.[245–247] In parallel, malonodinitrile (**56**) was efficiently dialkylated using 1,4-dibromobutane in combination with DBU as a base.[248] With these two starting materials in hands, L-Phg-Box-ligand **58** was synthesized in a step-economical procedure converting dinitrile **57** with amino alcohol **55** in the presence of stoichiometric amounts of anhydrous Zn(OTf)$_2$ directly into compound **58**. However, when substoichiometrical quantities of this LEWIS acid were used, mainly mono(oxazoline) formation occurred, which would need a higher effort in purification, as described by VILLALBA in 2005.[249] Although quantitative conversion could not get accomplished within this reaction step, the purification of ligand **58** worked smoothly and L-Phg-Box **58** could be isolated in its enantiomerically pure form in 51 % yield after flash column chromatography. Complexation with anhydrous CuCl$_2$ resulted in the quantitative formation of deeply green colored pre-catalyst **59**,[250] from which both remaining chlorides

had to be abstracted by AgSbF$_6$ prior to its use as active catalyst **60** in the enantioselective D$_{IELS}$-A$_{LDER}$ reaction (Scheme 28).[242,243]
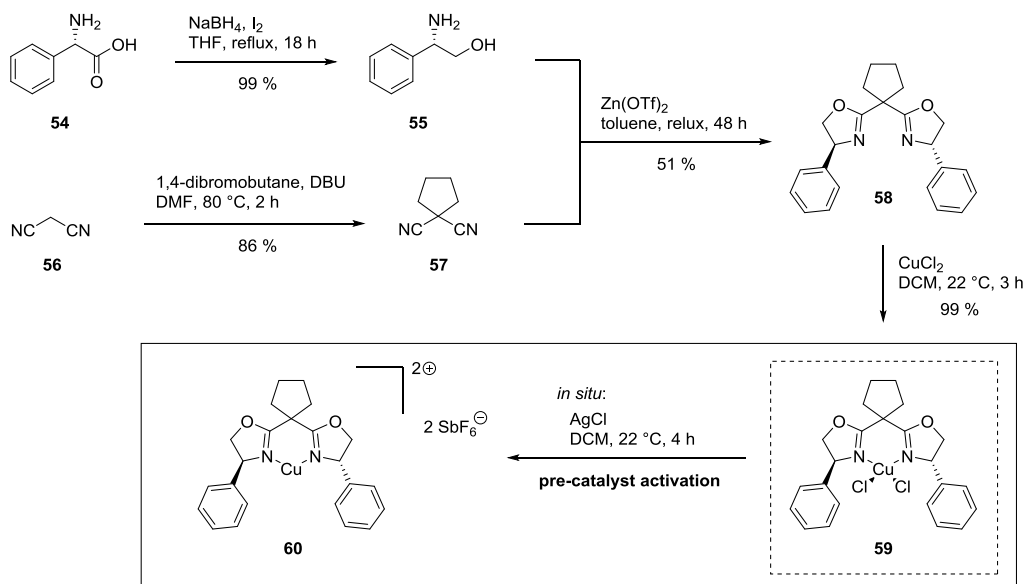
Scheme 28: Reaction sequence for the synthesis of optically pure catalyst **60** needed for the enantioselective D$_{IELS}$-A$_{LDER}$ reaction between furan (**12**) and dienophile **62**.[242,243,245–248,250]
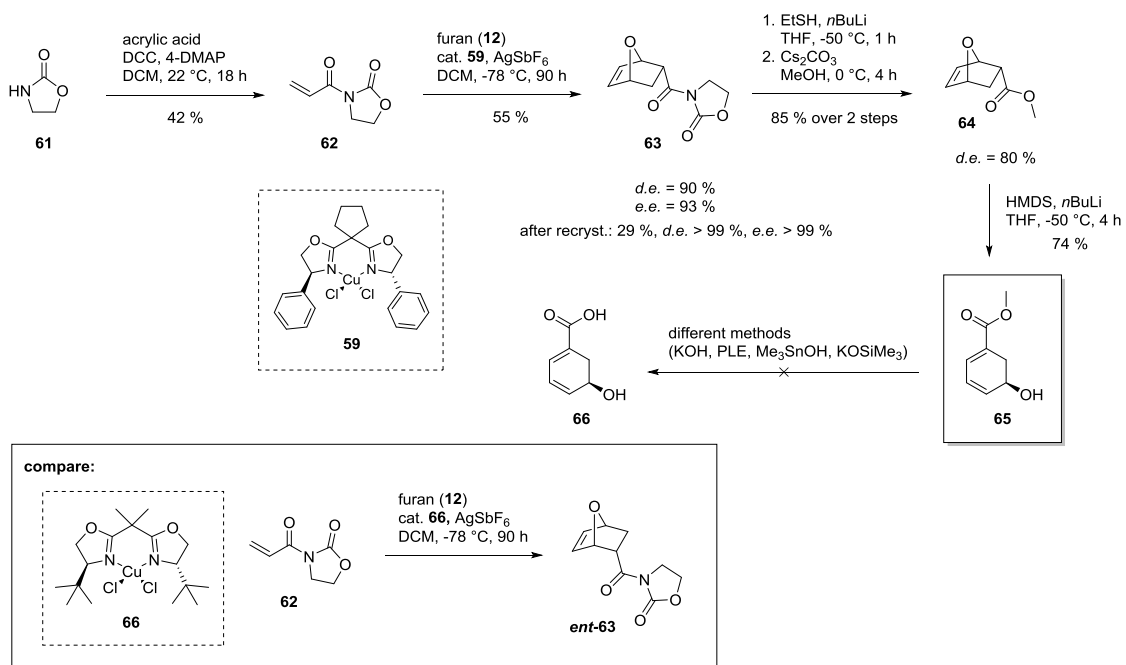
Scheme 29: Reaction sequence for the synthesis of enantiomerically pure ester **65**; Hydrolysis reactions of ester **65** failed so far due its high sensitivity towards elimination; Compare: Same enantiomers of pre-catalysts **59** and **66** result in the formation of opposite imides **63** and ***ent*-63**.[242,243,251]

Running a mild, DCC/4-DMAP-mediated imidation between acrylic acid and the rather non-nucleophilic oxazolidinone (**61**), dienophile **62** was isolated after chromatographic purification in 42 %.[251] In general, furan (**12**) is regarded as poor diene in DIELS-ALDER cycloadditions explaining why only a few examples of catalytic asymmetric DIELS-ALDER reactions have been reported in literature.[242–244,252] For reasonable yields together with excellent diastereo- as well as enantioselectivities, this pericyclic cycloaddition had to be performed at a temperature of -78 °C for 42 h. Therefore a special manufactured cryogenic reactor consisting of two nested Styrofoam boxes filled with dry ice was used to maintain the low temperatures over several hours (Figure 24). Interestingly, the same enantiomer of L-Phg-Box pre-catalyst **59** compared to the initially described L-*tert*-Leu-Box compound **66**,[242,243] preferentially resulted in the formation of opposite enantiomers of bicyclus **63**. Although this interesting effect is well-known in literature and is concluded to a possible geometry change at the copper atom,[253] we hypothesize that additionally attractive π-π-interactions instead of simple sterical clashes between the furan (**12**) and the aromatic moiety of catalyst **60** are responsible for the complete inversion of enantioselectivity. Nevertheless, by the use of L-Phg-Box **59** as ligand, bicyclus **63** was isolated in a yield of 55 % (*d.e.* = 90 % and *e.e.* = 93 %) and could be received in its optically and diastereomerically pure form (*e.e.* > 99 % and *d.e.* > 99 %) after recrystallization in an overall yield of 29 % (Scheme 23).[242,243]
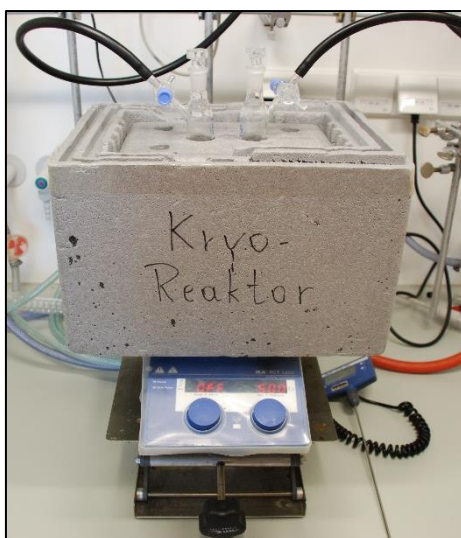
Figure 24: Cryogenic reactor of two nested Styrofoam boxes: Inner box filled with dry ice.

A direct LHMDS-mediated ring opening with imide **63** proved to be unsuccessful under a variety of conditions.[242,243] Two straightforward reesterification reactions with EtSH as well as MeOH in yields of 87 % and 98 %, respectively, were essential for this assisted

transformation. The significant loss of diastereomeric excess of bicyclic ester **63** (*d.e.* = 80 % and *e.e.* > 99 %) did not affect the ring opening at all due to the fast interconversion of both diastereomers under basic conditions. Herein, the facile use of *in situ* prepared LHMDS resulted in a smooth isomerization at -50 °C yielding 74 % isolated cyclohexadiene derivative **65** after flash column chromatography.[242,243] Although rather basic conditions and well coordinating Li$^+$ counter ions were established, only a small amount of side product formation resulting from elimination reactions was detected.[172–175] In general, compound **65** should be prone for mentioned degradation due to the absence of a *trans*-substituent adjacent to the hydroxyl moiety. Herein, an additional substituent would definitely prevent the hydroxy group in attaining an *anti*-periplanar conformation with a neighboring hydrogen atom, which is crucial for proceeding in an E_2 elimination reaction (compare DHHA (**1**)).

Finally, hydrolysis of the methyl ester should deliver DHHB (**52**) in its enantiomerically pure form. However, many attempts to succeed in this transformation failed due to the high sensitivity of intermediate **65** under acidic or basic conditions at room temperature. Neither ordinary or soft bases, such as LiOH.H$_2$O, KOH or KOSiMe$_3$,[172–175,254] nor enzymatic driven hydrolyses with PLE,[176–178] led to the formation of the favored product. Even the use of Me$_3$SnOH as an extraordinary soft reagent for hydrolysis did not succeed. Elimination occurred in any case, similarly at 0 °C, and resulted quantitatively in the generation of benzoic acid, the elimination product of this reaction after passed hydrolysis. Apart from that, slightly acidic or basic functional groups on the surface of PLE seemed sufficient enough for initiating the elimination process.[176] Regrettably, this soft type of enzymatic hydrolysis shows that derivative **65** is certainly inapplicable due to same reasons acting as a substrate in substrate scope investigations of WT PhzF.

Instead, DHHS (**51**) was subjected to our established time-resolved ^{1}H-NMR analyses at 15 °C for a better separation of individual signals.[34] Surprisingly, no product formation could be detected after prolonged reaction times indicating a complete loss of reactivity by changing the amino moiety into a second hydroxy residue in DHHS (**51**). In other words, the amino functionality is essential for the isomerization of DHHA (**1**) catalyzed by WT PhzF, whether for a better recognition of the substrate as well as binding to the active site and/or due to (stereo)electronical/mechanistic effects lowering the activation energy for the preferred reaction type (Figure 25). Fluorescence spectroscopy may figure out, if the affinity to WT PhzF alters significantly, when DHHS (**51**) is used compared to other tested competitive inhibitors, as 3-hydroxyanthranilic acid (**32**).
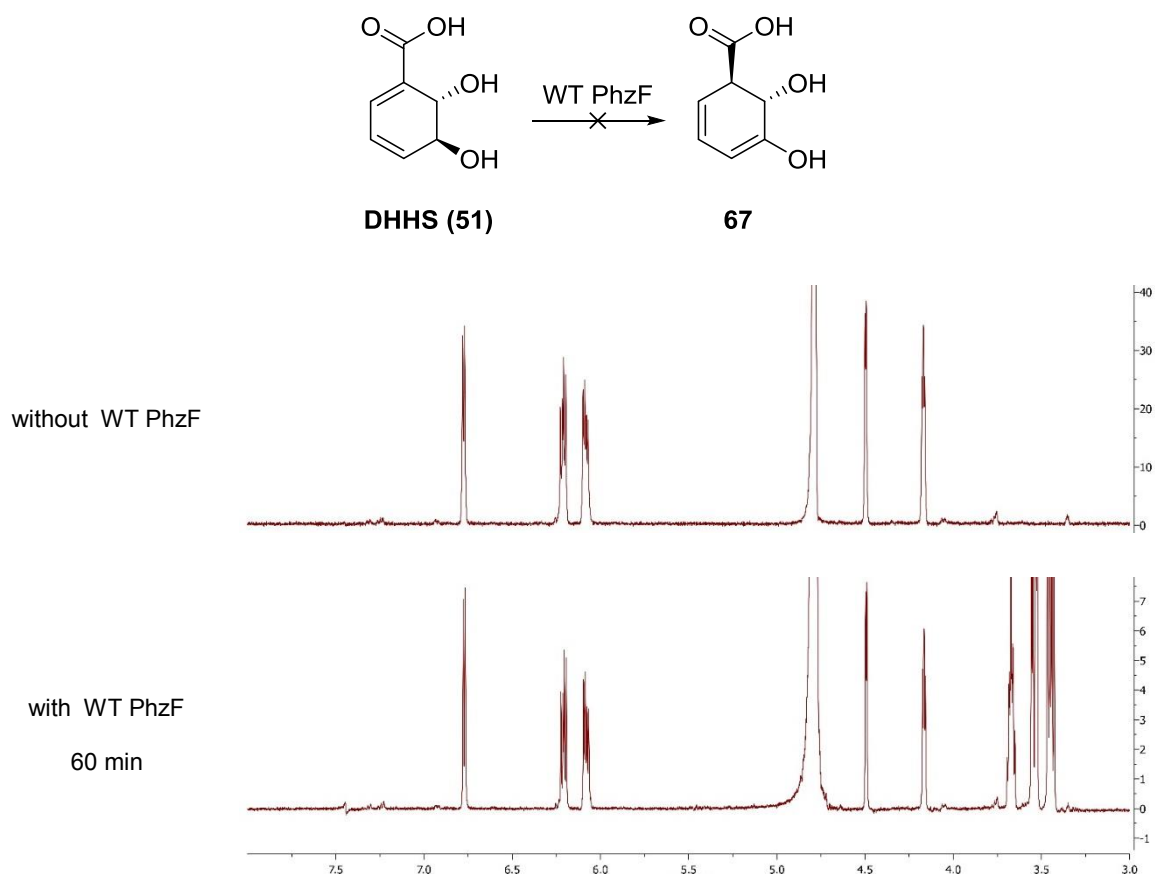
Figure 25: Time-resolved ^{1}H-NMR analyses of the WT PhzF catalyzed isomerization of DHHS (**51**).

4.16. pK$_a$ Determination of Protic Residues in DHHA (1) via Acid-Base Titration

Proven as crucial for enzyme activity, it was worth to determine the pK$_a$ of the amine moiety in DHHA (**1**) and to investigate, how this value may influence the reaction rate in the isomerization with WT PhzF. Accompanying the assignment of all other protic residues in DHHA (**1**), general acid-base titration is the method of choice, although high quantities of the natural substrate were needed for this purpose. Therefore, DHHA (**1**) was produced as racemic mixture on a multigram scale following the initially published and enhanced reaction procedure of STEEL (see chapter: Synthesis of DHHA (**1**)).[172–175]

In this connection, 750 µmol DHHA (**1**) of a 10 mM solution in 75 mL H$_2$O were titrated with 100 mM aqueous NaOH once and the method was validated by the titration of L-glycine (Lit.: pK$_a$(COOH) 2.3, pK$_a$(NH$_3^+$) 9.6; found: pK$_a$(COOH) 2.7, pK$_a$(NH$_3^+$) 9.6)[255,256] as well as malonic acid (Lit.: pK$_a$(COOH) 2.8, pK$_a$(NH$_3^+$) 5.7; found: pK$_a$(COOH) 2.8, pK$_a$(NH$_3^+$) 5.4).[257] Although one pK$_a$ value deviates in each reference material from that listed in literature, the

highest divergence was taken to serve for the standard deviation of the pK_a found in DHHA (**1**) (Scheme 30 and Figure 26).
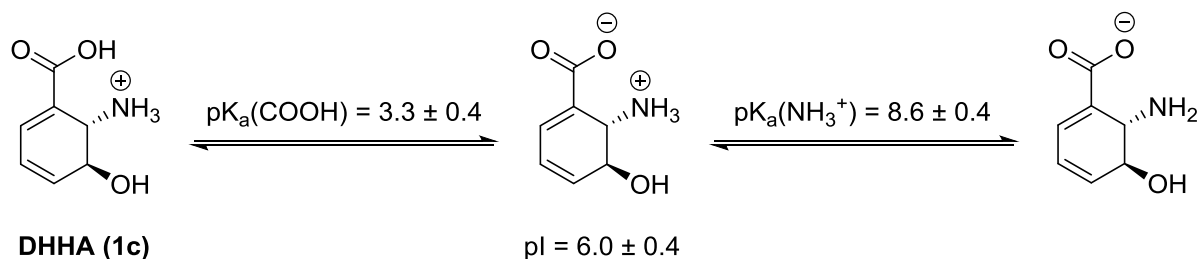
Scheme 30: pK_a values of DHHA (**1c**) determined by acid-base titration with 100 mM NaOH.
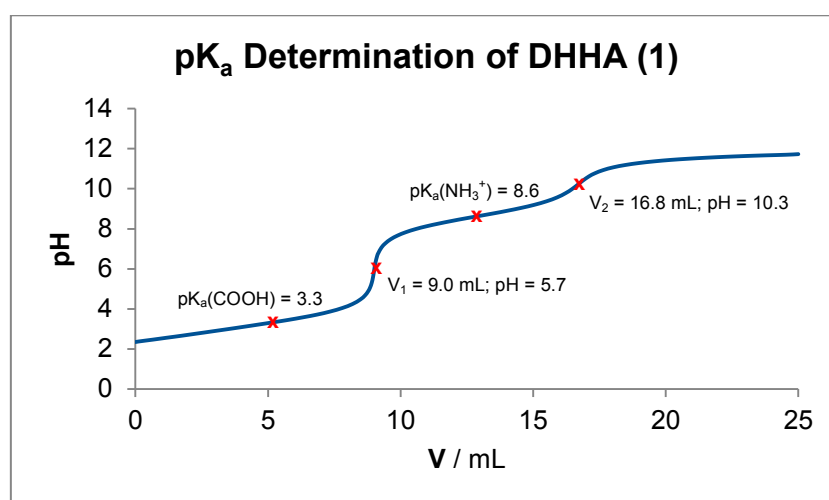
Figure 26: Titration curve for the pK_a determination of DHHA (**1**) by acid-base titration with 100 mM NaOH.

Table 6: pK_a values of comparable amino acids; pK_a of DHHA (**1**) determined by acid-base titration with 100 mM NaOH.

Entry	Compound	pK_a(COOH)	pK_a(NH$_3^+$)
1	DHHA (**1**)	3.3 ± 0.4	8.6 ± 0.4
2	α-serine[255]	2.2	9.2
3	α-threonine[255]	2.6	10.4
4	β-hydroxyglutamate[255]	2.1	9.2
5	β-alanine[255]	3.6	10.2

In comparison to referenced and related material, both pK_a values of DHHA (**1**) seemed quite reasonable for this natural β-amino acid. In general, β-amino acids exhibit an increased pK_a value for the carboxylic functionality compared to α-amino acids due to the absence of the polarizing amino substituent attached to the α-carbon atom. However, the measured pK_a value of the carboxylic moiety in DHHA (**1**) is even slightly decreased (pK_a(COOH) = 3.3 ± 0.4) in relation to β-alanine (pK_a(COOH) = 3.6), but still perfectly fits into the assured range for this substance class.[255,256] Interestingly, the amino group in DHHA (**1**) behaves quite differently. Featuring a remarkable low pK_a value for an amine functionality (pK_a(NH_3^+) = 8.6 ± 0.4), this observation can be explained by distinctive intramolecular hydrogen bond interactions within all functional groups of DHHA (**1**) by an optimal constitutional and conformational arrangement (Table 6).

However, a contrary behavior for the pK_a value of the amine group was primarily expected concerning a rate accelerating influence in a possible acid-base catalyzed isomerization. The more basic the amine of DHHA (**1**) acts, the higher the possibility for a pK_a lowering effect on the ε-proton by protonation in a protic mechanism. Nevertheless, the determined value of pK_a(NH_3^+) = 8.6 ± 0.4 is in principle sufficient enough to get protonated by histidine H74 (Lit.: pK_a(NH_3^+) = 6.0)[255,256] in WT PhzF. Whether this is the case in H74A, where H_2O molecules ensure the task of H74, has to be proven, but if an enzyme can handle a possible isomerization of DHHA (**1**) in an acid-base catalyzed mechanism, this would certainly be an easy exercise to accomplish.[34]

In conclusion, several attempts for the investigation of the mechanism in the WT PhzF catalyzed isomerization of DHHA (**1**) were undertaken, which have so far not led to results allowing the differentiation between both reaction types. Although the present thesis made highly pure mechanistic probes accessible, ongoing challenges are the realization of kinetic studies, which have to deliver enzyme characteristic parameters in terms of reaction rates and efficiencies. Once these obstacles get resolved, direct access to 1° KIEs will permit profound insight into the r.d.s. and will allow extensive conclusions of this migration process featuring hydrogen retention.

4.17. Exploring the Stereoselective Tautomerization in the WT PhzF Catalyzed Isomerization of DHHA (1)

Previous publications exploring the isomerization of DHHA (**1**) catalyzed by WT PhzF suggested next to the conservation of the migrating hydrogen atom an unexpected stereoselective tautomerization of enolic intermediate **2** to ketamine **68**. However, it could not

be proven so far, which side of enol **2** was effected by this proton migration and how this process occurred. There are two possible options discussed involving either a spontaneous tautomerization with H_2O from the bulk or specific catalysis by a solvent accessible functional group of the protein.[34] In this thesis, ^{1}H-NMR studies in combination with quantum-mechanical calculations should reveal, which face of enol **2** is preferentially protonated/deuterated within this tautomerization (Scheme 31).
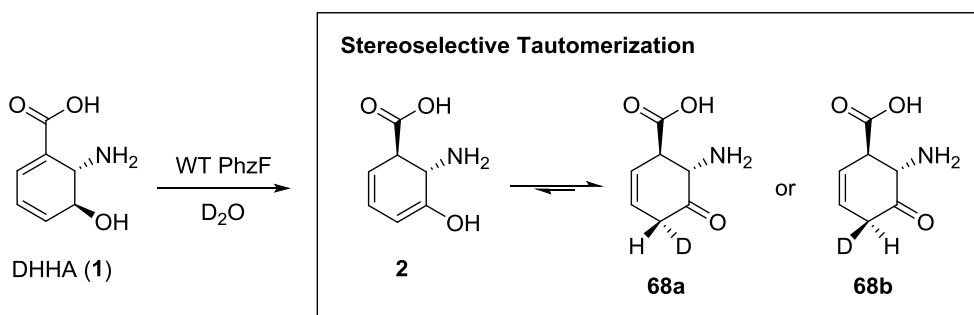
Scheme 31: WT PhzF catalyzed isomerization of DHHA (**1**) followed by a stereoselective tautomerization of enol **2** in D_2O.[34]

Chemical shifts (δ) of both hydrogen atoms were determined to values of δ = 3.19 ppm and δ = 2.92 ppm, as already observed in previous performed migration experiments with DHHA (**1**) as well as d-DHHA (**5**). Indicating the stereoselective tautomerization, only the corresponding signal at δ = 3.19 ppm was observed, when the isomerization was performed with DHHA (**1**) in D_2O as solvent (Figure 27).
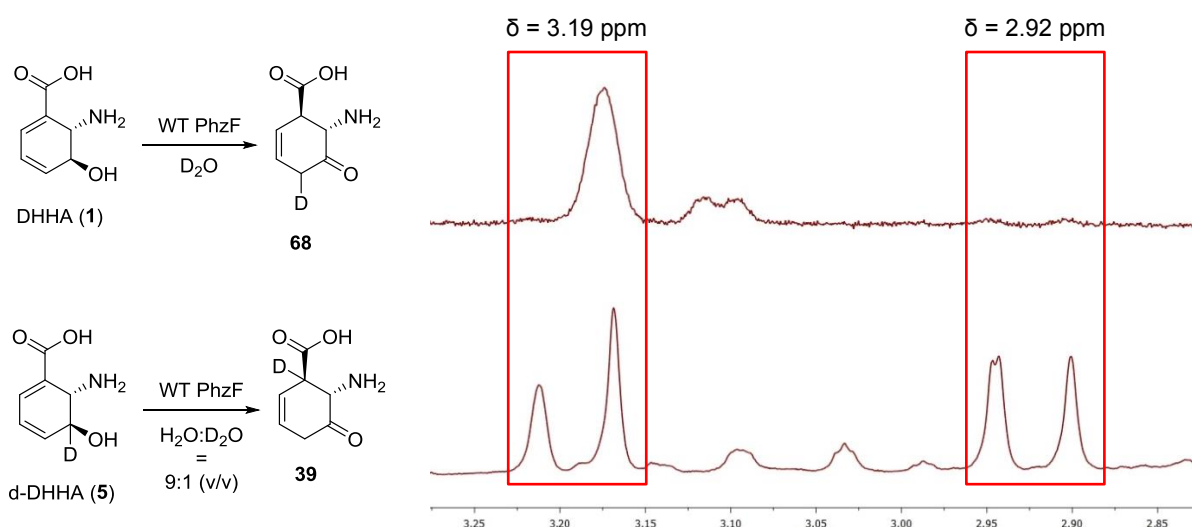
Figure 27: Characteristic signal multiplicities in ^{1}H-NMR spectra for α-protons/α-deuterons of ketamines **68** in D_2O and **39** in $H_2O:D_2O$ = 9:1 (v/v).

Hybrid DFT computations at the mPW1PW91/IGLO-II//mPW1PW91/6-31+G* level of theory made chemical shifts (δ) for both hydrogen atoms accessible, which should on the one hand support experimentally recorded data and on the other hand help in the differentiation of both hydrogen atoms. In this context, only the energetically most stable conformer of ketamine **3** (with two hydrogen atoms) was comprised due to sustained neutral conditions during the enzymatic transformation. Additionally, the polarized continuum model (PCM) was established to simulate aqueous conditions for ^{1}H-NMR analyses. All chemical shifts (δ) were referenced to tetramethylsilane (TMS).

In good agreement with experimental data, the following chemical shifts (δ) were calculated for these two considered hydrogen atoms: $\delta_{calc}(H_{ax})$ = 3.16 ppm and $\delta_{calc}(H_{eq})$ = 2.64 ppm. This led to the assumption that prochiral enol **2** abstracts only a proton/deuteron from its *Re*-face in a stereoselective manner, which maintains the possibility for confirming this observation by the measurement of a nuclear OVERHAUSER effect (NOE)[258,259] between H_{ax} and proton H_{C2}, as depicted in Figure 28.
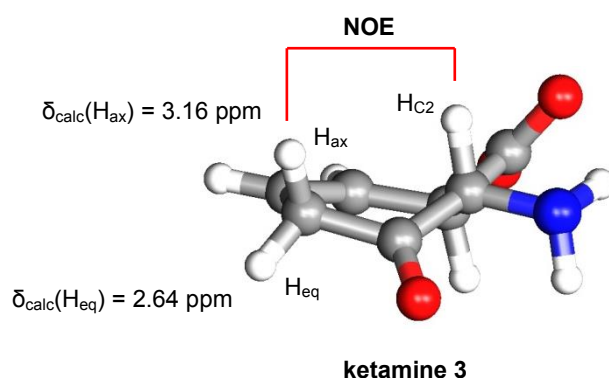
Figure 28: Calculated ^{1}H-NMR shifts of ketamine **3** at the mPW1PW91/IGLO-II//mPW1PW91/6-31+G* level of theory.[77–79,150,184,260]

Preliminary ^{1}H-NMR experiments with DHHA (**1**) under established reaction conditions demonstrated that all α-protons adjacent to the keto moiety in ketamine **3** were prone to exchange with proton/deuterons of the surrounding media over several hours quantitatively. To prevent this circumstance of rapid signal depletion, DHHA (**1**) in combination with WT PhzF in $H_2O:D_2O$ = 9:1 (v/v) was selected to ensure fast isomerization as well as tautomerization to enol **2** and postpone the time-dependent side product formation for an extended monitoring of compound **3** in solution. Once more, all experiments were performed at 15 °C in 100 mM NaH_2PO_4/Na_2HPO_4 buffer at pH 7.6 to retain similar reaction conditions,

as described before. Gratifyingly, a small NOE effect was detected after irradiation of H_{C2} ($\delta_{ex}(H_{C2})$ = 4.40 ppm) attesting the proposed, stereoselective tautomerization from the *Re*-face of enol **2**. Slight differences in chemical shifts can be explained by the strong temperature dependence of all chemical shifts and the utilization of aqueous buffer solutions as reaction media (Figure 29).
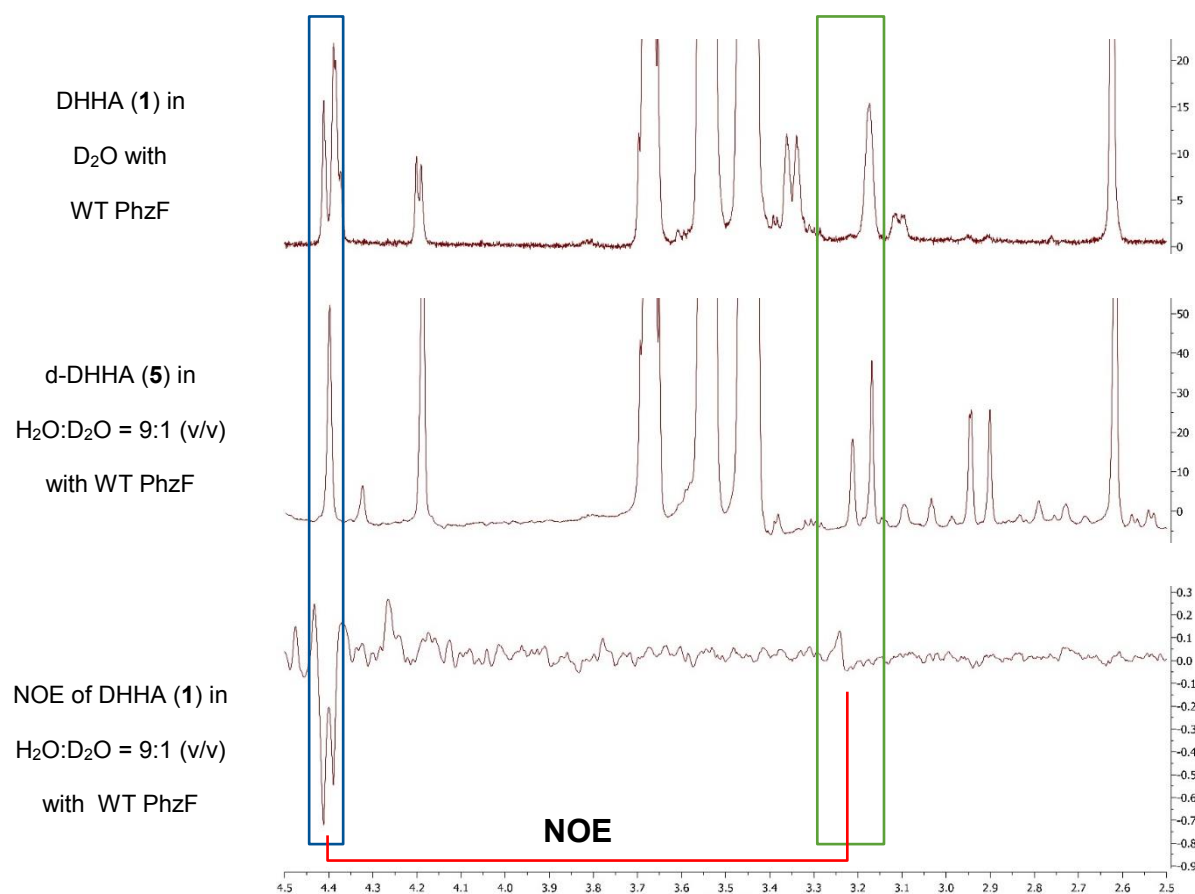
Figure 29: Determined nuclear OVERHAUSER effect (NOE) for the stereoselective tautomerization of DHHA (**1**) to ketamine **3**.

In this connection, the stereoselective tautomerization within the isomerization of DHHA (**1**) was conclusively examined exploiting the powerful combination of experimental research in combination with supporting quantum-mechanical calculations. Although a quantitative abstraction of a proton/deuteron to the *Re*-face of enol **2** was confirmed, it is still disputable at which site this controlled migration proceeds. Since the accessibility to enol **2** seems equally possible from both faces in an achiral environment, it is most likely that solvent accessible amino acid side residues of WT PhzF are involved in that process.

5. Summary of Scientific Research

5.1. Stereoselective Isomerization of DHHA (1): Suprafacial [1,5]-Prototropic Rearrangement vs. Acid-Base Catalysis

The investigation of biochemical pathways and their mechanisms of metabolite formation is indispensable for a profound understanding in disease control.[105] *Pseudomonas aeruginosa*, one potent phenazine producing bacterial pathogen, occurs as main virulence determinant in chronic and acute lung disease. Specific interference in the biosynthesis of these secondary metabolites should obtain a targeted treatment in infectious disease evoked by phenazine producing strains and should further provide tool compounds that can be employed as lead structures for pharmaceutical intervention.[13,23,34,35,47,108]
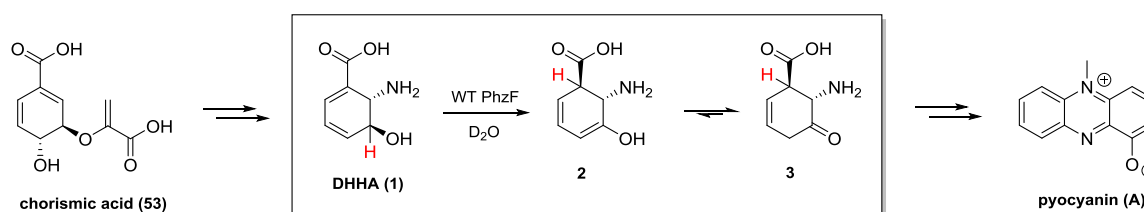
Scheme 32: WT PhzF catalyzed isomerization of DHHA (**1**), the key transformation in the biosynthesis of phenazines; Pyocyanin (**A**) as an example for highly redox-active phenazine species produced by *Pseudomonas aeruginosa* as pathogen in cyctic fibrosis.[34]

Central part of present thesis was laid on the elucidation of the phenazine biosynthesis, especially on the key step, the isomerization of DHHA (**1**) catalyzed by WT PhzF. Ketamine **3**, the product of this transformation, is the dominant player for the formation of the tricyclic ring system in phenazine producing bacteria strains (Scheme 32). Although several important details of this biosynthetic pathway have been explored, the WT PhzF catalyzed isomerization was by the time not fully understood.[13,34,35] By combining organic synthesis with quantum-mechanical calculations as well as biochemical techniques, it was investigated, if this isomerization follows an ordinary acid-base catalyzed mechanism or a so far in nature not described pericyclic reaction, namely the first example of a suprafacial [1,5]-prototropic rearrangement without the fragmentation of the substrate molecule. Main differences for both types of mechanism were elaborated and on the basis of these, experiments realized, which so far did not lead to an explicit exclusion either of an [1,5]-prototropic rearrangement or of a protic reaction type. However, indications for both mechanisms were collected. Results of

experiments are depicted and shortly discussed below demonstrating the thin line between argumentation and over-interpretation of collected data (Figure 30 and Figure 31).

Suprafacial [1,5]-Prototropic Rearrangement
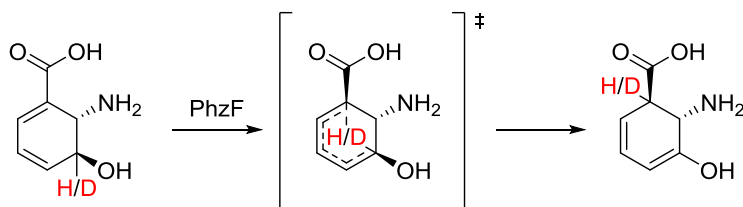
PROS:

quantitative migration of H/D

lowered calculated activation energy due to strong hydrogen bond interactions in TS of DHHA (**1**)

sulfate bound to active site of PhzF consistent with lowest activation energy in anionic DHHA (**1**)

CONS:

many mutants not active including E45D and E45Q

role of E45 not evident in pericyclic reaction

Figure 30: Collected arguments for and against the suprafacial [1,5]-prototropic rearrangement of DHHA (**1**) catalyzed by WT PhzF.

Acid-Base Catalyzed Isomerization

intermediate
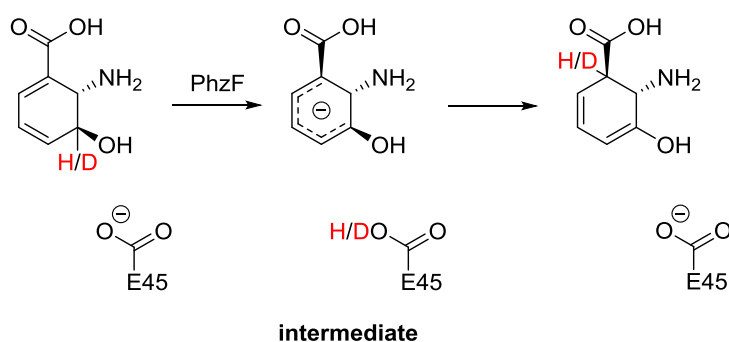
PROS:

role of E45 well described

short distance of 2.7 Å to E45 for an optimal arrangement between substrate and enzyme

many mutants not active including E45Q

compatable with quantitative migration of H/D

CONS:

sulfate bound to active site (cationic form of DHHA (**1**) essential for lowering pK_a)

active H74A mutant (missing imidazole of histidine probalby necessary for lowering pK_a)

$pK_{a,est}$(H/D) = 24-30

Figure 31: Collected arguments for and against an acid-base catalyzed isomerization of DHHA (**1**) by WT PhzF.

Preliminary assessments by quantum-mechanical calculations at the mPW1PW91/6-31+G* level of theory[77–79,150] account for a favored [1,5]-prototropic rearrangement in DHHA (**1**) due to stabilizing hydrogen bond interactions of the substituents in the TS compared to ordinary cyclohexadiene (**6**). Computations were either performed in gas phase or by surrounding five H_2O molecules to imitate the solvent. Collected data figured out that only the net charge of the molecule influences the activation energy for the considered sigmatropic rearrangement and not charge separation, as found in the zwitter ionic species of DHHA (**1d**). Taking all factors including conformational structures, total charges and solvent systems into account, a general guideline concerning the activation energy of DHHA (**1**) in a concerted suprafacial [1,5]-prototropic rearrangement was assembled reaching values from 131 kJ.mol^{-1} for the anionic form of DHHA (**1b**) to 175 kJ.mol^{-1} for cationic DHHA (**1c**), which exhibit approximately the same energy barrier than the conventional cyclohexadiene (**6**).[152,154]

ΔG_{AE}:	anionic **1b**	<	neutral **1a**	≈	zwitter ionic **1d**	<	cationic **1c**	≈	cyclohexadiene (**6**)
	131-141 kJ.mol^{-1}		145-151 kJ.mol^{-1}				161-175 kJ.mol^{-1}		172 kJ.mol^{-1}[152,154]

In collaboration with the research group of Prof. Wulf BLANKENFELDT and in particular Christina DIEDERICH, we achieved a deeper insight into the molecular structure of WT PhzF by X-ray crystallography. The enzyme consists of two independent active sites with mainly four amino acids located around the catalytic center: Serine S213, aspartate D208, histidine H74 and glutamate E45. Additionally, two α-helices surround the active center, whereby the positively polarized ends of both helical dipolar moments are directing towards this cavity.[34,47] This circumstance and an anionic sulfate bound to the active site led to the assumption that the substrate is fixed to the enzyme in its anionic form, which emphasizes the results of former quantum-mechanical calculations for lowering the activation energy in an [1,5]-prototropic rearrangement.

Mutation experiments, however, discovered only one mutant out of several prepared as around four times less active than WT PhzF. It was H74A, in which the histidine H74 was mutated to the smaller and nonpolar alanine. Noteworthy, the free space was filled up with additional crystal H_2O molecules to compensate the functionality of the imidazole moiety in histidine. Every mutant, in which glutamate E45 was substituted by another, but also comparable amino acid, as glutamine or aspartate, the enzyme activity was completely lost indicating the importance of this active site residue. E45 is directly located beneath the hydrogen atom, which migrates in the considered PhzF catalyzed isomerization, contrarily showing strong indication for an acid-base catalyzed mechanism. Apart from that, the distance between the carbon atom, at which the migrating hydrogen atom is bound, and the

oxygen of the E45 is fairly small and accounts for only 2.7 Å (Figure 32).[34] This may indicate an optimized arrangement between substrate and enzyme in a protic transformation, however, the estimated pK_a value of pK_a = 24-30, in reference to wildtype mandelate racemase (WT MR),[223,228,229] is from our point of view too high for an ordinary basic abstraction of the ε-proton in DHHA (1) by E45.
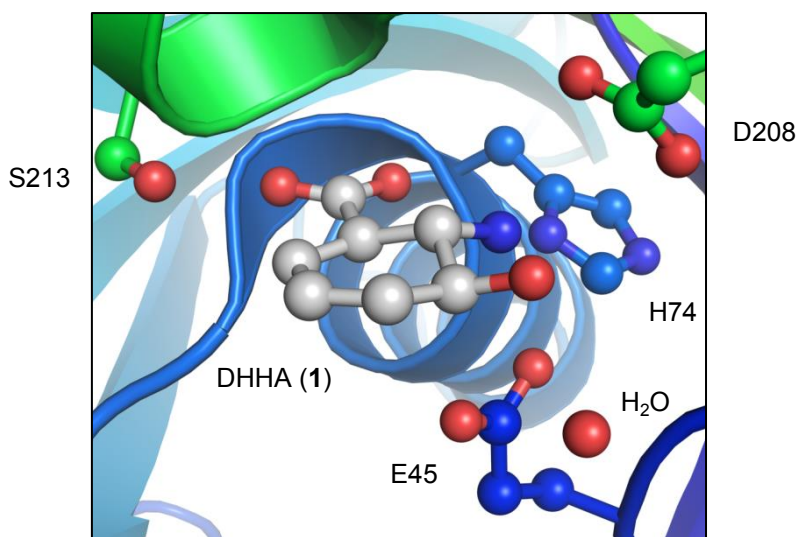
WT PhzF/DHHA (1)

Figure 32: X-ray crystal structure of WT PhzF with its presumably natural substrate DHHA (1) bound to the active site.[34]

The synthesis of mechanistic probes, such as deuterium labeled DHHA (d-DHHA) (5), as well as DHHA derivatives for substrate scope investigations, was essential for the exploration of this highly interesting enzyme mechanism. Most of these compounds were synthesized by adopting a reaction protocol for the synthesis of DHHA (1) published by STEEL in 2003.[172–175] This universal sequence led to the access of synthetical DHHA (1a) in high purity, d-DHHA (5a) (Scheme 33), as well as their *O*-alkylated analogues, such as Me-DHHA (*rac*-41a), Et-DHHA (*rac*-42a) and *n*Pr-DHHA (*rac*-43a) in form of TFA salts (Scheme 34). In addition, H_2-DHHA (34a) was prepared as a competitive inhibitor for obtaining better insight into the binding mode of DHHA (1) by a comparison of 3-hydroxyanthranilic acid (32) and H_2-DHHA (34) in crystal structures with WT PhzF.[34] Unexpectedly, single X-ray crystals with H_2-DHHA (34) were up to now not accessible neither by direct crystallization nor in soaking experiments, presumably caused by the approximately 15 % higher molecular volume of the ring system proved in computations at the mPW1PW91/6-31+G* level of theory.[77–79,150]
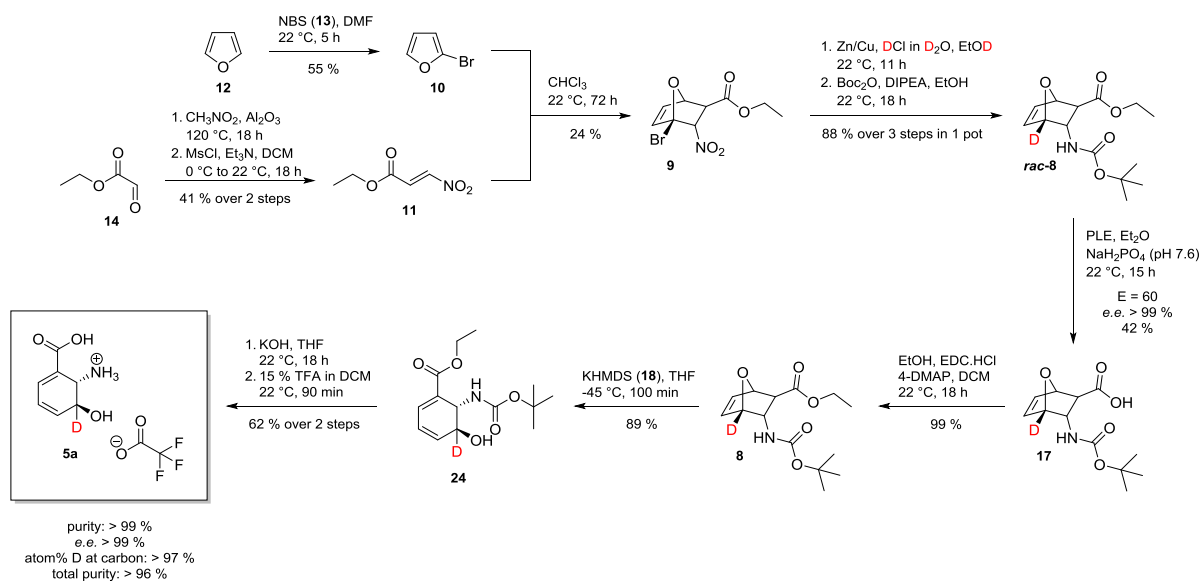
Scheme 33: Reaction sequence for the synthesis of enantiomerically pure d-DHHA in form of a TFA salt **5a** in analogy to the synthesis of DHHA (**1**) published by STEEL.[172–175]
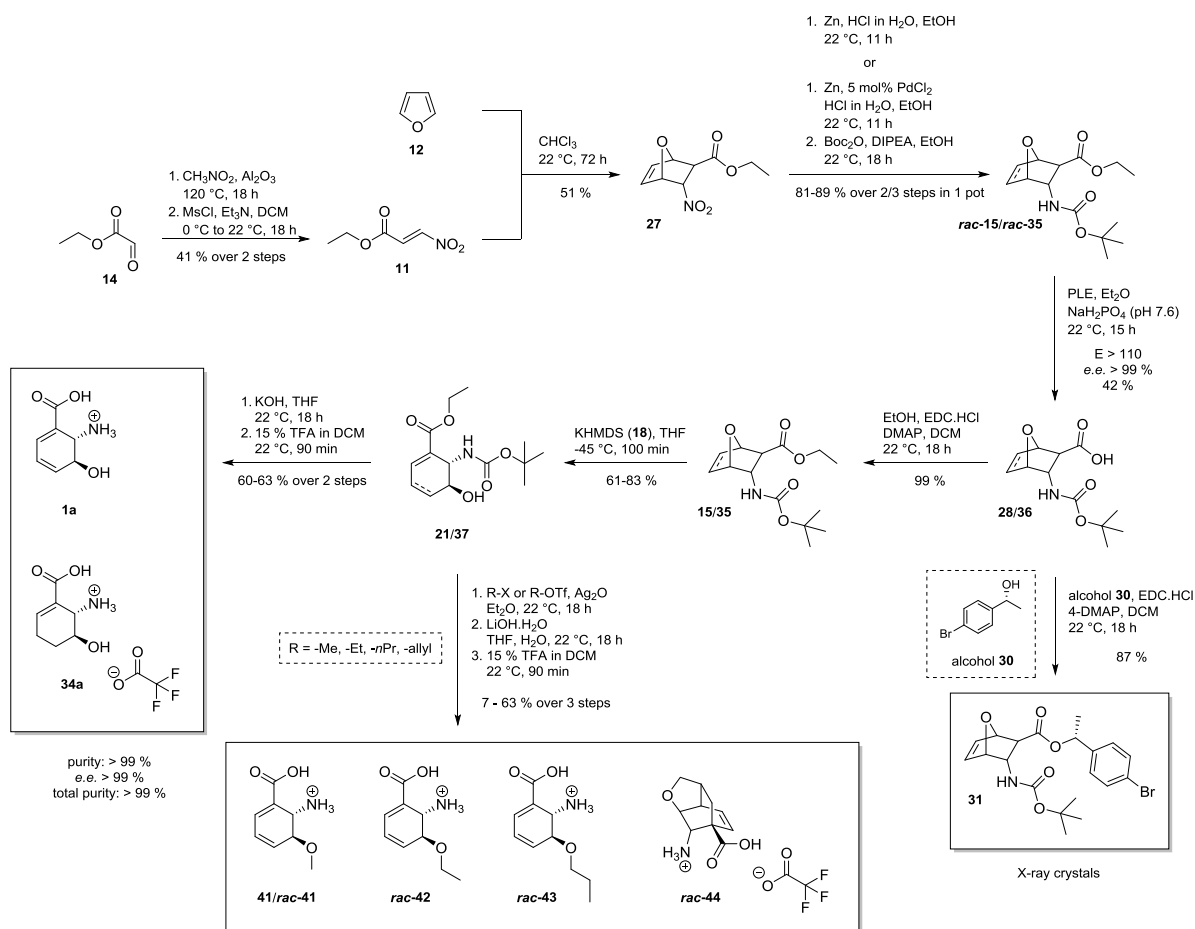
Scheme 34: Reaction sequence for the synthesis of enantiomerically pure DHHA (**1a**), H_2-DHHA (**34a**) and Me-DHHA (**41a**) as well as *O*-alkyl derivatives as racemates, all in form of TFA salts.[172–175]

Time-resolved ^{1}H-NMR analyses with DHHA (**1**) in D_2O as well as cross experiments with d-DHHA (**5**) in H_2O with WT PhzF and H74A, respectively, gave evidence for a quantitative transfer of the hydrogen atom within this isomerization (Figure 33).[34] Enzymatic assay with both compounds, however, did not result in the measurement of reliable enzymatic parameters for calculating a significant primary kinetic isotope effect (1° KIE) so far due to the high instability of formed ketamine **3**. *O*-Alkylated analogues of DHHA overcame this issue of reactiveness by preventing the tautomerization after the enzyme catalyzed isomerization step. Me-DHHA (***rac*-41**) as well as Et-DHHA (***rac*-42**) were likewise recognized and isomerized by WT PhzF, but spontaneous elimination to the corresponding benzoic acid esters were obtained. Similar reaction rates of the enzyme catalyzed isomerization and elimination in Me-DHHA (***rac*-41**) prohibited the exact determination of enzyme-characteristic kinetic parameters, as v_{max}, K_M and k_{cat}, which are essential for calculating 1° KIEs. Gratifyingly, Et-DHHA (***rac*-42**) fulfilled the task of decelerating the enzymatic transformation and becoming rate determining for the validation in upcoming enzymatic assays (Scheme 34).
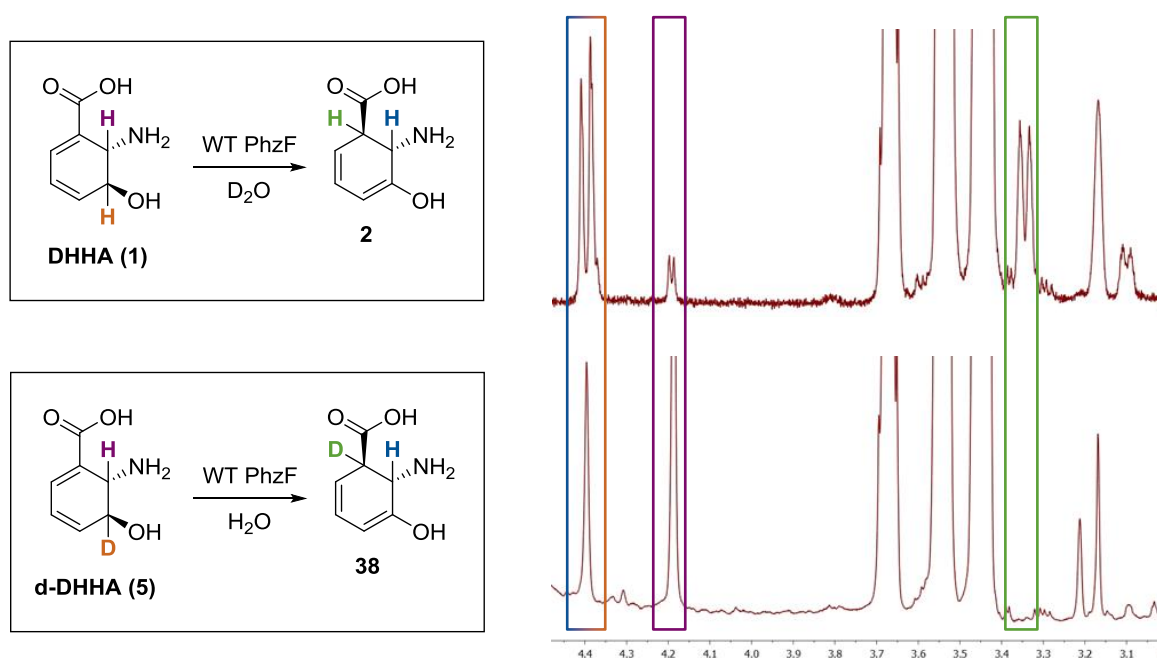
Figure 33: WT PhzF catalyzed isomerization of DHHA (**1**) and d-DHHA (**5**), respectively, as representative for the conserved hydrogen/deuterium migration observed in this enzymatic transformation.
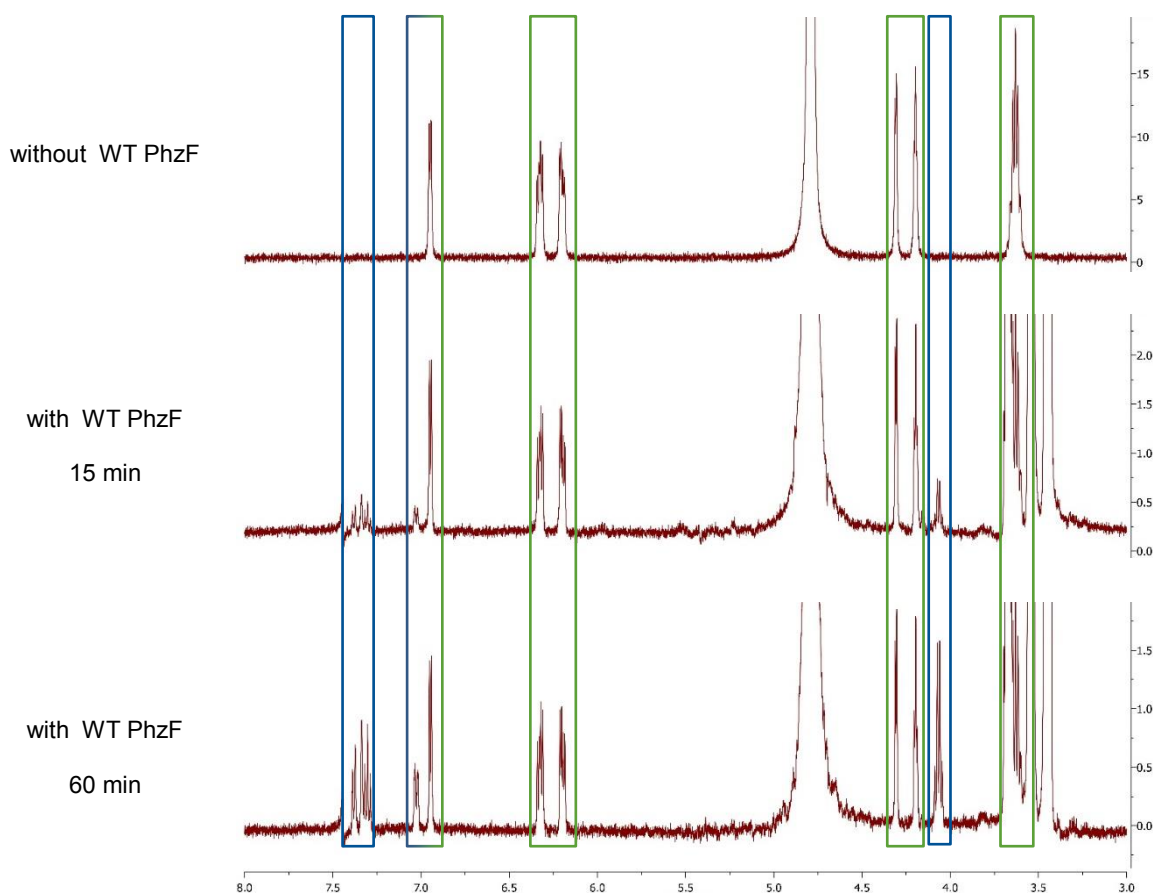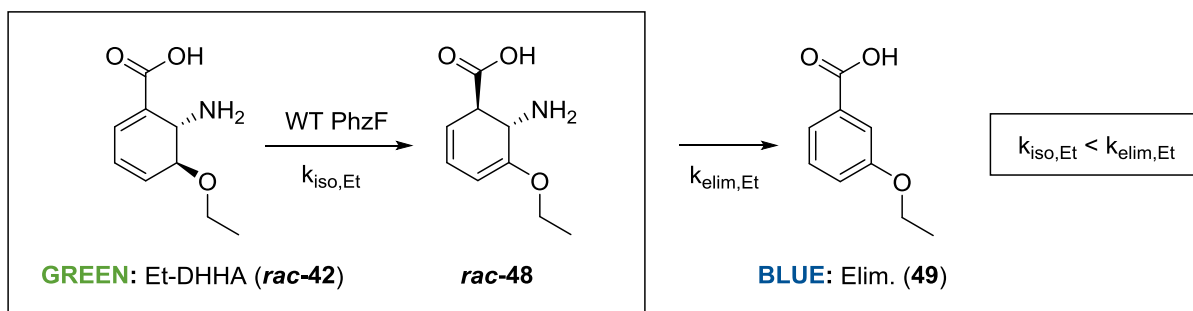
Figure 34: Time-resolved ^{1}H-NMR experiments with Et-DHHA (*rac*-42) and WT PhzF demonstrating the fast interconversion of intermediate *rac*-48 to 3-ethoxybenzoic acid (49) as defined compound of this enzyme catalyzed transformation.

Remarkable for WT PhzF was the observation that this highly specific enzyme similarly converted derivatives of its natural substrate DHHA (1). Substrate scope investigations indicated that only small residues attached to the hydroxy moiety, as in Me-DHHA (*rac*-41) and Et-DHHA (*rac*-42), were successfully isomerized by the enzyme. However, alterations on the amine functionality resulted in an unexpected unreactiveness with WT PhzF. This was impressively demonstrated in experiments with DHHS (51), a gift from Prof. Michael MÜLLER, in which the amine moiety was substituted by another hydroxy residue.[218,240] In other words, the amine in DHHA (1) is essential for enzyme activity either by reasons of binding to the

81

active site or by still unexplored mechanistic effects including basicity or essential enzyme-substrate interactions. In addition, pK_a values for DHHA (**1**) were obtained via standard acid-base titration protocols receiving $pK_a(COOH) = 3.3 \pm 0.4$ and $pK_a(NH_3^+) = 8.6 \pm 0.4$ in the predictable range for β-amino acids. However, the pK_a of the amino moiety seems significantly lowered probably caused by intramolecular hydrogen bond interactions between polar residues within DHHA (**1**).

5.2. *Re*-Face of Enol 2 Affected in the Stereoselective Tautomerization after the Isomerization of DHHA (1)

The tautomerization of enol **2** was explored, which is associated with the WT PhzF catalyzed isomerization of DHHA (**1**). Previous publications of BLANKENFELDT identified an unexpected stereoselective proton migration in the formation of ketamine **3** possibly influenced by solvent accessible amino acid side residues of the catalytic active protein. However, it has not been proven, which face of prochiral enol **2** was affected within this transformation.[34]

In this connection, ^{1}H-NMR analyses in combination with quantum-mechanical computations were performed to elucidate the mentioned stereoselective tautomerization. DHHA (**1**) in $H_2O:D_2O = 9:1$ (v/v) was selected as model system to ensure on the one hand fast interconversion to enol **2** by WT PhzF, on the other hand avoid rapid exchange of α-protons in ketamine **3** compared to experiments in D_2O. The measurement of a nuclear OVERHAUSER effect (NOE)[258,259] between hydrogen H_{C2} and H_{ax} of the involved methylene group provided evidence for a stereoselective *Re*-face protonation in enol **2**, which was in accordance with chemical shifts (δ) calculated for anionic ketamine **3** at the mPW1PW91/IGLO-II//mPW1PW91/6-31+G* level of theory (Figure 35).[77–79,150,184,260]
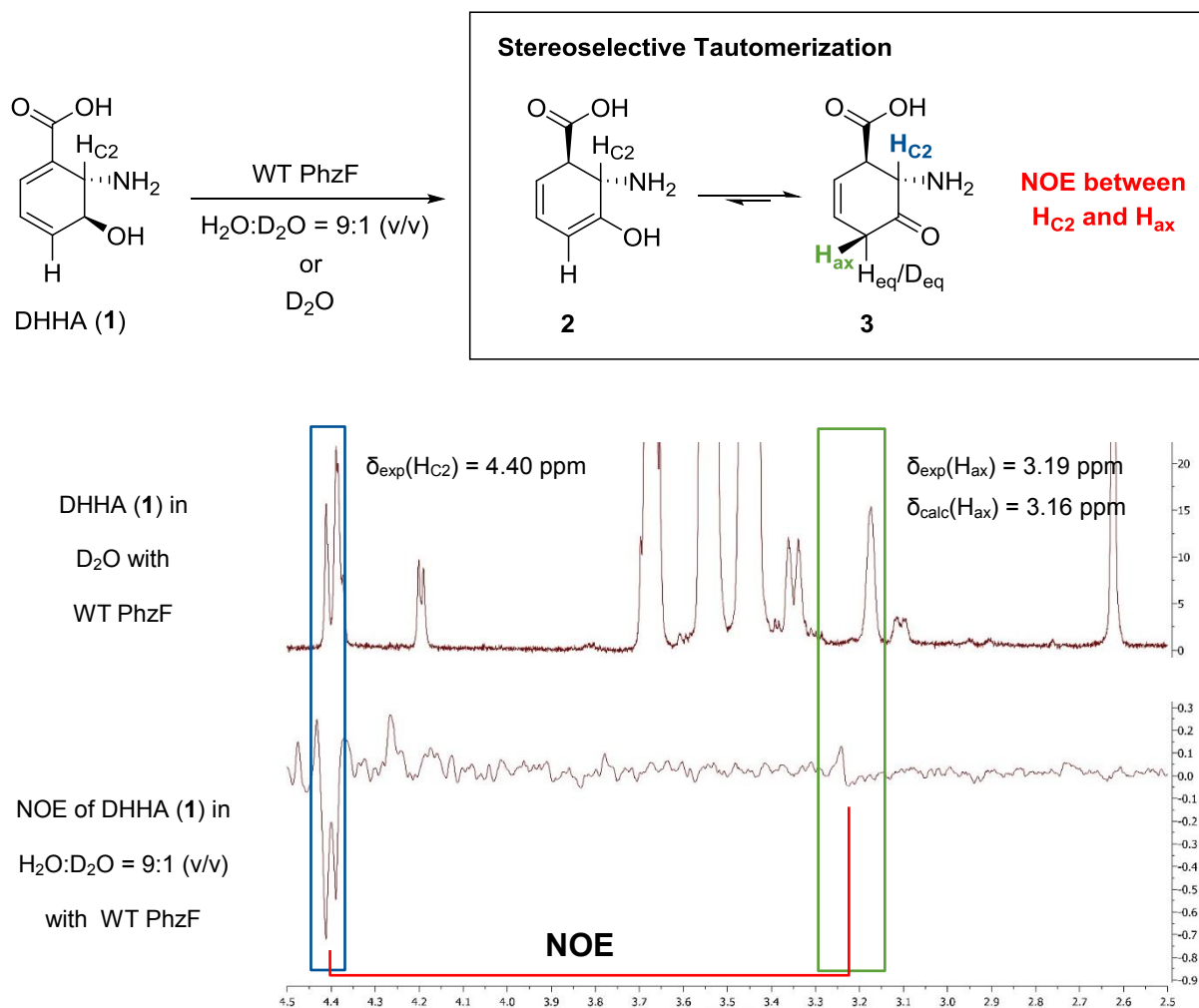
Figure 35: Stereoselective *Re*-face tautomerization of enol **2** proved by a nuclear OVERHAUSER effect (NOE);[258,259] Chemical Shifts (δ) calculated at the mPW1PW91/IGLO-II//mPW1PW91/6-31+G* level of theory[77–79,150,184,260] for anionic ketamine **3**.

6. Outlook

The present thesis demonstrates how delicate the exploration of a reaction mechanism is by combining diverse fields of Chemistry. Several attempts were undertaken to explore the WT PhzF catalyzed isomerization of DHHA (**1**) in the phenazine biosynthesis, but we are not yet able to classify the mechanism of action. It could be illustratively attested that nature developed an efficient catalytic system with a high degree of hydrogen conservation and in addition, collected data does not rule out the possibility of a rare [1,5]-prototropic rearrangement catalyzed by a native enzyme.

Major difficulties were discovered in the assembly of enzymatic assays, which are considered as highly indicatory for supporting enzymatic reaction types. Kinetic studies will not only provide important characteristic parameters, e.g. v_{max}, K_M and k_{cat}, but also allow the direct access to essential 1° KIEs.[4] Although a clear differentiation between both reaction types, the pericyclic and protic mechanism, was made so far, prospective studies should definitely consider the possibility of a mixed reaction form. Maybe WT PhzF managed to overcome the rather large activation barrier for a pericyclic rearrangement with the aid of using the essential glutamate E45 in a base supported, vibrational assisted hydrogen tunneling (VAT).[143,144,157] In this connection, enzymatic assays emerged as method of choice for determining temperature dependencies of 1° KIEs, which are usually indicative for quantum-mechanical effects, such as VAT.[142,144,145,157,261]

Based on described results and the solved X-ray crystal structure of WT PhzF,[34] QM/MM calculations[124,158] are currently performed in the research group of Prof. Matthias ULLMANN simulating the isomerization behavior of DHHA (**1**) in WT PhzF.[122,123,130] Due to the large enhancements of these methods in recent years,[123–128,130] gained results would allow trustworthy insights into the existing isomerization process. However, we recommend to consider and include also mentioned quantum-mechanical effects into these computations, which were proven to be existent in several enzymatic hydrogen transfer reactions, and to determine how these would affect the conversion of DHHA (**1**).

7. Experimental Section

7.1. Quantum-Mechanical Calculations

Supplementary computational studies were executed on a computing cluster with blade architecture using the Gaussian09 software package.[262] For every listed calculation mPW1PW91 was used as a hybrid DFT functional together with the 6-31+G* basis set of POPLE and coworkers on all atoms.[77–79,150] Molecular geometries were fully optimized in the gas phase and minimum structures were characterized by harmonic frequency calculations. Solvent effects were simulated by using either the polarized continuum model (PCM)[153] or by surrounding five H_2O molecules to imitate the solvent. Single point calculations were performed on optimized geometries. In the case of NMR calculations, IGLO-II basis sets in combination with the mPW1PW91 functional were used and chemical shifts were referenced to tetramethylsilane (TMS).[184,260] All structures were visualized using the Gabedit software package.[263]

For a complete set of computational studies concerning the [1,5]-prototropic rearrangement in DHHA (**1**) see Mario LEYPOLD's MSc thesis "Studien zur Synthese von mechanistischen Sonden des PhzF-Proteins". Herein, all calculated minimum structures, transition states, activation energies ΔG_{AE} and simulations in solvent systems for different ionization states of DHHA (**1**) are listed.[152]

7.2. General Aspects

All commercially available reagents and solvents were purchased from Sigma-Aldrich, Alfa, Aesar, ABCR, Fisher Scientific, Acros Organics, Roth or VWR, were of reagent grade or better and were used without further purification except otherwise stated. When it was required, e.g. with ethereal solvents, non-dry solvents were distilled before use. If reactions were performed under inert conditions, e.g. exclusion of water, oxygen of both, all experiments were carried out using classical Schenk techniques. Herein solvents were dried and/or degassed with common methods and afterwards stored under inert gas atmosphere (argon or N_2) over molecular sieves. In some cases, when explicitly mentioned, dry solvents were received from the mentioned suppliers. In general, when high vacuum was stated in experimental procedures, typically a vacuum of 10^{-2}-10^{-3} mbar was applied. All reactions were stirred with Teflon-coated magnetic stirring bars unless otherwise stated.

Degassing of solvents was performed by applying two different procedures. For small amounts of solvents (10 mL or less) vacuum was subjected to an appropriate reaction vessel, the solvent was frozen in liquid N_2, warmed to RT until the solvent or reaction mixture started to boil and was afterwards purged with an inert gas. This procedure was repeated at least for three times, depending also on the solvent volume. Larger amounts of solvents were degassed by bubbling argon from a balloon via cannula through the solvent during ultrasonification for about 20 min.

Molecular sieves (Sigma-Aldrich, beads with 8-12 mesh) were activated in a round-bottom flask with a gas inlet adapter by heating them carefully in a heating mantle at level 1 for approximately 12 h under high vacuum until complete dryness was obtained. These activated molecular sieves were stored at RT under argon atmosphere.

In general, temperatures were measured externally if not otherwise stated. When working at a temperature of 0 °C, an ice-water bath served as the cooling medium. Lower temperatures were achieved by either using an acetone/dry ice cooling bath or a cryostatic temperature regulator. Reactions, which were carried out at higher temperatures than RT, were heated in a silicon oil bath on a heating plate (RCT basic IKAMAG® safety control, 0-1500 rpm) equipped with an external temperature controller.

Solvents and chemicals listed below were prepared according to the following procedures:

Acetonitrile (MeCN): Anhydrous MeCN stored over 3 Å MS was purchased from Acros Organics. It was transferred into an amber 1000 mL Schenk bottle and stored over activated 3 Å MS under argon atmosphere (water content according to specification: <100 ppm).

Chloroform (CHCl$_3$): Anhydrous CHCl$_3$ stored over 4 Å MS (stabilized with amylene) was purchased from Acros Organics. It was transferred into an amber 1000 mL Schenk bottle and stored over activated 4 Å MS under argon atmosphere (water content according to specification: <50 ppm).

Dichloromethane (DCM): Anhydrous DCM was produced by pre-drying EtOH stabilized DCM over P_4O_{10} and afterwards heating it under reflux over CaH_2 for 24 h under argon atmosphere. It was distilled in an amber 1000 mL Schlenk bottle over activated 4 Å MS and under argon atmosphere.

Diethylether (Et$_2$O): Anhydrous Et$_2$O was produced by heating it over Na under reflux for 24 h under argon atmosphere until benzophenone indicated its dryness by turning into deep blue color. It was distilled over a 20 cm Vigreux column and immediately used afterwards.

***N,N*-Dimethylformamide (DMF):** Anhydrous DMF stored over 3 Å MS was purchased from Acros Organics. It was transferred into an amber 1000 mL Schenk bottle and stored over activated 3 Å MS under argon atmosphere (water content according to specification: <50 ppm).

Tetrahydrofuran (THF): Anhydrous THF was produced by heating it over Na under reflux for 48 h under argon atmosphere until benzophenone indicated its dryness by turning into deep blue color. It was distilled into an amber 1000 mL Schlenk bottle and stored over 4 Å MS and under argon atmosphere.

The following solvents were used in reactions as well as workup processes, which were directly performed under atmospheric conditions: Cyclohexane, dichloromethane (DCM) ethyl acetate (EtOAc) and methanol (MeOH) purchased from VWR or Fisher Scientific, diethylether (Et_2O), ethanol (EtOH) and tetrahydrofuran (THF) purchased from Roth as well as acetonitrile (MeCN) purchased from Riedel-de Haën. All solvent were used without further purification except Et_2O and THF. These two were distilled before use and stored over solid KOH in amber light glass bottles.

Saturated NaCl solution (brine): Solid NaCl was dissolved in H_2O until remaining solid was left.

Saturated $NaHCO_3$ solution: Solid $NaHCO_3$ was dissolved in H_2O until remaining solid was left.

Half saturated $NaHCO_3$ solution: Saturated $NaHCO_3$ solution was diluted with an equal volume of H_2O.

Saturated Na_2CO_3 solution: Solid Na_2CO_3 was dissolved in H_2O until remaining solid was left.

7.2.1. Thin Layer Chromatography (TLC)

Analytical thin layer chromatography (TLC) was carried out on Merck TLC silica gel aluminium sheets (silica gel 60, F_{254}, 20 x 20 cm). All separated compounds were visualized by UV light (λ = 254 nm and/or λ = 366 nm) and by the listed staining reagents followed by the development in the heat. Eluents and R_f-values are stated in the experimental descriptions.

Iodine (I_2 adsorbed on silica gel): Powdered iodine was mixed in a TLC chamber with silica gel.

Cerium ammonium molybdate (CAM): 50 g $(NH_4)_6Mo_7O_{24}$ were dissolved in 400 mL H_2O and afterwards 50 mL conc. H_2SO_4 as well as 2.0 g $Ce(SO_4)_2$ were added, respectively.

Potassium permanganate ($KMnO_4$): 0.3 g $KMnO_4$ as well as 20 g K_2CO_3 were dissolved in 300 mL H_2O and afterwards 5.0 mL 5 % aqueous NaOH were added.

7.2.2. Flash Column Chromatography

Flash column chromatography was performed on silica gel 60 from Acros Organics with particle sizes between 35 µm and 70 µm. Depending on the problem of separation, a 30 to 100 fold excess of silica gel was used with respect to the dry amount of crude material. The crude material was either dissolved in the eluent or in the case of an insoluble sample, it was dissolved in an appropriate solvent (EtOAc or DCM) and subsequently adsorbed on the 1.5 fold excess of silica gel. Afterwards the solvent was removed on a rotary evaporator and the adsorbed crude material dried under high vacuum. The dimension of the column was adjusted to the required amount of silica gel and formed a pad between 10 cm and 30 cm. In general, the silica gel was mixed with the eluent and the column was equilibrated. Subsequently, the dissolved or adsorbed crude material was loaded onto the top of the silica gel and the mobile phase was forced through the column using a rubber bulb pump. The volume of each collected fraction was adjusted between 20 % and 40 % of the silica gel volume.

7.2.3. Gas Chromatography with Mass Selective Detection (GC-MS)

GC-MS analyses were performed on an Agilent Technologies 7890A GC system equipped with a 5975C mass selective detector (inert MSD with Triple Axis Detector system) by electron-impact ionization (EI) with a potential of E = 70 eV. Herein, the samples were separated depending on their boiling point and polarity. The desired crude materials or pure compounds were dissolved either in DCM or EtOAc and the solutions were injected by employing the autosampler 7683B in a split mode 1/20 (inlet temperature: 280 °C; injection volume: 0.2 µL). Separations were carried out on an Agilent Technologies J&W GC HP-5MS capillary column ((5 %-phenyl)methylpolysiloxane, 30 m x 0.2 mm x 0.25 µm) with a constant helium flow rate (He 5.0 (Air Liquide), 1.085 mL.min^{-1}, average velocity: 41.6 cm.s^{-1}). A general gradient temperature method was used:

Method_GENERAL: initial temperature: 50 °C for 1 min, linear increase to 300 °C (40 °C.min^{-1}), hold for 5 min, 1 min post-run at 300 °C, detecting range: 50.0-550.0 amu, solvent delay: 2.80 min.

The conversion of starting material and/or product formation was determined by integrating the areas of the desired signals. All given values are only relative values due to the fact that no internal standard was used in all performed experiments. Retention times as well as relative intensities related to the basis peak are listed in the experimental procedures of the purified compounds.

7.2.4. High Performance Liquid Chromatography (HPLC)

Analytical HPLC-MS measurements were performed on a Shimadzu Nexera LCMS-2020 system (CBM-20A Prominence system controller, Nexera SIL-30AC autosampler, DGU-20A3 and DGU-20A5 on-line degassers, Nexera LC-30AD binary pump, FCV-20AH2 valve unit, CTO-20AC Prominence column oven, SPD-M20A Prominence photodiode array (PDA) detector (deuterium lamp, tungsten lamp, 190-800 nm)) equipped with single quadrupole ultra-fast LC/MS detector "LCMS-2020". Analytes were ionized using an electrospray ionization source (ESI) in the positive and/or negative mode. All of these separations were carried out on a reversed phase Agilent Poroshell 120 SB-C18 (100 x 3.0 mm, 2.7 µm) column equipped with a Merck LiChroCART® 4-4 pre-column. Samples were either dissolved in MeCN or MeOH and in the case of undissolved particles the suspension was filtered through syringe filters. The following methods were used for the separation:

Method_GENERAL: 0.0-0.5 min 70 % H$_2$O + 0.01 % HCOOH/30 % MeCN, 0.5-6.5 min linear gradient to 100 % MeCN, 6.5-7.2 min 100 % MeCN; 0.70 mL.min^{-1}; 40 °C.

Method_ESTER: 0.0-5.0 min 60 % H$_2$O + 0.01 % HCOOH/40 % MeCN, 5.0-5.1 min linear gradient to 100 % MeCN, 5.1-5.7 min 100 % MeCN; 0.70 mL.min^{-1}; 40 °C.

Method_IMIDE: isocratic with H$_2$O:MeCN = 95:5 + 0.01 % HCOOH (v/v/v); 0.70 mL.min^{-1}; 40 °C; 290 bar.

Method_MARFEY_A: 0.0-2.5 min 65 % H$_2$O + 0.01 % HCOOH/35 % MeCN, 2.5-2.6 min linear gradient to 100 % MeCN, 2.6-3.0 min 100 % MeCN; 0.70 mL.min^{-1}; 40 °C.

Method_MARFEY_B: 0.0-5.5 min 70 % H_2O + 0.01 % HCOOH/30 % MeCN, 5.5-5.6 min linear gradient to 100 % MeCN, 5.6-6.0 min 100 % MeCN; 0.70 mL.min^{-1}; 40 °C.

The determination of the enantiomeric excess was performed on an Agilent 1100 Series HPLC system equipped with a temperature controlled column oven. The separations were carried out on a chiral Daicel Chemical Industries Chiralpak® AD-H column (4.6 x 250 mm, 5.0 μm) for Method_ACID as well as Method_ESTER and on a chiral Daicel Chemical Industries Chiralcel® OD-H column (4.6 x 250 mm, 5.0 μm) for Method_IMIDE. Signals were detected using an Agilent Technologies 1200 Series MWD SL UV detector at λ = 210 nm. The following methods were used for performing the separations.

Method_ACID: isocratic with *n*-heptane:EtOH = 85:15 + 0.01 % TFA (v/v/v); 1.00 mL.min^{-1}; 15 °C; 65 bar.

Method_ESTER: isocratic with *n*-heptane:EtOH = 85:15 (v/v); 1.00 mL.min^{-1}; 15 °C; 65 bar.

Method_IMIDE: isocratic with *n*-heptane:2-PrOH = 75:25 (v/v); 0.80 mL.min^{-1}; 15 °C; 57 bar.

7.2.5. Nuclear Magnetic Resonance Spectroscopy (NMR)

^{1}H- and ^{13}C-NMR spectra were recorded on a Bruker AVANCE III 300 spectrometer (^{1}H: 300.36 MHz; ^{13}C: 75.53 MHz) with autosampler and ^{1}H-, ^{13}C- and ^{19}F-NMR spectra on a Varian Unity Inova 500 spectrometer (^{1}H: 499.88 MHz; ^{13}C: 125.69 MHz, ^{19}F: 470.35 MHz). Chemical shifts were either referenced to tetramethylsilane as internal standard or to the residual proton and carbon signal of the deuterated solvent (CDCl$_3$: δ = 7.26 ppm (^{1}H), 77.16 ppm (^{13}C); DMSO-d$_6$: δ = 2.50 ppm (^{1}H), 39.52 ppm (^{13}C)). Chemical shifts δ are given in ppm (parts per million) and coupling constants *J* in Hz (Hertz). If necessary, 1D spectra (APT and NOESY) as well as 2D spetra (HH-COSY, HSQC and HMBC) were recorded for the identification and confirmation of the structure. Signal multiplicities are abbreviated as s (singlet), bs (broad singlet), d (doublet), dd (doublet of doublet), ddd (doublet of doublet of doublet), td (triplet of doublet), t (triplet), dt (doublet of triplet), q (quadruplet), dq (doublet of quadruplet), p (pentet), h (hexet) and m (multiplet). Additionally, quarternary carbon atoms are designated as C$_q$. Deuterated solvents for nuclear resonance spectroscopy were purchased from euriso-top®. CDCl$_3$ was neutralized by filtering it through basic Alox (aluminium oxide activiated, basic type 5016A, 58 Å, particle size: 150 mesh, Brockmann Grade I) from Acros Organics.

7.2.6. High Resolution Mass Spectrometry (HRMS)

HRMS spectra were recorded in the research group of Prof. Robert SAF (ICTM, TU Graz) on a "Waters Micromass GCT Premier" system. Ionization was realized by an electron impact source (EI ionization) at a constant potential of 70 eV. Herein, individual samples were either inserted directly (direct inlet electron impact ionization; DI-EI) or prior to this gas chromatographically separated on a "Hewlett Packard BC 7890A" system. Molecule ions were analyzed by a time-of-flight (TOF) mass analyzer in the positive mode (TOF MS EI+). Besides molecular formulas, calculated as well as determined *m/z* ratios of each molecule peak are denoted.

7.2.7. Determination of Melting Points

Melting points were determined on a Mel-Temp® melting point apparatus from Electrothermal with an integrated microscopical support. They were measured in open capillary tubes with a mercury-in-glass thermometer and were not corrected.

7.2.8. Specific Optical Rotation

The specific optical rotation was determined on a Perkin Elmer Polarimeter 341 with an integrated sodium vapor lamp. All samples were measured at the D-line of the sodium light (λ = 589 nm) under non-tempered conditions between 25 °C and 34 °C. Concentrations between 5.0 g.L^{-1} (c = 0.50) and 10.0 g.L^{-1} (c = 1.00) depending on the solubility of the sample were chosen, whereas MeCN, CHCl$_3$, H$_2$O, MeOH and DMSO were used as solvents. All solvents were either purchased from Sigma-Aldrich or Fluka and had HPLC quality or higher.

7.2.9. Titration of Stock Solutions

Diverse stock solutions had to be titrated before their use in order to determine their exact concentration. Due to their sensitivity to hydrolysis of several reagents, some of these titrations had to be carried out under inert conditions in oven-dried, evacuated and argon purged Schlenk flaks. Each titration was performed at least for three times, whereas the mean value of the determined concentration was taken for further experiments. The prepared stock solutions were immediately used after their titration.

7.2.10. Titration of *n*-Butyllithium (*n*BuLi in *n*-Hexane)

Literature: W. G. Kofron, L. M. Baclawski, *J. Org. Chem.* **1976**, *41*, 1879-1880.

An oven-dried, evacuated and argon purged 15 mL Schlenk flask was charged with 400 mg (1.89 mmol, 1.0 eq) diphenylacetic acid. It was dissolved in 4.0 mL anhydrous THF and afterwards titrated with *n*BuLi in *n*-hexane via septum and syringe until a color change to a yellow suspension was maintained.

Concentration: 2.04 M.

7.2.11. Titration of KHMDS (18) in THF

Literature: R. E. Ireland, R. S. Meissner, *J. Org. Chem.* **1991**, *56*, 4566-4568.

An oven-dried, evacuated an argon purged 8 mL Schlenk flask was charged with 200 μL of the yellow 2-(6-butyl-1,6-dihydropyridin-2-yl)pyridine (**23**) solution (for preparation see chapter 7.3.3.). It was diluted with 1.0 mL of anhydrous THF and one droplet of KHMDS solution was added to eliminate the background noise, whereas a red solution was formed. Subsequently one droplet of a 1.0 M 2-butanol solution (in toluene) was added and afterwards exactly 2.0 mL of the KHMDS solution. The red solution was titrated via septum and syringe with the 1.0 M 2-butanol solution (in toluene) under vigorously stirring until a grey to yellowish suspension was formed indicating the equivalence point.

Concentration: 0.76 M.

7.2.12. Enzyme Catalyzed Reactions

Kinetic resolution experiments were performed with pig liver esterase (PLE) purchased from Fluka as a technical precipitate in a half saturated $(NH_4)_2SO_4$ solution. In order to provide a constant pH value, 100 mM NaH_2PO_4/Na_2HPO_4 buffer was added, which was prepared according to the following procedure.

> **100 mM NaH_2PO_4/Na_2HPO_4 buffer (pH 7.6):** 12.0 g solid and anhydrous NaH_2PO_4 purchased from Fluka were dissolved in 1.0 L deionized water and afterwards a 3.0 M NaOH solution was added under vigorously stirring until a calibrated pH-meter indicated pH 7.6.

7.2.13. Derivatization with MARFEY's reagent (25)

All mentioned stock-solutions were prepared with H_2O as a solvent. In a 1 mL Eppendorf vial 5 µL of a 22 mM ammonium salt stock-solution of compound **1a**, **5a**, **34a** and **41a** were converted with 20 µL of a 10 mM (*S*)-2-((5-fluoro-2,4-dinitrophenyl)amino)propanamide stock-solution (MARFEY's reagent). 2 µL 1 M $NaHCO_3$ were added to the yellow solution and the closed Eppendorf vial was mixed on a tempered shaker at 45 °C for 90 min. Afterwards the yellow solution was cooled to RT, acidified with 1 µL 2 M H_2SO_4 and diluted with 50 µL H_2O.

7.2.14. Trituration for the Purification of Polar Compounds

For purification purpose different polar compounds were suspended in proper solvents or solvent mixtures. These suspensions were ultrasonicated for 30 min and subsequently cooled in an ice-water bath to 0 °C. The solids were collected by filtration, washed with the same cold solvent or solvent mixture and finally dried under high vacuum.

7.3. Experimental Procedures

7.3.1. Recrystallization of *N*-Bromosuccinimide (NBS) (13)
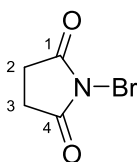
13

A 1000 mL round-bottom flask equipped with a Teflon-coated magnetic stirring bar and reflux condenser was charged with 50.0 g (281 mmol) *N*-bromosuccinimide (NBS) (**13**). 450 mL H_2O were added and the orange suspension was heated under reflux until NBS (**13**) was completely dissolved. Afterwards the orange solution was cooled to ambient temperature and subsequently in an ice-water bath to 0 °C. The colorless crystals were collected by filtration, washed with cold H_2O (2 x 50 mL) and Et_2O (1 x 50 mL), respectively, and finally dried under high vacuum.

Yield: 31.7 g (178 mmol, 63 %); colorless crystals.

^{1}H-NMR (300.36 MHz, $CDCl_3$): δ = 2.96 (s, 4H, H-2, H-3).

^{13}C-NMR (75.53 MHz, CDCl$_3$): δ = 173.2 (C$_q$, C-1, C-4), 28.8 (C-2, C-3).

7.3.2. Potassium hexamethyldisilazide (KHMDS) (18)

18
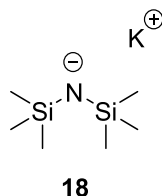
Literature: J. Åhman, P. Somfai, *Synth. Comm.* **1995**, *25*, 2301-2303.

An oven-dried, evacuated and argon purged 100 mL three-necked round-bottom flask equipped with a Teflon-coated magnetic stirring bar, gas inlet adapter, reflux condenser and bubbler was charged with 2.36 g (20.6 mmol, 1.1 eq) KH suspension (35 % (w/w) in mineral oil). It was dispersed in 10 mL anhydrous *n*-hexane, the supernatant was removed and the remaining solid was washed with *n*-hexane (3 x 5 mL) as described above. Afterwards the greyish solid was carefully dried under high vacuum, diluted with 20 mL anhydrous THF and 3.8 mL (18.4 mmol, 1.0 eq) 1,1,1,3,3,3-hexamethyldisilazane were added in one portion. The greyish suspension was ultrasonicated in an oil bath for 4 h under argon atmosphere. After a short induction time, heavily gas bubbling was observed and a yellowish suspension was formed. Subsequently, the yellowish suspension was allowed to stand at RT under argon atmosphere for 15 h and the supernatant was transferred into an oven-dried, evacuated and argon purged 80 mL Schlenk flask by cannuling. It can be stored in a freezer at -24 °C under argon atmosphere for several weeks without significant degradation, but has to be titrated before use.

Concentration: 0.76 M (after titration with 1.0 M 2-butanol (in toluene) and 2-(6-butyl-1,6-dihydropyridin-2-yl)pyridine (**23**) in THF as indicator solution).

7.3.3.   2-(6-Butyl-1,6-dihydropyridin-2-yl)pyridine (23)
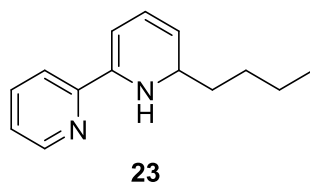
23

Literature: R. E. Ireland, R. S. Meissner, *J. Org. Chem.* **1991**, *56*, 4566-4568.

An oven-dried, evacuated and argon purged 15 mL Schlenk flask equipped with a Teflon-coated magnetic stirring bar was charged with 5.0 mg (32 µmol, 1.0 eq) 2,2'-bipyridine. It was dissolved in 3.0 mL anhydrous THF and 63 µL (128 µmol, 4.0 eq) *n*BuLi (2.04 M in *n*-hexane) were added over a period of 5 min via septum and syringe under argon atmosphere at RT, which resulted in the formation of a deeply red colored solution. Afterwards 1.0 M 2-butanol (in toluene) was dropwise added under vigorous stirring until a yellowish solution was consistent, which was immediately used after this preparation.

7.3.4.   2-Bromofuran (10)

10
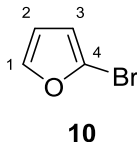
Literature: M. A. Raheem, J. R. Nagireddy, R. Durham, W. Tam, *Synth. Comm.* **2010**, *40*, 2138-2146.

An oven-dried, evacuated and argon purged 250 mL three-necked round-bottom flask equipped with a Teflon-coated magnetic stirring bar, gas inlet adapter, 100 mL dropping funnel, internal thermometer and bubbler was charged with 15.3 g (225 mmol, 2.0 eq) furan (**12**), which was subsequently dissolved in 40 mL anhydrous DMF. Afterwards a deep orange solution consisting of 20.0 g (112 mmol, 1.0 eq) NBS (**13**) in 60 mL anhydrous DMF was added via the dropping funnel at RT over a period of 50 min. The temperature did not exceed 35 °C, whereas the brownish reaction mixture was vigorously stirred at RT for additional 5 h. Afterwards the brown solution was concentrated on a rotary evaporator (10 mbar, 35 °C) to remove the excess of unreacted furan (**12**). The remaining solution was purified by water steam distillation. Therefore the storage vessel filled with H_2O was heated in an oil bath to 140 °C, the brown solution, however, in a second oil bath to 105 °C. Due to contamination with furan (**12**), the first few drops of condensate were discarded. The collected colorless condensate was washed with H_2O (1 x 30 mL) to remove residual DMF and finally the

colorless, clear product was stored in an inert 25 mL Schlenk flask over dried K_2CO_3 under argon atmosphere in a freezer at -20 °C for several weeks.

Yield: 9.03 g (61.4 mmol, 55 %); clear, colorless liquid.

C_4H_3BrO [146.97 g.mol^{-1}].

b_p = 65-67 °C (350 mbar).

^{1}H-NMR (300.36 MHz, CDCl$_3$): δ = 7.43-7.42 (m, 1H, H-1), 6.38-6.36 (m, 1H, H-2), 6.31-6.30 (m, 1H, H-3).

^{13}C-NMR (75.53 MHz, CDCl$_3$): δ = 144.5 (C-1), 122.1 (C$_q$, C-4), 112.6 (C-2), 111.3 (C-3).

7.3.5. Ethyl 2-hydroxy-3-nitropropanoate (69)

69
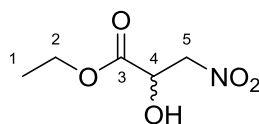
Literature: J. K. Addo, P. Teesdale-Spittle, J. O. Hoberg, *Synthesis* **2005**, 12, 1923-1925.

An oven-dried 100 mL two-necked round-bottom flask equipped with a Teflon-coated magnetic stirring bar, reflux condenser and a CaCl$_2$ drying tube was charged with 15.0 g (73.5 mmol, 1.0 eq) ethyl glyoxalate solution (~50 % (w/w) in toluene). It was dissolved in 35 mL nitromethane and 15.0 g Al$_2$O$_3$ (neutral, activated, Brockmann Grade I) were added to the colorless solution. The resulting yellowish suspension was heated under reflux in an oil bath at 120 °C for 18 h. Afterwards the resulting orange suspension was cooled down to RT, filtered through a pad of Celite$^®$ (diameter: 8.0 cm, height: 4.0 cm) and the filter cake was washed with EtOAc (4 x 30 mL) in order to elute the whole amount of product. The solvent of the orange solution was evaporated on a rotary evaporator and the brownish, oily crude material was purified via flash column chromatography (520 g SiO$_2$, 22.0 x 8.0 cm, eluent: cyclohexane:EtOAc = 2:1 (v/v), R$_f$ = 0.26). Finally, the light orange, needle shaped crystals were dried under high vacuum.

Yield: 7.78 g (48.2 mmol, 66 %); light orange, needle shaped crystals.

$C_5H_9NO_5$ [163.13 g.mol^{-1}].

R$_f$ = 0.26 (cyclohexane:EtOAc = 2:1 (v/v), UV and CAM).

m_p = 41-42 °C.

GS-MS (METHOD_GENERAL): t_R = 4.61 min; *m/z* = 116 (6 %), 100 (6 %), 90 (53 %), 71 (38 %), 62 (100 %).

^{1}H-NMR (300.36 MHz, CDCl$_3$): δ = 4.77 (d, $^3J_{HH}$ = 4.2 Hz, 2H, H-5), 4.63 (q, $^3J_{HH}$ = 4.3 Hz, 1H, H-4), 4.40-4.29 (m, 2H, H-2), 3.40 (d, $^3J_{HH}$ = 4.7 Hz, 1H, OH), 1.33 (t, $^3J_{HH}$ = 7.2 Hz, 3H, H-1).

^{13}C-NMR (75.53 MHz, CDCl$_3$): δ = 170.8 (C$_q$, C-3), 76.9 (C-5), 67.7 (C-4), 63.3 (C-2), 14.2 (C-1).

7.3.6. Ethyl (*E*)-3-nitroacrylate (11)
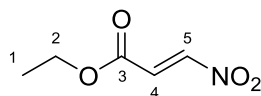
11

An oven-dried, evacuated and argon purged 500 mL three-necked round-bottom flask equipped with a Teflon-coated magnetic stirring bar and gas inlet adapter was charged with 8.00 g (49.0 mmol, 1.0 eq) ethyl 2-hydroxy-3-nitropropanoate (**69**), which was dissolved in 100 mL anhydrous DCM. The yellowish solution was cooled in an acetone/dry ice bath to -20 °C. Consecutively, 11.4 mL (147 mmol, 3.0 eq) methanesulfonyl chloride (MsCl) and 20.9 mL (147 mmol, 3.0 eq) Et$_3$N were added via a syringe and septum over a period of 15 min each and the brownish suspension was vigorously stirred at -20 °C for additional 3 h. Afterwards the suspension was poured into 450 mL ice-cooled H$_2$O, warmed to ambient temperature and stirred for 15 min. The phases were separated and the yellow aqueous phase was extracted with DCM (3 x 100 mL). The combined brownish organic layers were washed with H$_2$O (3 x 150 mL) and brine (1 x 150 mL), dried over MgSO$_4$, filtered and the solvent was removed under reduced pressure on a rotary evaporator. Finally, the brownish, liquid crude material was purified by fractional distillation (38-39 °C, 0.52 mbar) and the residual MsCl was carefully removed by drying the intensively yellow colored liquid at 1.0 mbar at RT for 15 h.

Yield: 4.34 g (29.9 mmol, 61 %); yellow, penetrative smelling liquid.

C$_5$H$_7$NO$_4$ [145.11 g.mol^{-1}].

R_f = 0.26 (cyclohexane:EtOAc = 12:1 (v/v), UV and CAM).

b_p = 38-39 °C (0.52 mbar).

GS-MS (METHOD_GENERAL): t_R = 3.94 min; *m/z* = 118 (5 %), 100 (100 %), 85 (19 %), 71 (12 %), 53 (52 %).

^{1}H-NMR (300.36 MHz, CDCl$_3$): δ = 7.67 (d, $^3J_{HH}$ = 13.5 Hz, 1H, H-5), 7.08 (d, $^3J_{HH}$ = 13.5 Hz, 1H, H-4), 4.32 (q, $^3J_{HH}$ = 7.1 Hz, 2H, H-2), 1.34 (t, $^3J_{HH}$ = 7.1 Hz, 3H, H-1).

^{13}C-NMR (75.53 MHz, CDCl$_3$): δ = 162.8 (C$_q$, C-3), 149.1 (C-5), 127.8 (C-4), 62.6 (C-2), 14.2 (C-1).

7.3.7. Ethyl (1*R*,2*S*,3*S*,4*R*)-4-bromo-3-nitro-7-oxabicyclo[2.2.1]hept-5-ene-2-carboxylate (9)
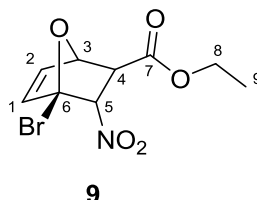
9

An oven-dried 50 mL round-bottom flask equipped with a Teflon-coated magnetic stirring bar was charged with 2.47 g (17.0 mmol, 1.0 eq) ethyl (*E*)-3-nitroacrylate (**11**). It was dissolved in 8 mL anhydrous CHCl$_3$ and afterwards 3.75 g (25.5 mmol, 1.5 eq) 2-bromofuran (**10**) were added in one portion. The yellowish solution was stirred in the closed flask at RT for 72 h. The solvent and all non-reacted volatile starting materials were removed on a rotary evaporator (10 mbar, 35 °C). Finally, the oily, orange crude material was purified via flash column chromatography (440 g SiO$_2$, 21.5 x 7.5 cm, eluent: cyclohexane:EtOAc = 12:1 (v/v), R_f = 0.17) and the resulting colorless solid dried under high vacuum.

Yield: 1.18 g (4.0 mmol, 24 %); colorless solid.

C$_9$H$_{10}$NO$_5$Br [292.08 g.mol^{-1}].

R_f = 0.60 (cyclohexane:EtOAc = 2:1 (v/v), UV and CAM).

m_p = 40-41 °C.

HPLC-MS (Method_ESTER): t_R = 4.55 min.

^{1}H-NMR (300.36 MHz, CDCl$_3$): δ = 6.69 (dd, $^3J_{HH}$ = 5.6 Hz, $^3J_{HH}$ = 2.1 Hz, 1H, H-2), 6.45 (d, $^3J_{HH}$ = 5.6 Hz, 1H, H-1), 5.51 (d, $^3J_{HH}$ = 3.2 Hz, 1H, H-5), 5.31 (d, $^3J_{HH}$ = 1.7 Hz, 1H, H-3),

4.29 (q, $^3J_{HH}$ = 7.1 Hz, 2H, H-8), 3.31 (d, $^3J_{HH}$ = 3.2 Hz, 1H, H-4), 1.33 (t, $^3J_{HH}$ = 7.1 Hz, 3H, H-9).

^{13}C-NMR (75.53 MHz, CDCl$_3$): δ = 168.4 (C$_q$, C-7), 138.5 (C-2), 138.2 (C-1), 90.3 (C-5), 88.0 (C$_q$, C-6), 82.1 (C-3), 62.7 (C-8), 52.7 (C-4), 14.2 (C-9).

HRMS (DI-EI): calculated for C$_9$H$_{10}$NO$_5$Br $^+$: 290.9742; found: 290.9729.

7.3.8. Ethyl (1*S*,2*R*,3*S*,4*R*)-1-bromo-3-nitro-7-oxabicyclo[2.2.1]hept-5-ene-2-carboxylate (70)

70
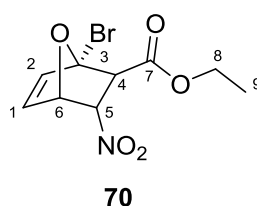
C$_9$H$_{10}$NO$_5$Br [292.08 g.mol^{-1}].

R$_f$ = 0.60 (cyclohexane:EtOAc = 2:1 (v/v), UV and CAM).

HPLC-MS (Method_ESTER): t$_R$ = 3.97 min.

^{1}H-NMR (300.36 MHz, CDCl$_3$): δ = 6.70 (d, $^3J_{HH}$ = 5.6 Hz, 1H, H-2), 6.45 (dd, $^3J_{HH}$ = 5.6 Hz, $^3J_{HH}$ = 1.7 Hz, 1H, H-1), 5.59 (dd, $^3J_{HH}$ = 4.9 Hz, $^3J_{HH}$ = 3.4 Hz, 1H, H-5), 5.46 (dd, $^3J_{HH}$ = 5.1 Hz, $^3J_{HH}$ = 1.6 Hz, 1H, H-6), 4.43-4.25 (m, 2H, H-8), 3.52 (d, $^3J_{HH}$ = 3.3 Hz, 1H, H-4), 1.38 (t, $^3J_{HH}$ = 7.2 Hz, 3H, H-9).

^{13}C-NMR (75.53 MHz, CDCl$_3$): δ = 168.2 (C$_q$, C-7), 143.2 (C-2), 135.1 (C-1), 91.1 (C$_q$, C-3), 85.8 (C-5), 77.9 (C-6), 62.6 (C-8), 54.6 (C-4), 14.4 (C-9).

7.3.9. Ethyl (1*S*,2*S*,3*S*,4*S*)-4-bromo-3-nitro-7-oxabicyclo[2.2.1]hept-5-ene-2-carboxylate (71)

71
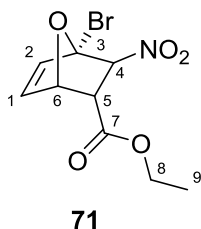
$C_9H_{10}NO_5Br$ [292.08 g.mol^{-1}].

R_f = 0.49 (cyclohexane:EtOAc = 2:1 (v/v), UV and CAM).

HPLC-MS (Method_ESTER): t_R = 3.86 min.

^{1}H-NMR (300.36 MHz, CDCl$_3$): δ = 6.63 (dd, $^3J_{HH}$ = 5.6 Hz, $^3J_{HH}$ = 1.7 Hz, 1H, H-1), 6.48 (d, $^3J_{HH}$ = 5.6 Hz, 1H, H-2), 5.35 (dd, $^3J_{HH}$ = 4.9 Hz, $^3J_{HH}$ = 1.5 Hz, 1H, H-6), 5.08 (d, $^3J_{HH}$ = 3.4 Hz, 1H, H-4), 4.17 (q, $^3J_{HH}$ = 7.1 Hz, 2H, H-8), 4.06 (dd, $^3J_{HH}$ = 4.8 Hz, $^3J_{HH}$ = 3.5 Hz, 1H, H-5), 1.26 (t, $^3J_{HH}$ = 7.1 Hz, 3H, H-9).

^{13}C-NMR (75.53 MHz, CDCl$_3$): δ = 167.7 (C$_q$, C-7), 140.0 (C-1), 138.7 (C-2), 90.5 (C$_q$, C-3), 90.5 (C-4), 78.5 (C-6), 62.3 (C-8), 52.5 (C-5), 14.2 (C-9).

7.3.10. Ethyl (1*R*,2*R*,3*S*,4*R*)-1-bromo-3-nitro-7-oxabicyclo[2.2.1]hept-5-ene-2-carboxylate (72)

72
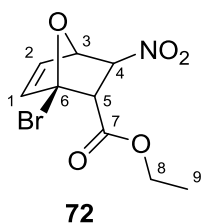
$C_9H_{10}NO_5Br$ [292.08 g.mol^{-1}].

R_f = 0.49 (cyclohexane:EtOAc = 2:1 (v/v), UV and CAM).

HPLC-MS (Method_ESTER): t_R = 4.28 min.

^{1}H-NMR (300.36 MHz, CDCl$_3$): δ = 6.60 (d, $^3J_{HH}$ = 5.6 Hz, 1H, H-1), 6.50 (dd, $^3J_{HH}$ = 5.6 Hz, $^3J_{HH}$ = 2.0 Hz, 1H, H-2), 5.49 (d, $^3J_{HH}$ = 2.1 Hz, 1H, H-3), 4.85 (d, $^3J_{HH}$ = 3.1 Hz, 1H, H-4), 4.32-4.16 (m, 2H, H-8), 4.08 (d, $^3J_{HH}$ = 3.1 Hz, 1H, H-5), 1.32 (t, $^3J_{HH}$ = 7.1 Hz, 3H, H-9).

^{13}C-NMR (75.53 MHz, CDCl$_3$): δ = 167.7 (C$_q$, C-7), 142.6 (C-1), 133.9 (C-2), 88.3 (C-4), 87.7 (C$_q$, C-6), 82.8 (C-3), 62.5 (C-8), 57.6 (C-5), 14.2 (C-9).

7.3.11. Ethyl (1*R*,2*S*,3*S*,4*S*)-3-((*tert*-butoxycarbonyl)amino)-7-oxabicyclo[2.2.1]-hept-5-ene-2-carboxylate-4-*d* (*rac*-8)

rac-8
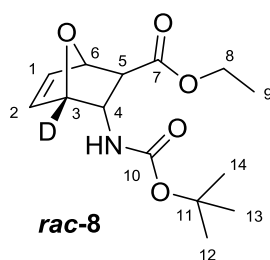
An oven-dried 250 mL three-necked round-bottom flask equipped with a Teflon-coated magnetic stirring bar, gas inlet adapter and bubbler was charged with 3.65 g (12.5 mmol, 1.0 eq) bicyclic DIELS-ALDER compound **9**. It was dissolved in 110 mL EtOD and afterwards cooled in an ice-water bath to 0 °C. Consecutively, 25.8 mL conc. DCl (~38 % (w/w) in D$_2$O, 99.5 atom% D) and 24.5 g (375 mmol, 30.0 eq) Zn/Cu couple (max. 3 % Cu) were added in small portions to the colorless solution in an argon counter flow. Immediately after the addition of the Zn/Cu couple intense D$_2$ gas formation was observed. After 30 min of vigorously stirring at 0 °C, the ice-water bath was removed and the grey suspension was additionally stirred at RT for 10 h. It was filtered through a pad of anhydrous Celite® (diameter: 3.0 cm, height: 4.0 cm) and the filter cake was washed with EtOD (2 x 20 mL). The filtrate was collected in an oven-dried 500 mL round-bottom flask equipped with a Teflon-coated magnetic stirring bar. 52.4 mL (300 mmol, 24.0 eq) DIPEA and 4.91 g (22.5 mmol, 1.8 eq) Boc$_2$O were added successively and the resulting colorless suspension was vigorously stirred at RT for 16 h. Subsequently it was carefully concentrated under high vacuum, the colorless solid residue was diluted with 600 mL EtOAc, washed with H$_2$O (1 x 600 mL) and the cloudy, colorless aqueous phase was reextracted with EtOAc (2 x 600 mL). The combined yellowish organic layers were washed with saturated NaHCO$_3$ (1 x 600 mL), dried over MgSO$_4$, filtered and the solvent was removed under reduced pressure on a rotary evaporator. Finally, the colorless solid crude material was purified via flash column chromatography (350 g SiO$_2$, 17.0 x 8.0 cm, eluent: cyclohexane:EtOAc = 3:1 (v/v), R$_f$ = 0.24) and the resulting colorless solid dried under high vacuum.

Yield: 3.12 g (11.0 mmol, 88 %); colorless solid.

C$_{14}$H$_{20}$DNO$_5$ [284.33 g.mol^{-1}].

R_f = 0.33 (cyclohexane:EtOAc = 2:1 (v/v), UV and CAM).

m_p = 88-89 °C.

HPLC-MS (Method_GENERAL): t_R = 3.05 min; m/z + Na$^+$ = 307.

^{1}H-NMR (300.36 MHz, CDCl$_3$): δ = 6.60 (dd, $^3J_{HH}$ = 5.8 Hz, $^3J_{HH}$ = 1.4 Hz, 1H, H-1), 6.46 (d, $^3J_{HH}$ = 5.8 Hz, 1H, H-2), 5.12 (bs, 1H, H-6), 4.53 (bs, 1H, H-4), 4.29 (d, $^3J_{HH}$ = 7.8 Hz, 1H, NH), 4.21 (q, $^3J_{HH}$ = 7.1 Hz, 2H, H-8), 2.05 (d, $^3J_{HH}$ = 3.4 Hz, 1H, H-5), 1.43 (s, 9H, H-12, H-13, H-14), 1.28 (t, $^3J_{HH}$ = 7.1 Hz, 3H, H-9).

^{13}C-NMR (75.53 MHz, CDCl$_3$): δ = 171.9 (C$_q$, C-7), 155.2 (C$_q$, C-10), 137.9 (C-1), 134.5 (C-2), 82.2 (C-6), 80.1 (C$_q$, C-11), 78.8 ($^1J_{CD}$ = 25.5 Hz, C-3), 61.4 (C-8), 52.5 (C-4), 28.4 (C-12, C-13, C-14), 14.3 (C-9).

7.3.12. (1*R*,2*S*,3*S*,4*S*)-3-((*tert*-Butoxycarbonyl)amino)-7-oxabicyclo[2.2.1]-hept-5-ene-2-carboxylic-4-*d* acid (17)

17
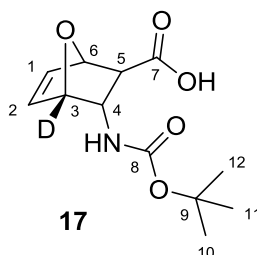
This preparation (total amount of deuterated bicyclic ester *rac*-8: 2.70 g (9.50 mmol, 1.0 eq)) was divided into three smaller preparations with 900 mg (3.17 mmol, 1.0 eq) of compound *rac*-8 each!

Each 250 mL round-bottom flask equipped with a Teflon-coated magnetic stirring bar was charged with 900 mg (3.17 mmol, 1.0 eq) deuterated bicyclic ester *rac*-8. It was dissolved in 36 mL Et$_2$O and to the colorless solutions 64 mL NaH$_2$PO$_4$/Na$_2$HPO$_4$ buffer (pH 7.6, 100 mM) were added, respectively. After addition of 3.6 mL PLE-precipitate (in half saturated (NH$_4$)$_2$SO$_4$, unknown activity) to each preparation the yellowish two-phasic mixtures were stirred with 150 rpm in closed systems at RT for 22 h until the non-hydrolyzed enantiomer of compound *ent*-8 reached an *e.e.* value between 73-75 % (E = 60).

The combined yellowish reaction mixtures were phase separated and the aqueous phase was washed with Et$_2$O (2 x 300 mL). In order to obtain a better phase separation the mixture was centrifuged. The yellowish aqueous layer was acidified with 30 mL of saturated KHSO$_4$

to pH 1-2 and the product was extracted with DCM (4 x 300 mL). The combined yellowish organic layers were dried over $MgSO_4$, filtered and the solvent was removed under reduced pressure on a rotary evaporator. For purification the brownish crude material was triturated in 12 mL cyclohexane:EtOAc = 2:1 (v/v), collected by filtration, washed with cold cyclohexane:EtOAc = 2:1 (v/v) (2 x 2.0 mL) and the resulting colorless powder was dried under high vacuum.

Yield: 1.03 g (4.00 mmol, 42 %); colorless powder.

chiral HPLC (Method_ACID): t_R = 11.31 min (major enantiomer) and 13.15 min (minor enantiomer); *e.e.* = 93 %.

In order to gain perfect *e.e.* values, this procedure was repeated with 650 mg (2.29 mmol, 1.0 eq) of the enantiomerically enriched deuterated bicyclic ester **8** (*e.e.* = 93 %) as starting material. After reaching an *e.e.* = 67 % of non-hydrolyzed ester ***ent*-8**, the work-up as well as the purification was performed as described above.

Yield: 407 mg (1.58 mmol, 69 %); colorless powder.

$C_{12}H_{16}DNO_5$ [256.27 g.mol^{-1}].

R_f = 0.24 (EtOAc:MeOH:AcOH = 1000:4:1 (v/v/v), UV and CAM).

m_p = 123-124 °C.

$[\alpha]_D^{31-32\ °C}$ = -189.3 ° (c = 0.50 in DMSO).

HPLC-MS (Method_GENERAL): t_R = 1.72 min; *m/z* + Na$^+$ = 279.

chiral HPLC (Method_ACID): t_R = 11.31 min (major enantiomer) and 13.15 min (minor enantiomer); *e.e.* > 99 %.

^{1}H-NMR (300.36 MHz, DMSO-d$_6$): δ = 12.44 (s, 1H, COOH), 6.83 (bs, 1H, NH), 6.56 (d, $^3J_{HH}$ = 4.2 Hz, 1H, H-1), 6.36 (d, $^3J_{HH}$ = 4.7 Hz, 1H, H-2), 4.99 (s, 1H, H-6), 4.07 (bs, 1H, H-4), 2.24 (s, 1H, H-5), 1.38 (s, 9H, H-10, H-11, H-12).

^{13}C-NMR (75.53 MHz, DMSO-d$_6$): δ = 173.3 (C$_q$, C-7), 155.3 (C$_q$, C-8), 137.0 (C-1), 134.1 (C-2), 81.6 (C-6), 78.2 ($^1J_{CD}$ = 25.2 Hz, C-3), 78.0 (C$_q$, C-9), 52.6 (C-4), 49.6 (C-5), 28.1 (C-10, C-11, C-12).

HRMS (DI-EI): calculated for $[C_{12}H_{16}DNO_5 - C_4H_3DO]^+$: 187.0845; found: 187.0852.

7.3.13. Ethyl (1*R*,2*S*,3*S*,4*S*)-3-((*tert*-butoxycarbonyl)amino)-7-oxabicyclo[2.2.1]-hept-5-ene-2-carboxylate-4-*d* (8)
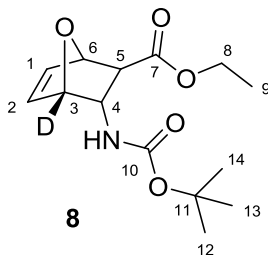
An oven-dried, evacuated and argon purged 100 mL Schlenk flask with a Teflon-coated magnetic stirring bar was charged with 980 mg (3.82 mmol, 1.0 eq) deuterium labeled bicyclic carboxylic acid **17** (*e.e.* = 93 %). It was dissolved in 40 mL anhydrous DCM and 335 µL (5.74 mmol, 1.5 eq) anhydrous EtOH as well as 46.7 mg (382 µmol, 10 mol%) 4-DMAP were added in an argon counter flow, respectively. Afterwards the colorless solution was cooled in an ice-water bath to 0 °C and 1.10 g (5.74 mmol, 1.5 eq) EDC.HCl were added in one portion. Immediately after the addition of coupling reagent the ice-water bath was removed, the Schlenk flask equipped with a bubbler and the colorless solution was stirred at RT for 16 h under argon atmosphere. Afterwards the colorless solution was diluted with 40 mL DCM and washed with H_2O (3 x 40 mL). The colorless organic phase was dried over $MgSO_4$, filtered and concentrated on a rotary evaporator. Finally, the yellowish solid was purified via flash column chromatography (55 g SiO_2, 13.0 x 3.0 cm, eluent: cyclohexane:EtOAc = 3:1 (v/v), R_f = 0.24) and the resulting colorless, crystalline solid was dried under high vacuum.

Yield: 1.07 g (3.76 mmol, 99 %); colorless, crystalline solid.

chiral HPLC (Method_ESTER): t_R = 11.15 min (minor enantiomer) and 13.18 min (major enantiomer); *e.e.* = 93 %.

This procedure was repeated with 360 mg (1.40 mmol, 1.0 eq) of the enantiomerically pure deuterated bicyclic carboxylic acid **17** (*e.e.* > 99 %) as starting material.

Yield: 394 mg (1.39 mmol, 99 %); colorless, crystalline solid.

$C_{14}H_{20}DNO_5$ [284.33 g.mol^{-1}].

R_f = 0.33 (cyclohexane:EtOAc = 2:1 (v/v), UV and CAM).

m_p = 101-102 °C.

$[\alpha]_D^{33-34\,°C}$ = -142.7 ° (c = 1.00 in $CHCl_3$).

HPLC-MS (Method_GENERAL): t_R = 3.05 min; m/z + Na^+ = 307.

chiral HPLC (Method_ESTER): t_R = 11.15 min (minor enantiomer) and 13.18 min (major enantiomer); *e.e.* > 99 %.

^{1}H-NMR (300.36 MHz, CDCl$_3$): δ = 6.60 (dd, $^3J_{HH}$ = 5.8 Hz, $^3J_{HH}$ = 1.4 Hz, 1H, H-1), 6.46 (d, $^3J_{HH}$ = 5.8 Hz, 1H, H-2), 5.12 (bs, 1H, H-6), 4.53 (bs, 1H, H-4), 4.29 (d, $^3J_{HH}$ = 7.8 Hz, 1H, NH), 4.21 (q, $^3J_{HH}$ = 7.1 Hz, 2H, H-8), 2.05 (d, $^3J_{HH}$ = 3.4 Hz, 1H, H-5), 1.43 (s, 9H, H-12, H-13, H-14), 1.28 (t, $^3J_{HH}$ = 7.1 Hz, 3H, H-9).

^{13}C-NMR (75.53 MHz, CDCl$_3$): δ = 171.9 (C$_q$, C-7), 155.2 (C$_q$, C-10), 137.9 (C-1), 134.5 (C-2), 82.2 (C-6), 80.1 (C$_q$, C-11), 78.8 ($^1J_{CD}$ = 25.5 Hz, C-3), 61.4 (C-8), 52.5 (C-4), 28.4 (C-12, C-13, C-14), 14.3 (C-9).

HRMS (DI-EI): calculated for [C$_{14}$H$_{20}$DNO$_5$ − C$_4$H$_3$DO]$^+$: 215.1158; found: 215.1170.

7.3.14. Ethyl (5*S*,6*S*)-6-(((*tert*-butoxycarbonyl)amino)-5-hydroxycyclohexa-1,3-diene-1-carboxylate-5-*d* (7)
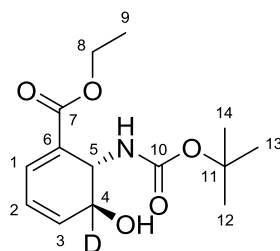
7

An oven-dried, evacuated and argon purged 15 mL Schlenk flask with a Teflon-coated magnetic stirring bar was charged with 420 mg (1.48 mmol, 1.0 eq) deuterium labeled bicyclic ester **8** (*e.e.* > 99 %). It was dissolved in 6.5 mL anhydrous THF and afterwards the resulting colorless solution was cooled in an acetone/dry ice bath to -45 °C under argon atmosphere. In parallel 5.4 mL (4.43 mmol, 3.0 eq) of a 0.829 M KHMDS solution (in anhydrous THF) were transferred into a second oven-dried, evacuated and argon purged 80 mL Schlenk flask and diluted with 7.6 mL anhydrous THF. This yellowish, cloudy solution was also cooled in an acetone/dry ice bath to -45 °C under inert atmosphere. In an argon counter flow the colorless solution of starting material was added to the yellowish KHMDS solution in one portion, the Schlenk flask with the former solution of ester **8** was rinsed with 2.0 mL anhydrous THF and the resulting yellow suspension was vigorously stirred at -45 °C in the acetone/dry ice bath for 100 min. Afterwards the resulting orange, cloudy solution was

poured into 40 mL saturated NH_4Cl and extracted with EtOAc (3 x 30 mL). The combined yellowish, organic layers were dried over $MgSO_4$, filtered and concentrated on a rotary evaporator. Finally, the yellow, oily crude material was purified via flash column chromatography (55 g SiO_2, 12.0 x 4.0 cm, eluent: cyclohexane:EtOAc = 5:4 (v/v), R_f = 0.22) and the resulting yellowish, highly viscous liquid was dried under high vacuum.

Yield: 375 mg (1.32 mmol, 89 %); yellowish, highly viscous liquid.

$C_{14}H_{20}DNO_5$ [284.33 g.mol^{-1}].

R_f = 0.31 (cyclohexane:EtOAc = 2:3 (v/v), UV and CAM).

$[\alpha]_D^{33-34\ °C}$ = +298.3 ° (c = 1.50 in $CHCl_3$); *e.e.* > 99 %.

HPLC-MS (Method_GENERAL): t_R = 2.61 min; *m/z* + Na^+ = 307.

^{1}H-NMR (300.36 MHz, $CDCl_3$): δ = 7.17-7.15 (m, 1H, H-1), 6.29-6.22 (m, 2H, H-2, H-3), 4.75 (d, $^3J_{HH}$ = 8.0 Hz, 1H, H-5), 4.46 (bs, 1H, NH), 4.31-4.13 (m, 2H, H-8), 3.09 (bs, 1H, OH), 1.42 (s, 9H, H-12, H-13, H-14), 1.28 (t, $^3J_{HH}$ = 7.1 Hz, 3H, H-9).

^{13}C-NMR (75.53 MHz, $CDCl_3$): δ = 166.0 (C_q, C-7), 155.6 (C_q, C-10), 133.6 (C-1), 132.7 (C-3), 127.5 (C_q, C-6), 124.7 (C-2), 80.2 (C_q, C-11), 67.4 ($^1J_{CD}$ = 22.5 Hz, C-4), 61.0 (C-8), 50.2 (C-5), 28.5 (C-12, C-13, C-14), 14.3 (C-9).

HRMS (DI-EI): calculated for $C_{14}H_{20}DNO_5^+$: 284.1483; found: 284.1489.

7.3.15. (5*S*,6*S*)-6-((*tert*-Butoxycarbonyl)amino)-5-hydroxycyclohexa-1,3-diene-1-carboxylic-5-*d* acid (24)
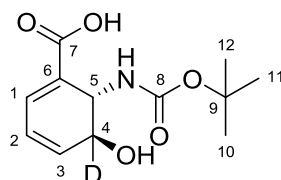
24

A 10 mL round-bottom flask with a Teflon-coated magnetic stirring bar was charged with 370 mg (1.30 mmol, 1.0 eq) deuterium labeled ester **7** (*e.e.* > 99 %). It was dissolved in 6.0 mL THF and to the colorless solution 650 µL (6.50 mmol, 5.0 eq) 10 M KOH in H_2O were added in one portion. The resulting light orange solution was vigorously stirred at RT for 15 h. Afterwards it was concentrated on a rotary evaporator and the brownish, oily residue was dissolved in 30 mL H_2O. The brownish aqueous phase was washed with EtOAc (2 x

30 mL) and subsequently acidified with 2.0 mL saturated $KHSO_4$ to pH 1-2. The product was extracted with EtOAc (4 x 50 mL), the combined yellow organic phases were dried over $MgSO_4$, filtered and the solvent was removed on a rotary evaporator. Finally, the crude material was purified via flash column chromatography (35 g SiO_2, 25.0 x 2.0 cm, eluent: EtOAc:AcOH = 1000:1 (v/v), R_f = 0.18) and the resulting colorless powder was dried under high vacuum.

Yield: 264 mg (1.03 mmol, 79 %); colorless powder.

$C_{12}H_{16}DNO_5$ [256.27 g.mol^{-1}].

R_f = 0.28 (EtOAc:MeOH:AcOH = 1000:30:1 (v/v/v), UV and CAM).

m_p = 168-169 °C (decomposition).

$[\alpha]_D^{32-33\,°C}$ = +420.8 ° (c = 1.00 in DMSO); *e.e.* > 99 %.

HPLC-MS (Method_GENERAL): t_R = 2.59 min; *m/z* + Na$^+$ = 279.

^{1}H-NMR (300.36 MHz, DMSO-d$_6$): δ = 12.26 (s, 1H, COOH), 7.00-6.98 (m, 1H, H-1), 6.56 (d, $^3J_{HH}$ = 6.9 Hz, 1H, NH), 6.20-6.16 (m, 2H, H-2, H-3), 5.03 (s, 1H, OH), 4.43 (d, $^3J_{HH}$ = 7.2 Hz, 1H, H-5), 1.37 (s, 9H, H-10, H-11, H-12).

^{13}C-NMR (75.53 MHz, DMSO-d$_6$): δ = 167.4 (C_q, C-7), 155.1 (C_q, C-8), 133.2 (C-1), 133.0 (C-3), 126.9 (C_q, C-6), 123.9 (C-2), 77.7 (C_q, C-9), 65.7 ($^1J_{CD}$ = 21.6 Hz, C-4), 49.0 (C-5), 28.2 (C-10, C-11, C-12).

HRMS (DI-EI): calculated for $C_{12}H_{16}DNO_5^+$: 256.1169; found: 256.1184.

7.3.16. (1*S*,6*S*)-2-Carboxy-6-hydroxycyclohexa-2,4-diene-6-*d*-1-ammonium 2,2,2-trifluoroacetate (5a)
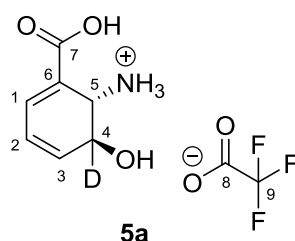
5a

An oven-dried 10 mL round-bottom flask equipped with a Teflon-coated magnetic stirring bar was charged with 235 mg (917 µmol, 1.0 eq) deuterium labeled carboxylic acid **24** (*e.e.* > 99 %). Afterwards the starting material was suspended in 3.5 mL DCM and to the colorless

suspension 525 µL TFA were added (15 % TFA in DCM (v/v)), respectively. A yellowish solution was immediately formed after the addition of TFA, it turned brownish by the time and the desired product precipitated in the form of a brownish solid. The suspension was stirred at RT for 90 min. Subsequently it was cooled in an ice-water bath to 0 °C, the precipitate was collected by filtration and washed with a small amount of cooled DCM (2 x 400 µL). Finally, the brownish, powdery crude material was purified by trituration in 1.0 mL DCM:MeCN = 2:1 (v/v). It was collected by filtration, washed with cold DCM:MeCN = 2:1 (v/v) (2 x 200 µL) and the resulting colorless powder was dried under high vacuum.

Yield: 193 mg (714 µmol, 78 %); colorless powder.

$C_9H_9DF_3NO_5$ [270.18 g.mol^{-1}].

m_p = 161-162 °C (decomposition).

$[\alpha]_D^{32\text{-}33\,°C}$ = +364.4 ° (c = 0.50 in DMSO); *e.e.* > 99 %.

^{1}H-NMR (300.36 MHz, D$_2$O): δ = 7.47 (d, $^3J_{HH}$ = 5.2 Hz, 1H, H-1), 6.53-6.43 (m, 2H, H-2, H-3), 4.40 (s, 1H, H-5).

^{1}H-NMR (300.36 MHz, DMSO-d$_6$): δ = 13.06 (bs, 1H, COOH), 8.05 (bs, 3H, NH$_3^+$), 7.24-7.23 (m, 1H, H-1), 6.37-6.30 (m, 2H, H-2, H-3), 5.60 (s, 1H, OH), 4.04 (s, 1H, H-5).

^{13}C-NMR (125.69 MHz, D$_2$O): δ = 168.5 (C$_q$, C-7), 162.9 (C$_q$, q, $^2J_{CF}$ = 35.4 Hz, C-8), 137.7 (C-1), 131.8 (C-3), 125.2 (C$_q$, C-6), 122.1 (C-2), 116.3 (C$_q$, q, $^1J_{CF}$ = 292 Hz, C-9), 63.7 ($^1J_{CD}$ = 22.4 Hz, C-4), 48.8 (C-5).

^{19}F-NMR (470.35 MHz, DMSO-d$_6$): δ = -73.5 (decoupled, CF$_3$).

HRMS (DI-EI): calculated for $C_7H_8DNO_3^+$: 156.0645; found: 156.0651.

7.3.17. (5*S*,6*S*)-6-((5-(((*S*)-1-Amino-1-oxopropan-2-yl)amino)-2,4-dinitrophenyl)-amino)-5-hydroxycyclohexa-1,3-diene-1-carboxylic-5-*d* acid (26a)

26a
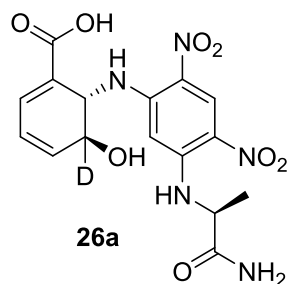
According to the general procedure (derivatization with MARFEY's reagent) ammonium salt **5a** was derivatized with MARFEY's reagent in order to determine the *e.e.* value of compound **5**.

HPLC-MS (Method_MARFEY_A): t_R = 1.51 min (minor diastereomer) and 1.80 min (major diastereomer); *d.e.* > 99 %, consequently *e.e.* > 99 % of compound **5**.
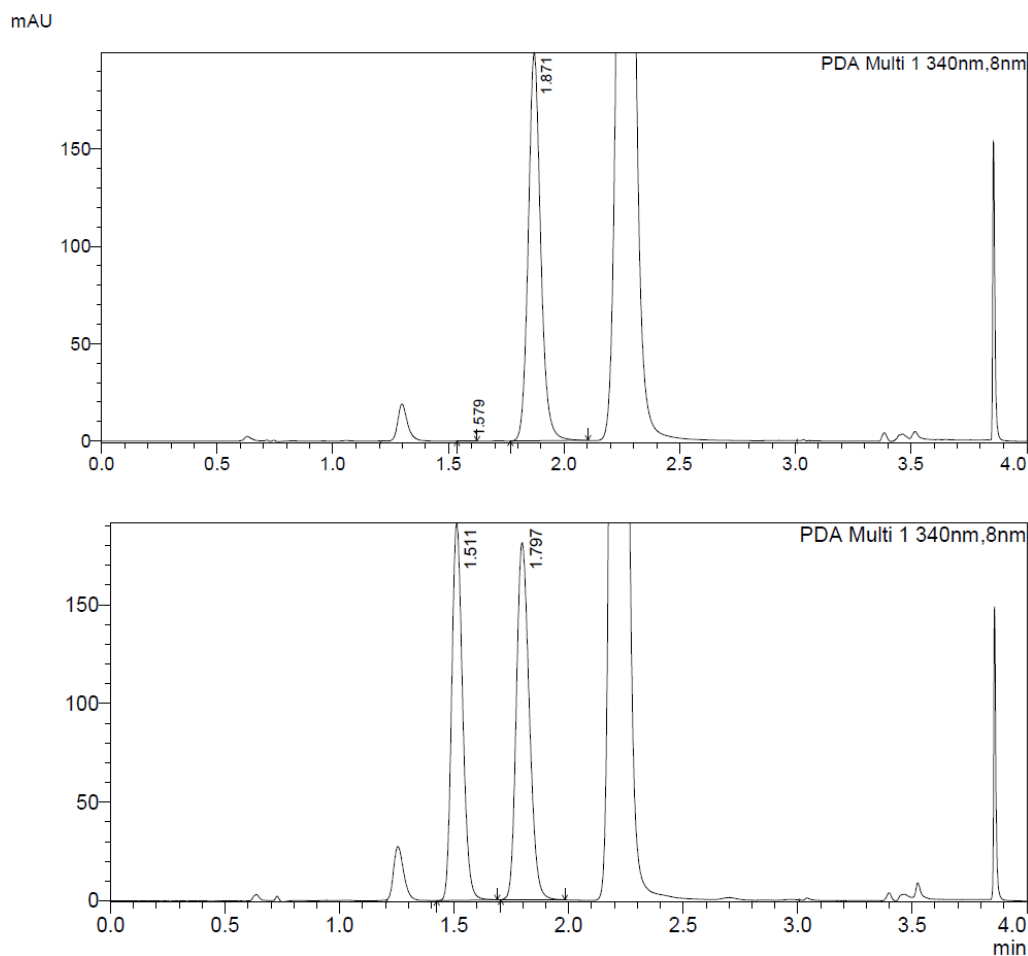
Figure 36: HPLC-MS chromatograms of **26a** and **rac-26** for the determination of the diastereomeric excess (*d.e.*).

7.3.18. Ethyl (1*R*,2*S*,3*S*,4*S*)-3-nitro-7-oxabicyclo[2.2.1]hept-5-ene-2-carboxylate (27)
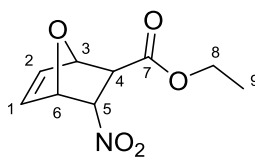
27

Literature: I. B. Masesane, A. S. Batsanov, J. A. K. Howard, R. Mondal, P. G. Steel, *Beilstein J. Org. Chem.* **2006**, *9*, 1-6.

An oven-dried 50 mL round-bottom flask equipped with a Teflon-coated magnetic stirring was charged with 3.63 g (25.0 mmol, 1.0 eq) ethyl (*E*)-3-nitroacrylate (**11**). It was dissolved in 13 mL anhydrous $CHCl_3$ and 3.64 mL (50.0 mmol, 2.0 eq) furan (**12**) were added in one portion, consecutively. The yellow solution was vigorously stirred at RT in the closed flask for 28 h. Afterwards the solvent and all non-reacted volatile starting materials were removed on a rotary evaporator (10 mbar, 35 °C). Finally, the brownish crude material was purified via flash column chromatography (520 g SiO_2, 21.0 x 8.0 cm, eluent: cyclohexane:EtOAc = 3:1 (v/v), R_f = 0.23) and the resulting yellowish, crystalline solid was dried under high vacuum.

Yield: 2.70 g (12.7 mmol, 51 %); yellowish, crystalline solid.

$C_9H_{11}NO_5$ [213.19 g.mol^{-1}].

R_f = 0.42 (cyclohexane:EtOAc = 3:1 (v/v), UV and CAM).

m_p = 54-55 °C.

HPLC-MS (Method_ESTER): t_R = 2.28 min.

^{1}H-NMR (300.36 MHz, $CDCl_3$): δ = 6.72 (dd, $^3J_{HH}$ = 5.8 Hz, $^3J_{HH}$ = 1.8 Hz, 1H, H-2), 6.38 (dd, $^3J_{HH}$ = 5.8 Hz, $^3J_{HH}$ = 1.4 Hz, 1H, H-1), 5.53 (dd, $^3J_{HH}$ = 4.8 Hz, $^3J_{HH}$ = 3.0 Hz, 1H, H-5), 5.46 (d, $^3J_{HH}$ = 4.8 Hz, 1H, H-6), 5.33 (d, $^3J_{HH}$ = 0.7 Hz, 1H, H-3), 4.26 (q, $^3J_{HH}$ = 7.1 Hz, 2H, H-8), 3.21 (d, $^3J_{HH}$ = 2.9 Hz, 1H, H-4), 1.32 (t, $^3J_{HH}$ = 7.1 Hz, 3H, H-9).

^{13}C-NMR (75.53 MHz, $CDCl_3$): δ = 169.8 (C_q, C-7), 139.0 (C-2), 133.8 (C-1), 84.4 (C-5), 83.4 (C-3), 79.1 (C-6), 62.3 (C-8), 49.1 (C-4), 14.3 (C-9).

7.3.19. Ethyl (1*S*,2*S*,3*S*,4*R*)-3-nitro-7-oxabicyclo[2.2.1]hept-5-ene-2-carboxylate (73)

73
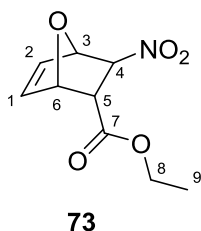
$C_9H_{11}NO_5$ [213.19 g.mol^{-1}].

R_f = 0.33 (cyclohexane:EtOAc = 3:1 (v/v), UV and CAM).

m_p = 34-35 °C.

HPLC-MS (Method_ESTER): t_R = 2.11 min.

^{1}H-NMR (300.36 MHz, CDCl$_3$): δ = 6.54 (dd, $^3J_{HH}$ = 5.8 Hz, $^3J_{HH}$ = 1.4 Hz, 1H, H-1), 6.51 (dd, $^3J_{HH}$ = 5.8 Hz, $^3J_{HH}$ = 1.6 Hz, 1H, H-2), 5.50 (s, 1H, H-3), 5.32 (d, $^3J_{HH}$ = 4.8 Hz, 1H, H-6), 4.83 (d, $^3J_{HH}$ = 3.0 Hz, 1H, H-4), 4.16 (q, $^3J_{HH}$ = 7.1 Hz, 2H, H-8), 3.94 (dd, $^3J_{HH}$ = 4.8 Hz, $^3J_{HH}$ = 3.0 Hz, 1H, H-5), 1.26 (t, $^3J_{HH}$ = 7.1 Hz, 3H, H-9).

^{13}C-NMR (75.53 MHz, CDCl$_3$): δ = 168.9 (C$_q$, C-7), 138.5 (C-1), 134.4 (C-2), 86.8 (C-4), 84.2 (C-3), 79.3 (C-6), 61.9 (C-8), 49.8 (C-5), 14.2 (C-9).

7.3.20. Ethyl (1*R*,2*S*,3*S*,4*S*)-3-((*tert*-butoxycarbonyl)amino)-7-oxabicyclo[2.2.1]-hept-5-ene-2-carboxylate (*rac*-15)
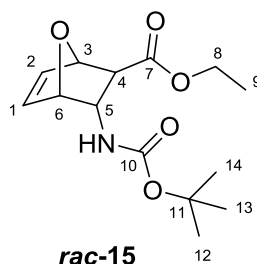
***rac*-15**

Literature: I. B. Masesane, A. S. Batsanov, J. A. K. Howard, R. Mondal, P. G. Steel, *Beilstein J. Org. Chem.* **2006**, *9*, 1-6.

An oven-dried 500 mL round-bottom flask equipped with a Teflon-coated magnetic stirring bar was charged with 4.26 g (20.0 mmol, 1.0 eq) bicyclic DIELS-ALDER compound **27**. It was dissolved in 200 mL EtOH and afterwards cooled in an ice-water bath to 0 °C. Consecutively,

27 mL conc. HCl (~36 % (w/w) in H_2O) and 26.2 g (400 mmol, 20.0 eq) activated Zn (Zn washed with 1 M HCl, H_2O as well as MeOH and afterwards dried under high vacuum) were added in small portions to the colorless solution. Immediately after the addition of the Zn an intense H_2 gas formation was observed. After 30 min of vigorously stirring at 0 °C, the ice-water bath was removed and the grey suspension was additionally stirred at RT for 8 h. It was filtered through a pad of Celite® (diameter: 6.0 cm, height: 5.0 cm) and the filter cake was carefully washed with EtOH (2 x 50 mL). The filtrate was collected in an oven-dried 1000 mL round-bottom flask equipped with a Teflon-coated magnetic stirring bar. 55.9 mL (320 mmol, 16.0 eq) DIPEA and 7.76 g (36.0 mmol, 1.8 eq) Boc_2O were added successively and the resulting colorless suspension was vigorously stirred at RT for 22 h. Subsequently it was carefully concentrated under high vacuum, the colorless solid residue was diluted with 800 mL EtOAc and washed with H_2O (1 x 800 mL). The cloudy, colorless aqueous phase was reextracted with EtOAc (2 x 800 mL), the combined yellowish organic layers washed with saturated $NaHCO_3$ (1 x 800 mL), dried over $MgSO_4$, filtered and the solvent was removed under reduced pressure on a rotary evaporator. Finally, the colorless solid crude material was purified via flash column chromatography (250 g SiO_2, 19.0 x 6.0 cm, eluent: cyclohexane:EtOAc = 3:1 (v/v), R_f = 0.24) and the resulting colorless solid dried under high vacuum.

Yield: 4.99 g (17.6 mmol, 88 %); colorless solid.

$C_{14}H_{21}NO_5$ [283.32 g.mol^{-1}].

R_f = 0.33 (cyclohexane:EtOAc = 2:1 (v/v), UV and CAM).

m_p = 97-98 °C.

HPLC-MS (Method_GENERAL): t_R = 3.05 min; m/z + Na^+ = 306.

^{1}H-NMR (300.36 MHz, $CDCl_3$): δ = 6.60 (dd, $^3J_{HH}$ = 5.8 Hz, $^3J_{HH}$ = 1.7 Hz, 1H, H-2), 6.46 (dd, $^3J_{HH}$ = 5.8 Hz, $^3J_{HH}$ = 1.5 Hz, 1H, H-1), 5.12 (s, 1H, H-3), 5.06 (bs, 1H, H-6), 4.54 (bs, 1H, H-5), 4.31 (d, $^3J_{HH}$ = 7.8 Hz, 1H, NH), 4.21 (q, $^3J_{HH}$ = 7.1 Hz, 2H, H-8), 2.05 (d, $^3J_{HH}$ = 3.5 Hz, 1H, H-4), 1.43 (s, 9H, H-12, H-13, H-14), 1.28 (t, $^3J_{HH}$ = 7.1 Hz, 3H, H-9).

^{13}C-NMR (75.53 MHz, $CDCl_3$): δ = 171.9 (C_q, C-7), 155.1 (C_q, C-10), 138.0 (C-2), 134.6 (C-1), 82.2 (C-3), 80.1 (C_q, C-11), 79.1 (C-6), 61.4 (C-8), 53.5 (C-5), 52.5 (C-4), 28.5 (C-12, C-13, C-14), 14.3 (C-9).

7.3.21. (1*R*,2*S*,3*S*,4*S*)-3-((*tert*-Butoxycarbonyl)amino)-7-oxabicyclo[2.2.1]hept-5-ene-2-carboxylic acid (28)

28
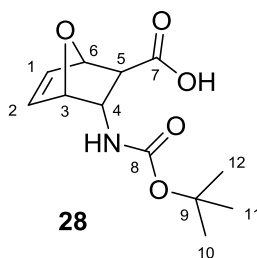
Literature: M. E. Bunnage, T. Ganesh, I. B. Masesane, D. Orton, P. G. Steel, *Org. Lett.* **2003**, *5*, 239-242.

This preparation (total amount of bicyclic ester **rac-15**: 4.92 g (17.4 mmol, 1.0 eq)) was divided into five smaller preparations with 984 mg (3.47 mmol, 1.0 eq) of compound **rac-15** each!

Each 250 mL round-bottom flask equipped with a Teflon-coated magnetic stirring bar was charged with 984 mg (3.47 mmol, 1.0 eq) bicyclic ester **rac-15**. It was dissolved in 40 mL Et_2O and to the colorless solutions 70 mL NaH_2PO_4/Na_2HPO_4 buffer (pH 7.6, 100 mM) were added, respectively. After addition of 3.6 mL PLE-precipitate (in half saturated $(NH_4)_2SO_4$, unknown activity) to each preparation the yellowish two-phasic mixtures were stirred with 200 rpm in the closed flask at RT for 22 h until the non-hydrolyzed enantiomer of compound **ent-15** reached an *e.e.* value between 94-96 % (E = 180).

The combined yellowish reaction mixtures were phase separated and the aqueous phase was washed with Et_2O (2 x 600 mL). In order to obtain a better phase separation the mixture was centrifuged. The yellowish aqueous layer was acidified with 50 mL of saturated $KHSO_4$ to pH 1-2 and the product was extracted with DCM (4 x 500 mL). The combined yellowish organic layers were dried over $MgSO_4$, filtered and the solvent was removed under reduced pressure on a rotary evaporator. For purification the brownish crude material was triturated in 15 mL cyclohexane:EtOAc = 2:1 (v/v), collected by filtration, washed with cold cyclohexane:EtOAc = 2:1 (v/v) (2 x 2.0 mL) and the resulting colorless powder was dried under high vacuum.

Yield: 1.96 g (7.68 mmol, 44 %); colorless powder.

chiral HPLC (Method_ACID): t_R = 11.31 min (major enantiomer) and 13.15 min (minor enantiomer); *e.e.* = 96 %.

In order to gain perfect *e.e.* values, this procedure was repeated with 2.10 g (7.41 mmol, 1.0 eq) of the enantiomerically enriched bicyclic ester **15** (*e.e.* = 96 %) as starting material. After reaching an *e.e.* = 38 % of non-hydrolyzed ester ***ent*-15**, the work-up as well as the purification was performed as described above.

Yield: 1.57 g (6.15 mmol, 83 %); colorless powder.

$C_{12}H_{17}NO_5$ [255.26 g.mol^{-1}].

R_f = 0.24 (EtOAc:MeOH:AcOH = 1000:4:1 (v/v/v), UV and CAM).

m_p = 133-134 °C.

$[\alpha]_D^{31-32\ °C}$ = -189.0 ° (c = 1.00 in DMSO).

HPLC-MS (Method_GENERAL): t_R = 1.68 min; *m/z* + Na$^+$ = 278.

chiral HPLC (Method_ACID): t_R = 11.31 min (major enantiomer) and 13.15 min (minor enantiomer); *e.e.* > 99 %.

^{1}H-NMR (300.36 MHz, DMSO-d$_6$): δ = 12.45 (s, 1H, COOH), 6.84 (d, $^3J_{HH}$ = 4.1 Hz, 1H, NH), 6.56 (d, $^3J_{HH}$ = 5.1 Hz, 1H, H-1), 6.36 (d, $^3J_{HH}$ = 4.6 Hz, 1H, H-2), 4.99 (s, 1H, H-6), 4.92 (d, $^3J_{HH}$ = 3.5 Hz, 1H, H-3), 4.07 (bs, 1H, H-4), 2.24 (s, 1H, H-5), 1.38 (s, 9H, H-10, H-11, H-12).

^{13}C-NMR (75.53 MHz, DMSO-d$_6$): δ = 173.4 (C$_q$, C-7), 155.4 (C$_q$, C-8), 137.0 (C-1), 134.1 (C-2), 81.6 (C-6), 78.5 (C-3), 78.0 (C$_q$, C-9), 52.6 (C-4), 49.6 (C-5), 28.2 (C-10, C-11, C-12).

7.3.22. Ethyl (1*R*,2*S*,3*S*,4*S*)-3-((*tert*-butoxycarbonyl)amino)-7-oxabicyclo[2.2.1]-hept-5-ene-2-carboxylate (15)
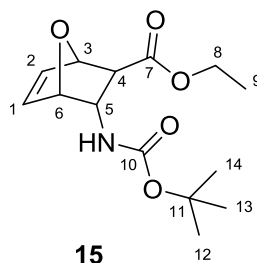
15

An oven-dried, evacuated and argon purged 250 mL Schlenk flask with a Teflon-coated magnetic stirring bar was charged with 1.93 g (7.56 mmol, 1.0 eq) bicyclic carboxylic acid **28** (*e.e.* = 96 %). It was dissolved in 70 mL anhydrous DCM and 661 µL (11.3 mmol, 1.5 eq) anhydrous EtOH as well as 92.4 mg (756 µmol, 10 mol%) 4-DMAP were added in an argon counter flow, respectively. Afterwards the colorless solution was cooled in an ice-water bath

to 0 °C and 2.17 g (11.3 mmol, 1.5 eq) EDC.HCl were added in one portion. Immediately after the addition of the coupling reagent the ice-water bath was removed, the Schlenk flask equipped with a bubbler and the colorless solution was stirred at RT for 16 h under argon atmosphere. Afterwards the colorless solution was diluted with 50 mL DCM, washed with H_2O (3 x 60 mL) and the product was reextracted from the colorless aqueous phase with DCM (2 x 30 mL). The combined colorless organic layers were dried over $MgSO_4$, filtered and concentrated on a rotary evaporator. Finally the yellowish crude material was purified via flash column chromatography (80 g SiO_2, 25.0 x 3.0 cm, eluent: cyclohexane:EtOAc = 3:1 (v/v), R_f = 0.24) and the resulting colorless, crystalline solid was dried under high vacuum.

Yield: 2.11 g (7.45 mmol, 99 %); colorless, crystalline solid.

chiral HPLC (Method_ESTER): t_R = 11.15 min (minor enantiomer) and 13.18 min (major enantiomer); *e.e.* = 96 %.

This procedure was repeated with 1.55 g (6.07 mmol, 1.0 eq) of the enantiomerically enriched bicyclic carboxylic acid **28** (*e.e.* > 99 %) as starting material.

Yield: 1.71 g (6.04 mmol, 99 %); colorless, crystalline solid.

$C_{14}H_{21}NO_5$ [283.32 g.mol^{-1}].

R_f = 0.43 (cyclohexane:EtOAc = 3:2 (v/v), UV and CAM).

m_p = 104-105 °C.

$[\alpha]_D^{31\text{-}32\,°C}$ = -142.0 ° (c = 1.00 in $CHCl_3$).

HPLC-MS (Method_GENERAL): t_R = 3.08 min; *m/z* + Na^+ = 306.

chiral HPLC (Method_ESTER): t_R = 11.15 min (minor enantiomer) and 13.18 min (major enantiomer); *e.e.* > 99 %.

^{1}H-NMR (300.36 MHz, CDCl$_3$): δ = 6.60 (dd, $^3J_{HH}$ = 5.8 Hz, $^3J_{HH}$ = 1.7 Hz, 1H, H-2), 6.46 (dd, $^3J_{HH}$ = 5.8 Hz, $^3J_{HH}$ = 1.5 Hz, 1H, H-1), 5.12 (s, 1H, H-3), 5.06 (bs, 1H, H-6), 4.54 (bs, 1H, H-5), 4.31 (d, $^3J_{HH}$ = 7.8 Hz, 1H, NH), 4.21 (q, $^3J_{HH}$ = 7.1 Hz, 2H, H-8), 2.05 (d, $^3J_{HH}$ = 3.5 Hz, 1H, H-4), 1.43 (s, 9H, H-12, H-13, H-14), 1.28 (t, $^3J_{HH}$ = 7.1 Hz, 3H, H-9).

^{13}C-NMR (75.53 MHz, CDCl$_3$): δ = 171.9 (C$_q$, C-7), 155.1 (C$_q$, C-10), 138.0 (C-2), 134.6 (C-1), 82.2 (C-3), 80.1 (C$_q$, C-11), 79.1 (C-6), 61.4 (C-8), 53.5 (C-5), 52.5 (C-4), 28.5 (C-12, C-13, C-14), 14.3 (C-9).

7.3.23. (*R*)-1-(4-Bromophenyl)ethyl (1*R*,2*S*,3*S*,4*S*)-3-((*tert*-butoxycarbonyl)-amino)-7-oxabicyclo[2.2.1]hept-5-ene-2-carboxylate (31)
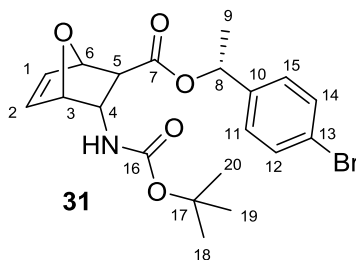
An oven-dried, evacuated and argon purged 30 mL Schlenk flask with a Teflon-coated magnetic stirring bar was charged with 153 mg (600 µmol, 1.0 eq) bicyclic carboxylic acid **28** (*e.e.* > 99 %). It was dissolved in 7.0 mL anhydrous DCM and 110 µL (720 µmol, 1.2 eq) (*R*)-1-(4-bromophenyl)ethan-1-ol (**30**) as well as 7.3 mg (60.0 µmol, 10 mol%) 4-DMAP were added in an argon counter flow, respectively. Afterwards the colorless solution was cooled in an ice-water bath to 0 °C and 138 mg (720 mmol, 1.2 eq) EDC.HCl were added in one portion. Immediately after the addition of the coupling reagent the ice-water bath was removed, the Schlenk flask equipped with a bubbler and the colorless solution was stirred at RT for 14 h under argon atmosphere. Afterwards the colorless solution was diluted with 10 mL DCM and washed with H_2O (3 x 7.0 mL). The colorless organic phase was dried over $MgSO_4$, filtered and concentrated on a rotary evaporator. Finally, the colorless, solid crude material was purified via flash column chromatography (32 g SiO_2, 21.0 x 2.0 cm, eluent: cyclohexane:EtOAc = 3:1 (v/v), R_f = 0.24) and the resulting colorless, crystalline solid was dried under high vacuum.

Yield: 224 mg (510 µmol, 85 %); colorless, crystalline solid.

$C_{20}H_{24}BrNO_5$ [438.31 g.mol^{-1}].

R_f = 0.34 (cyclohexane:EtOAc = 2:1 (v/v), UV and CAM).

m_p = 121-122 °C.

$[\alpha]_D^{33-34\,°C}$ = -59.5 ° (c = 1.00 in CHCl$_3$).

HPLC-MS (Method_GENERAL): t_R = 5.06 min; *m/z* + Na$^+$ = 460 and 462 (1:1).

^{1}H-NMR (300.36 MHz, CDCl$_3$): δ = 7.47 (d, $^3J_{HH}$ = 8.3 Hz, 2H, H-12, H-14), 7.25 (d, $^3J_{HH}$ = 7.2 Hz, 2H, H-11, H-15), 6.61 (d, $^3J_{HH}$ = 5.5 Hz, 1H, H-1), 6.47 (d, $^3J_{HH}$ = 5.5 Hz, 1H, H-2), 5.89 (q, $^3J_{HH}$ = 6.5 Hz, 1H, H-8), 5.12 (s, 1H, H-6), 5.03 (bs, 1H, H-3), 4.54 (bs, 1H, H-4), 4.23 (bs, 1H, NH), 2.06 (d, $^3J_{HH}$ = 3.4 Hz, 1H, H-5), 1.54 (d, $^3J_{HH}$ = 6.6 Hz, 3H, H-9), 1.41 (s, 9H, H-18, H-19, H-20).

^{13}C-NMR (75.53 MHz, CDCl$_3$): δ = 171.1 (C$_q$, C-7), 155.1 (C$_q$, C-16), 140.6 (C$_q$, C-10), 138.0 (C-1), 134.6 (C-2), 131.8 (C-12, C-14), 128.0 (C-11, C-15), 122.0 (C$_q$, C-13), 82.1 (C-6), 80.1 (C$_q$, C-17), 79.1 (C-3), 72.6 (C-8), 53.4 (C-4), 52.7 (C-5), 28.4 (C-18, C-19, C-20), 22.3 (C-9).

HRMS (DI-EI): calculated for [C$_{20}$H$_{24}$BrNO$_5$ – C$_4$H$_4$O]$^+$: 369.0576 and 371.0557; found: 369.0601 and 371.0581.

X-ray crystals of compound **31** were grown by dissolving 50 mg of ester **31** in a GC-vial in 1.0 mL MTBE at RT. For a slow evaporation of the solvent, a thin blood capillary with the capacity of 5 µL was fixed to the cap of the GC-Vial. The crystal growing was maintained at RT for 7 d.

7.3.24. Ethyl (5*S*,6*S*)-6-(((*tert*-butoxycarbonyl)amino)-5-hydroxycyclohexa-1,3-diene-1-carboxylate (21)
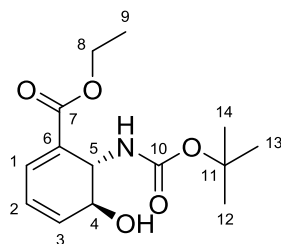
21

Literature: M. E. Bunnage, T. Ganesh, I. B. Masesane, D. Orton, P. G. Steel, *Org. Lett.* **2003**, *5*, 239-242.

An oven-dried, evacuated and argon purged 30 mL Schlenk flask with a Teflon-coated magnetic stirring bar was charged with 1.13 g (4.00 mmol, 1.0 eq) bicyclic ester **28** (*e.e.* > 99 %). It was dissolved in 17 mL anhydrous THF and afterwards the resulting colorless solution was cooled in an acetone/dry ice bath to -45 °C under argon atmosphere. In parallel 13 mL (12.0 mmol, 3.0 eq) of a 0.923 M KHMDS solution (in anhydrous THF) were transferred into a second oven-dried, evacuated and argon purged 250 mL Schlenk flask and diluted with 20 mL anhydrous THF. This yellowish suspension was also cooled in an acetone/dry ice bath to -45 °C under inert atmosphere. In an argon counter flow the colorless solution of starting material was added to the yellowish, cloudy KHMDS solution in one portion, the Schlenk flask with the former solution of ester **28** was rinsed with 10 mL anhydrous THF and the resulting yellow solution was vigorously stirred at -45 °C in an acetone/dry ice bath for 100 min. Afterwards the resulting orange, cloudy solution was poured into 100 mL saturated NH$_4$Cl and extracted with EtOAc (3 x 60 mL). The combined

yellowish, organic layers were dried over MgSO$_4$, filtered and concentrated on a rotary evaporator. Finally, the orange, oily crude material was purified via flash column chromatography (130 g SiO$_2$, 14.0 x 5.0 cm, eluent: cyclohexane:EtOAc = 1:1 (v/v), R$_f$ = 0.25) and the resulting yellowish, highly viscous liquid was dried under high vacuum.

Yield: 1.02 g (3.60 mmol, 90 %); yellowish, highly viscous liquid.

C$_{14}$H$_{21}$NO$_5$ [283.32 g.mol^{-1}].

R$_f$ = 0.39 (cyclohexane:EtOAc = 2:3 (v/v), UV and CAM).

[α]$_D^{31-32\,°C}$ = +300.1 ° (c = 1.50 in CHCl$_3$); *e.e.* > 99 %.

HPLC-MS (Method_GENERAL): t$_R$ = 2.59 min; *m/z* + Na$^+$ = 306.

^{1}H-NMR (300.36 MHz, CDCl$_3$): δ = 7.16 (d, $^3J_{HH}$ = 3.6 Hz, 1H, H-1), 6.30-6.22 (m, 2H, H-2, H-3), 4.76 (d, $^3J_{HH}$ = 7.2 Hz, 1H, H-5), 4.47 (bs, 1H, NH), 4.32 (bs, 1H, H-4), 4.28-4.13 (m, 2H, H-8), 3.03 (bs, 1H, OH), 1.42 (s, 9H, H-12, H-13, H-14), 1.28 (t, $^3J_{HH}$ = 7.1 Hz, 3H, H-9).

^{13}C-NMR (75.53 MHz, CDCl$_3$): δ = 166.0 (C$_q$, C-7), 155.6 (C$_q$, C-10), 133.6 (C-1), 132.8 (C-3), 127.5 (C$_q$, C-6), 124.6 (C-2), 80.2 (C$_q$, C-11), 67.9 (C-4), 61.0 (C-8), 50.3 (C-5), 28.5 (C-12, C-13, C-14), 14.3 (C-9).

7.3.25. (5*S*,6*S*)-6-((*tert*-Butoxycarbonyl)amino)-5-hydroxycyclohexa-1,3-diene-1-carboxylic acid (29)
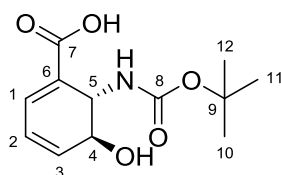
29

Literature: M. E. Bunnage, T. Ganesh, I. B. Masesane, D. Orton, P. G. Steel, *Org. Lett.* **2003**, *5*, 239-242.

A 10 mL round-bottom flask with a Teflon-coated magnetic stirring bar was charged with 567 mg (2.00 mmol, 1.0 eq) ester **21** (*e.e.* > 99 %). It was dissolved in 11 mL THF and to the colorless solution 1.0 mL (10.0 mmol, 5.0 eq) 10 M KOH in H$_2$O were added in one portion. The resulting light orange solution was vigorously stirred at RT for 19 h. Afterwards it was concentrated on a rotary evaporator and the brownish, oily residue was dissolved in 50 mL H$_2$O. The brownish aqueous phase was washed with EtOAc (2 x 50 mL), the product from

the organic phase reextracted with H_2O (2 x 10 mL) and the combined brownish aqueous layers subsequently acidified with 5.0 mL saturated $KHSO_4$ to pH 1-2. The product was extracted with EtOAc (4 x 100 mL), the combined yellow organic phases were dried over $MgSO_4$, filtered and the solvent was removed on a rotary evaporator. Finally, the crude material was purified via flash column chromatography (50 g SiO_2, 10.0 x 3.5 cm, eluent: EtOAc:AcOH = 1000:1 (v/v), R_f = 0.18) and the resulting colorless powder was dried under high vacuum.

Yield: 383 mg (1.50 mmol, 79 %); colorless solid.

$C_{12}H_{17}NO_5$ [255.27 g.mol^{-1}].

R_f = 0.31 (EtOAc:MeOH:AcOH = 1000:100:1 (v/v/v), UV and CAM).

m_p = 168-169 °C (decomposition).

$[\alpha]_D^{31-32\,°C}$ = +466.4 ° (c = 1.00 in DMSO); *e.e.* > 99 %.

HPLC-MS (Method_GENERAL): t_R = 1.31 min; m/z + Na$^+$ = 278.

^{1}H-NMR (300.36 MHz, DMSO-d$_6$): δ = 12.28 (s, 1H, COOH), 7.00-6.98 (m, 1H, H-1), 6.58 (d, $^3J_{HH}$ = 7.4 Hz, 1H, NH), 6.20-6.13 (m, 2H, H-2, H-3), 5.07 (d, $^3J_{HH}$ = 5.6 Hz, 1H, OH), 4.43 (d, $^3J_{HH}$ = 7.2 Hz, 1H, H-5), 3.91 (bs, 1H, H-4), 1.36 (s, 9H, H-10, H-11, H-12).

^{13}C-NMR (75.53 MHz, DMSO-d$_6$): δ = 167.4 (C$_q$, C-7), 155.1 (C$_q$, C-8), 133.3 (C-1), 133.1 (C-3), 126.9 (C$_q$, C-6), 123.9 (C-2), 77.7 (C$_q$, C-9), 66.2 (C-4), 49.0 (C-5), 28.2 (C-10, C-11, C-12).

7.3.26. (1*S*,6*S*)-2-Carboxy-6-hydroxycyclohexa-2,4-diene-1-ammonium 2,2,2-trifluoroacetate (1a)
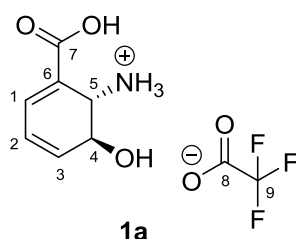
1a

An oven-dried 25 mL round-bottom flask equipped with a Teflon-coated magnetic stirring bar was charged with 383 mg (1.50 mmol, 1.0 eq) carboxylic acid **29** (*e.e.* > 99 %). Afterwards the starting material was suspended in 5.0 mL DCM and to the colorless suspension 750 µL TFA were added (15 % TFA in DCM (v/v)), respectively. A yellowish solution was

119

immediately formed after the addition of TFA, it turned brownish by the time and the desired product precipitated in the form of a brownish solid. The suspension was stirred at RT for 90 min. Subsequently it was cooled in an ice-water bath to 0 °C, the precipitate was collected by filtration and washed with a small amount of cooled DCM (2 x 700 µL). Finally the brownish, powdery crude material was purified by trituration in 1.6 mL DCM:MeCN = 2:1 (v/v). It was collected by filtration, washed with cold DCM:MeCN = 2:1 (v/v) (2 x 300 µL) and the resulting colorless powder was dried under high vacuum.

Yield: 323 mg (1.20 mmol, 80 %); colorless powder.

$C_9H_{10}F_3NO_5$ [269.17 g.mol^{-1}].

m_p = 161-162 °C (decomposition).

$[\alpha]_D^{32-33\,°C}$ = +364.4 ° (c = 0.50 in DMSO); *e.e.* > 99 %.

^{1}H-NMR (300.36 MHz, D_2O): δ = 7.45 (d, $^3J_{HH}$ = 5.3 Hz, 1H, H-1), 6.51-6.40 (m, 2H, H-2, H-3), 4.47-4.45 (m, 1H, H-4), 4.38 (d, $^3J_{HH}$ = 3.0 Hz, 1H, H-5).

^{1}H-NMR (300.36 MHz, DMSO-d_6): δ = 13.08 (bs, 1H, COOH), 8.07 (bs, 3H, NH_3^+), 7.25-7.22 (m, 1H, H-1), 6.37-6.29 (m, 2H, H-2, H-3), 5.64 (bs, 1H, OH), 4.16 (s, 1H, H-4), 4.04 (s, 1H, H-5).

^{13}C-NMR (125.69 MHz, D_2O): δ = 168.4 (C_q, C-7), 162.9 (C_q, q, $^2J_{CF}$ = 35.5 Hz, C-8), 137.6 (C-1), 131.8 (C-3), 125.1 (C_q, C-6), 122.0 (C-2), 116.2 (C_q, q, $^1J_{CF}$ = 292 Hz, C-9), 64.0 (C-4), 48.7 (C-5).

^{19}F-NMR (470.35 MHz, D_2O): δ = -75.7 (decoupled, CF_3).

7.3.27. (5*S*,6*S*)-6-((5-(((*S*)-1-Amino-1-oxopropan-2-yl)amino)-2,4-dinitrophenyl)-amino)-5-hydroxycyclohexa-1,3-diene-1-carboxylic acid (74a)

74a
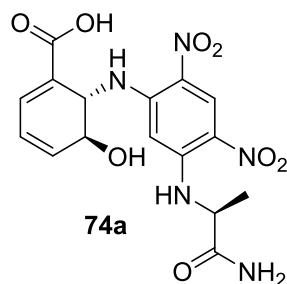
According to the general procedure (derivatization with MARFEY's reagent) ammonium salt **1a** was derivatized with MARFEY's reagent in order to determine the *e.e.* value of this compound.

HPLC-MS (Method_MARFEY_A): t_R = 1.51 min (minor diastereomer) and 1.80 min (major diastereomer); *d.e.* > 99 %, consequently *e.e.* > 99 % of compound **1**.
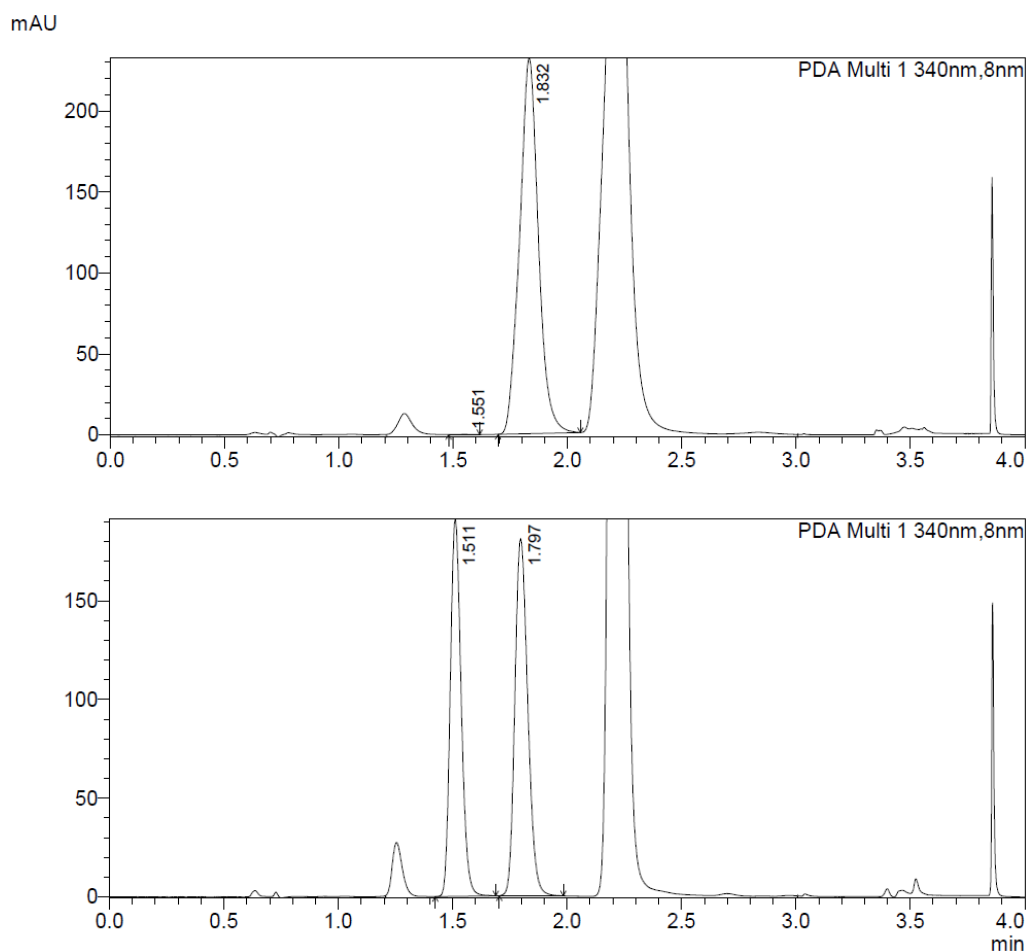
Figure 37: HPLC-MS chromatograms of **74a** and *rac*-**74** for the determination of the diastereomeric excess (*d.e.*).

7.3.28. Ethyl (1*R*,2*S*,3*S*,4*S*)-3-((*tert*-butoxycarbonyl)amino)-7-oxabicyclo[2.2.1]-heptane-2-carboxylate (*rac*-35)

***rac*-35**
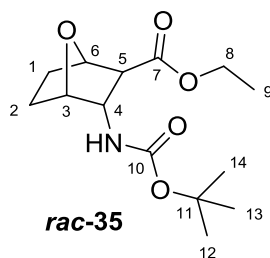
An oven-dried 250 mL round-bottom flask equipped with a Teflon-coated magnetic stirring bar was charged with 2.66 g (12.5 mmol, 1.0 eq) bicyclic DIELS-ALDER compound **27**. It was dissolved in 120 mL EtOH and afterwards cooled in an ice-water bath to 0 °C. Consecutively, 17.2 mL conc. HCl (~36 % (w/w) in H_2O), 16.4 g (250 mmol, 20.0 eq) activated Zn (Zn washed with 1 M HCl, H_2O as well as MeOH and afterwards dried under high vacuum) as well as 111 mg (625 µmol, 5.0 mol%) $PdCl_2$ were added in small portions to the colorless solution. Immediately after the addition of Zn intense H_2 gas formation was observed. After 30 min of vigorous stirring at 0 °C, the ice-water bath was removed and the grey suspension was additionally stirred at RT for 7 h. It was filtered through a pad of Celite® (diameter: 6.0 cm, height: 4.0 cm) and the filter cake was carefully washed with EtOH (2 x 30 mL). The filtrate was collected in an oven-dried 500 mL round-bottom flask equipped with a Teflon-coated magnetic stirring bar. 34.9 mL (25.8 g, 200 mmol, 16.0 eq) DIPEA and 4.91 g (22.5 mmol, 1.8 eq) Boc_2O were added successively and the resulting colorless suspension was vigorously stirred at RT for 16 h. Subsequently it was carefully concentrated under high vacuum, the colorless solid residue was diluted with 600 mL EtOAc and washed with H_2O (1 x 600 mL). The cloudy, colorless aqueous phase was reextracted with EtOAc (2 x 600 mL), the combined yellowish organic layers washed with saturated $NaHCO_3$ (1 x 600 mL), dried over $MgSO_4$, filtered and the solvent was removed under reduced pressure on a rotary evaporator. Finally, the colorless solid crude material was purified via flash column chromatography (320 g SiO_2, 22.0 x 6.0 cm, eluent: cyclohexane:EtOAc = 3:1 (v/v), R_f = 0.25) and the resulting colorless solid dried under high vacuum.

Yield: 2.89 g (10.1 mmol, 81 %), colorless, crystalline solid.

$C_{14}H_{23}NO_5$ [285.34 g.mol^{-1}].

R_f = 0.36 (cyclohexane:EtOAc = 2:1 (v/v), UV and CAM).

m_p = 116-117 °C.

HPLC-MS (Method_GENERAL): t_R = 3.22 min; *m/z* + Na$^+$ = 308.

^{1}H-NMR (300.36 MHz, CDCl$_3$): δ = 4.81 (bs, 1H, NH), 4.72-4.71 (d, 2H, H-3, H-6), 4.27-4.23 (m, 1H, H-4), 4.17 (q, $^3J_{HH}$ = 7.1 Hz, 2H, H-8), 2.15 (d, $^3J_{HH}$ = 5.0 Hz, 1H, H-5), 1.87-1.78 (m, 2H, H-1, H-2), 1.70-1.64 (m, 1H, H-2), 1.59-1.51 (m, 1H, H-1), 1.43 (s, 9H, H-12, H-13, H-14), 1.26 (t, $^3J_{HH}$ = 7.1 Hz, 3H, H-9).

^{13}C-NMR (75.53 MHz, CDCl$_3$): δ = 172.2 (C$_q$, C-7), 155.6 (C$_q$, C-10), 79.9 (C$_q$, C-11), 79.8 (C-3), 78.5 (C-6), 61.3 (C-8), 56.5 (C-4), 55.2 (C-5), 30.2 (C-1), 28.4 (C-12, C-13, C-14), 22.5 (C-2), 14.3 (C-9).

7.3.29. (1*R*,2*S*,3*S*,4*S*)-3-((*tert*-Butoxycarbonyl)amino)-7-oxabicyclo[2.2.1]hept-ane-2-carboxylic acid (36)

36
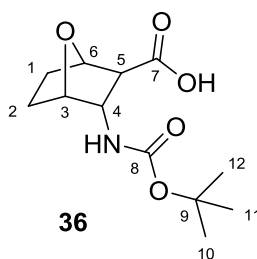
This preparation (total amount of bicyclic ester *rac*-35: 2.67 g (9.36 mmol, 1.0 eq)) was divided into three smaller preparations with 890 mg (3.12 mmol, 1.0 eq) of compound *rac*-35 each!

Each 250 mL round-bottom flask with a Teflon-coated magnetic stirring bar was charged with 890 mg (3.12 mmol, 1.0 eq) bicyclic ester *rac*-35. It was dissolved in 36 mL Et$_2$O and to the colorless solutions 62 mL NaH$_2$PO$_4$/Na$_2$HPO$_4$ buffer (pH 7.6, 100 mM) were added, respectively. After addition of 3.6 mL PLE-precipitate (in half saturated (NH$_4$)$_2$SO$_4$, unknown activity) to each preparation the yellowish two-phasic mixtures were stirred with 250 rpm in the closed flask at RT for 22 h until the non-hydrolyzed enantiomer of compound *ent*-35 reached an *e.e.* value between 96-98 % (E = 110).

The combined yellowish reaction mixtures were phase separated and the aqueous phase was washed with Et$_2$O (2 x 300 mL). In order to obtain a better phase separation the mixture was centrifuged. The yellowish aqueous layer was acidified with 25 mL of saturated KHSO$_4$ to pH 1-2 and the product was extracted with DCM (4 x 300 mL). The combined yellowish organic layers were dried over MgSO$_4$, filtered and the solvent was removed under reduced pressure on a rotary evaporator. For purification the brownish crude material was triturated in 12 mL cyclohexane:EtOAc = 2:1 (v/v), collected by filtration, washed with cold

cyclohexane:EtOAc = 2:1 (v/v) (2 x 1.0 mL) and the resulting colorless powder was dried under high vacuum.

Yield: 1.14 g (4.44 mmol, 47 %); colorless powder.

chiral HPLC (Method_ACID): t_R = 8.87 min (major enantiomer) and 11.10 min (minor enantiomer); *e.e.* = 93 %.

In order to gain perfect *e.e.* values, this procedure was repeated with 1.18 g (4.14 mmol, 1.0 eq) of the enantiomerically enriched bicyclic ester **35** (*e.e.* = 93 %) as starting material. After reaching an *e.e.* = 47 % of non-hydrolyzed ester ***ent*-35**), the work-up as well as the purification was performed as described above.

Yield: 890 mg (3.46 mmol, 84 %); colorless powder.

$C_{12}H_{19}NO_5$ [257.28 g.mol^{-1}].

R_f = 0.16 (EtOAc:MeOH:AcOH = 1000:4:1 (v/v/v), UV and CAM).

m_p = 145-146 °C.

$[\alpha]_D^{31\text{-}32\,°C}$ = -23.1 ° (c = 1.00 in CHCl$_3$).

HPLC-MS (Method_GENERAL): t_R = 1.89 min; *m/z* + Na$^+$ = 280.

chiral HPLC (Method_ACID): t_R = 8.87 min (major enantiomer) and 11.10 min (minor enantiomer); *e.e.* > 99 %.

^{1}H-NMR (300.36 MHz, DMSO-d$_6$): δ = 12.38 (s, 1H, COOH), 7.28 (d, $^3J_{HH}$ = 5.1 Hz, 1H, NH), 4.56 (s, 1H, H-6), 4.46-4.43 (m, 1H, H-3), 4.00-3.94 (m, 1H, H-4), 2.38 (d, $^3J_{HH}$ = 3.6 Hz, 1H, H-5), 1.80-1.71 (m, 1H, H-2a), 1.59-1.55 (m, 2H, H-1), 1.39 (s, 10H, H-2b, H-10, H-11, H-12).

^{13}C-NMR (75.53 MHz, DMSO-d$_6$): δ = 173.5 (C$_q$, C-7), 155.4 (C$_q$, C-8), 79.2 (C-6), 78.0 (C$_q$, C-9), 77.5 (C-3), 55.4 (C-4), 52.1 (C-5), 29.3 (C-1), 28.2 (C-10, C-11, C-12), 22.1 (C-2).

HRMS (DI-EI): calculated for $C_{12}H_{19}NO_5^+$: 257.1263; found: 257.1284.

7.3.30. Ethyl (1*R*,2*S*,3*S*,4*S*)-3-((*tert*-butoxycarbonyl)amino)-7-oxabicyclo[2.2.1]-heptane-2-carboxylate (35)
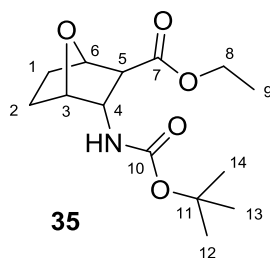
35

An oven-dried, evacuated and argon purged 100 mL Schlenk flask with a Teflon-coated magnetic stirring bar was charged with 1.04 g (4.20 mmol, 1.0 eq) bicyclic carboxylic acid **36** (*e.e.* = 93 %). It was dissolved in 40 mL anhydrous DCM and 367 µL (6.30 mmol, 1.5 eq) anhydrous EtOH as well as 51.3 mg (420 µmol, 10 mol%) 4-DMAP were added in an argon counter flow, respectively. Afterwards the colorless solution was cooled in an ice-water bath to 0 °C and 1.21 g (6.30 mmol, 1.5 eq) EDC.HCl were added in one portion. Immediately after the addition of the coupling reagent the ice-water bath was removed, the Schlenk flask equipped with a bubbler and the colorless solution was stirred at RT for 15 h under argon atmosphere. Afterwards the colorless solution was diluted with 40 mL DCM and washed with H_2O (3 x 40 mL). The colorless organic phase was dried over $MgSO_4$, filtered and concentrated on a rotary evaporator. Finally, the yellowish crude material was purified via flash column chromatography (50 g SiO_2, 10 x 3.5 cm, eluent: cyclohexane:EtOAc = 2:1 (v/v), R_f = 0.24) and the resulting colorless, crystalline solid was dried under high vacuum.

Yield: 1.18 g (4.14 mmol, 98 %); colorless, crystalline solid.

chiral HPLC (Method_ESTER): t_R = 8.07 min (minor enantiomer) and 9.73 min (major enantiomer); *e.e.* = 93 %.

This procedure was repeated with 797 g (3.10 mmol, 1.0 eq) of the enantiomerically enriched bicyclic carboxylic acid **36** (*e.e.* > 99 %) as starting material.

Yield: 871 mg (3.05 mmol, 98 %); colorless, crystalline solid.

$C_{14}H_{23}NO_5$ [285.34 g.mol^{-1}].

R_f = 0.50 (cyclohexane:EtOAc = 3:2 (v/v), UV and CAM).

m_p = 136-137 °C.

$[\alpha]_D^{31-32\ °C}$ = -58.6 ° (c = 1.00 in CHCl$_3$).

HPLC-MS (Method_GENERAL): t_R = 3.22 min; *m/z* + Na$^+$ = 308.

chiral HPLC (Method_ESTER): t_R = 8.07 min (minor enantiomer) and 9.73 min (major enantiomer); *e.e.* > 99 %.

^{1}H-NMR (300.36 MHz, CDCl$_3$): δ = 4.81 (bs, 1H, NH), 4.72-4.71 (d, 2H, H-3, H-6), 4.27-4.23 (m, 1H, H-4), 4.17 (q, $^3J_{HH}$ = 7.1 Hz, 2H, H-8), 2.15 (d, $^3J_{HH}$ = 5.0 Hz, 1H, H-5), 1.87-1.78 (m, 2H, H-1a, H-2a), 1.70-1.64 (m, 1H, H-2b), 1.59-1.51 (m, 1H, H-1b), 1.43 (s, 9H, H-12, H-13, H-14), 1.26 (t, $^3J_{HH}$ = 7.1 Hz, 3H, H-9).

^{13}C-NMR (75.53 MHz, CDCl$_3$): δ = 172.2 (C$_q$, C-7), 155.6 (C$_q$, C-10), 79.9 (C$_q$, C-11), 79.8 (C-3), 78.5 (C-6), 61.3 (C-8), 56.5 (C-4), 55.2 (C-5), 30.2 (C-1), 28.4 (C-12, C-13, C-14), 22.5 (C-2), 14.3 (C-9).

HRMS (DI-EI): calculated for C$_{14}$H$_{23}$NO$_5$$^+$: 285.1576; found: 285.1573.

7.3.31. Ethyl (5*S*,6*S*)-6-((*tert*-butoxycarbonyl)amino)-5-hydroxycyclohex-1-ene-1-carboxylate (37)

37

An oven-dried, evacuated and argon purged 30 mL Schlenk flask with a Teflon-coated magnetic stirring bar was charged with 800 mg (2.80 mmol, 1.0 eq) bicyclic ester **35** (*e.e.* > 99 %). It was dissolved in 12 mL anhydrous THF and afterwards the resulting colorless solution was cooled in an acetone/dry ice bath to -45 °C under argon atmosphere. In parallel 10 mL (8.40 mmol, 3.0 eq) of a 0.840 M KHMDS solution (in anhydrous THF) were transferred into a second oven-dried, evacuated and argon purged 80 mL Schlenk flask and diluted with 14 mL anhydrous THF. This yellowish, cloudy solution was also cooled in an acetone/dry ice bath to -45 °C under inert atmosphere. In an argon counter flow the colorless solution of starting material was added via syringe to the yellowish KHMDS solution in one portion, the Schlenk flask with the former solution of ester **35** was rinsed with 4 mL anhydrous THF and the resulting yellow suspension solution was vigorously stirred at -45 °C in the acetone/dry ice bath for 120 min. Afterwards the resulting orange, cloudy solution was poured onto 70 mL saturated NH$_4$Cl and extracted with EtOAc (3 x 40 mL). The combined yellowish, organic layers were dried over MgSO$_4$, filtered and concentrated on a rotary

evaporator. Finally, the yellowish, oily crude material was purified via flash column chromatography (100 g SiO_2, 16.0 x 4.0 cm, eluent: cyclohexane:EtOAc = 11:9 (v/v), R_f = 0.24 and R_f = 0.32) and the resulting colorless, highly viscous liquids were dried under high vacuum.

Yield: 247 mg (866 µmol, 31 %); colorless, highly viscous liquid.

$C_{14}H_{23}NO_5$ [285.34 g.mol^{-1}].

R_f = 0.28 (cyclohexane:EtOAc = 1:1 (v/v), UV and CAM).

$[α]_D^{31\text{-}32\,°C}$ = +84.9 ° (c = 1.00 in $CHCl_3$); *e.e.* > 99 %.

HPLC-MS (Method_GENERAL): t_R = 2.61 min; m/z + Na$^+$ = 308.

^{1}H-NMR (300.36 MHz, $CDCl_3$): δ = 7.19-7.16 (m, 1H, H-2), 4.56 (d, $^3J_{HH}$ = 6.0 Hz, 1H, NH), 4.37-4.35 (m, 1H, H-6), 4.28-4.08 (m, 2H, H-8), 4.04 (bs, 1H, H-5), 2.95 (bs, 1H, OH), 2.49-2.37 (m, 1H, H-3), 2.25-2.14 (m, 1H, H-3), 1.85-1.64 (m, 2H, H-4), 1.43 (s, 9H, H-12, H-13, H-14), 1.26 (t, $^3J_{HH}$ = 7.1 Hz, 3H, H-14).

^{13}C-NMR (75.53 MHz, $CDCl_3$): δ = 166.3 (C_q, C-7), 155.7 (C_q, C-10), 143.7 (C-2), 128.0 (C_q, C-1), 80.0 (C_q, C-11), 69.0 (C-5), 60.7 (C-8), 50.8 (C-6), 28.5 (C-12, C-13, C-14), 21.8 (C-3), 14.3 (C-9).

HRMS (DI-EI): calculated for $C_{14}H_{23}NO_5^+$: 285.1576; found: 285.1581.

7.3.32. Ethyl (5*S*,6*S*)-6-((*tert*-butoxycarbonyl)amino)-5-hydroxycyclohex-2-ene-1-carboxylate (38)

38

Yield: 237 mg (831 µmol, 30 %); colorless, highly viscous liquid.

$C_{14}H_{23}NO_5$ [285.34 g.mol^{-1}].

R_f = 0.40 (cyclohexane:EtOAc = 1:1 (v/v), UV and CAM).

$[\alpha]_D^{31\text{-}32\,°C}$ = +138.5 ° (c = 1.00 in CHCl$_3$); *e.e.* > 99 %.

HPLC-MS (Method_GENERAL): t_R = 2.87 min; *m/z* + Na$^+$ = 308.

^{1}H-NMR (300.36 MHz, CDCl$_3$): δ = 5.76-5.68 (m, 2H, H-2, H-3), 5.23 (d, $^3J_{HH}$ = 7.6 Hz, 1H, NH), 4.23-4.07 (m, 3H, H-5, H-8), 4.03-3.95 (m, 1H, H-6), 3.58-3.55 (m, 1H, H-1), 2.58-2.51 (m, 2H, H-4, OH), 2.12 (dd, $^3J_{HH}$ = 18.1 Hz, $^3J_{HH}$ = 6.4 Hz, 2H, H-4), 1.42 (s, 9H, H-12, H-13, H-14), 1.25 (t, $^3J_{HH}$ = 7.1 Hz, 3H, H-9).

^{13}C-NMR (75.53 MHz, CDCl$_3$): δ = 172.5 (C$_q$, C-7), 156.5 (C$_q$, C-10), 127.3 (C-2), 122.8 (C-3), 80.0 (C$_q$, C-11), 66.6 (C-5), 61.1 (C-8), 52.6 (C-6), 44.5 (C-1), 33.0 (C-4), 28.5 (C-12, C-13, C-14), 14.3 (C-9).

HRMS (DI-EI): calculated for C$_{14}$H$_{23}$NO$_5$$^+$: 285.1576; found: 285.1588.
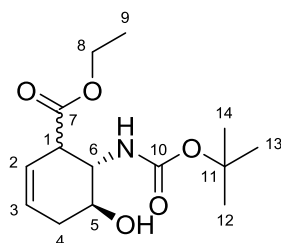
7.3.33. (5*S*,6*S*)-6-((*tert*-Butoxycarbonyl)amino)-5-hydroxycyclohex-1-ene-1-carboxylic acid (75)
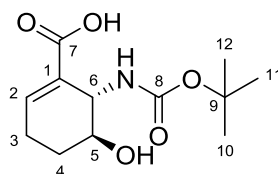
75

A 10 mL round-bottom flask with a Teflon-coated magnetic stirring bar was charged with 240 mg (840 µmol, 1.0 eq) ester **37** (*e.e.* > 99 %). It was dissolved in 5 mL THF and to the colorless solution 840 µL (8.40 mmol, 10.0 eq) 10 M KOH solution in H$_2$O were added in one portion. The resulting yellowish solution was vigorously stirred at RT for 17 h. Afterwards it was concentrated on a rotary evaporator and the orange, oily residue was dissolved in 20 mL H$_2$O. The brownish aqueous phase was washed with EtOAc (2 x 20 mL), the product from the organic phase was reextracted with H$_2$O (2 x 5 mL) and the combined brownish aqueous layers subsequently acidified with 3 mL saturated KHSO$_4$ to pH 1-2. The product was extracted with EtOAc (4 x 40 mL), the combined yellow organic phases were dried over MgSO$_4$, filtered and the solvent was removed on a rotary evaporator. Finally, the brownish crude material was purified via flash column chromatography (20 g SiO$_2$, 14.0 x 2.0 cm, eluent: EtOAc:AcOH = 1000:1 (v/v), R$_f$ = 0.24) and the resulting colorless powder was dried under high vacuum.

Yield: 179 mg (696 µmol, 83 %); colorless solid.

$C_{12}H_{19}NO_5$ [257.28 g.mol^{-1}].

R_f = 0.48 (EtOAc:MeOH:AcOH = 1000:100:1 (v/v/v), UV and CAM).

m_p = 204-205 °C.

$[\alpha]_D^{29-30\ °C}$ = +149.6 ° (c = 1.00 in DMSO); *e.e.* > 99 %.

HPLC-MS (Method_GENERAL): t_R = 1.32 min; *m/z* + Na$^+$ = 280.

^{1}H-NMR (300.36 MHz, DMSO-d$_6$): δ = 12.02 (bs, 1H, COOH), 6.94 (s, 1H, H-H-2), 6.74 (d, $^3J_{HH}$ = 7.7 Hz, 1H, NH), 4.76 (s, 1H, OH), 4.14 (d, $^3J_{HH}$ = 6.5 Hz, 1H, H-6), 3.69 (s, 1H, H-5), 2.27-2.15 (m, 1H, H-3), 2.07-1.96 (m, 1H, H-3), 1.67-1.50 (m, 2H, H-4), 1.37 (s, 9H, H-10, H-11, H-12).

^{13}C-NMR (75.53 MHz, DMSO-d$_6$): δ = 167.5 (C$_q$, C-7), 154.7 (C$_q$, C-8), 142.0 (C-2), 127.8 (C$_q$, C-1), 77.4 (C$_q$, C-9), 66.7 (C-5), 48.4 (C-6), 28.3 (C-10, C-11, C-12), 22.6 (C-4), 20.8 (C-3).

HRMS (DI-EI): calculated for $C_{12}H_{19}NO_5^+$: 257.1263; found: 257.1289.

7.3.34. (1*S*,6*S*)-2-Carboxy-6-hydroxycyclohex-2-ene-1-ammonium 2,2,2-trifluoroacetate (34a)
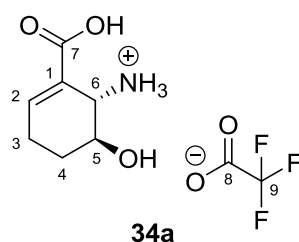
34a

An oven-dried 5 mL round-bottom flask equipped with a Teflon-coated magnetic stirring bar was charged with 154 mg (600 µmol, 1.0 eq) carboxylic acid **75** (*e.e.* > 99 %). Afterwards the starting material was suspended in 2.0 mL DCM and to the colorless suspension 300 µL TFA were added (15 % TFA in DCM (v/v)), respectively. A yellowish solution was immediately formed after the addition of TFA, it turned brownish by the time and the desired product precipitated in the form of a brownish solid. The suspension was stirred at RT for 90 min. Subsequently it was cooled in an ice-water bath to 0 °C, the precipitate was collected by filtration and washed with a small amount of cooled DCM (2 x 300 µL). Finally, the colorless, powdery crude material was purified by trituration in 600 µL DCM:MeCN = 2:1 (v/v). It was

collected by filtration, washed with cold DCM:MeCN = 2:1 (v/v) (2 x 150 µL) and the resulting colorless powder was dried under high vacuum.

Yield: 113 mg (417 mmol, 69 %); colorless powder.

$C_9H_{12}F_3NO_5$ [271.19 g.mol^{-1}].

m_p = 154-155 °C.

$[\alpha]_D^{32-33\,°C}$ = +55.0 ° (c = 0.50 in DMSO); *e.e.* > 99 %.

^{1}H-NMR (300.36 MHz, D$_2$O): δ = 7.44 (t, $^3J_{HH}$ = 3.5 Hz, 1H, H-2), 4.10-4.02 (m, 2H, H-5, H-6), 2.54-2.37 (m, 2H, H-3), 2.01-1.91 (m, 1H, H-4), 1.88-1.76 (m, 1H, H-4).

^{1}H-NMR (300.36 MHz, DMSO-d$_6$): δ = 13.00 (bs, 1H, COOH), 7.99 (bs, 3H, NH$_3^+$), 7.21 (t, $^3J_{HH}$ = 3.5 Hz, 1H, H-2), 5.37 (s, 1H, OH), 3.91 (s, 1H, H-5), 3.71 (s, 1H, H-6), 2.40-2.19 (m, 2H, H-3), 1.83-1.76 (m, 1H, H-4), 1.68-1.61 (m, 1H, H-4).

^{13}C-NMR (125.69 MHz, D$_2$O): δ = 168.6 (C$_q$, C-7), 162.9 (C$_q$, q, $^2J_{CF}$ = 35.5 Hz, C-8), 148.9 (C-2), 123.4 (C$_q$, C-1), 116.2 (C$_q$, q, $^1J_{CF}$ = 292 Hz, C-9), 67.2 (C-5), 51.4 (C-6), 25.4 (C-4), 22.8 (C-3).

^{19}F-NMR (470.35 MHz, D$_2$O): δ = -75.7 (decoupled, CF$_3$).

HRMS (DI-EI): calculated for $C_7H_{11}NO_3^+$: 157.0739; found: 157.0729.

7.3.35. (5S,6S)-6-((5-(((S)-1-Amino-1-oxopropan-2-yl)amino)-2,4-dinitrophenyl)-amino)-5-hydroxycyclohex-1-ene-1-carboxylic acid (76a)
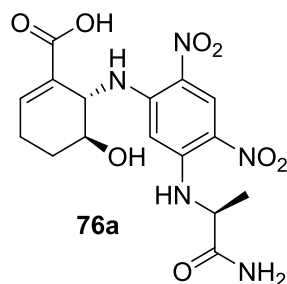
According to the general procedure (derivatization with MARFEY's reagent) ammonium salt **34a** was derivatized with MARFEY's reagent in order to determine the *e.e.* value of this compound.

HPLC-MS (Method_MARFEY_A): t_R = 1.47 min (minor diastereomer) and 1.87 min (major diastereomer); *d.e.* > 99 %, consequently *e.e.* > 99 % of compound **34**.
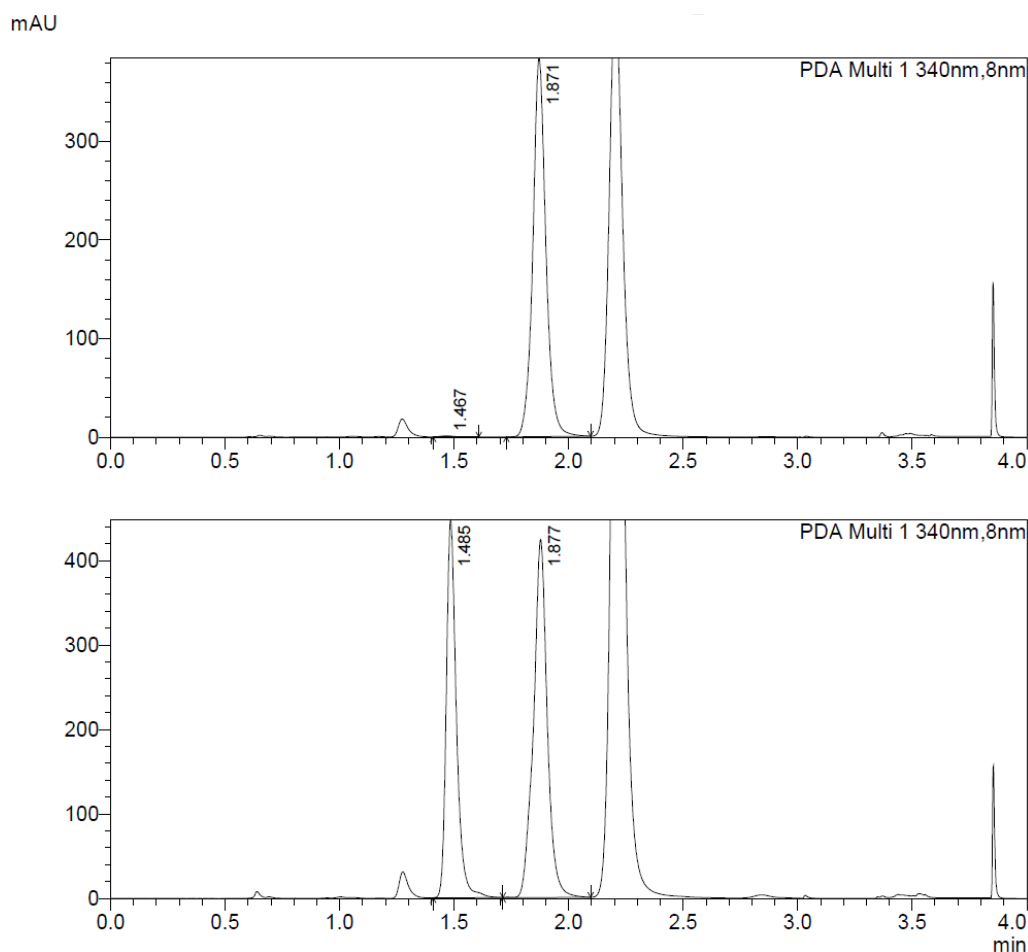
Figure 38: HPLC-MS chromatograms of **76a** and ***rac*-76** for the determination of the diastereomeric excess (*d.e.*).

7.3.36. Ethyl (5S,6S)-6-((*tert*-butoxycarbonyl)amino)-5-methoxycyclohexa-1,3-diene-1-carboxylate (77)
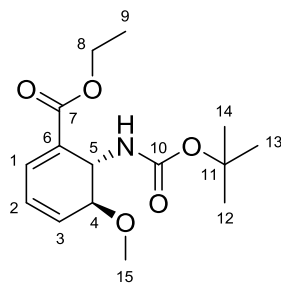
77

An oven-dried 25 mL round-bottom flask equipped with a Teflon-coated magnetic stirring bar was charged with 312 mg (1.10 mmol, 1.0 eq) ester **21** (*e.e.* > 99 %). It was dissolved in 13 mL Et_2O and to the yellowish solution 510 mg (2.20 mmol, 2.0 eq) Ag_2O were added. After the addition of 2.0 g 4 Å MS and 411 µL (6.60 mmol, 6.0 eq) iodomethane (MeI), the black suspension was stirred in the closed flask at RT for 22 h. Subsequently it was filtered through a pad of Celite® (diameter: 3.0 cm, height: 4.0 cm), the filter cake was washed with EtOAc (3 x 50 mL) and the solvent was removed on a rotary evaporator. Finally, the yellow, viscous crude material was purified via flash column chromatography (33 g SiO_2, 21.0 x 2.0 cm, eluent: cyclohexane:EtOAc = 3:1 (v/v), R_f = 0.28) and the resulting colorless, highly viscous liquid was dried under high vacuum.

Yield: 307 mg (1.03 mmol, 94 %); colorless, highly viscous liquid.

$C_{15}H_{23}NO_5$ [297.34 g.mol^{-1}].

R_f = 0.60 (cyclohexane:EtOAc = 1:1 (v/v), UV and CAM).

$[α]_D^{31\text{-}32\,°C}$ = +312.8 ° (c = 1.00 in $CHCl_3$); *e.e.* > 99 %.

HPLC-MS (Method_GENERAL): t_R = 3.55 min; *m/z* + Na^+ = 320.

^{1}H-NMR (300.36 MHz, $CDCl_3$): δ = 7.15 (d, $^3J_{HH}$ = 5.0 Hz, 1H, H-1), 6.32-6.22 (m, 2H, H-2, H-3), 4.90 (d, $^3J_{HH}$ = 7.0 Hz, 1H, H-5), 4.31-4.13 (m, 3H, H-8, NH), 3.86 (bs, 1H, H-4), 3.48 (s, 3H, H-15), 1.43 (s, 9H, H-12, H-13, H-14), 1.28 (t, $^3J_{HH}$ = 7.1 Hz, 3H, H-9).

^{13}C-NMR (75.53 MHz, $CDCl_3$): δ = 165.8 (C_q, C-7), 155.1 (C_q, C-10), 133.4 (C-1), 130.5 (C-3), 128.1 (C_q, C-6), 125.6 (C-2), 79.9 (C_q, C-11), 75.9 (C-4), 60.9 (C-8), 56.8 (C-15), 45.6 (C-5), 28.5 (C-12, C-13, C-14), 14.3 (C-9).

HRMS (DI-EI): calculated for $C_{15}H_{23}NO_5^+$: 297.1576; found: 297.1567.

7.3.37. (5*S*,6*S*)-6-((*tert*-Butoxycarbonyl)amino)-5-methoxycyclohexa-1,3-diene-1-carboxylic acid (78)
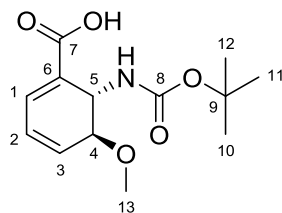
78

A 25 mL round-bottom flask equipped with a Teflon-coated magnetic stirring bar was charged with 279 mg (940 µmol, 1.0 eq) methoxy ester **77**. It was dissolved in 8.0 mL THF and to the colorless solution 400 µL H_2O as well as 158 mg (3.76 mmol, 4.0) $LiOH.H_2O$ were added, respectively. The resulting yellowish, milky solution was stirred in a closed system at RT for 90 h. Afterwards it was concentrated on a rotary evaporator and the oily residue was dissolved in 25 mL H_2O. The yellowish aqueous phase was washed with EtOAc (2 x 25 mL), the product from the organic phase reextracted with H_2O (2 x 5 mL) and the combined yellowish aqueous layers subsequently acidified with 2.0 mL saturated $KHSO_4$ to pH 1-2. The product was extracted with EtOAc (3 x 25 mL), the combined yellowish organic phases were dried over $MgSO_4$, filtered and the solvent was removed on a rotary evaporator. Finally, the crude material was purified via flash column chromatography (36 g SiO_2, 22.5 x 2.0 cm, eluent: cyclohexane:EtOAc:AcOH = 1000:5000:1 (v/v/v), R_f = 0.22) and the resulting colorless, viscous liquid was dried under high vacuum.

Yield: 248 mg (921 µmol, 98 %); colorless, viscous liquid.

$C_{13}H_{19}NO_5$ [269.29 g.mol^{-1}].

R_f = 0.49 (EtOAc:AcOH = 1000:1 (v/v), UV and CAM).

$[\alpha]_D^{31\text{-}32\,°C}$ = +325.9 ° (c = 0.50 in DMSO); *e.e.* > 99 %.

HPLC-MS (Method_GENERAL): t_R = 2.15 min; *m/z* + Na$^+$ = 292.

^{1}H-NMR (300.36 MHz, DMSO-d$_6$): δ = 12.40 (bs, 1H, COOH), 7.00 (d, $^3J_{HH}$ = 5.1 Hz, 1H, H-1), 6.75 (d, $^3J_{HH}$ = 7.1 Hz, 1H, NH), 6.31-6.20 (m, 2H, H-2, H-3), 4.54 (d, $^3J_{HH}$ = 6.9 Hz, 1H, H-5), 3.69 (d, $^3J_{HH}$ = 3.8 Hz, 1H, H-4), 3.30 (s, 3H, H-13), 1.37 (s, 9H, H-10, H-11, H-12).

^{13}C-NMR (75.53 MHz, DMSO-d$_6$): δ = 167.1 (C$_q$, C-7), 155.0 (C$_q$, C-8), 133.1 (C-1), 129.7 (C-3), 127.4 (C$_q$, C-6), 125.8 (C-2), 77.9 (C$_q$, C-9), 75.2 (C-4), 55.5 (C-13), 45.6 (C-5), 28.2 (C-10, C-11, C-12).

HRMS (DI-EI): calculated for $C_{13}H_{19}NO_5^+$: 269.1263; found: 269.1271.

7.3.38. (1*S*,6*S*)-2-Carboxy-6-methoxycyclohexa-2,4-diene-1-ammonium 2,2,2-trifluoroacetate (41a)
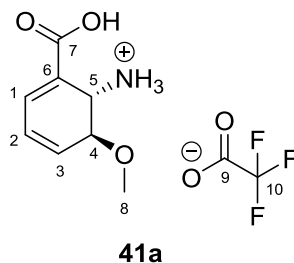
41a

An oven-dried 10 mL round-bottom flask equipped with a Teflon-coated magnetic stirring bar was charged with 249 mg (925 µmol, 1.0 eq) methoxy carboxylic acid **78** (*e.e.* > 99 %). Afterwards the starting material was dissolved in 3.0 mL DCM and 450 µL TFA (15 % TFA in DCM (v/v)) were added to the colorless solution, respectively. A brownish solution was immediately formed after the addition of TFA, which turned greenish over the time. It was stirred at RT for 120 min. Subsequently the solvent was removed on a rotary evaporator and the remaining brownish solid was triturated in 3.0 mL DCM. The resulting brownish suspension was cooled in an ice-water bath to 0 °C, the precipitate was collected by filtration and washed with a small amount of cooled DCM (2 x 500 µL). Finally, the brownish, powdery crude material was purified by a second trituration step in 2.0 mL DCM:MeCN = 4:1 (v/v). It was collected by filtration, washed with cold DCM:MeCN = 4:1 (v/v) (2 x 400 µL) and the resulting colorless powder was dried under high vacuum.

Yield: 177 mg (625 µmol, 68 %); colorless powder.

$C_{10}H_{12}F_3NO_5$ [283.20 g.mol^{-1}].

m_p = 144-145 °C.

$[\alpha]_D^{32\text{-}33\,°C}$ = +313.8 ° (c = 0.50 in DMSO); *e.e.* > 99 %.

^{1}H-NMR (300.36 MHz, D$_2$O): δ = 7.44 (d, $^3J_{HH}$ = 5.2 Hz, 1H, H-1), 6.57-6.47 (m, 2H, H-2, H-3), 4.51 (d, $^3J_{HH}$ = 2.8 Hz, 1H, H-5), 4.23-4.21 (m, 1H, H-4), 3.45 (s, 3H, H-8).

^{1}H-NMR (300.36 MHz, DMSO-d$_6$): δ = 13.03 (bs, 1H, COOH), 8.21 (bs, 3H, NH$_3^+$), 7.24 (dd, $^3J_{HH}$ = 4.2 Hz, $^3J_{HH}$ = 1.9 Hz, 1H, H-1), 6.48-6.40 (m, 2H, H-2, H-3), 4.18 (d, $^3J_{HH}$ = 1.7 Hz, 1H, H-5), 3.98 (s, 1H, H-4), 3.30 (s, 3H, H-8).

^{13}C-NMR (125.69 MHz, D$_2$O): δ = 168.2 (C$_q$, C-7), 162.9 (C$_q$, q, $^2J_{CF}$ = 35.6 Hz, C-9), 137.4 (C-1), 129.3 (C-3), 126.3 (C-2), 122.5 (C$_q$, C-6), 116.2 (C$_q$, q, $^1J_{CF}$ = 292 Hz, C-10), 72.7 (C-4), 56.1 (C-8), 45.7 (C-5).

^{19}F-NMR (470.35 MHz, D$_2$O): δ = -75.7 (decoupled, CF$_3$).

HRMS (DI-EI): calculated for C$_8$H$_{11}$NO$_3^+$: 169.0739; found: 169.0738.

7.3.39. (5*S*,6*S*)-6-((5-(((*S*)-1-Amino-1-oxopropan-2-yl)amino)-2,4-dinitrophenyl)-amino)-5-methoxycyclohexa-1,3-diene-1-carboxylic acid (79a)

79a
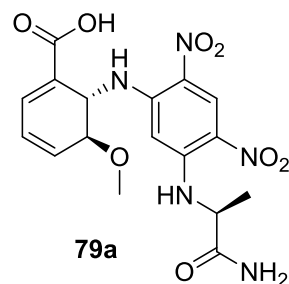
According to the general procedure (derivatization with MARFEY's reagent) ammonium salt **41a** was derivatized with MARFEY's reagent in order to determine the *e.e.* value of this compound.

HPLC-MS (Method_MARFEY_B): t_R = 4.16 min (minor diastereomer) and 5.58 min (major diastereomer); *d.e.* > 99 %, consequently *e.e.* > 99 % of compound **41**.
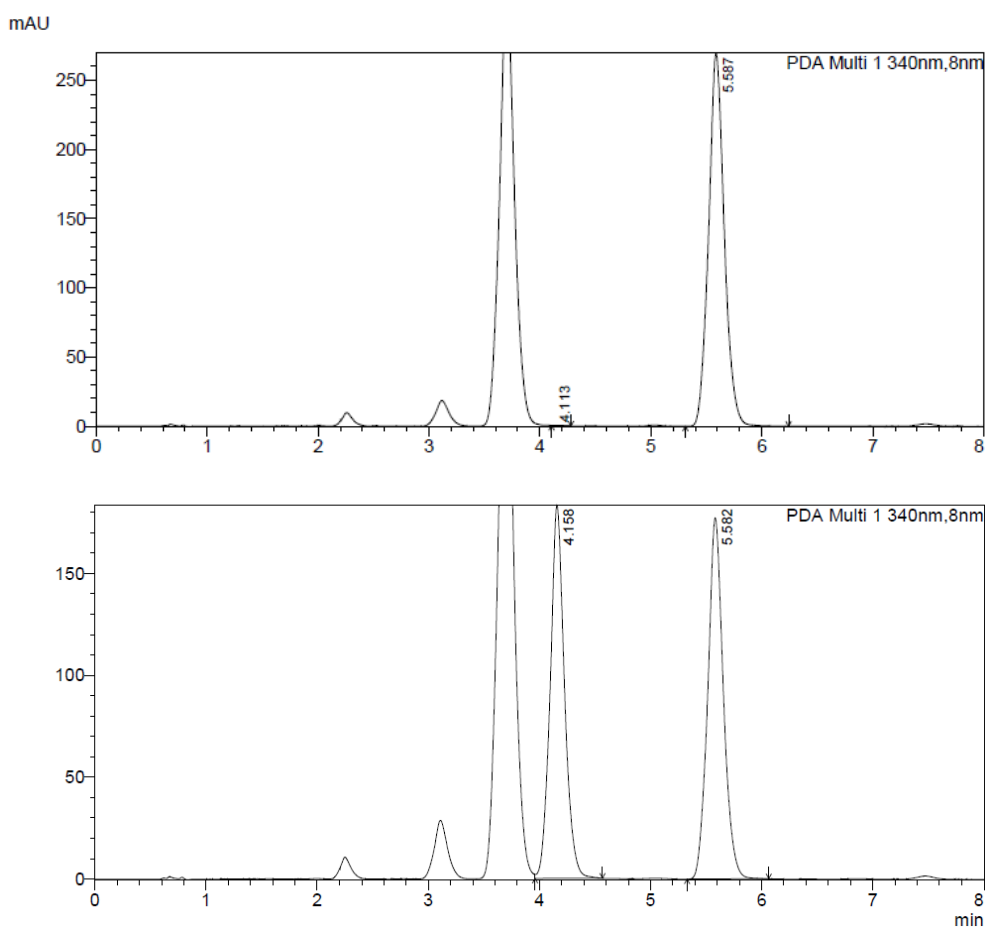
Figure 39: HPLC-MS chromatograms of **79a** and *rac*-**79** for the determination of the diastereomeric excess (*d.e.*).

7.3.40. Ethyl (5*S*,6*S*)-6-((*tert*-Butoxycarbonyl)amino)-5-ethoxycyclohexa-1,3-diene-1-carboxylate (*rac*-80)
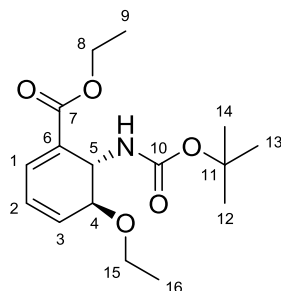
rac-80

An oven-dried, evacuated and argon purged 25 mL two-necked round-bottom flask equipped with a Teflon-coated magnetic stirring bar and gas inlet adapter was charged with 283 mg (1.00 mmol, 1.0 eq) racemic ester *rac*-21. It was dissolved in 12 mL anhydrous Et_2O and 463 mg (2.00 mmol, 2.0 eq) Ag_2O were added to the yellowish solution. After the addition of 2.0 g 3 Å MS and 778 µL (6.00 mmol, 6.0 eq) ethyl trifluoromethanesulfonate in an argon counter flow, the black suspension was stirred in the closed flask under argon atmosphere at RT for 70 h. Subsequently it was filtered through a pad of Celite® (diameter: 3.0 cm, height: 4.0 cm), the filter cake was washed with EtOAc (4 x 50 mL) and the solvent was removed on a rotary evaporator. Finally, the yellow, viscous crude material was purified via flash column chromatography (50 g SiO_2, 30.0 x 3.0 cm, eluent: cyclohexane:EtOAc = 4:1 (v/v), R_f = 0.18) and the resulting yellowish, highly viscous liquid was dried under high vacuum.

Yield: 78 mg (250 µmol, 25 %); yellowish, highly viscous liquid.

$C_{16}H_{25}NO_5$ [311.38 g.mol^{-1}].

R_f = 0.68 (cyclohexane:EtOAc = 1:1 (v/v), UV and CAM).

HPLC-MS (Method_GENERAL): t_R = 4.00 min; m/z + Na$^+$ = 334.

^{1}H-NMR (300.36 MHz, CDCl$_3$): δ = 7.17 (d, $^3J_{HH}$ = 5.1 Hz, 1H, H-1), 6.31-6.18 (m, 2H, H-2, H-3), 4.89 (d, $^3J_{HH}$ = 7.1 Hz, 1H, H-5), 4.32-4.13 (m, 3H, H-8, NH), 3.96 (d, $^3J_{HH}$ = 3.9 Hz, 1H, H-4), 3.88-3.84 (m, 1H, H-15), 3.69-3.59 (m, 1H, H-15), 1.44 (s, 9H, H-12, H-13, H-14), 1.29 (t, $^3J_{HH}$ = 7.1 Hz, 3H, H-9), 1.19 (t, $^3J_{HH}$ = 7.0 Hz, 3H, H-16).

^{13}C-NMR (75.53 MHz, CDCl$_3$): δ = 166.0 (C$_q$, C-7), 155.1 (C$_q$, C-10), 133.6 (C-1), 131.0 (C-3), 128.0 (C$_q$, C-6), 125.2 (C-2), 79.9 (C$_q$, C-11), 74.6 (C-4), 64.8 (C-15), 60.9 (C-8), 46.1 (C-5), 28.5 (C-12, C-13, C-14), 15.7 (C-16), 14.4 (C-9).

HRMS (DI-EI): calculated for $C_{16}H_{25}NO_5^+$: 311.1733; found: 311.1747.

7.3.41. (5*S*,6*S*)-6-((*tert*-Butoxycarbonyl)amino)-5-ethoxycyclohexa-1,3-diene-1-carboxylic acid (*rac*-81)
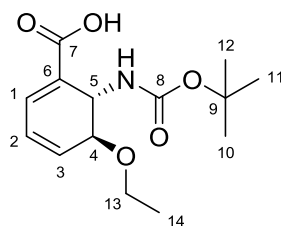
***rac*-81**

A 25 mL round-bottom flask equipped with a Teflon-coated magnetic stirring bar was charged with 78 mg (250 µmol, 1.0 eq) ethoxy ester ***rac*-80**. It was dissolved in 2.0 mL THF and to the colorless solution 175 µL H_2O as well as 63 mg (1.50 mmol, 6.0 eq) $LiOH.H_2O$ were added, respectively. The resulting yellowish, milky solution was stirred in the closed flask at RT for 6 d. Afterwards it was concentrated on a rotary evaporator and the oily residue was dissolved in 10 mL H_2O. The yellowish aqueous phase was washed with EtOAc (2 x 10 mL), the product from the organic phase reextracted with H_2O (2 x 2.0 mL) and the combined yellowish aqueous layers subsequently acidified with 1.0 mL saturated $KHSO_4$ to pH 1-2. The product was extracted with EtOAc (3 x 20 mL), the combined yellowish organic phases were dried over $MgSO_4$, filtered and the solvent was removed on a rotary evaporator. Finally, the crude material was purified via flash column chromatography (7.0 g SiO_2, 25.0 x 0.8 cm, eluent: cyclohexane:EtOAc:AcOH = 1000:5000:1 (v/v/v), R_f = 0.24) and the resulting colorless solid was dried under high vacuum.

Yield: 67 mg (238 µmol, 95 %); colorless solid.

$C_{14}H_{21}NO_5$ [283.32 g.mol^{-1}].

R_f = 0.52 (EtOAc:AcOH = 1000:1 (v/v), UV and CAM).

m_p = 53-54 °C.

HPLC-MS (Method_GENERAL): t_R = 2.60 min; m/z + Na^+ = 306.

^{1}H-NMR (300.36 MHz, DMSO-d_6): δ = 12.37 (bs, 1H, COOH), 7.00 (d, $^3J_{HH}$ = 4.8 Hz, 1H, H-1), 6.74 (d, $^3J_{HH}$ = 7.2 Hz, 1H, NH), 6.20-6.19 (m, 2H, H-2, H-3), 4.53 (d, $^3J_{HH}$ = 7.1 Hz, 1H, H-5), 3.77 (d, $^3J_{HH}$ = 3.8 Hz, 1H, H-4), 3.70-3.59 (m, 1H, H-13), 3.57-3.46 (m, 1H, H-13), 1.37 (s, 9H, H-10, H-11, H-12), 1.07 (t, $^3J_{HH}$ = 7.0 Hz, 3H, H-14).

^{13}C-NMR (75.53 MHz, DMSO-d_6): δ = 167.2 (C_q, C-7), 155.1 (C_q, C-8), 133.2 (C-1), 130.3 (C-3), 127.3 (C_q, C-6), 125.4 (C-2), 77.9 (C_q, C-9), 73.8 (C-4), 63.1 (C-13), 46.1 (C-5), 28.2 (C-10, C-11, C-12), 15.5 (C-14).

HRMS (DI-EI): calculated for $C_{14}H_{21}NO_5^+$: 283.1420; found: 283.1442.

7.3.42. (1*S*,6*S*)-2-Carboxy-6-ethoxycyclohexa-2,4-diene-1-ammonium 2,2,2-trifluoroacetate (*rac*-42a)
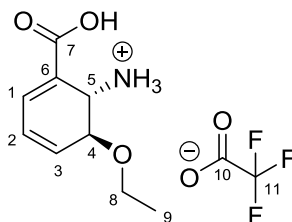
rac-42a

An oven-dried 5 mL round-bottom flask equipped with a Teflon-coated magnetic stirring bar was charged with 54 mg (190 µmol, 1.0 eq) ethoxy carboxylic acid **rac-81**. Afterwards the starting material was dissolved in 500 µL DCM and 75 µL TFA (15 % TFA in DCM (v/v)) were added to the colorless solution, respectively. A brownish solution was immediately formed after the addition of TFA, which was stirred at RT for 100 min. Subsequently the solvent was removed on a rotary evaporator and the remaining brownish solid was triturated in 500 µL DCM. The resulting brownish suspension was cooled in an ice-water bath to 0 °C, the precipitate was collected by filtration and washed with a small amount of cooled DCM (2 x 100 µL). Finally the brownish, powdery crude material was purified by a second trituration step in 200 µL DCM:MeCN = 6:1 (v/v). It was collected by filtration, washed with cold DCM:MeCN = 6:1 (v/v) (2 x 50 µL) and the resulting colorless powder was dried under high vacuum.

Yield: 18 mg (59 µmol, 31 %); colorless powder.

$C_{11}H_{14}F_3NO_5$ [297.23 g.mol^{-1}].

m_p = 133-134 °C.

^{1}H-NMR (300.36 MHz, D$_2$O): δ = 7.44 (d, $^3J_{HH}$ = 5.3 Hz, 1H, H-1), 6.56-6.45 (dd, $^3J_{HH}$ = 9.6 Hz, $^3J_{HH}$ = 5.5 Hz, 1H, H-2), 6.47 (dd, $^3J_{HH}$ = 9.0 Hz, $^3J_{HH}$ = 4.8 Hz, 1H, H-3), 4.51 (d, $^3J_{HH}$ = 2.5 Hz, 1H, H-5), 4.29 (dd, $^3J_{HH}$ = 4.4 Hz, $^3J_{HH}$ = 2.8 Hz, 1H, H-4), 3.82-3.66 (m, 2H, H-8), 1.18 (t, $^3J_{HH}$ = 7.0 Hz, 3H, H-9).

^{13}C-NMR (125.69 MHz, D$_2$O): δ = 168.4 (C$_q$, C-7), 162.9 (C$_q$, q, $^2J_{CF}$ = 35.5 Hz, C-10), 137.3 (C-1), 129.6 (C-3), 126.0 (C-2), 116.2 (C$_q$, q, $^1J_{CF}$ = 292 Hz, C-11), 71.2 (C-4), 65.2 (C-8), 45.9 (C-5), 14.3 (C-9).

^{19}F-NMR (470.35 MHz, D$_2$O): δ = -75.7 (decoupled, CF$_3$).

HRMS (DI-EI): calculated for C$_9$H$_{13}$NO$_3$$^+$: 183.0895; found: 183.0886.

7.3.43. Propyl trifluoromethanesulfonate (82)
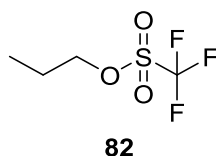
82

An oven-dried, evacuated and argon purged 50 mL Schlenk flask equipped with a Teflon-coated magnetic stirring bar was charged with 1.33 mL (16.5 mmol, 1.10 eq) pyridine. It was dissolved in 15 mL anhydrous DCM and afterwards cooled in an acetone/dry ice bath under argon atmosphere to -20 °C. To this cooled, colorless solution 2.65 mL (15.8 mmol, 1.05 eq) Tf$_2$O were added via a syringe and septum over a period of 10 min, which resulted in the formation of a colorless suspension. This suspension was additionally stirred at -20 °C in the acetone/dry ice bath under argon for 10 min. Afterwards 1.12 mL (15.0 mmol, 1.00 eq) *n*-PrOH were added dropwise via a syringe over a period of 10 min, the cooling bath was removed and the colorless suspension was stirred under argon at RT for 15 min. It was filtered through a Schlenk frit, the filter cake was washed with anhydrous DCM (2 x 10 mL) and the colorless filtrate was carefully concentrated in the vacuum of an oil pump to approximately 5 mL, which resulted in the precipitation of a colorless solid. Subsequently the colorless suspension was treated with 30 mL anhydrous *n*-pentane and again filtered through a second Schlenk frit in an oven-dried, evacuated and argon purged 80 mL Schlenk flask. The filter cake was washed with anhydrous *n*-pentane (2 x 5 mL) and the solvent of the colorless filtrate was carefully removed in the vacuum of an oil pump. Finally, the brownish, oily residue was dried at 5 mbar for 5 min. It was immediately used in the propylation step without further purification.

Yield: 2.88 g (15.0 mmol, 100 %); brownish, viscous liquid.

7.3.44. Ethyl (5S,6S)-6-((*tert*-butoxycarbonyl)amino)-5-propoxycyclohexa-1,3-diene-1-carboxylate (*rac*-83)
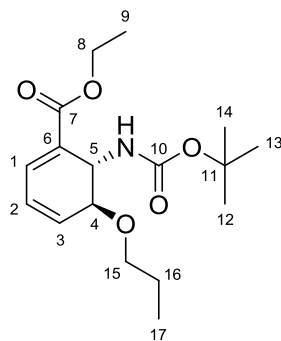
rac-83

An oven-dried, evacuated and argon purged 50 mL two-necked round-bottom flask equipped with a Teflon-coated magnetic stirring bar and gas inlet adapter was charged with 425 mg (1.50 mmol, 1.0 eq) racemic ester *rac*-21. It was dissolved in 10 mL anhydrous Et_2O and to the colorless solution 695 mg (2.00 mmol, 2.0 eq) Ag_2O as well as 3.0 g 3 Å MS were added in an argon counter flow, respectively, which resulted in the formation of a black suspension. In parallel 2.88 g (15.0 mmol, 10.0 eq) of the freshly prepared propyl trifluoromethanesulfonate (**82**) were dissolved in 7.5 mL anhydrous Et_2O under argon in the same Schlenk flask, in which this compound was dried. This solution was added to the black suspension via a syringe and septum in one portion, the Schlenk flask was rinsed with anhydrous Et_2O (1 x 2.5 mL) and the black suspension was vigorously stirred in the closed flask at RT for 120 h. Afterwards it was filtered through a pad of Celite® (diameter: 3.0 cm, height: 4.0 cm), the filter cake was washed with EtOAc (4 x 50 mL) and the solvent was removed on a rotary evaporator. Finally, the orange, viscous crude material was purified via flash column chromatography (80 g SiO_2, 25.0 x 2.5 cm, eluent: cyclohexane:EtOAc = 9:2 (v/v), R_f = 0.24) and the resulting yellowish, highly viscous liquid was dried under high vacuum.

Yield: 56 mg (172 µmol, 11 %); yellowish, highly viscous liquid.

$C_{17}H_{27}NO_5$ [325.40 g.mol^{-1}].

R_f = 0.70 (cyclohexane:EtOAc = 1:1 (v/v), UV and CAM).

HPLC-MS (Method_GENERAL): t_R = 4.49 min; m/z + Na$^+$ = 348.

^{1}H-NMR (300.36 MHz, CDCl$_3$): δ =7.16 (d, $^3J_{HH}$ = 4.9 Hz, 1H, H-1), 6.31-6.17 (m, 2H, H-2, H-3), 4.89 (d, $^3J_{HH}$ = 7.1 Hz, 1H, H-5), 4.33-4.13 (m, 3H, H-8, NH), 3.94 (d, $^3J_{HH}$ = 2.8 Hz, 1H, H-4), 3.77-3.66 (m, 1H, H-15a), 3.60-3.47 (m, 1H, H-15b), 1.57 (h, $^3J_{HH}$ = 7.2 Hz, 2H, H-16),

1.43 (s, 9H, H-12, H-13, H-14), 1.29 (t, $^3J_{HH}$ = 7.1 Hz, 3H, H-9), 0.89 (t, $^3J_{HH}$ = 7.4 Hz, 3H, H-17).

^{13}C-NMR (75.53 MHz, CDCl$_3$): δ = 166.0 (C$_q$, C-7), 155.2 (C$_q$, C-10), 133.6 (C-1), 131.0 (C-3), 128.0 (C$_q$, C-6), 125.2 (C-2), 79.8 (C$_q$, C-11), 74.6 (C-4), 71.0 (C-15), 60.9 (C-8), 46.0 (C-5), 28.5 (C-12, C-13, C-14), 23.4 (C-16), 14.3 (C-9), 10.6 (C-17).

7.3.45. (5*S*,6*S*)-6-((*tert*-Butoxycarbonyl)amino)-5-propoxycyclohexa-1,3-diene-1-carboxylic acid (*rac*-84)
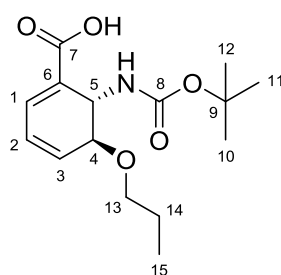
***rac*-84**

A 5 mL round-bottom flask equipped with a Teflon-coated magnetic stirring bar was charged with 49 mg (150 µmol, 1.0 eq) propoxy ester ***rac*-83**. It was dissolved in 1.2 mL THF and to the yellowish solution 70 µL H$_2$O as well as 38 mg (900 µmol, 6.0 eq) LiOH.H$_2$O were added, respectively. The resulting yellowish, milky solution was stirred in the closed flask at RT for 7 d. Afterwards it was concentrated on a rotary evaporator and the oily residue was dissolved in 5.0 mL H$_2$O. The yellowish aqueous phase was washed with EtOAc (2 x 5.0 mL), the product from the organic phase reextracted with H$_2$O (2 x 500 µL) and the combined yellowish aqueous layers subsequently acidified with 750 µL saturated KHSO$_4$ to pH 1-2. The product was extracted with EtOAc (3 x 5.0 mL), the combined yellowish organic phases were dried over MgSO$_4$, filtered and the solvent was removed on a rotary evaporator. Finally, the crude material was purified via flash column chromatography (6.0 g SiO$_2$, 23.0 x 0.8 cm, eluent: cyclohexane:EtOAc:AcOH = 1000:5000:1 (v/v/v), R$_f$ = 0.26) and the resulting yellowish, viscous liquid was dried under high vacuum.

Yield: 44 mg (148 µmol, 99 %); yellowish, viscous liquid.

C$_{15}$H$_{23}$NO$_5$ [297.35 g.mol^{-1}].

R$_f$ = 0.58 (EtOAc:AcOH = 1000:1 (v/v), UV and CAM).

HPLC-MS (Method_GENERAL): t$_R$ = 3.17 min; *m/z* + Na$^+$ = 320.

^{1}H-NMR (300.36 MHz, DMSO-d$_6$): δ = 12.31 (bs, 1H, COOH), 7.00 (d, $^3J_{HH}$ = 4.9 Hz, 1H, H-1), 6.74 (d, $^3J_{HH}$ = 7.0 Hz, 1H, NH), 6.29-6.19 (m, 2H, H-2, H-3), 4.54 (d, $^3J_{HH}$ = 7.0 Hz, 1H, H-5), 3.76 (d, $^3J_{HH}$ = 3.5 Hz, 1H, H-4), 3.58-3.51 (m, 1H, H-13), 3.46-3.41 (m, 1H, H-13), 1.51-1.42 (m, 2H, H-14), 1.37 (s, 9H, H-10, H-11, H-12), 0.82 (t, $^3J_{HH}$ = 7.3 Hz, 3H, H-15).

^{13}C-NMR (75.53 MHz, DMSO-d$_6$): δ =167.2 (C$_q$, C-7), 155.1 (C$_q$, C-8), 133.2 (C-1), 130.3 (C-3), 127.3 (C$_q$, C-6), 125.4 (C-2), 77.9 (C$_q$, C-9), 73.9 (C-4), 69.4 (C-13), 46.0 (C-5), 28.2 (C-10, C-11, C-12), 22.8 (C-14), 10.5 (C-15).

7.3.46. (1*S*,6*S*)-2-Carboxy-6-propoxycyclohexa-2,4-diene-1-ammonium 2,2,2-trifluoroacetate (*rac*-43a)
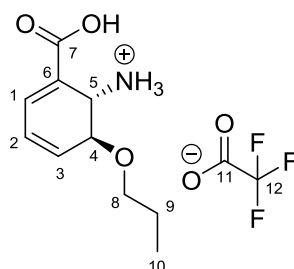
rac-43a

An oven-dried 5 mL round-bottom flask equipped with a Teflon-coated magnetic stirring bar was charged with 30 mg (100 µmol, 1.0 eq) propoxy carboxylic acid *rac*-84. Afterwards the starting material was dissolved in 300 µL DCM and 45 µL TFA (15 % TFA in DCM (v/v)) were added to the colorless solution, respectively. A brownish solution was immediately formed after the addition of TFA, which was stirred at RT for 120 min. Subsequently the solvent was removed on a rotary evaporator and the remaining brownish solid was triturated in 500 µL DCM:*n*-pentane = 1:1 (v/v). The resulting brownish suspension was cooled in an ice-water bath to 0 °C, the precipitate was collected by filtration and washed with cold DCM:*n*-pentane = 1:1 (v/v) (2 x 100 µL). Finally, the brownish powder was dried under high vacuum.

Yield: 17 mg (55 µmol, 55 %); brownish powder.

C$_{12}$H$_{16}$F$_3$NO$_5$ [311.26 g.mol^{-1}].

m$_p$ = 109-110 °C.

^{1}H-NMR (300.36 MHz, DMSO-d$_6$): δ = 12.95 (bs, 1H, COOH), 8.19 (bs, 3H, NH$_3^+$), 7.24 (dd, $^3J_{HH}$ = 4.2 Hz, $^4J_{HH}$ = 1.5 Hz, 1H, H-1), 6.46-6.38 (m, 2H, H-2, H-3), 4.17 (s, 1H, H-5), 4.04 (bs, 1H, H-4), 3.52-3.42 (m, 2H, H-8), 1.47 (h, $^3J_{HH}$ = 7.0 Hz, 2H, H-9), 0.82 (t, $^3J_{HH}$ = 7.4 Hz, 3H, H-10).

^{13}C-NMR (75.53 MHz, DMSO-d$_6$): δ = 166.5 (C$_q$, C-7), 157.9 (C$_q$, q, $^2J_{CF}$ = 30.7 Hz, C-11), 135.2 (C-1), 130.2 (C-3), 125.3 (C-2), 117.3 (C$_q$, q, $^1J_{CF}$ = 301 Hz, C-12), 70.7 (C-4), 69.6 (C-8), 45.7 (C-5), 22.5 (C-9), 10.3 (C-10).

^{19}F-NMR (470.35 MHz, DMSO-d$_6$): δ = -73.5 (decoupled, CF$_3$).

7.3.47. Ethyl (3*S*,3a*R*,6*S*,7*S*,7a*S*)-7-((*tert*-butoxycarbonyl)amino)-3,3a,7,7a-tetra-hydro-3,6-methanobenzofuran-6(2*H*)-carboxylate (*rac*-85)
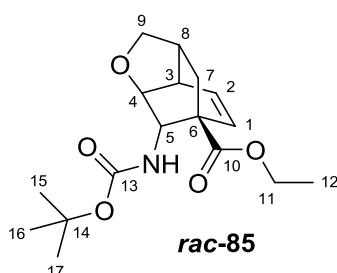
rac-85

An oven-dried 50 mL round-bottom flask equipped with a Teflon-coated magnetic stirring bar was charged with 425 mg (1.50 mmol, 1.0 eq) racemic ester *rac*-21. It was dissolved in 18 mL Et$_2$O and 695 mg (3.00 mmol, 2.0 eq) Ag$_2$O as well as 125 mg (750 μmol, 50 mol%) KI were added to the yellowish solution, respectively. After the addition of 2.7 g 4 Å MS and 1.6 mL (2.22 g, 18.0 mmol, 12.0 eq) allyl bromide, the black suspension was stirred in the closed flask at RT for 6 d. Subsequently it was filtered through a pad of Celite® (diameter: 3.0 cm, height: 4.0 cm), the filter cake was washed with EtOAc (3 x 150 mL) in order to elute the whole amount of product and the solvent was removed on a rotary evaporator. Finally, the yellow, viscous crude material was purified via flash column chromatography (30 g SiO$_2$, 23.0 x 2.0 cm, eluent: cyclohexane:EtOAc = 9:2 (v/v), R$_f$ = 0.24) and the resulting colorless solid was dried under high vacuum.

Yield: 298 mg (922 μmol, 61 %); colorless solid.

C$_{17}$H$_{25}$NO$_5$ [323.17 g.mol^{-1}].

R$_f$ = 0.64 (cyclohexane:EtOAc = 1:1 (v/v), UV and KMnO$_4$).

m$_p$ = 105-107 °C.

HPLC-MS (Method_GENERAL): t$_R$ = 3.86 min; *m/z* + Na$^+$ = 346.

^{1}H-NMR (300.36 MHz, CDCl$_3$): δ = 6.62 (d, $^3J_{HH}$ = 8.2 Hz, 1H, H-1), 6.24 (dd, $^3J_{HH}$ = 8.0 Hz, $^3J_{HH}$ = 7.0 Hz,1H, H-2), 4.31-4.08 (m, 3H, H-11, NH), 3.97 (d, $^3J_{HH}$ = 9.6 Hz, 1H, H-5), 3.82 (dd, $^2J_{HH}$ = 7.5 Hz, $^3J_{HH}$ = 3.2 Hz, 1H, H-9a), 3.74 (d, $^3J_{HH}$ = 5.3 Hz, 1H, H-4), 3.71 (d, $^3J_{HH}$ =

7.8 Hz, 1H, H-9b), 3.00 (dd, $^3J_{HH}$ = 9.8 Hz, $^3J_{HH}$ = 5.2 Hz, 1H, H-3), 2.19-2.12 (m, 1H, H-8), 1.80 (d, $^2J_{HH}$ = 13.1 Hz, 1H, H-7a), 1.65 (dd, $^2J_{HH}$ = 13.0 Hz, $^3J_{HH}$ = 10.4 Hz, 1H, H-7b), 1.38 (s, 9H, H-15, H-16, H-17), 1.27 (t, $^3J_{HH}$ = 7.1 Hz, 3H, H-12).

^{13}C-NMR (75.53 MHz, CDCl$_3$): δ = 173.7 (C$_q$, C-10), 154.6 (C$_q$, C-13), 132.0 (C-1), 128.6 (C-2), 82.7 (C-4), 79.4 (C$_q$, C-14), 74.6 (C-9), 61.3 (C-11), 61.3 (C-5), 47.3 (C$_q$, C-6), 41.5 (C-3), 36.8 (C-7), 35.2 (C-8), 28.4 (C-15, C-16, C-17), 14.3 (C-12).

HRMS (DI-EI): calculated for C$_{17}$H$_{25}$NO$_5^+$: 323.1733; found: 323.1744.

7.3.48. (3*S*,3a*R*,6*S*,7*S*,7a*S*)-7-((*tert*-Butoxycarbonyl)amino)-3,3a,7,7a-tetra-hydro-3,6-methanobenzofuran-6(2*H*)-carboxylic acid (*rac*-86)
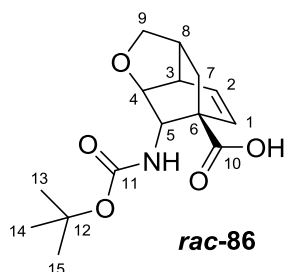
rac-86

A 25 mL round-bottom flask equipped with a Teflon-coated magnetic stirring bar was charged with 275 mg (850 µmol, 1.0 eq) ester *rac*-85. It was dissolved in 7.0 mL THF and to the colorless solution 600 µL H$_2$O as well as 214 mg (5.10 mmol, 6.0) LiOH.H$_2$O were added, respectively. The resulting yellowish, milky solution was stirred in a closed system at RT for 60 h. Afterwards it was concentrated on a rotary evaporator and the oily residue was dissolved in 25 mL H$_2$O. The yellowish aqueous phase was washed with EtOAc (2 x 25 mL), the product from the organic phase reextracted with H$_2$O (2 x 5 mL) and the combined yellowish aqueous layers subsequently acidified with 2.0 mL saturated KHSO$_4$ to pH 1-2. The product was extracted with EtOAc (3 x 25 mL), the combined yellowish organic phases were dried over MgSO$_4$, filtered and the solvent was removed on a rotary evaporator. Finally, the crude material was purified via flash column chromatography (30 g SiO$_2$, 22.0 x 2.0 cm, eluent: cyclohexane:EtOAc:AcOH = 1000:5000:1 (v/v/v), R$_f$ = 0.25) and the resulting colorless solid was dried under high vacuum.

Yield: 244 mg (825 µmol, 97 %); colorless solid.

C$_{15}$H$_{21}$NO$_5$ [295.34 g.mol^{-1}].

R$_f$ = 0.56 (EtOAc:AcOH = 1000:1 (v/v), UV and CAM).

m_p = 104-106 °C.

HPLC-MS (Method_GENERAL): t_R = 2.22 min; m/z + Na^+ = 318.

^{1}H-NMR (300.36 MHz, DMSO-d_6): δ = 12.35 (bs, 1H, COOH), 6.46 (d, $^3J_{HH}$ = 8.3 Hz, 1H, H-1), 6.14 (t, $^3J_{HH}$ = 7.5 Hz, 1H, H-2), 5.79 (d, $^3J_{HH}$ = 8.5 Hz, 1H, NH), 3.68-3.65 (m, 2H, H-5, H-9a), 3.58-3.56 (m, 2H, H-4, H-9b), 2.93-2.87 (m, 1H, H-3), 2.11-2.06 (m, 1H, H-8), 1.61-1.49 (m, 2H, H-7), 1.34 (s, 9H, H-13, H-14, H-15).

^{13}C-NMR (75.53 MHz, DMSO-d_6): δ = 174.9 (C_q, C-10), 154.5 (C_q, C-11), 132.0 (C-1), 127.4 (C-2), 81.9 (C-4), 77.8 (C_q, C-12), 73.6 (C-9), 61.1 (C-5), 46.1 (C_q, C-6), 40.7 (C-3), 36.9 (C-7), 34.3 (C-8), 28.1 (C-13, C-14, C-15).

HRMS (DI-EI): calculated for $C_{15}H_{21}NO_5^+$: 295.1420; found: 295.1443.

7.3.49. (3S,3aR,6S,7S,7aS)-6-Carboxy-2,3,3a,7,7a-hexahydro-3,6-methano-benzofuran-7-ammonium 2,2,2-trifluoroacetate (*rac*-44a)
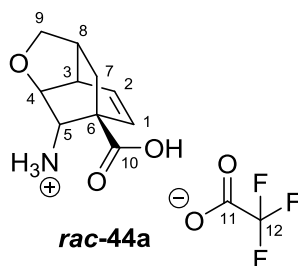
An oven-dried 10 mL round-bottom flask equipped with a Teflon-coated magnetic stirring bar was charged with 236 mg (800 µmol, 1.0 eq) carboxylic acid **rac-86**. Afterwards the starting material was dissolved in 3.0 mL DCM and 450 µL TFA (15 % TFA in DCM (v/v)) were added to the colorless solution, respectively. A yellow solution was immediately formed after the addition of TFA. It was stirred at RT for 90 min. Subsequently the solvent was removed on a rotary evaporator and the remaining brownish solid was triturated in 4.0 mL DCM. The resulting brownish suspension was cooled in an ice-water bath to 0 °C, the precipitate was collected by filtration and washed with a small amount of cooled DCM (2 x 700 µL). Finally the brownish, powdery crude material was purified by a second trituration step in 4.0 mL DCMC:MeCN = 6:1 (v/v). It was collected by filtration, washed with cold DCM:MeCN = 6:1 (v/v) (2 x 400 µL) and the resulting colorless powder was dried under high vacuum.

Yield: 158 mg (512 µmol, 64 %); colorless powder.

$C_{12}H_{14}F_3NO_5$ [309.24 g.mol^{-1}].

m_p = 167-169 °C.

^{1}H-NMR (300.36 MHz, D$_2$O): δ = 6.50-6.41 (m, 2H, H-1, H-2), 4.00 (d, $^3J_{HH}$ = 5.2 Hz, 1H, H-4), 3.85 (dd, $^3J_{HH}$ = 7.9 Hz, $^3J_{HH}$ = 3.4 Hz, 1H, H-9a), 3.75 (d, $^3J_{HH}$ = 7.9 Hz, 1H, H-9b), 3.53 (s, 1H, H-5), 3.24 (dd, $^3J_{HH}$ = 9.1 Hz, $^3J_{HH}$ = 4.4 Hz, 1H, H-3), 2.39-2.33 (m, 1H, H-8), 1.98 (dd, $^2J_{HH}$ = 13.3 Hz, $^3J_{HH}$ = 10.7 Hz, 1H, H-7a), 1.72 (d, $^2J_{HH}$ = 13.5 Hz, 1H, H-7b).

^{1}H-NMR (300.36 MHz, DMSO-d$_6$): δ = 13.35 (bs, 1H, COOH), 7.81 (bs, 3H, NH$_3^+$), 6.37-6.31 (m, 2H, H-1, H-2), 3.85 (d, $^3J_{HH}$ = 5.1 Hz, 1H, H-4), 3.69 (dd, $^3J_{HH}$ = 7.4 Hz, $^3J_{HH}$ = 2.9 Hz, 1H, H-9a), 3.62 (d, $^3J_{HH}$ = 7.5 Hz, 1H, H-9b), 3.18 (s, 1H, H-5), 3.11-3.04 (m, 1H, H-3), 2.24-2.16 (m, 1H, H-8), 1.76 (dd, $^2J_{HH}$ = 13.1 Hz, $^3J_{HH}$ = 10.5 Hz, 1H, H-7a), 1.58 (d, $^2J_{HH}$ = 13.1 Hz, 1H, H-7b).

^{13}C-NMR (125.69 MHz, D$_2$O): δ = 176.7 (C$_q$, C-10), 162.9 (C$_q$, q, $^2J_{CF}$ = 35.4 Hz, C-11), 130.5 (C-1), 129.3 (C-2), 116.2 (C$_q$, q, $^1J_{CF}$ = 292 Hz, C-12), 77.1 (C-4), 74.1 (C-9), 58.7 (C-5), 45.3 (C$_q$, C-6), 40.5 (C-3), 36.7 (C-7), 33.6 (C-8).

^{19}F-NMR (470.35 MHz, D$_2$O): δ = -75.7 (decoupled, CF$_3$).

HRMS (DI-EI): calculated for C$_{10}$H$_{13}$NO$_3^+$: 195.0895; found: 195.0903.

7.3.50. (*S*)-2-Amino-2-phenylethan-1-ol (55)

55
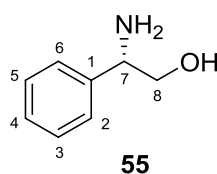
Literature: X. Shi, W. He, H. Li, X. Zhang, *Tetrahedron Lett.* **2011**, *52*, 3204-3207.

A 500 mL three-necked round-bottom flask equipped with a Teflon-coated magnetic stirring bar, 100 mL dropping funnel, air condenser and CaCl$_2$ drying tube was charged with 7.56 g (50.0 mmol, 1.0 eq) L-(+)-phenylglycine (**54**). Afterwards it was suspended in 200 mL THF, 4.73 g (125 mmol, 2.5 eq) NaBH$_4$ were added in one portion and the colorless suspension was cooled in an ice-water bath to 0 °C. A solution of 15.2 g (60.0 mmol, 1.2 eq) I$_2$ in 100 mL THF was added via the dropping funnel over a period of 30 min, whereas gas formation was observed form the beginning of addition. The brownish suspension was additionally stirred at 0 °C in the ice-water bath for 30 min, afterwards the cooling media was removed and the light orange suspension was heated under reflux in an oil bath at 75 °C for 18 h, whereas discoloration occurred over the time. Subsequently the colorless suspension was cooled to

RT, carefully quenched by addition of 100 mL MeOH via the dropping funnel and the resulting clear, colorless solution was stirred at RT for 30 min. It was concentrated on a rotary evaporator. The colorless, oily residue was dissolved in 200 mL 20 % aqueous NaOH (w/w) and the colorless solution stirred at RT for 24 h. Finally, the product was extracted with DCM (3 x 250 mL), the colorless, organic phases dried over $MgSO_4$, filtered, the solvent removed on a rotary evaporator and the resulting colorless solid dried under high vacuum.

Yield: 6.79 g (49.5 mmol, 99 %); colorless solid.

$C_8H_{11}NO$ [137.18 g.mol^{-1}].

R_f = 0.37 (EtOAc:MeOH:Et$_3$N = 1000:100:1 (v/v/v), UV and CAM).

m_p = 64-66 °C.

^{1}H-NMR (300.36 MHz, CDCl$_3$): δ = 7.30-7.19 (m, 5H, H-2, H-3, H-4, H-5, H-6), 3.96 (dd, $^3J_{HH}$ = 7.9 Hz, $^3J_{HH}$ = 4.0 Hz, 1H, H-7), 3.65 (dd, $^2J_{HH}$ = 10.7 Hz, $^3J_{HH}$ = 4.0 Hz, 1H, H-8a), 3.54-3.41 (m, 1H, H-8b), 2.28 (bs, 3H, NH$_2$, OH).

^{13}C-NMR (75.53 MHz, CDCl$_3$): δ = 142.7 (C$_q$, C-1), 128.7 (C-3, C-5), 127.6 (C-4), 126.6 (C-2, C-6), 68.1 (C-8), 57.5 (C-7).

7.3.51. Cyclopentane-1,1-dicarbonitrile (57)

57
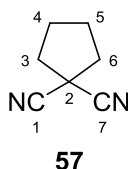
Literature: T.-Y. Tsai, K.-S. Shia, H.-J. Liu, *Synlett* **2003**, 97-101.

A 1000 mL three-necked round-bottom flask equipped with a Teflon-coated magnetic stirring bar, 100 mL dropping funnel, air condenser and CaCl$_2$ drying tube was charged with 6.60 g (100 mmol, 1.0 eq) malonodinitrile (**56**). It was dissolved in 450 mL DMF, 13.1 mL (23.8 g, 110 mmol, 1.1 eq) 1,4-dibromobutane were added in one portion and the colorless solution was cooled in an ice-water bath to 0 °C. Afterwards a solution of 32.9 mL (33.5 g, 220 mmol, 2.2 eq) 1,8-diazabicyclo[5.4.0]undec-7-ene (DBU) in 50 mL DMF was added via the dropping funnel over a period of 20 min. The resulting yellow solution was warmed to RT and later heated in an oil bath at 80 °C for 3 h. Subsequently, the orange solution was cooled to RT and concentrated on a rotary evaporator. The remaining brownish residue was dissolved in 200 mL 2 M HCl and the product extracted with Et$_2$O (3 x 200 mL). The combined, yellowish

organic phases were washed with saturated NaHCO$_3$ (1 x 200 mL), dried over MgSO$_4$, filtered and concentrated on a rotary evaporator. Finally, the brownish, oily crude material was purified via flash column chromatography (100 g SiO$_2$, 30.0 x 2.5 cm, eluent: DCM, detection via GC-MS) and the colorless, gelatinous solid was dried under high vacuum.

Yield: 10.3 g (85.7 mmol, 86 %); colorless, gelatinous solid.

C$_7$H$_8$N$_2$ [120.15 g.mol^{-1}].

GS-MS (METHOD_GENERAL): t$_R$ = 4.05 min; *m/z* = 119 (11 %), 105 (20 %), 92 (34 %), 79 (100 %), 64 (34 %), 52 (38 %).

^{1}H-NMR (300.36 MHz, CDCl$_3$): δ = 2.42-2.38 (m, 4H, H-3, H-6), 1.99-1.94 (m, 4H, H-4, H-5).

^{13}C-NMR (75.53 MHz, CDCl$_3$): δ = 116.7 (C$_q$, C-1, C-7), 39.4 (C-3, C-6), 33.8 (C$_q$, C-2), 24.1 (C-4, C-5).

7.3.52. (4*S*,4'*S*)-2,2'-(Cyclopentane-1,1-diyl)bis(4-phenyl-4,5-dihydrooxazole) (L-Phg-Box) (58)
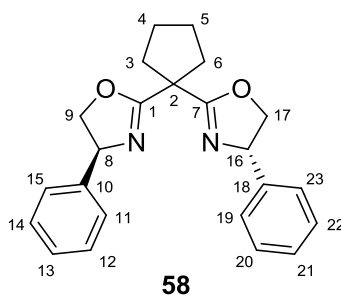
Literature: A. Cornejo, J. M. Fraile, J. I. Garcia, M. J. Gil, V. Martinez-Merino, J. A. Mayoral, E. Pires, I. Villalba, *Synlett* **2005**, *15*, 2321-2324.

An oven-dried, evacuated and argon purged 500 mL three-necked round-bottom flask equipped with a Teflon-coated magnetic stirring bar, 100 mL dropping funnel, reflux condenser, gas inlet adapter and bubbler was charged with 1.56 g (13.0 mmol, 1.0 eq) dinitrile **57**. It was dissolved in 90 mL anhydrous toluene and 4.73 g (13.0 mmol, 1.0 eq) anhydrous Zn(OTf)$_2$ were added to the colorless solution in the argon counter flow. Afterwards a solution of 3.75 g (27.3 mmol, 2.1 eq) amino alcohol **55** in 40 mL anhydrous toluene, dissolved by warming with a heat gun, was added via dropping funnel to the colorless suspension over a period of 10 min and the colorless suspension was heated under reflux in an oil bath at 120 °C for 15 h under argon atmosphere. The resulting brownish suspension was cooled down to RT and was washed with saturated NaHCO$_3$ (3 x 130 mL)

as well as brine (3 x 130 mL), respectively. Subsequently, the brownish organic phase was dried over $MgSO_4$, filtered and the solvent was removed on a rotary evaporator. Finally, the brownish, viscous crude material was purified via flash column chromatography (250 g SiO_2, 16.0 x 6.0 cm, eluent: cyclohexane:EtOAc = 5:2 (v/v), R_f = 0.26) and the resulting colorless powder was dried under high vacuum.

Yield: 2.38 g (6.60 mmol, 51 %); colorless solid.

$C_{23}H_{24}N_2O_2$ [360.46 g.mol^{-1}].

R_f = 0.56 (cyclohexane:EtOAc = 1:1 (v/v), UV and $KMnO_4$).

m_p = 65-67 °C.

$[\alpha]_D^{31\text{-}32\,°C}$ = -121.9 ° (c = 1.00 in $CHCl_3$); *e.e.* > 99 % and *d.e.* > 99 %.

GS-MS (METHOD_GENERAL): t_R = 9.55 min; *m/z* = 360 (10 %), 319 (37 %), 241 (14 %), 215 (34 %), 104 (100 %), 91 (30 %).

^{1}H-NMR (300.36 MHz, $CDCl_3$): δ = 7.29-7.19 (m, 10H, H-11, H-12, H-13, H-14, H-15, H-19, H-20, H-21, H-22, H-23), 5.17 (dd, $^3J_{HH}$ = 9.8 Hz, $^3J_{HH}$ = 8.0 Hz, 2H, H-8, H-16), 4.62 (dd, $^3J_{HH}$ = 9.9 Hz, $^2J_{HH}$ = 8.6 Hz, 2H, H-9a, H-17a), 4.10 (t, $^2J_{HH}$ = 8.0 Hz, $^3J_{HH}$ = 8.0 Hz, 2H, H-9b, H-17b), 2.40-2.31 (m, 4H, H-3, H-6), 1.79-1.74 (m, 4H, H-4, H-5).

^{13}C-NMR (75.53 MHz, $CDCl_3$): δ = 169.9 (C_q, C-1, C-7), 142.6 (C_q, C-10, C-18), 128.8 (C-12, C-14, C-20, C-22), 127.7 (C-13, C-21), 126.8 (C-11, C-15, C-19, C-23), 75.7 (C-9, C-17), 69.6 (C-8, C-16), 49.5 (C_q, C-2), 35.8 (C-3, C-6), 25.3 (C-4, C-5).

7.3.53. [Dichlorido-((4*S*,4'*S*)-2,2'-(cyclopentane-1,1-diyl)bis(4-phenyl-4,5-dihydrooxazole))] copper(II) (59)

59
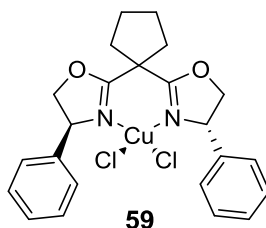
Literature: D. A. Evans, J. S. Johnson, E. J. Olhava, *J. Am. Chem. Soc.* **2000**, *122*, 1635-1649.

An oven-dried, evacuated and argon purged 100 Schlenk flask with a Teflon-coated magnetic stirring bar was charged with 1.08 g (3.00 mmol, 1.0 eq) L-Phg-Box-ligand **58**. It was dissolved in 30 mL anhydrous DCM and 403 mg (3.00 mmol, 1.0 eq) anhydrous CuCl$_2$ were added to the colorless solution in one portion. Afterwards the brownish suspension was vigorously stirred at RT for 3 h under argon atmosphere, whereas an intensively green colored solution was formed over reaction time. It was filtered through a small pad of oven-dried Celite$^®$ in a Schlenk frit under argon pressure directly into another oven-dried, evacuated and argon purged 100 mL Schlenk flask. The pad of Celite$^®$ was washed with anhydrous DCM (3 x 10 mL), the solvent was removed carefully in the vacuum of an oil pump and finally the resulting green, powdery solid was dried under high vacuum.

Yield: 1.47 g (2.97 mmol, 99 %); green, powdery solid.

7.3.54. 3-Acryloyloxazolidin-2-one (62)
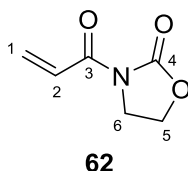
62

An oven-dried, evacuated and argon purged 250 mL three-necked round-bottom flask equipped with a Teflon-coated magnetic stirring bar, gas inlet adapter and bubbler was charged with 4.35 g (50.0 mmol, 1.0 eq) oxazolidin-2-one (**61**). It was dissolved in 50 mL anhydrous DCM, 6.9 mL (7.21 g, 100 mmol, 2.0 eq) and 916 mg (7.50 mmol, 15 mol%) 4-DMAP were added in an argon counter flow, respectively. The colorless solution was cooled in an ice-water bath to 0 °C, 20.6 g (100 mmol, 2.0 eq) DCC were added in one portion and the resulting colorless suspension was stirred at 0 °C under argon for 10 min.

Afterwards the ice-water bath was removed and the colorless suspension stirred at RT under argon atmosphere for 16 h. The resulting yellow suspension was filtered and the filter cake was washed with DCM (3 x 150 mL). Subsequently, the yellow organic phase was washed with saturated $NaHCO_3$ (1 x 200 mL), dried over $MgSO_4$, filtered and the solvent was removed on a rotary evaporator. Finally, the orange, viscous crude material was purified via flash column chromatography (220 g SiO_2, 18.0 x 6.0 cm, eluent: cyclohexane:EtOAc = 2:1 (v/v), R_f = 0.25) and the resulting colorless, crystalline solid was dried under high vacuum.

Yield: 2.98 g (21.1 mmol, 42 %); colorless, crystalline solid.

$C_6H_7NO_3$ [141.12 g.mol^{-1}].

R_f = 0.51 (cyclohexane:EtOAc = 1:1 (v/v), UV and $KMnO_4$).

m_p = 77-79 °C.

GS-MS (METHOD_GENERAL): t_R = 4.99 min; m/z = 141 (15 %), 113 (48 %), 55 (100 %).

^{1}H-NMR (300.36 MHz, $CDCl_3$): δ = 7.48 (dd, $^3J_{HH}$ = 17.0 Hz, $^3J_{HH}$ = 10.5 Hz, 1H, H-2), 6.55 (dd, $^3J_{HH}$ = 17.0 Hz, $^2J_{HH}$ = 1.6 Hz, 1H, H-1a), 5.89 (dd, $^3J_{HH}$ = 10.5 Hz, $^2J_{HH}$ = 1.6 Hz, 1H, H-1b), 4.43 (t, $^3J_{HH}$ = 8.0 Hz, 2H, H-5), 4.07 (t, $^3J_{HH}$ = 8.0 Hz, 2H, H-6).

^{13}C-NMR (75.53 MHz, $CDCl_3$): δ = 165.2 (C_q, C-3), 153.5 (C_q, C-4), 131.9 (C-2), 127.1 (C-1), 62.3 (C-5), 42.7 (C-6).

7.3.55. 3-((1*R*,2*R*,4*R*)-7-oxabicyclo[2.2.1]hept-5-ene-2-carbonyl)oxazolidin-2-one (63)
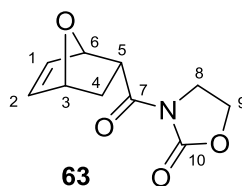
Literature: D. A. Evans, D. M. Barnes, J. S. Johnson, T. Lectka, P. von Matt, S. J. Miller, J. A. Murry, R. D. Norcross, E. A. Shaughnessy, K. R. Campos, *J. Am. Chem. Soc.* **1999**, *121*, 7582-7594.

An oven-dried, evacuated and argon purged 50 mL Schlenk flask equipped with a Teflon-coated magnetic stirring bar was charged with 495 mg (1.00 mmol, 5.0 mol%) pre-catalyst **59**. It was dissolved in 15 mL anhydrous DCM and to the deeply green colored solution 687 mg (2.00 mmol, 10 mol%) AgSbF$_6$ were added in an argon counter flow. The resulting blueish green solution was protected from light and vigorously stirred at RT for 4 h, whereas AgCl precipitated as a brownish solid by the time. In parallel, a second oven-dried, evacuated and argon purged 80 mL Schlenk flask equipped with a Teflon-coated magnetic stirring bar was charged with 2.82 g (20.0 mmol, 10.0 eq) 3-acryloyloxazolidin-2-one (**62**). Afterwards it was dissolved in 20 mL anhydrous DCM and the resulting colorless solution was cooled in an acetone/dry ice cooling bath to -78 °C under argon atmosphere. To this cooled, resulting suspension 14.5 mL (13.6 g, 200 mmol, 10.0 eq) furan (**12**) were added in one portion and afterwards it was stirred in the acetone/dry ice cooling bath at -78 °C for additional 15 min. The blueish green catalyst suspension was filtered through a Schlenk frit filled with a small pad of oven-dried Celite® under argon pressure directly into the cooled, colorless suspension of starting material. Afterwards the Celite® was washed with anhydrous DCM (2 x 1.0 mL), likewise added and the resulting blueish green suspension was stirred in a special manufactured cryogenic reactor (see Figure 40) consisting of two nested Styrofoam boxes filled with dry ice at -78 °C for 90 h under argon atmosphere. Subsequently, it was quenched by the addition of 6.0 mL NH$_3$ ammonia solution (~25 % (w/w) in H$_2$O) at -78 °C and the deeply blue colored two-phasic system was vigorously stirred at this temperature for additional 15 min. Later it was warmed to RT, 80 mL of H$_2$O were added in small portions and the deeply blue colored two-phasic system was stirred at ambient temperature for 30 min. Phases were separated and the blue aqueous phase was extracted with DCM (3 x 6.0 mL). The combined colorless organic phases were washed with brine (1 x 150 mL), dried over MgSO$_4$, filtered and concentrated on a rotary evaporator. Finally, the orange, viscous crude material was purified via flash column chromatography (200 g SiO$_2$, 17.0 x 6.0 cm,

eluent: cyclohexane:EtOAc = 1:1 (v/v), R_f = 0.21) and the resulting colorless, crystalline solid was dried under high vacuum.
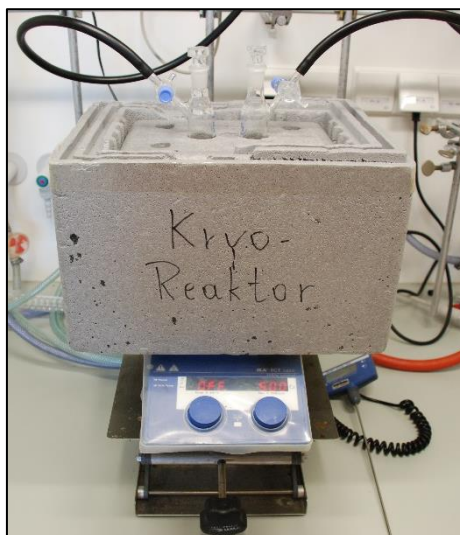
Figure 40: Cryogenic reactor of two nested Styrofoam boxes: Inner box filled with dry ice.

Yield: 2.29 g (10.9 mmol, 55 %); colorless, crystalline solid.

chiral HPLC (Method_IMIDE): t_R = 36.74 min (major enantiomer) and 29.66 min (minor enantiomer); t_R = 40.51 min and 59.42 min (other stereoisomers); *e.e.* = 93 % and *d.e.* > 90 %.

In order to achieve perfect optical and diastereomeric purities the chromatographed material was recrystallized in 24 mL *n*-pentane:EtOAc = 1:1 (v/v). The resulting rhombic formed, colorless crystal were collected by filtration, washed with cold *n*-pentane:EtOAc = 1:1 (v/v) (2 x 4.0 mL) and finally dried under high vacuum.

Yield: 1.23 g (5.88 mmol, 29 %); colorless, rhombic shaped crystals.

$C_{10}H_{11}NO_4$ [209.19 g.mol^{-1}].

R_f = 0.29 (cyclohexane:EtOAc = 2:3 (v/v), UV and $KMnO_4$).

m_p = 98-100 °C.

$[\alpha]_D^{30-31\ °C}$ = +85.7 ° (c = 1.00 in $CHCl_3$); *e.e.* > 99 % and *d.e.* > 99 %.

HPLC-MS (Method_IMIDE): t_R = 6.48 min.

chiral HPLC (Method_IMIDE): t_R = 36.74 min (major enantiomer) and 29.66 min (minor enantiomer); t_R = 40.51 min and 59.42 min (other stereoisomers); *e.e.* > 99 % and *d.e.* > 99 %.

^{1}H-NMR (300.36 MHz, CDCl$_3$): δ = 6.47 (dd, $^3J_{HH}$ = 5.8 Hz, $^3J_{HH}$ = 1.5 Hz, 1H, H-2), 6.19 (dd, $^3J_{HH}$ = 5.8 Hz, $^3J_{HH}$ = 1.2 Hz, 1H, H-1), 5.31 (d, $^3J_{HH}$ = 4.0 Hz, 1H, H-6), 5.05 (dd, $^3J_{HH}$ = 4.7 Hz, $^3J_{HH}$ = 1.0 Hz, 1H, H-3), 4.47-4.35 (m, 2H, H-9), 4.06 (dt, $^3J_{HH}$ = 8.8 Hz, $^3J_{HH}$ = 4.2 Hz, 1H, H-5), 4.00-3.88 (m, 2H, H-8), 2.19 (ddd, $^2J_{HH}$ = 11.3 Hz, $^3J_{HH}$ = 9.1 Hz, $^3J_{HH}$ = 4.7 Hz, 1H, H-5), 1.65 (dd, $^2J_{HH}$ = 11.3 Hz, $^3J_{HH}$ = 4.1 Hz, 1H, H-4).

^{13}C-NMR (75.53 MHz, CDCl$_3$): δ = 172.1 (C$_q$, C-7), 153.3 (C$_q$, C-10), 137.1 (C-2), 132.2 (C-1), 79.4 (C-3), 79.3 (C-6), 62.2 (C-9), 43.3 (C-5), 42.9 (C-8), 29.5 (C-4).

7.3.56. *S*-Ethyl (1*R*,2*R*,4*R*)-7-oxabicyclo[2.2.1]hept-5-ene-2-carbothioate (87)
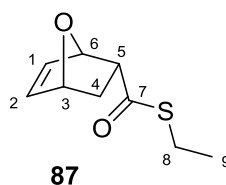
87

Literature: D. A. Evans, D. M. Barnes, J. S. Johnson, T. Lectka, P. von Matt, S. J. Miller, J. A. Murry, R. D. Norcross, E. A. Shaughnessy, K. R. Campos, *J. Am. Chem. Soc.* **1999**, *121*, 7582-7594.

An oven-dried, evacuated and argon purged 100 mL Schlenk flask equipped with a Teflon-coated magnetic stirring bar was charged with 447 µL (376 mg, 6.05 mmol, 1.10 eq) EtSH. It was dissolved in 30 mL anhydrous THF and afterwards cooled in an acetone/dry ice bath to -78 °C under argon atmosphere. 2.86 mL (5.78 mmol, 1.05 eq) *n*BuLi (2.02 M in *n*-hexane) were added via septum and syringe at this temperature dropwise over a period of 10 min. The colorless solution was warmed to 0 °C and the resulting colorless suspension additionally stirred for 30 min under argon atmosphere in the ice-water bath and again cooled to -78 °C. In parallel, an oven-dried, evacuated and argon purged 100 mL Schlenk flask equipped with a Teflon-coated magnetic stirring bar was charged with 1.15 g (5.50 mmol, 1.00 eq) of optically and diastereomerically pure imide **63** (*e.e.* > 99 % and *d.e.* > 99 %). It was dissolved in 30 mL anhydrous THF and likewise cooled to -78 °C in the acetone/dry ice bath. The cooled imide solution was transferred to the colorless lithium thioethanolate suspension in one portion and the flask was rinsed with 5.0 mL anhydrous THF. Afterwards the colorless suspension was warmed to -50 °C and stirred at this temperature under argon atmosphere for 1 h. Subsequently, it was poured into 30 mL saturated NH$_4$Cl solution, diluted

with 30 mL H_2O and the product extracted with EtOAc (3 x 80 mL). The combined, colorless organic phases were dried over $MgSO_4$, filtered and the solvent was removed on the rotary evaporator. Finally, the yellowish liquid was purified via flash column chromatography (60 g SiO_2, 14.0 x 3.5 cm, eluent: cyclohexane:EtOAc = 10:1 (v/v), R_f = 0.23) and the resulting colorless, nasty smelling liquid was dried in the vacuum of a membrane pump at 6.0 mbar for 20 min.

Yield: 886 mg (4.81 mmol, 87 %); colorless, nasty smelling liquid (sum of both diastereomers); *e.e.* > 99 % and *d.e.* = 80 %.

$C_9H_{12}O_2S$ [184.25 g.mol^{-1}].

R_f = 0.63 (cyclohexane:EtOAc = 3:1 (v/v), UV and $KMnO_4$).

^{1}H-NMR (300.36 MHz, $CDCl_3$): δ = 6.45 (dd, $^3J_{HH}$ = 5.8 Hz, $^3J_{HH}$ = 1.4 Hz, 1H, H-1), 6.21 (dd, $^3J_{HH}$ = 5.8 Hz, $^3J_{HH}$ = 1.1 Hz, 1H, H-2), 5.19 (d, $^3J_{HH}$ = 4.3 Hz, 1H, H-3), 5.03 (d, $^3J_{HH}$ = 3.7 Hz, 1H, H-6), 3.34 (td, $^3J_{HH}$ = 8.7 Hz, $^3J_{HH}$ = 4.3 Hz, 1H, H-4), 2.85 (dq, $^3J_{HH}$ = 7.4 Hz, $^5J_{HH}$ = 1.2 Hz, 2H, H-8), 2.07 (ddd, $^2J_{HH}$ = 11.5 Hz, $^3J_{HH}$ = 9.1 Hz, $^3J_{HH}$ = 4.7 Hz, 1H, H-5a), 1.67 (dd, $^2J_{HH}$ = 11.4 Hz, $^3J_{HH}$ = 3.8 Hz, 1H, H-5b), 1.22 (t, $^3J_{HH}$ = 7.4 Hz, 3H, H-9).

^{13}C-NMR (75.53 MHz, $CDCl_3$): δ = 198.0 (C_q, C-7), 137.2 (C-1), 132.2 (C-2), 79.8 (C-3), 79.5 (C-6), 52.1 (C-4), 28.8 (C-5), 23.5 (C-8), 14.8 (C-9).

7.3.57. *S*-Ethyl (1*R*,2*S*,4*R*)-7-oxabicyclo[2.2.1]hept-5-ene-2-carbothioate (88)
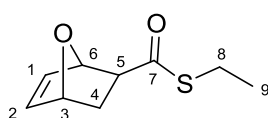
88

$C_9H_{12}O_2S$ [184.25 g.mol^{-1}].

R_f = 0.54 (cyclohexane:EtOAc = 3:1 (v/v), UV and $KMnO_4$).

^{1}H-NMR (300.36 MHz, $CDCl_3$): δ = 6.40 (dd, $^3J_{HH}$ = 5.8 Hz, $^3J_{HH}$ = 1.3 Hz, 1H, H-1), 6.36 (dd, $^3J_{HH}$ = 5.7 Hz, $^3J_{HH}$ = 1.2 Hz, 1H, H-2), 5.15 (s, 1H, H-3), 5.10 (d, $^3J_{HH}$ = 4.2 Hz, 1H, H-6), 2.91 (q, $^3J_{HH}$ = 7.4 Hz, 2H, H-8), 2.63 (dd, $^3J_{HH}$ = 8.4 Hz, $^4J_{HH}$ = 3.9 Hz, 1H, H-4), 2.17 (td, $^2J_{HH}$ = 11.5 Hz, $^3J_{HH}$ = 4.2 Hz, 1H, H-5a), 1.56 (dd, $^2J_{HH}$ = 11.6 Hz, $^3J_{HH}$ = 8.5 Hz, 1H, H-5b), 1.26 (t, $^3J_{HH}$ = 7.4 Hz, 3H, H-9).

^{13}C-NMR (75.53 MHz, CDCl$_3$): δ = 200.2 (C$_q$, C-7), 137.4 (C-1), 134.8 (C-2), 81.6 (C-3), 78.2 (C-6), 51.6 (C-4), 29.8 (C-5), 23.6 (C-8), 14.8 (C-9).

7.3.58. Methyl (1*R*,2*R*,4*R*)-7-oxabicyclo[2.2.1]hept-5-ene-2-carboxylate (64)
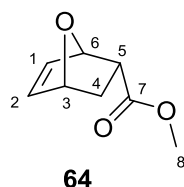
64

Literature: D. A. Evans, D. M. Barnes, J. S. Johnson, T. Lectka, P. von Matt, S. J. Miller, J. A. Murry, R. D. Norcross, E. A. Shaughnessy, K. R. Campos, *J. Am. Chem. Soc.* **1999**, *121*, 7582-7594.

A 100 mL two-necked round-bottom flask equipped with a Teflon-coated magnetic stirring bar and CaCl$_2$ drying tube was charged with 2.30 g (7.05 mmol, 1.5 eq) Cs$_2$CO$_3$. It was dissolved in 50 mL MeOH and afterwards cooled to -20 °C in an acetone/dry ice bath. A solution of 866 mg (4.70 mmol, 1.0 eq) optically pure thioester **87** (*e.e.* > 99 % and *d.e.* = 80 %) in 20 mL MeOH was added in one portion and the colorless solution was stirred in the cooling bath at -20 °C for additional 15 min. Afterwards the cooling media was removed and the colorless solution stirred in an ice-water bath at 0 °C for 3 h. 25 mL saturated NH$_4$Cl as well as 25 mL brine were added and the product was extracted with EtOAc (4 x 50 mL). The combined, colorless organic phases were dried over MgSO$_4$, filtered and the solvent was removed on the rotary evaporator. Finally, the yellow liquid was purified via flash column chromatography (15 g SiO$_2$, 16.0 x 1.5 cm, eluent: cyclohexane:EtOAc = 3:1 (v/v), R$_f$ = 0.20) furnishing a yellowish liquid. It was dissolved in 20 mL DCM, the solvent was removed on the rotary evaporator and the final product was dried in the vacuum of a membrane pump at 6.0 mbar for 30 min.

Yield: 662 mg (4.29 mmol, 91 %); yellowish liquid (sum of both diastereomers) *e.e.* > 99 % and *d.e.* = 80 %.

C$_8$H$_{10}$O$_3$ [154.16 g.mol^{-1}].

R$_f$ = 0.44 (cyclohexane:EtOAc = 2:1 (v/v), UV and KMnO$_4$).

[α]$_D$$^{30\text{-}31\,°C}$ = +96.8 ° (c = 1.00 in CHCl$_3$); *e.e.* > 99 % and *d.e.* > 99 %.

^{1}H-NMR (300.36 MHz, CDCl$_3$): δ = 6.43 (dd, $^3J_{HH}$ = 5.8 Hz, $^3J_{HH}$ = 1.3 Hz, 1H, H-2), 6.22 (dd, $^3J_{HH}$ = 5.8 Hz, $^3J_{HH}$ = 1.3 Hz, 1H, H-2), 5.16 (d, $^3J_{HH}$ = 4.4 Hz, 1H, H-6), 5.02 (d, $^3J_{HH}$ = 3.7 Hz,

1H, H-3), 3.64 (s, 3H, H-8), 3.11 (p, $^3J_{HH}$ = 4.4 Hz, 1H, H-5), 2.10 (ddd, $^2J_{HH}$ = 11.4 Hz, $^3J_{HH}$ = 9.5 Hz, $^3J_{HH}$ = 4.7 Hz, 1H, H-4a), 1.58 (dd, $^2J_{HH}$ = 11.5 Hz, $^3J_{HH}$ = 3.7 Hz, 1H, H-4b).

^{13}C-NMR (75.53 MHz, CDCl$_3$): δ = 172.8 (C$_q$, C-7), 137.2 (C-2), 132.7 (C-1), 79.2 (C-3), 78.9 (C-6), 51.9 (C-8), 42.8 (C-5), 28.7 (C-4).

7.3.59. Methyl (*R*)-5-hydroxycyclohexa-1,3-diene-1-carboxylate (65)
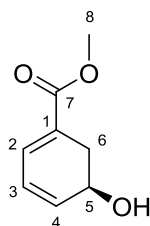
65

Literature: D. A. Evans, D. M. Barnes, J. S. Johnson, T. Lectka, P. von Matt, S. J. Miller, J. A. Murry, R. D. Norcross, E. A. Shaughnessy, K. R. Campos, *J. Am. Chem. Soc.* **1999**, *121*, 7582-7594.

An oven-dried, evacuated and argon purged 50 mL Schlenk flask equipped with a Teflon-coated magnetic stirring bar was charged with 488 µL (378 mg, 2.34 mmol, 1.3 eq) hexamethyldisilazane. It was dissolved in 12 mL anhydrous THF and the colorless solution was cooled in an acetone/dry ice bath to -78 °C under argon atmosphere. Afterwards 1.02 mL (2.34 mmol, 1.3 eq) *n*BuLi (2.30 M in *n*-hexane) were added via septum and syringe dropwise over a period 5 min The cooling media was removed and the colorless solution stirred in an ice-water bath at 0 °C under argon atmosphere for 30 min. Subsequently, it was again cooled in an acetone/dry ice bath to -78 °C. In parallel, an oven-dried, evacuated and argon purged 50 mL Schlenk flask equipped with a Teflon-coated magnetic stirring bar was charged with 277 mg (1.80 mmol, 1.0 eq) optically pure ester **64** (*e.e.* > 99 % and *d.e.* = 80 %). It was dissolved in 4.0 mg anhydrous THF and the colorless solution was cooled in an acetone/dry ice to -78 °C under argon atmosphere. Afterwards the cold solution of bicyclic ester **64** was added to the cold LHMDS solution in one portion in an argon counter flow and the Schlenk flask was rinsed with anhydrous THF (2 x 1.0 mL). The resulting yellowish solution was allowed to warm to -50 °C in the acetone/dry ice bath and was stirred at this temperature for additional 4 h under argon atmosphere. Subsequently, it was poured into 50 mL saturated NH$_4$Cl and the product was extracted from the yellowish aqueous phase with EtOAc (3 x 50 mL). The combined, colorless organic layers were dried over MgSO$_4$, filtered and the solvent was concentrated on a rotary evaporator. Finally, the yellow, oily

crude material was purified via flash column chromatography (9.0 g SiO_2, 25.0 x 0.8 cm, eluent: cyclohexane:EtOAc = 2:1 (v/v), R_f = 0.24) furnishing a colorless, viscous liquid. It was dissolved in 20 mL DCM, the solvent was removed on a rotary evaporator and the final product was dried in the vacuum of a membrane pump at 6.0 mbar for 30 min.

Yield: 232 mg (1.50 mmol, 84 %); colorless, viscous liquid.

$C_8H_{10}O_3$ [154.16 g.mol^{-1}].

R_f = 0.40 (cyclohexane:EtOAc = 1:1 (v/v), UV and $KMnO_4$).

$[\alpha]_D^{30-31\,°C}$ = +401.4 ° (c = 1.00 in $CHCl_3$); *e.e.* > 99 %.

chiral HPLC (Method_ESTER): t_R = 12.27 min (minor enantiomer) and 17.31 min (major enantiomer); *e.e.* > 99 %.

^{1}H-NMR (300.36 MHz, $CDCl_3$): δ = 7.10-7.07 (m, 1H, H-1), 6.28-6.18 (m, 2H, H-2, H-3), 4.40-4.35 (m, 1H, H-4), 3.76 (s, 3H, H-8), 2.91 (dd, $^2J_{HH}$ = 18.9 Hz, $^3J_{HH}$ = 5.3 Hz, 1H, H-5a), 2.63 (ddd, $^2J_{HH}$ = 18.8 Hz, $^3J_{HH}$ = 7.6 Hz, $^3J_{HH}$ = 2.1 Hz, 1H, H-5b), 1.82 (bs, 1H, OH).

^{13}C-NMR (75.53 MHz, $CDCl_3$): δ = 167.6 (C_q, C-7), 133.4 (C-3), 131.6 (C-1), 127.0 (C_q, C-6), 124.9 (C-2), 63.3 (C-4), 52.0 (C-8), 31.3 (C-5).
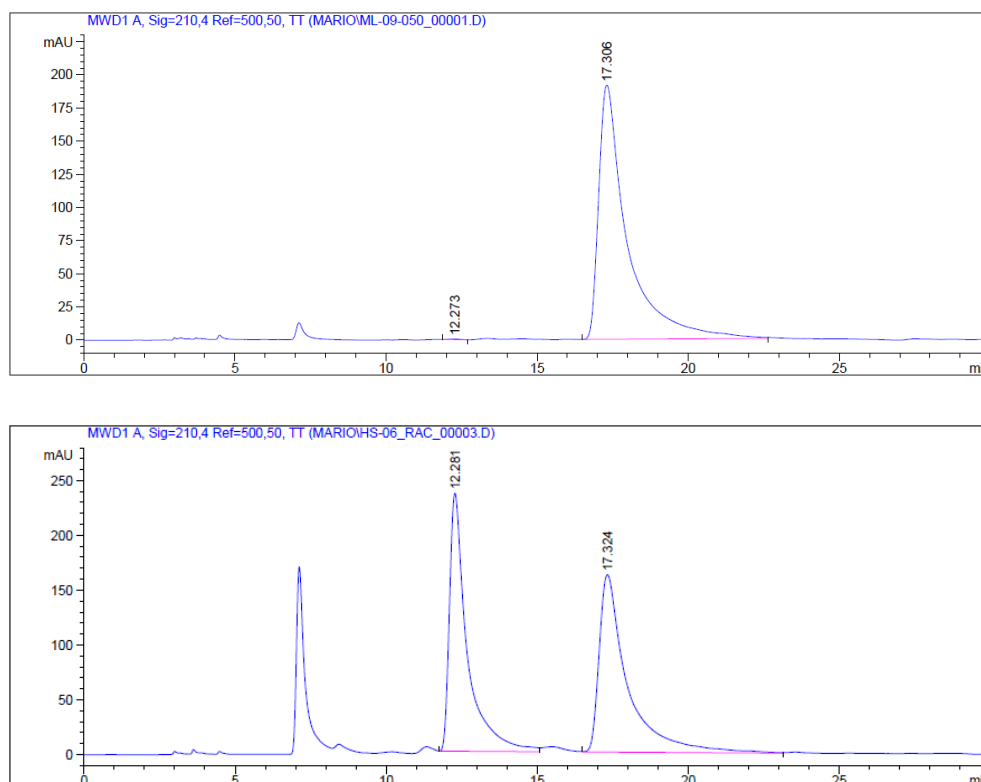
Figure 41: Chiral HPLC chromatograms of **65** and ***rac*-65** for the determination of the enantiomeric excess (*e.e.*).

7.4. Time-Resolved ^{1}H-NMR Experiments Investigating the Isomerization of DHHA (1) and its Derivatives Catalyzed by PhzF

All ^{1}H-NMR experiments described in this section were performed together with Prof. Hansjörg WEBER on a Varian Unity Inova 500 spectrometer (^{1}H: 499.88 MHz) in NMR tubes (178 x 4.95 mm, 300 MHz) of the Duran Group. For best signal separation, measurements were executed at a temperature of 15 °C. Herein, 50 mM NaH_2PO_4/Na_2HPO_4 buffer either in H_2O:D_2O = 9:1 (v/v) with pH 7.5 or in D_2O with pD 7.5 were used as a solvent. Before a stock-solution of WT PhzF was added to the solution of the corresponding DHHA derivative, all relevant parameter for ^{1}H-NMR analyses were set on the instrument. WT PhzF as well as H74A were received from Christina DIEDERICH from the BLANKENFELDT lab.

50 mM NaH_2PO_4/Na_2HPO_4 buffer in H_2O:D_2O = 9:1 (v/v) (pH 7.5): 60.0 mg solid and anhydrous NaH_2PO_4 with 16.0 mg NaOH were dissolved in 10 mL degassed H_2O:D_2O = 9:1 (v/v) in an oven-dried, evacuated and argon purged 25 mL Schlenk flask. For testing purpose, the pH was measured with a calibrated pH-meter in a separately prepared buffer solution.

50 mM NaH_2PO_4/Na_2HPO_4 buffer (pD 7.5): 60.0 mg solid and anhydrous NaH_2PO_4 with 16.0 mg NaOH were dissolved in 10 mL degassed D_2O in an oven-dried, evacuated and argon purged 25 mL Schlenk flask. For testing purpose, the pD was measured with a calibrated pH-meter in a separately prepared buffer solution.

Each NMR tube was charged with 6.30 µmol of DHHA (**1a**) or its corresponding derivative, was put afterwards in a size fitting Schlenk flask, which was subsequently evacuated and purged with argon. All substrates were dissolved in 650 µL of the degassed 50 mM NaH_2PO_4/Na_2HPO_4 buffer solutions either in H_2O:D_2O = 9:1 (v/v) (pH 7.5) or in D_2O (pD 7.5) under argon atmosphere. After measurement of the initial ^{1}H-NMR spectrum, 10 µL of the WT PhzF stock-solution (321 µM = 20.7 mg.mL^{-1} or 88 µM = 5.7 mg.mL^{-1} in 20 mM NaH_2PO_4/Na_2HPO_4 buffer in H_2O, pH 7.5, stabilized with glycerol) were rapidly added, the NMR tube was vigorously shaken and conversion was automatically measured by time-resolved ^{1}H-NMR analyses. Each spectrum was recorded after 5 min reaction time with a number of 8 scans.

7.4.1. ^{1}H-NMR Experiments for the Hydrogen/Deuterium Migration in DHHA (1)/d-DHHA (5) with WT PhzF and H74A

Cross experiments were performed either with wildtype PhzF or the H742A in order to investigate the migration behavior of the hydrogen in DHHA (**1**) and the deuterium in d-DHHA (**5**), respectively.

According to the general procedure, 6.30 µmol DHHA (**1a**) were dissolved in 650 µL degassed 50 mM NaH_2PO_4/Na_2HPO_4 in D_2O (pD 7.5) and in cross experiments 6.30 µmol d-DHHA (**5a**) in 650 µL degassed 50 mM NaH_2PO_4/Na_2HPO_4 in $H_2O{:}D_2O$ = 9:1 (v/v) (pH 7.5) under argon atmosphere. Both experiments were performed with 10 µL wildtype PhzF stock-solution (321 µM = 20.7 mg.mL^{-1} in 20 mM NaH_2PO_4/Na_2HPO_4 buffer in H_2O, pH 7.5, stabilized with glycerol) and with 90 µL H74A mutant stock-solution (275 µM = 17.7 mg.mL^{-1} in 20 mM NaH_2PO_4/Na_2HPO_4 buffer in H_2O, pH 7.5, stabilized with glycerol). In all measurements H_2O suppression was adjusted.

7.4.1.1. Migration Experiments: Time-Resolved ^{1}H-NMR Analysis of DHHA (1) in D$_2$O with WT PhzF
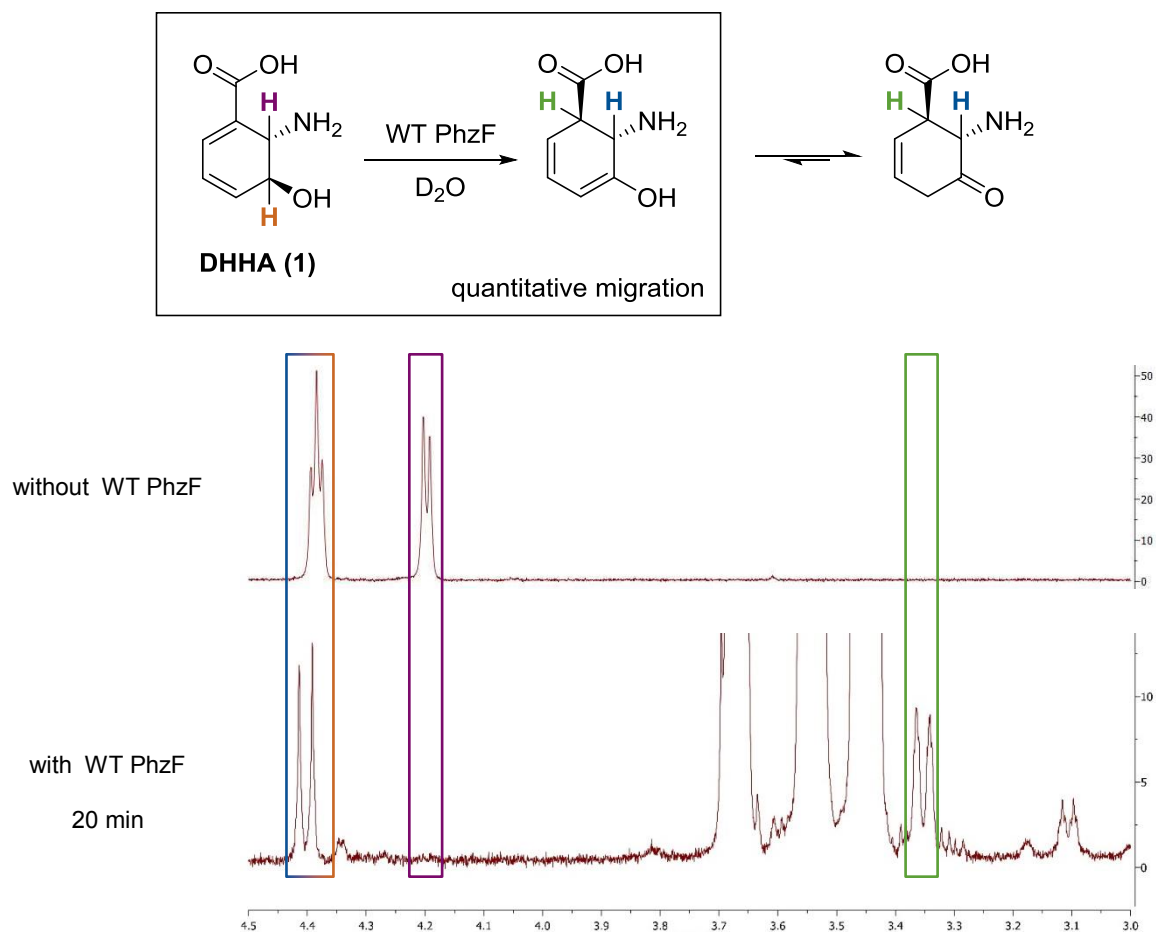
Figure 42: Time-resolved ^{1}H-NMR experiments with DHHA (**1**) and WT PhzF in D$_2$O.

7.4.1.2. Migration Experiments: Time-Resolved ^{1}H-NMR Analysis of d-DHHA (5) in H$_2$O:D$_2$O = 9:1 (v/v) with WT PhzF
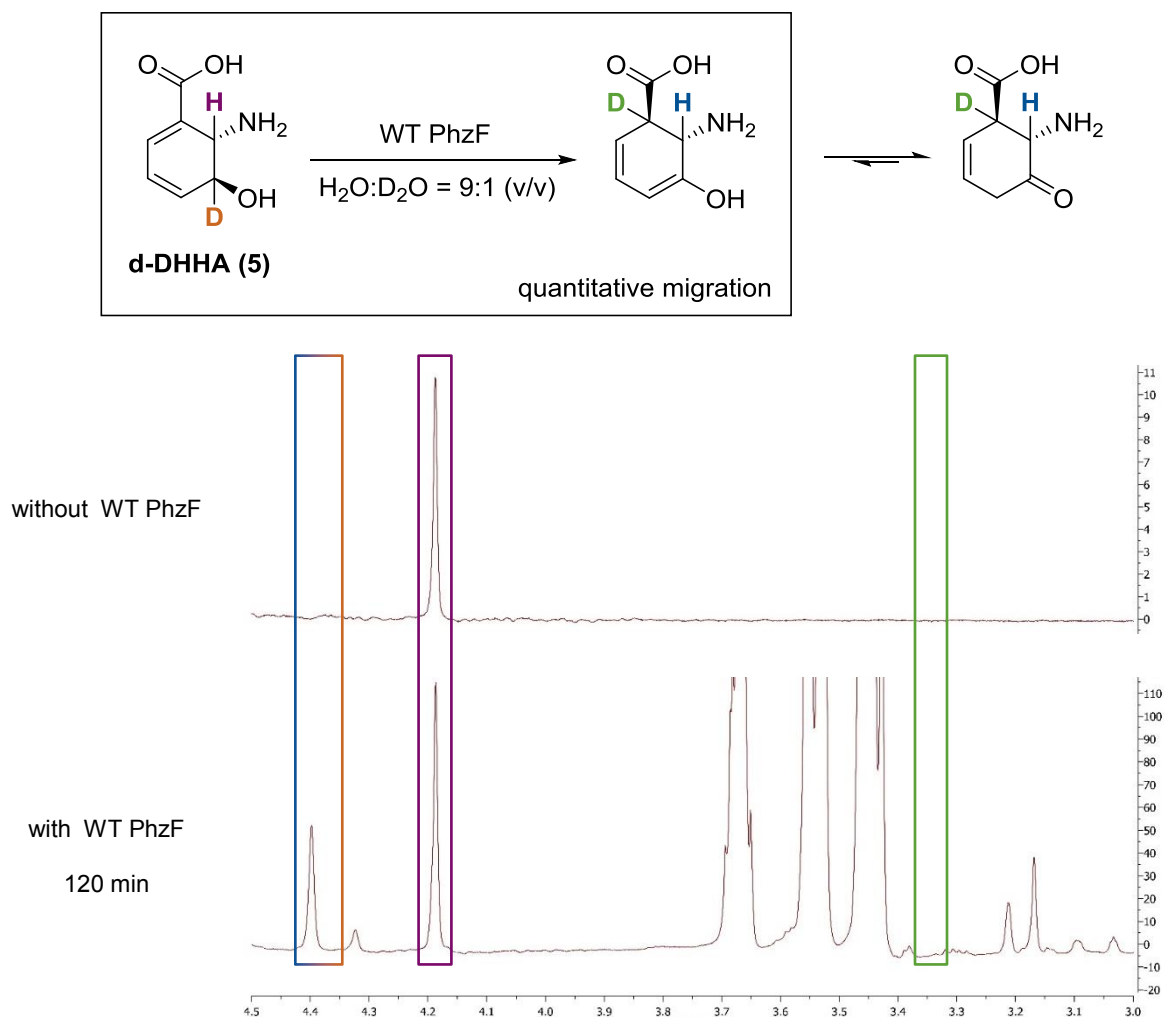
Figure 43: Time-resolved ^{1}H-NMR experiments with d-DHHA (**5**) and WT PhzF in H$_2$O:D$_2$O = 9:1 (v/v).

7.4.1.3. Migration Experiments: Time-Resolved ^{1}H-NMR Analysis of DHHA (1) in D$_2$O with H74A
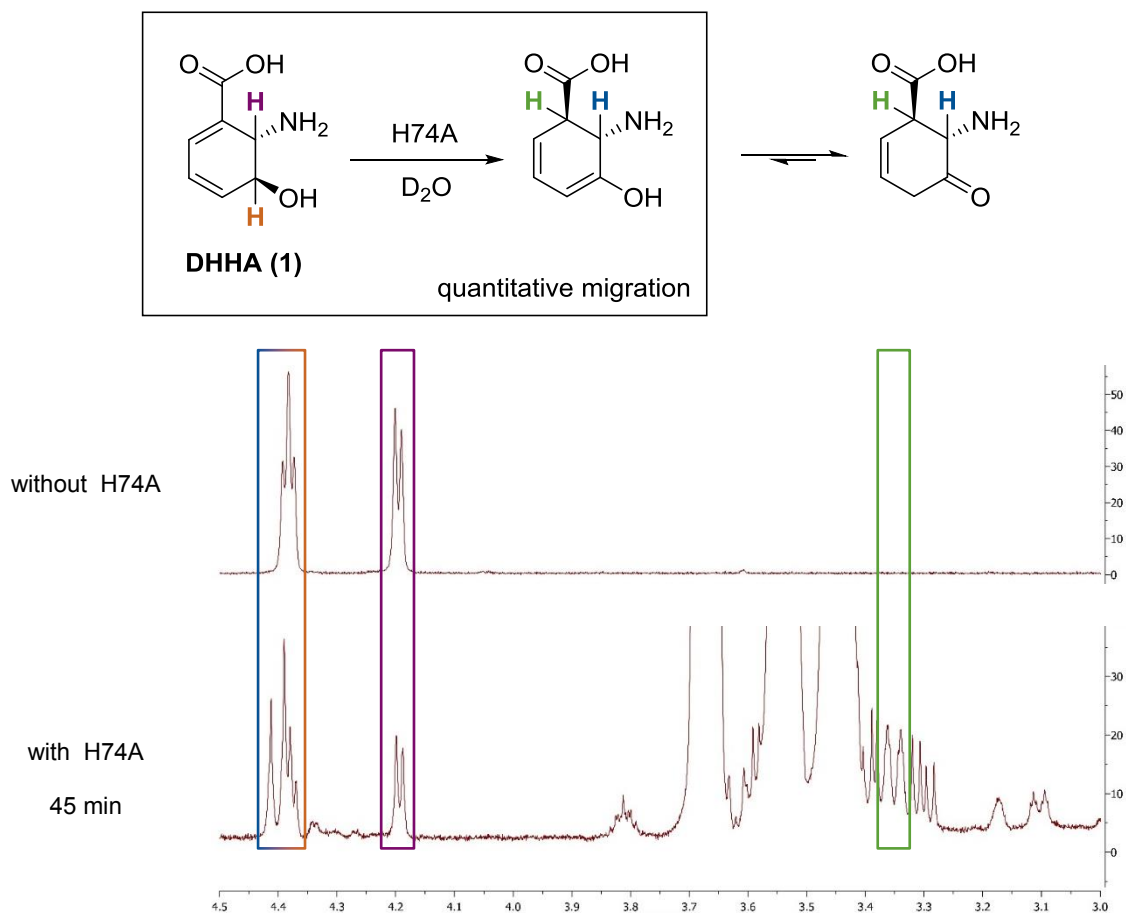
Figure 44: Time-resolved ^{1}H-NMR experiments with DHHA (**1**) and H74A in D$_2$O.

7.4.1.4. Migration Experiments: Time-Resolved ^{1}H-NMR Analysis of d-DHHA (5) in H$_2$O:D$_2$O = 9:1 (v/v) with H74A
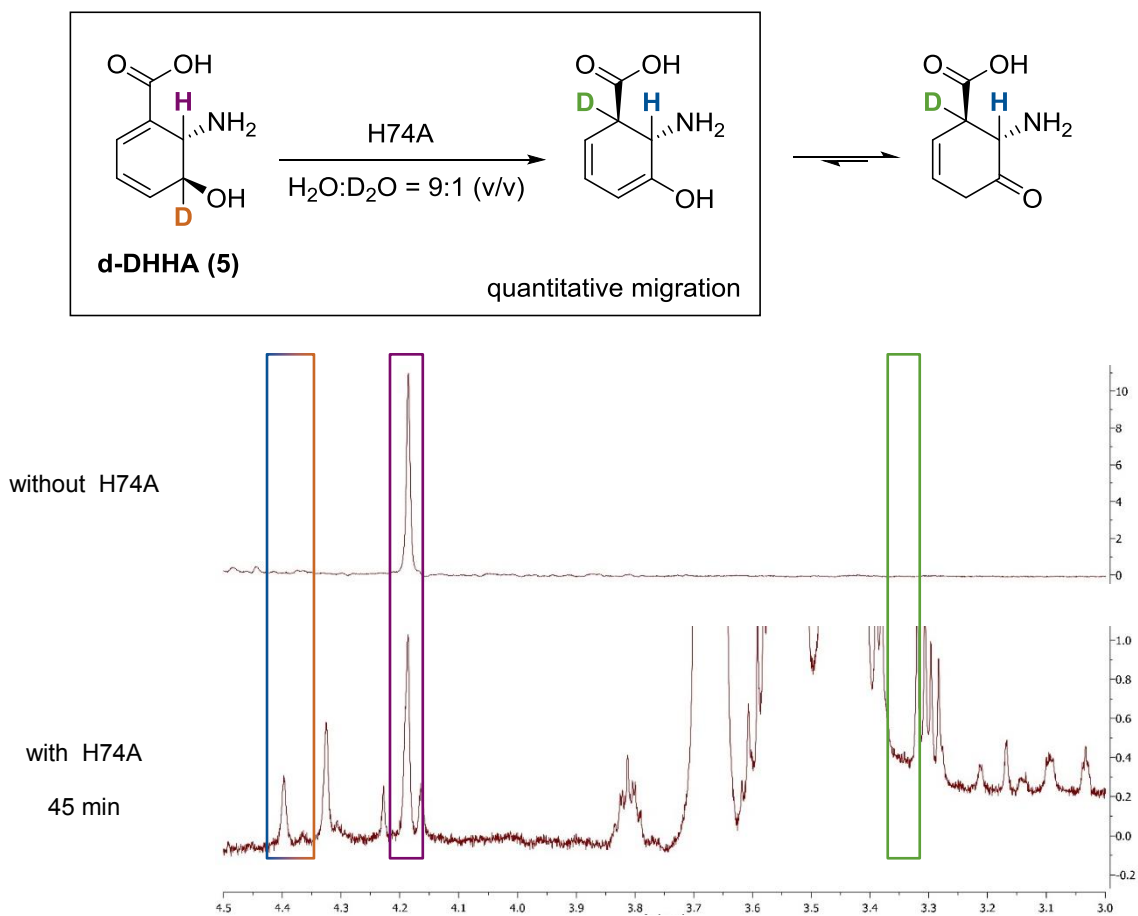
Figure 45: Time-resolved ^{1}H-NMR experiments with d-DHHA (**5**) and H74A in H$_2$O:D$_2$O = 9:1 (v/v).

7.4.2. ^{1}H-NMR Experiments for Substrate Scope Investigations of WT PhzF

Substrate scope investigations of PhzF were performed with the following racemic DHHA derivatives: Me-DHHA (*rac*-41a), Et-DHHA (*rac*-42a) and *n*Pr-DHHA (*rac*-43a). Herein racemic DHHA (*rac*-1a) was used as reference. Additional experiments were executed with optically pure starting materials: DHHA (1a), Me-DHHA (41a) as well as DHHS (51).

According to the general procedure, 6.30 µmol DHHA TFA salt derivate were dissolved in 650 µL degassed 50 mM NaH_2PO_4/Na_2HPO_4 in D_2O (pD 7.5) under argon atmosphere and afterwards 10 µL wildtype PhzF stock-solution (88 µM = 5.7 mg.mL^{-1} in 20 mM NaH_2PO_4/Na_2HPO_4 buffer in H_2O, pH 7.5, stabilized with glycerol) were added. Herein, no H_2O suppression was adjusted.

7.4.2.1. Substrate Scope Investigations: Time-Resolved ^{1}H-NMR Analysis of DHHA (*rac*-1) with WT PhzF
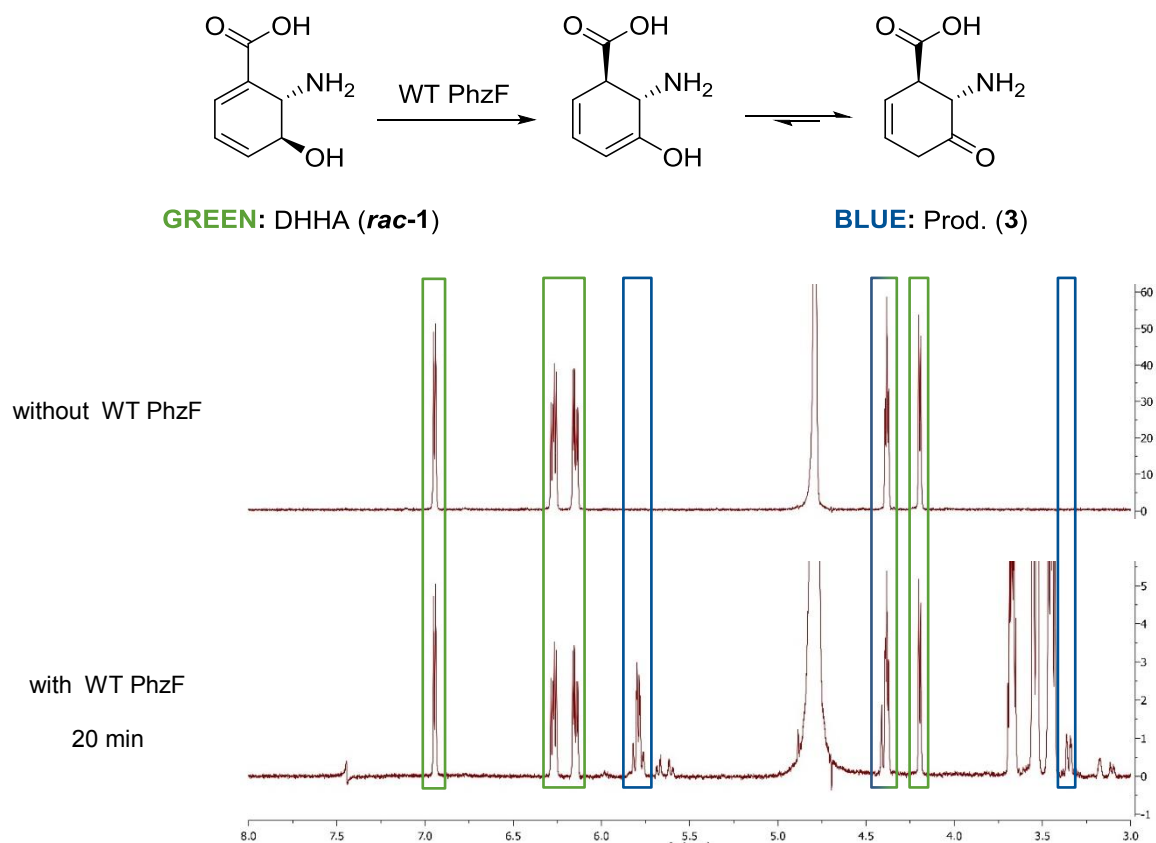
Figure 46: Time-resolved ^{1}H-NMR experiments with DHHA (*rac*-1) and WT PhzF in D_2O.

7.4.2.2. Substrate Scope Investigations: Time-Resolved ^{1}H-NMR Analysis of Me-DHHA (*rac*-41) with WT PhzF
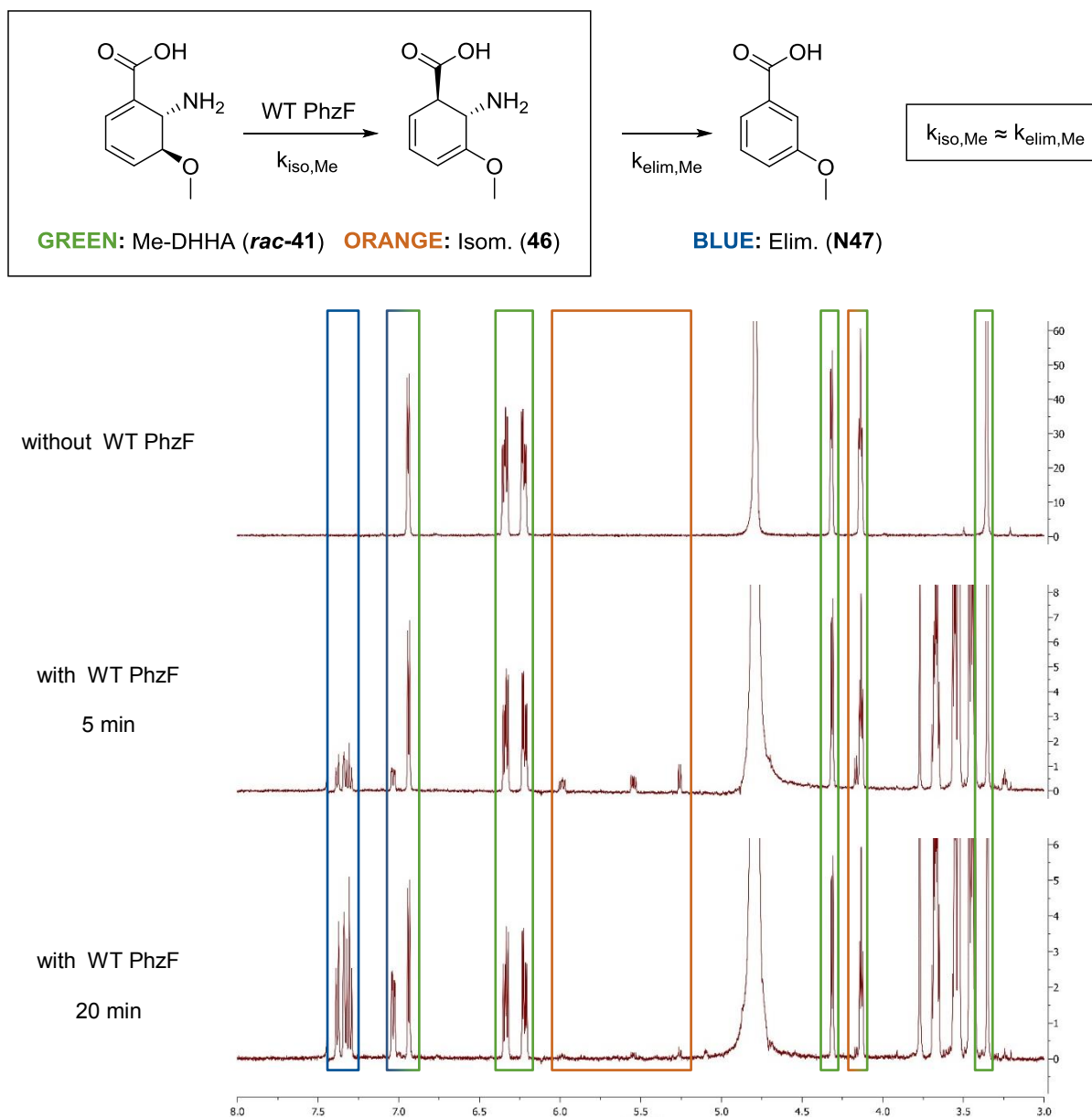
Figure 47: Time-resolved ^{1}H-NMR experiments with Me-DHHA (*rac*-41) and WT PhzF in D$_2$O.

7.4.2.3. Substrate Scope Investigations: Time-Resolved ^{1}H-NMR Analysis of Et-DHHA (*rac*-42) with WT PhzF
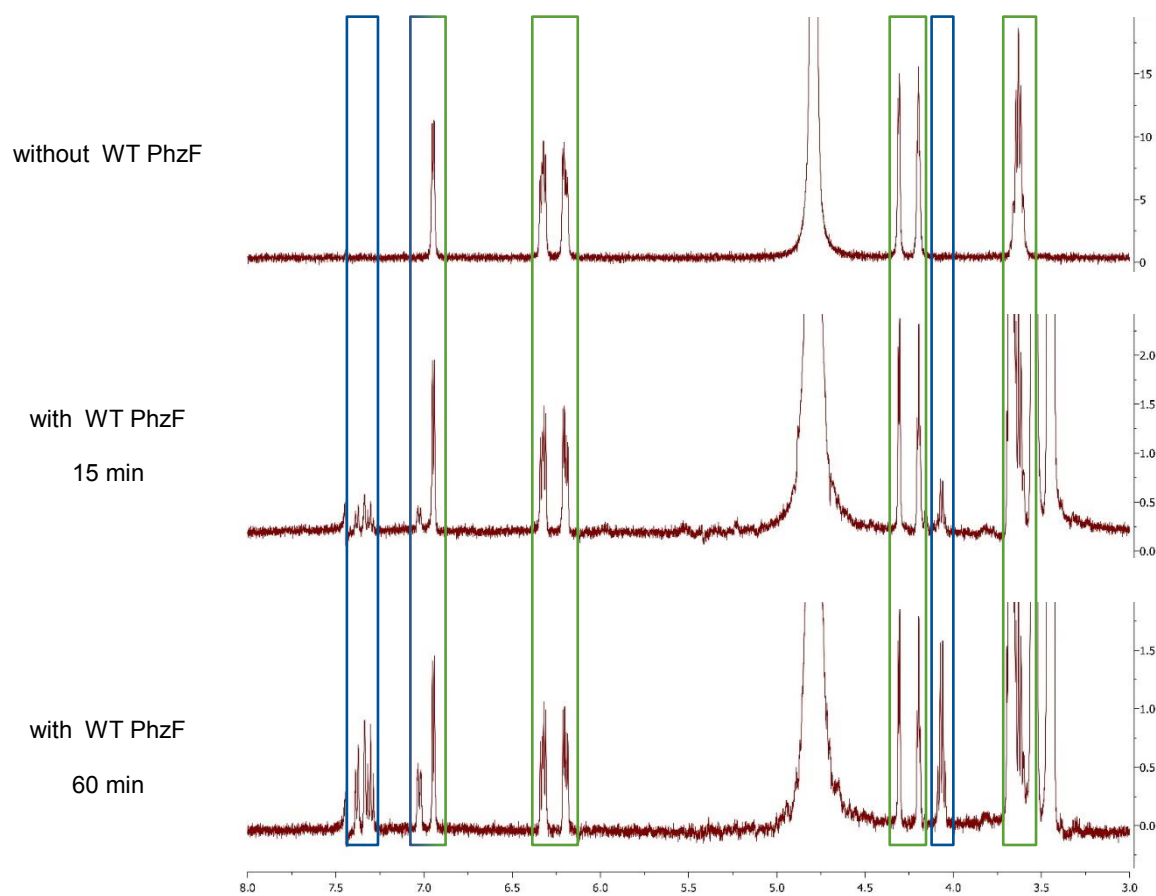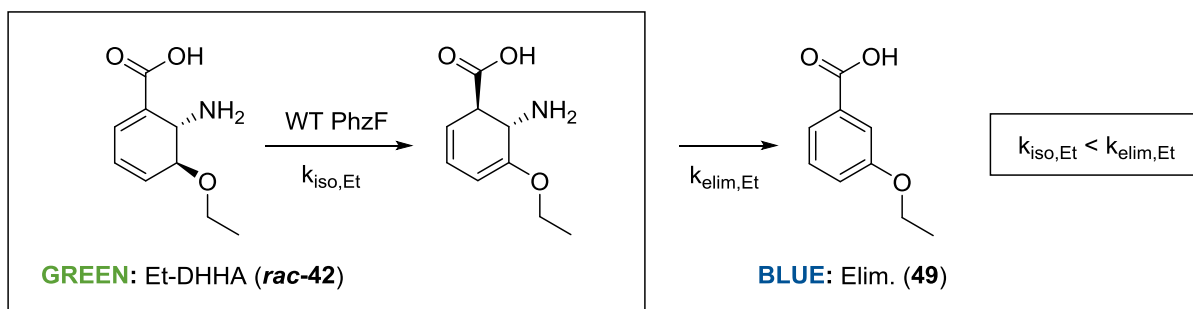
Figure 48: Time-resolved ^{1}H-NMR experiments with Et-DHHA (*rac*-42) and WT PhzF in D_2O.

7.4.2.4. Substrate Scope Investigations: Time-Resolved ¹H-NMR Analysis of *n*Pr-DHHA (*rac*-43) with WT PhzF
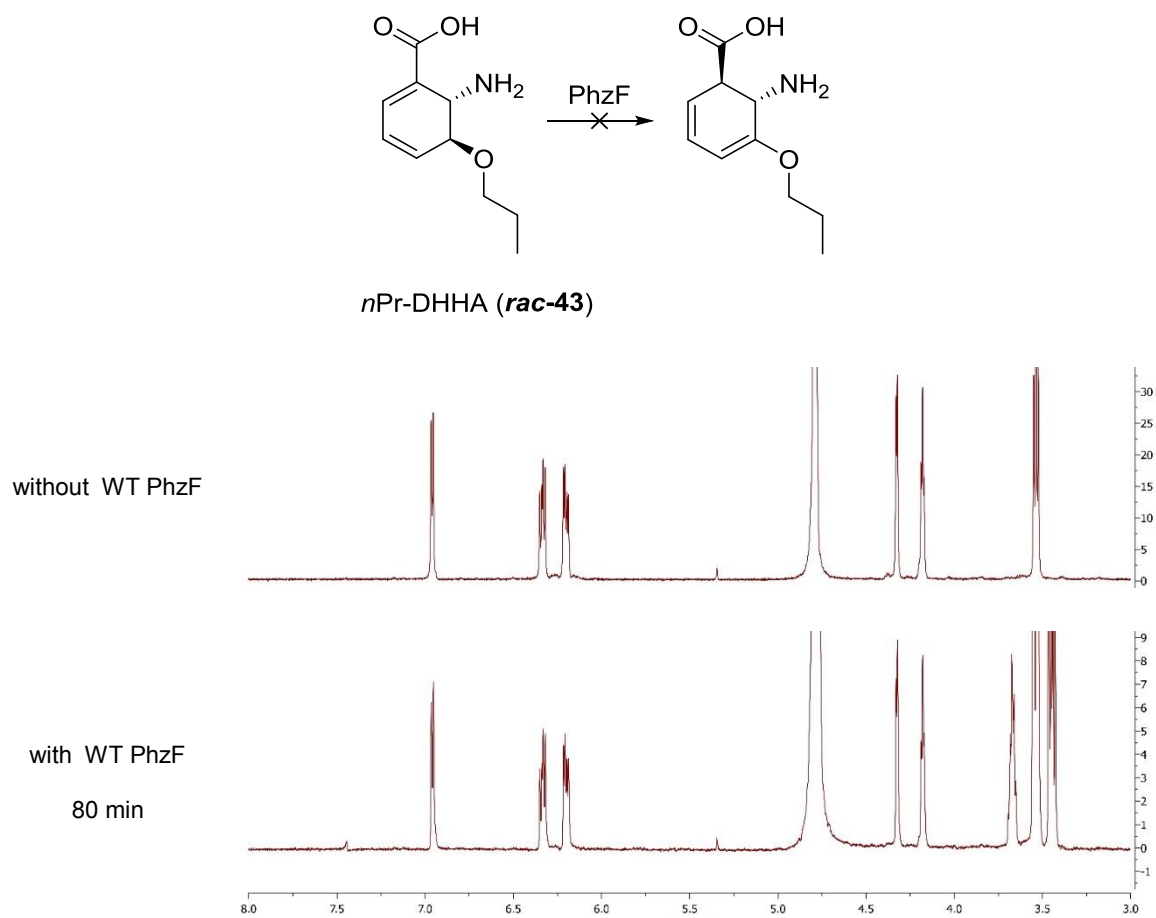
*n*Pr-DHHA (*rac*-43)

Figure 49: Time-resolved ¹H-NMR experiments with *n*Pr-DHHA (*rac*-43) and WT PhzF in D₂O.

7.4.2.5. Substrate Scope Investigations: Time-Resolved ^{1}H-NMR Analysis of DHHA (1) with WT PhzF

GREEN: DHHA (**1**)   **BLUE**: Prod. (**3**)
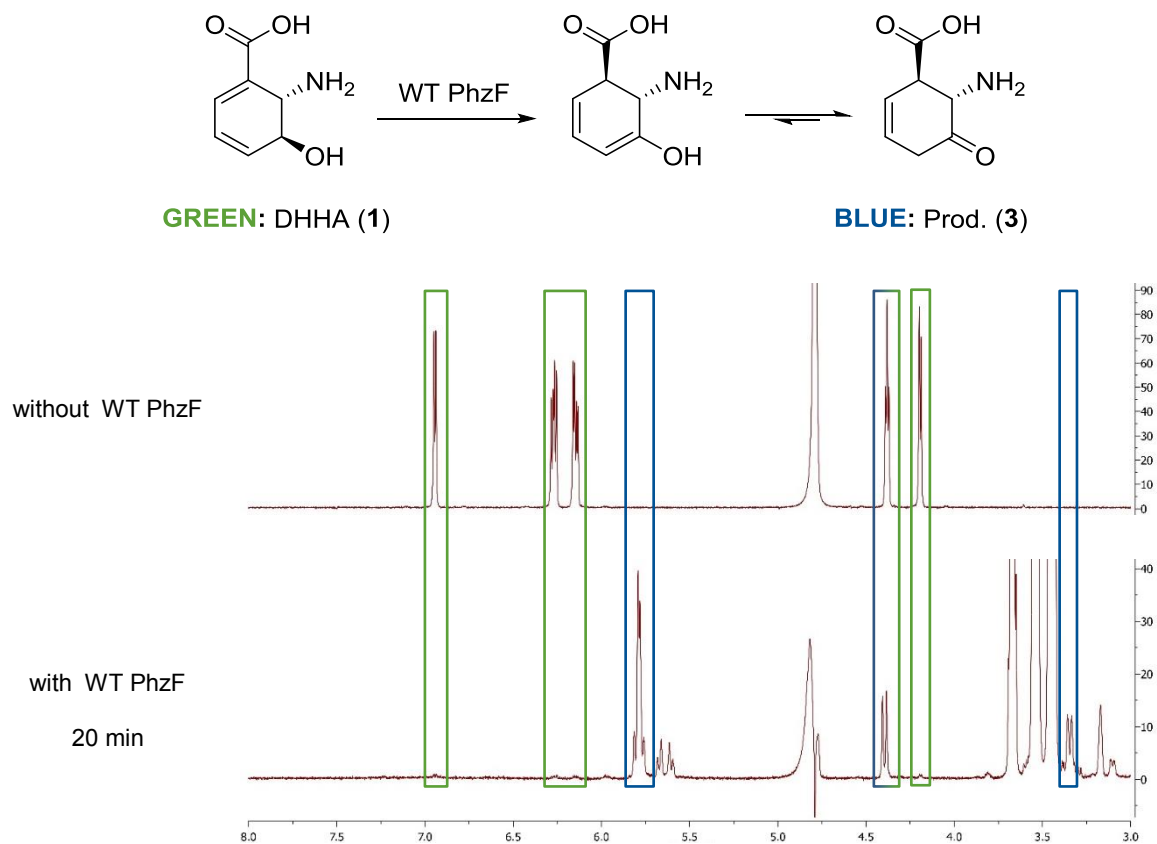
Figure 50: Time-resolved ^{1}H-NMR experiments with DHHA (**1**) and WT PhzF in D_2O.

7.4.2.6. Substrate Scope Investigations: Time-Resolved ^{1}H-NMR Analysis of Me-DHHA (41) with WT PhzF
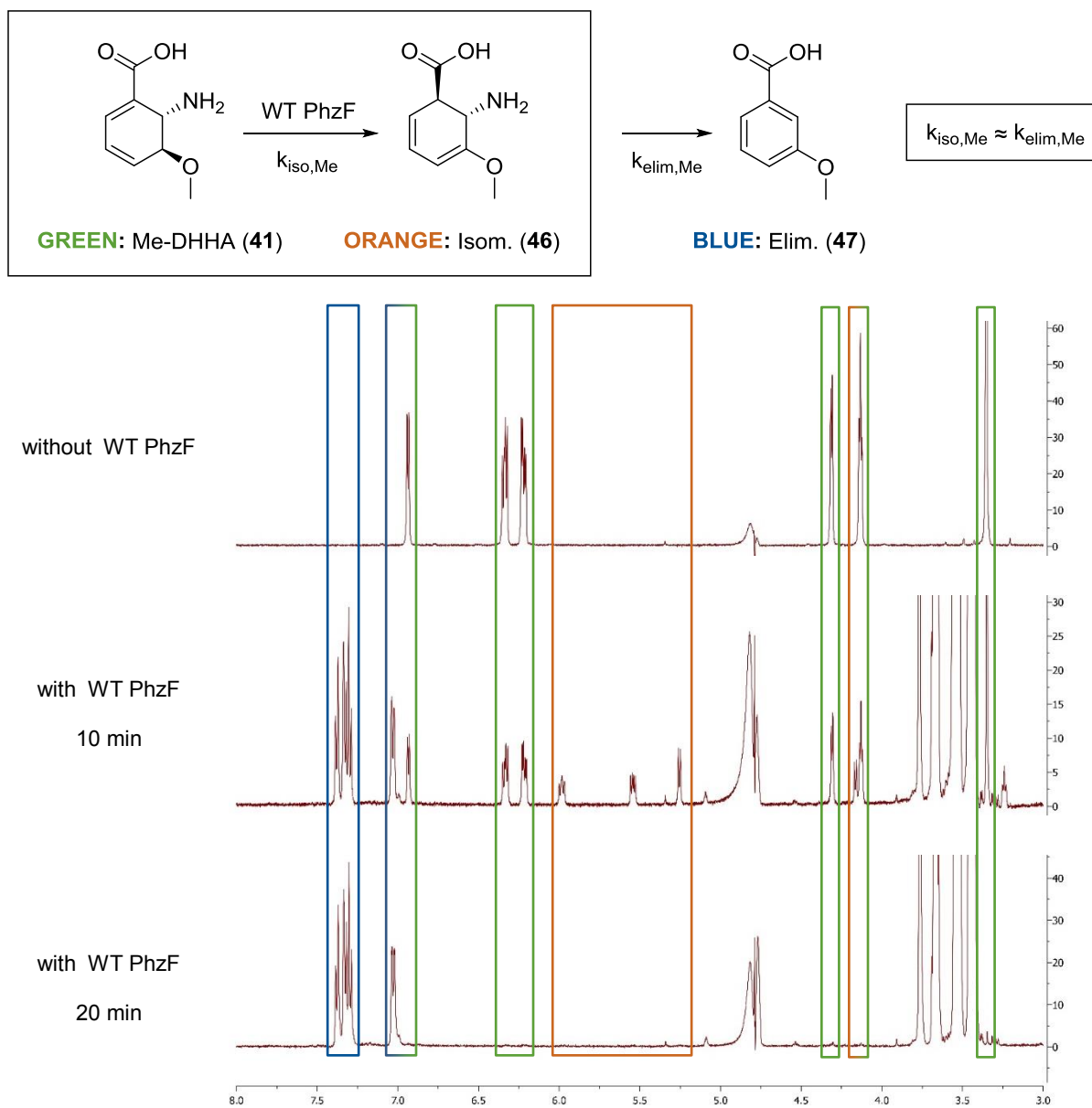
Figure 51: Time-resolved ^{1}H-NMR experiments with Me-DHHA (**41**) and WT PhzF in D_2O.

7.4.2.7. Substrate Scope Investigations: Time-Resolved ^{1}H-NMR Analysis of DHHS (51) with WT PhzF
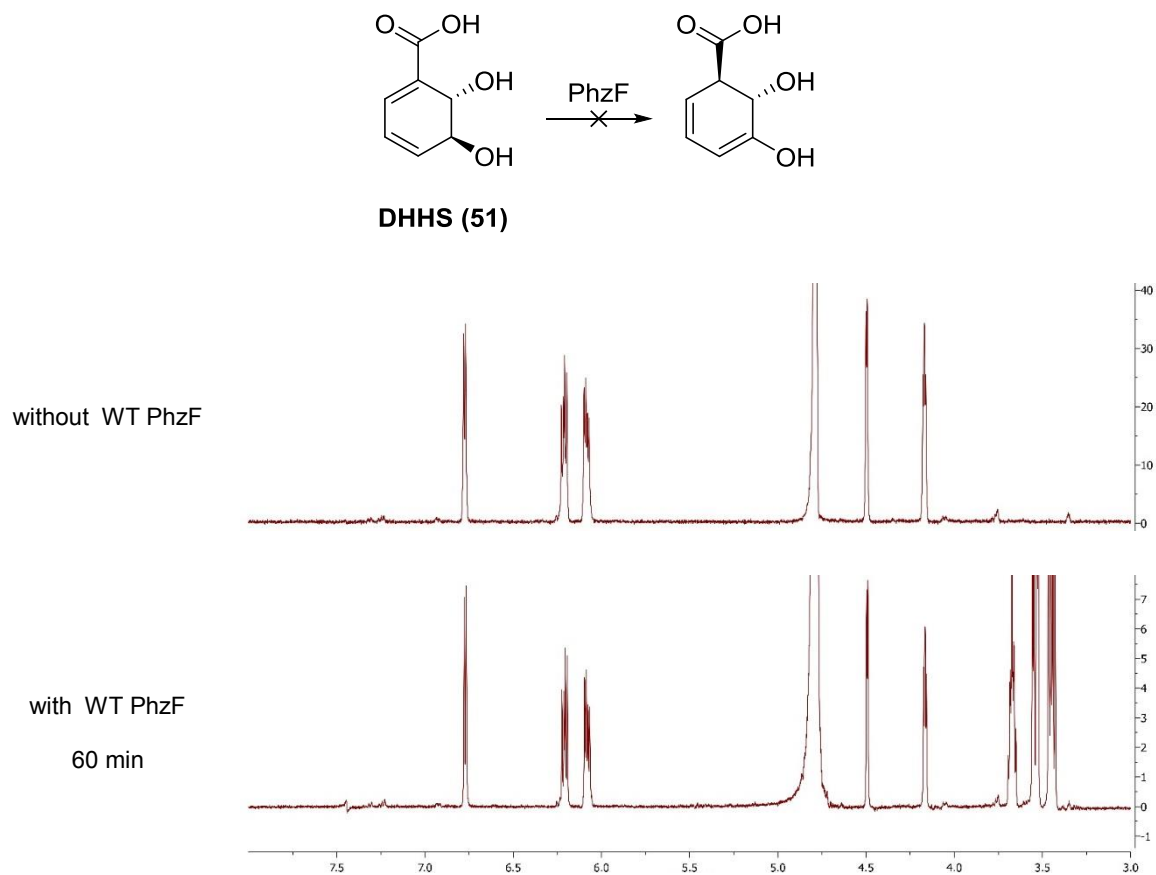
Figure 52: Time-resolved ^{1}H-NMR experiments with DHHS (**51**) and WT PhzF in D_2O.

7.5. Nuclear OVERHAUSER Effect (NOE) for the Determination of the Stereoselective Tautomerization in DHHA (1)

According to the general procedure, 6.30 µmol DHHA (**1**) were dissolved in 650 µL degassed 50 mM NaH_2PO_4/Na_2HPO_4 in D_2O (pD 7.5) under argon atmosphere and afterwards 10 µL WT PhzF stock-solution (88 µM = 5.7 mg.mL^{-1} in 20 mM NaH_2PO_4/Na_2HPO_4 buffer in H_2O, pH 7.5, stabilized with glycerol) were added. Herein, the blue marked hydrogen atom with the chemical shift of δ = 4.28 ppm was irradiated and no H_2O suppression was adjusted within this experiment.
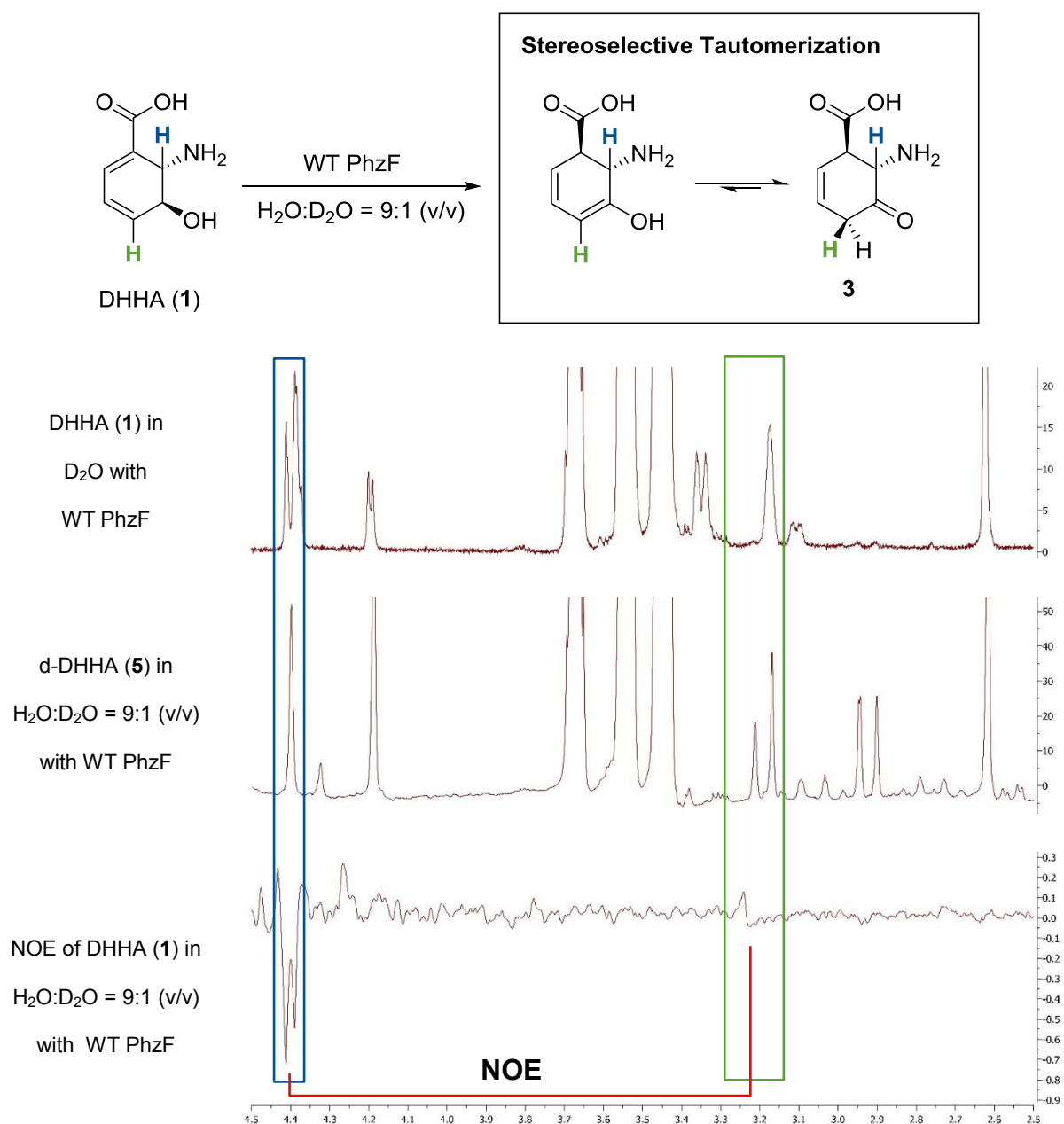
Figure 53: Determined nuclear OVERHAUSER effect (NOE) for the stereoselective tautomerization of DHHA (**1**) to ketamine **3**.

7.6. pK$_a$ Determination of DHHA (*rac*-1) by Acid-Base Titration with 100 mM NaOH

202 mg (750 µmol) DHHA (*rac*-1a) were dissolved in a 250 mL beaker equipped with a Teflon-coated magnetic stirring bar in 75 mL H$_2$O. The acid-base titration was performed on a "702 SM Titrino" Autotitrator from Metrohm with 100 mM NaOH ROTI®VOLUM standard solution from Roth and was repeated twice. For validation purpose, L-glycine was titrated with the same method (Ref.: pK$_a$(COOH) 2.3, pK$_a$(NH$_3^+$) 9.6; found: pK$_a$(COOH) 2.7, pK$_a$(NH$_3^+$) 9.6).
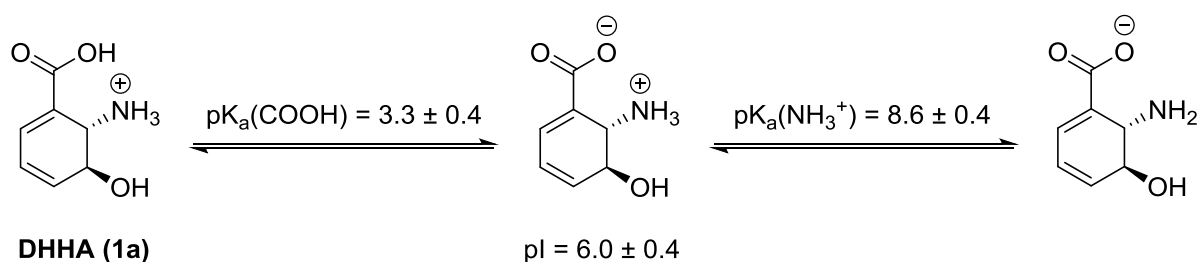
Scheme 35: pK$_a$ values of DHHA (**1a**) determined by acid-base titration with 100 mM NaOH.
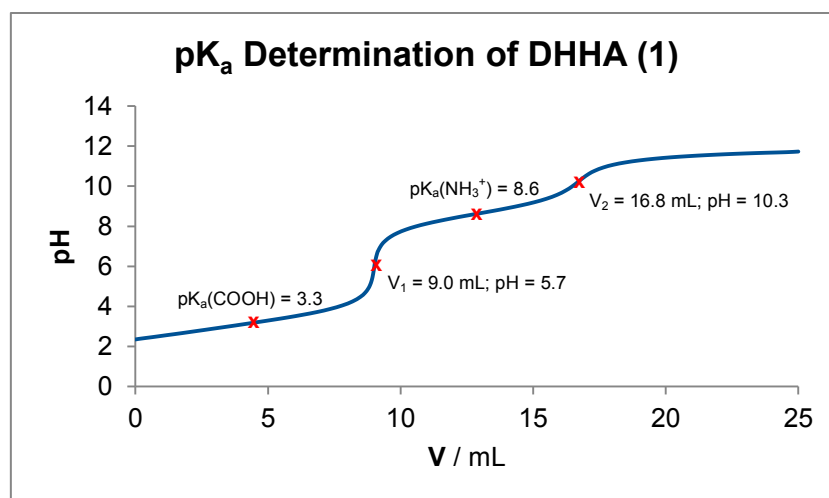
Figure 54: Titration curve for the pK$_a$ determination of DHHA (**1**) by acid-base titration with 100 mM NaOH.
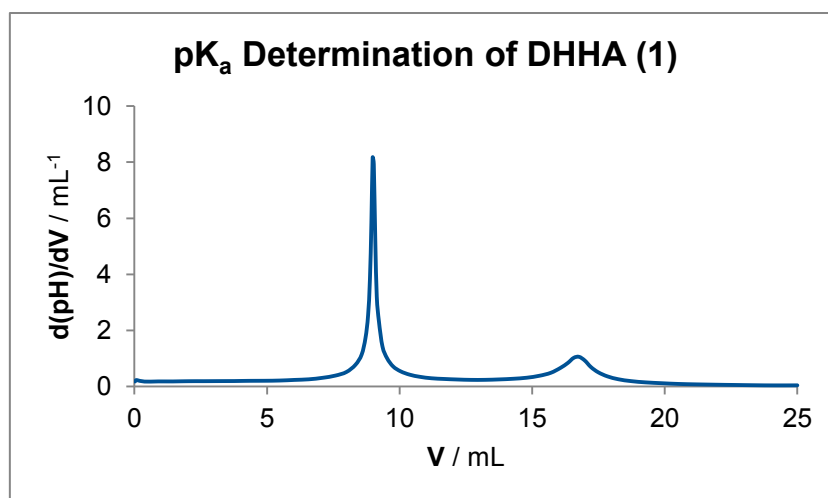
Figure 55: First derivative of the titration curve for the pK$_a$ determination of DHHA (**1**) by acid-base titration with 100 mM NaOH.

8.   References

[1]   M.-C. Maurel, J.-L. Dcout, *Tetrahedron* **1999**, *55*, 3141–3182.

[2]   B. Alberts, *Molecular Biology of the Cell*, Garland Science, New York, **2008**.

[3]   G. Caetano-Anollés, M. Wang, D. Caetano-Anollés, J. E. Mittenthal, *Biochem. J.* **2009**, *417*, 621–637.

[4]   A. Kohen, H.-H. Limbach, *Isotope Effects in Chemistry and Biology*, Taylor & Francis, Boca Raton, **2006**.

[5]   A. Choutko, A. P. Eichenberger, W. F. van Gunsteren, J. Dolenc, *Protein Sci.* **2013**, *22*, 809–822.

[6]   L. Pauling, *Nature* **1948**, *161*, 707–709.

[7]   V. L. Schramm, *Methods Enzymol.* **1999**, *308*, 301–348.

[8]   P. A. Bartlett, C. R. Johnson, *J. Am. Chem. Soc.* **1985**, *107*, 7792–7793.

[9]   P. A. Bartlett, Y. Nakagawa, C. R. Johnson, S. H. Reich, A. Luis, *J. Org. Chem.* **1988**, *53*, 3195–3210.

[10]   W. W. Smith, P. A. Bartlett, *J. Org. Chem.* **1993**, *58*, 7308–7309.

[11]   D. Antoniou, S. D. Schwartz, *J. Phys. Chem. B* **2001**, *105*, 5553–5558.

[12]   W. Blankenfeldt, J. F. Parsons, *Curr. Opin. Struct. Biol.* **2014**, *29*, 26–33.

[13]   M. Mentel, E. G. Ahuja, D. V. Mavrodi, R. Breinbauer, L. S. Thomashow, W. Blankenfeldt, *ChemBioChem* **2009**, *10*, 2295–2304.

[14]   J. B. Laursen, J. Nielsen, *Chem. Rev.* **2004**, *104*, 1663–1686.

[15]   a) M. J. Fordos, *Recl. Trav. Soc. d'Emul. Sci. Pharm.* **1859**, *3*, 30; b) M. J. Fordos, *Hebd. Seances Acad. Sci.* **1860**, *51*, 215–217.

[16]   a) D. V. Mavrodi, W. Blankenfeldt, L. S. Thomashow, *Annu. Rev. Phytopathol.* **2006**, *44*, 417–445; b) A. Price-Whelan, L. E. P. Dietrich, D. K. Newman, *Nat. Chem. Biol.* **2006**, *2*, 71–78.

[17]   M. C. Gessard, *C. R. Hebd. Seances Acad. Sci.* **1882**, *165*, 536.

[18]   a) J. Emerson, M. Rosenfeld, S. McNamara, B. Ramsey, R. L. Gibson, *Pediatr. Pulmonol.* **2002**, *34*, 91–100; b) J. M. Courtney, J. Bradley, J. Mccaughan, T. M. O'Connor, C. Shortt, C. P. Bredin, I. Bradbury, J. S. Elborn, *Pediatr. Pulmonol.* **2007**, *42*, 525–532; c) G. M. Nixon, D. S. Armstrong, R. Carzino, J. B. Carlin, A. Olinsky, C. F. Robertson, K. Grimwood, *J. Pedriatr.* **2001**, *138*, 699–704; d) A. R. Hauser, M. Jain, M. Bar-Meir, S. A. McColley, *Clin. Microbiol. Rev.* **2011**, *24*, 29–70.

[19]   H. Hillemann, *Ber. Dtsch. Chem. Ges. B* **1938**, *71*, 46–52.

[20]   a) E. Friedheim, L. Michaelis, *J. Biol. Chem.* **1931**, *91*, 355–368; b) K. A. Jensen, C. H. Holten, A. Melaja, A. Kainulainen, A. Halonen, E. Pulkkinen, *Acta Chem. Scand.* **1949**, *3*, 1446–1447; c) H. McCombie, H. A. Scarborough, *J. Chem. Soc., Trans.* **1923**, *123*, 3279.

[21]   P. Ernst, *Z. Hyg. Infektionskr.* **1887**, *2*, 369.

[22]   a) G. W. Lau, D. J. Hassett, H. Ran, F. Kong, *Trends Mol. Med.* **2004**, *10*, 599–606; b) D. Haas, G. Défago, *Nat. Rev. Microbiol.* **2005**, *3*, 307–319; c) L. S. Pierson, E. A. Pierson, *Appl. Microbiol. Biotechnol.* **2010**, *86*, 1659–1670; d) B. Rada, T. L. Leto, *Trends Microbiol.* **2013**, *21*, 73–81.

[23]   A. Price-Whelan, L. E. P. Dietrich, D. K. Newman, *J. Bacteriol.* **2007**, *189*, 6372–6381.

[24]   H.-J. Abken, M. Tietze, J. Brodersen, S. Baumer, U. Beifuss, U. Deppenmeier, *J. Bacteriol.* **1998**, *180*, 2027–2032.

[25]   D. V. Mavrodi, T. L. Peever, O. V. Mavrodi, J. A. Parejko, J. M. Raaijmakers, P. Lemanceau, S. Mazurier, L. Heide, W. Blankenfeldt, D. M. Weller et al., *Appl. Environ. Microbiol.* **2010**, *76*, 866–879.

[26]   J. M. Turner, A. J. Messenger, *Adv. Microb. Ecol.* **1986**, *27*, 211.

[27]   M. C. Gessard, *Ann. Inst. Pasteur* **1892**, *6*, 801.

[28]   a) M. Kurachi, *Bull. Inst. Chem. Res. Kyoto Univ.* **1959**, *37*, 85–100; b) B. D. Davis, *J. Biol. Chem.* **1951**, *191*, 315–325; c) R. E. Carter, J. H. Richards, *J. Am. Chem. Soc.* **1961**, *83*, 495–496.

[29]   a) D. H. Calhoun, M. Carson, R. A. Jensen, *J. Gen. Microbiol.* **1972**, *72*, 581–583; b) R. P. Longley, J. E. Halliwell, J. J. R. Campbell, W. M. Ingledew, *Can. J. Microbiol.* **1972**, *18*, 1357–1363.

[30]   R. C. Millican, *Biochim. Biophys. Acta* **1962**, *57*, 407–409.

[31]   H. M. Berman, *Nucleic Acids Res.* **2000**, *28*, 235–242.

[32]   Q.-A. Li, D. V. Mavrodi, L. S. Thomashow, M. Roessle, W. Blankenfeldt, *J. Biol. Chem.* **2011**, *286*, 18213–18221.

[33]   J. F. Parsons, K. Calabrese, E. Eisenstein, J. E. Ladner, *Biochemistry* **2003**, *42*, 5684–5693.

[34]   W. Blankenfeldt, A. P. Kuzin, T. Skarina, Y. Korniyenko, L. Tong, P. Bayer, P. Janning, L. S. Thomashow, D. V. Mavrodi, *Proc. Natl. Acad. Sci. U.S.A.* **2004**, *101*, 16431–16436.

[35]   E. G. Ahuja, P. Janning, M. Mentel, A. Graebsch, R. Breinbauer, W. Hiller, B. Costisella, L. S. Thomashow, D. V. Mavrodi, W. Blankenfeldt, *J. Am. Chem. Soc.* **2008**, *130*, 17053–17061.

[36]   N. Xu, E. G. Ahuja, P. Janning, D. V. Mavrodi, L. S. Thomashow, W. Blankenfeldt, *Acta Crystallogr. D Biol. Crystallogr.* **2013**, *69*, 1403–1413.

[37]   L. Schrödinger, *The PyMOL Molecular Graphics System*, **2010**.

[38]   M. D. Galbraith, S. R. Giddens, H. K. Mahanty, B. Clark, *Can. J. Microbiol.* **2004**, *50*, 877–881.

[39]   a) T. Knochel, A. Ivens, G. Hester, A. Gonzalez, R. Bauerle, M. Wilmanns, K. Kirschner, J. N. Jansonius, *Proc. Natl. Acad. Sci. U.S.A.* **1999**, *96*, 9479–9484; b) A. A. Morollo, M. J. Eck, *Nat. Struct. Biol.* **2001**, *8*, 243–247; c) G. Spraggon, C. Kim, X. Nguyen-Huu, M. C. Yee, C. Yanofsky, S. E. Mills, *Proc. Natl. Acad. Sci. U.S.A.* **2001**, *98*, 6021–6026.

[40]   J. R. D. McCormick, J. Reichenthal, U. Hirsch, N. O. Sjolander, *J. Am. Chem. Soc.* **1962**, *84*, 3711–3714.

[41]   M. McDonald, D. V. Mavrodi, L. S. Thomashow, H. G. Floss, *J. Am. Chem. Soc.* **2001**, *123*, 9459–9460.

[42]   E. J. Drake, D. A. Nicolai, A. M. Gulick, *Chem. Biol.* **2006**, *13*, 409–419.

[43]   R. B. Herbert, F. G. Holliman, P. N. Ibberson, J. B. Sheridan, *J. Chem. Soc., Perkin Trans. 1* **1979**, 2411–2415.

[44]   M. Cirilli, R. Zheng, G. Scapin, J. S. Blanchard, *Biochemistry* **1998**, *37*, 16452–16458.

[45]   A. Buschiazzo, M. Goytia, F. Schaeffer, W. Degrave, W. Shepard, C. Grégoire, N. Chamond, A. Cosson, A. Berneman, N. Coatnoan et al., *Proc. Natl. Acad. Sci. U.S.A.* **2006**, *103*, 1705–1710.

[46]   G. S. Garvey, C. J. Rocco, J. C. Escalante-Semerena, I. Rayment, *Protein Sci.* **2007**, *16*, 1274–1284.

[47]   J. F. Parsons, F. Song, L. Parsons, K. Calabrese, E. Eisenstein, J. E. Ladner, *Biochemistry* **2004**, *43*, 12427–12435.

[48]   D. V. Mavrodi, N. Bleimling, L. S. Thomashow, W. Blankenfeldt, *Acta Cryst. D* **2004**, *60*, 184–186.

[49]   a) U. Hollstein, D. A. McCamey, *J. Org. Chem.* **1973**, *38*, 3415–3417; b) R. B. Herbert, F. G. Holliman, J. B. Sheridan, *Tetrahedron Lett.* **1976**, *17*, 639–642; c) U. Hollstein, D. L. Mock, R. R. Sibbitt, U. Roisch, F. Lingens, *Tetrahedron Lett.* **1978**, *19*, 2987–2990.

[50]   S. W. Kim, S. S. Cha, H. S. Cho, J. S. Kim, N. C. Ha, M. J. Cho, S. Joo, K. K. Kim, K. Y. Choi, B. H. Oh, *Biochemistry* **1997**, *36*, 14030–14036.

[51]   S. R. Giddens, Y. Feng, H. K. Mahanty, *Mol. Microbiol.* **2002**, *45*, 769–783.

[52]   J. F. Parsons, K. Calabrese, E. Eisenstein, J. E. Ladner, *Acta Crystallogr. D Biol. Crystallogr.* **2004**, *60*, 2110–2113.

[53]   Z. Rui, M. Ye, S. Wang, K. Fujikawa, B. Akerele, M. Aung, H. G. Floss, W. Zhang, T.-W. Yu, *Chem. Biol.* **2012**, *19*, 1116–1125.

[54]   O. Saleh, B. Gust, B. Boll, H.-P. Fiedler, L. Heide, *J. Biol. Chem.* **2009**, *284*, 14439–14447.

[55]   R. B. Woodward, R. Hoffman, *J. Am. Chem. Soc.* **1965**, *78*, 2511–2513.

[56]   R. B. Woodward, R. Hoffmann, *Angew. Chem. Int. Ed.* **1969**, *8*, 781–853.

[57]   M. S. DeClue, K. K. Baldridge, D. E. Künzler, P. Kast, D. Hilvert, *J. Am. Chem. Soc.* **2005**, *127*, 15002–15003.

[58]   D. J. Gustin, P. Mattei, P. Kast, O. Wiest, L. Lee, W. W. Cleland, D. Hilvert, *J. Am. Chem. Soc.* **1999**, *121*, 1756–1757.

[59]   A. L. Lamb, *Biochemistry* **2011**, *50*, 7476–7483.

[60]   A. Y. Lee, P. A. Karplus, B. Ganem, J. Clardy, *J. Am. Chem. Soc.* **1995**, *117*, 3627–3628.

[61]   J. V. Gray, D. Eren, J. R. Knowles, *Biochemistry* **1990**, *29*, 8872–8878.

[62]   J. V. Gray, J. R. Knowles, *Biochemistry* **1994**, *33*, 9953–9959.

[63]   Y. Li, A. I. D. Alanine, R. A. Vishwakarma, S. Balachandran, F. J. Leeper, A. R. Battersby, *J. Chem. Soc., Chem. Commun.* **1994**, 2507.

[64]   L. W. Shipman, D. Li, C. A. Roessner, A. I. Scott, J. C. Sacchettini, *Structure* **2001**, *9*, 587–596.

[65]   L. Y. P. Luk, Q. Qian, M. E. Tanner, *J. Am. Chem. Soc.* **2011**, *133*, 12342–12345.

[66]   D. Schwarzer, P. Gritsch, T. Gaich, *Synlett* **2013**, *24*, 1025–1031.

[67]   H. J. Kim, M. W. Ruszczycky, H.-W. Liu, *Curr. Opin. Chem. Biol.* **2012**, *16*, 124–131.

[68]   K. Auclair, A. Sutherland, J. Kennedy, D. J. Witter, Van den Heever, Johan P., C. R. Hutchinson, J. C. Vederas, *J. Am. Chem. Soc.* **2000**, *122*, 11519–11520.

[69]   E. M. Stocking, R. M. Williams, *Angew. Chem. Int. Ed.* **2003**, *42*, 3078–3115.

[70]   G. Pohnert, *ChemBioChem* **2001**, *2*, 873–875.

[71] T. Ose, K. Watanabe, T. Mie, M. Honma, H. Watanabe, M. Yao, H. Oikawa, I. Tanaka, *Nature* **2003**, *422*, 185–189.

[72] B. A. Hess, L. Smentek, *Org. Biomol. Chem.* **2012**, *10*, 7503–7509.

[73] H. J. Kim, M. W. Ruszczycky, S.-h. Choi, Y.-n. Liu, H.-W. Liu, *Nature* **2011**, *473*, 109–112.

[74] C. D. Fage, E. A. Isiorho, Y. Liu, D. T. Wagner, H.-W. Liu, A. T. Keatinge-Clay, *Nat. Chem. Biol.* **2015**, *11*, 256–258.

[75] C. Poulsen, R. Verpoorte, *Phytochemistry* **1991**, *30*, 377–386.

[76] A. D. Becke, *J. Chem. Phys.* **1993**, *98*, 5648.

[77] R. Ditchfield, *J. Chem. Phys.* **1971**, *54*, 724.

[78] P. C. Hariharan, J. A. Pople, *Theoret. Chim. Acta* **1973**, *28*, 213–222.

[79] W. J. Hehre, *J. Chem. Phys.* **1972**, *56*, 2257.

[80] a) S. D. Copley, J. R. Knowles, *J. Am. Chem. Soc.* **1985**, *107*, 5306–5308; b) S. G. Sogo, T. S. Widlanski, J. H. Hoare, C. E. Grimshaw, G. A. Berchtold, J. R. Knowles, *J. Am. Chem. Soc.* **1984**, *106*, 2701–2703.

[81] L. Addadi, E. K. Jaffe, J. R. Knowles, *Biochemistry* **1983**, *22*, 4494–4501.

[82] W. J. Guilford, S. D. Copley, J. R. Knowles, *J. Am. Chem. Soc.* **1987**, *109*, 5013–5019.

[83] M. Haynes, E. Stura, D. Hilvert, I. Wilson, *Science* **1994**, *263*, 646–652.

[84] P. Kast, Y. B. Tewari, O. Wiest, D. Hilvert, K. N. Houk, R. N. Goldberg, *J. Phys. Chem. B* **1997**, *101*, 10976–10982.

[85] a) Y. M. Chook, H. Ke, W. N. Lipscomb, *Proc. Natl. Acad. Sci. U.S.A.* **1993**, *90*, 8600–8603; b) Y. M. Chook, J. V. Gray, H. Ke, W. N. Lipscomb, *J. Mol. Biol.* **1994**, *240*, 476–500; c) W. B. Knight, P. M. Weiss, W. W. Cleland, *J. Am. Chem. Soc.* **1986**, *108*, 2759–2761.

[86] M. S. DeClue, K. K. Baldridge, P. Kast, D. Hilvert, *J. Am. Chem. Soc.* **2006**, *128*, 2043–2051.

[87] Q. Luo, K. M. Meneely, A. L. Lamb, *J. Am. Chem. Soc.* **2011**, *133*, 7229–7233.

[88] Q. Luo, J. Olucha, A. L. Lamb, *Biochemistry* **2009**, *48*, 5239–5245.

[89] S. Martí, J. Andrés, V. Moliner, E. Silla, I. Tuñón, J. Bertrán, *J. Am. Chem. Soc.* **2009**, *131*, 16156–16161.

[90] M. W. Schmidt, K. K. Baldridge, J. A. Boatz, S. T. Elbert, M. S. Gordon, J. H. Jensen, S. Koseki, N. Matsunaga, K. A. Nguyen, S. Su et al., *J. Comput. Chem.* **1993**, *14*, 1347–1363.

[91] a) S.-M. Li, *Nat. Prod. Rep.* **2010**, *27*, 57–78; b) N. Steffan, A. Grundmann, W.-B. Yin, A. Kremer, S.-M. Li, *Curr. Med. Chem.* **2009**, *16*, 218–231.

[92] D. D. Schwarzer, P. J. Gritsch, T. Gaich, *Angew. Chem. Int. Ed.* **2012**, *51*, 11514–11516.

[93] H. Oikawa, K. Katayama, Y. Suzuki, A. Ichihara, *J. Chem. Soc., Chem. Commun.* **1995**, 1321.

[94] a) K. Auclair, A. Sutherland, J. Kennedy, D. J. Witter, Van den Heever, Johan P., C. R. Hutchinson, J. C. Vederas, *J. Am. Chem. Soc.* **2000**, *122*, 11519–11520; b) S. M. Ma, J. W.-H. Li, J. W. Choi, H. Zhou, K. K. M. Lee, V. A. Moorthie, X. Xie, J. T. Kealey, N. A. Da Silva, J. C. Vederas et al., *Science* **2009**, *326*, 589–592.

[95] C. R. W. Guimarães, M. Udier-Blagović, W. L. Jorgensen, *J. Am. Chem. Soc.* **2005**, *127*, 3577–3588.

[96] H. Oikawa, K. Yagi, K. Watanabe, M. Honma, A. Ichihara, *Chem. Commun.* **1997**, 97–98.

[97] H. Oikawa, K. Watanabe, K. Yagi, S. Ohashi, T. Mie, A. Ichihara, M. Honma, *Tetrahedron Lett.* **1999**, *40*, 6983–6986.

[98] J. M. Serafimov, D. Gillingham, S. Kuster, D. Hilvert, *J. Am. Chem. Soc.* **2008**, *130*, 7798–7799.

[99] G. Pohnert, *ChemBioChem* **2003**, *4*, 713–715.

[100] a) S. Eberhardt, N. Zingler, K. Kemter, G. Richter, M. Cushman, A. Bacher, *Eur. J. Biochem.* **2001**, *268*, 4315–4323; b) R.-R. Kim, B. Illarionov, M. Joshi, M. Cushman, C. Y. Lee, W. Eisenreich, M. Fischer, A. Bacher, *J. Am. Chem. Soc.* **2010**, *132*, 2983–2990.

[101] I. Sakurai, H. Suzuki, S. Shimizu, Y. Yamamoto, *Chem. Pharm. Bull.* **1985**, *33*, 5141–5143.

[102] T. P. M. Goumans, A. W. Ehlers, K. Lammertsma, E.-U. Würthwein, S. Grimme, *Chem. Eur. J.* **2004**, *10*, 6468–6475.

[103] a) R. H. Fillingame, W. Jiang, O. Y. Dmitriev, *J. Exp. Biol.* **2000**, *203*, 9–17; b) L. Stryer, *Biochemistry*, Freeman, New York, **1995**.

[104] a) H. Haruki, M. G. Pedersen, K. I. Gorska, F. Pojer, K. Johnsson, *Science* **2013**, *340*, 987–991; b) B. Kobe, I. G. Jennings, House, C, M., B. J. Michell, K. E. Goodwill, B. D. Santarsiero, R. C. Stevens, R. G. Cotton, B. E. Kemp, *Nat. Struct. Biol.* **1999**, *6*, 442–448; c) E. Richelson, E. J. Thompson, *Nat. New Biol.* **1973**, *241*, 201–204; d) S. Scafidi, G. Fiskum, S. L. Lindauer, P. Bamford, D. Shi, I. Hopkins, M. C. McKenna, *J. Neurochem.* **2010**, *114*, 820–831.

[105] J. Z. Long, B. F. Cravatt, *Chem. Rev.* **2011**, *111*, 6022–6063.

[106] a) S. T.-C. Eey, M. J. Lear, *Chem. Eur. J.* **2014**, *20*, 11556–11573; b) R. C. F. Jones, J. P. Bullous, C. C. M. Law, M. R. J. Elsegood, *Chem. Commun.* **2014**, *50*, 1588–1590; c) W. Eisenreich, T. Dandekar, J. Heesemann, W. Goebel, *Nat. Rev. Microbiol.* **2010**, *8*, 401–412.

[107] a) L. Rohmer, D. Hocquet, S. I. Miller, *Trends Microbiol.* **2011**, *19*, 341–348; b) I. E. Brodsky, R. Medzhitov, *Nat. Cell Biol.* **2009**, *11*, 521–526; c) L. Diacovich, J.-P. Gorvel, *Nat. Rev. Microbiol.* **2010**, *8*, 117–128; d) A. Haraga, M. B. Ohlson, S. I. Miller, *Nat. Rev. Microbiol.* **2008**, *6*, 53–66.

[108] G. W. Lau, H. Ran, F. Kong, D. J. Hassett, D. Mavrodi, *Infect. Immun.* **2004**, *72*, 4275–4278.

[109] W. W. Cleland, *Adv. Enzymol. Relat. Areas Mol. Biol.* **1977**, *45*, 273–387.

[110] W. W. Cleland, *J. Biol. Chem.* **2003**, *278*, 51975–51984.

[111] Z. D. Nagel, J. P. Klinman, *Nat. Chem. Biol.* **2009**, *5*, 543–550.

[112] Z. Wang, A. Kohen, *J. Am. Chem. Soc.* **2010**, *132*, 9820–9825.

[113] Y.-I. Lin, J. Gao, *J. Am. Chem. Soc.* **2011**, *133*, 4398–4403.

[114] M. D. Toney, J. N. Castro, T. A. Addington, *J. Am. Chem. Soc.* **2013**, *135*, 2509–2511.

[115] H. F. Fisher, *Molecules* **2013**, *18*, 8230–8242.

[116] H. Gu, S. Zhang, *Molecules* **2013**, *18*, 9278–9292.

[117] M. A. Rishavy, W. W. Cleland, *Can. J. Chem.* **1999**, *77*, 967–977.

[118] R. Pongdee, H.-W. Liu, *Bioorg. Chem.* **2004**, *32*, 393–437.

[119] J. Hiratake, *Chem. Rec.* **2005**, *5*, 209–228.

[120] a) S. Wang, A. M. Haapalainen, F. Yan, Q. Du, P. C. Tyler, G. B. Evans, A. Rinaldo-Matthis, R. L. Brown, G. E. Norris, S. C. Almo et al., *Biochemistry* **2012**, *51*, 6892–6894; b) L. Dzhekieva, M. Rocaboy, F. Kerff, P. Charlier, E. Sauvage, R. F. Pratt, *Biochemistry* **2010**, *49*, 6411–6419; c) Y. Tanaka, N. Nakagawa, S. Kuramitsu, S. Yokoyama, R. Masui, *J. Biochem.* **2005**, *138*, 263–275; d) S. Decherchi, A. Berteotti, G. Bottegoni, W. Rocchia, A. Cavalli, *Nat. Commun.* **2015**, *6*, 6155.

[121] a) A. B. Penenory, J. E. Arguello, M. Puiatti, *Eur. J. Org. Chem.* **2005**, 114–122; b) P. H. Toy, M. Newcomb, P. F. Hollenberg, *J. Am. Chem. Soc.* **1998**, *120*, 7719–7729.

[122] P. F. Faulder, G. Tresadern, K. K. Chohan, N. S. Scrutton, M. J. Sutcliffe, I. H. Hillier, N. A. Burton, *J. Am. Chem. Soc.* **2001**, *123*, 8604–8605.

[123] Z. Islam, T. S. Strutzenberg, I. Gurevic, A. Kohen, *J. Am. Chem. Soc.* **2014**, *136*, 9850–9853.

[124] N. Lawan, K. E. Ranaghan, F. R. Manby, A. J. Mulholland, *Chem. Phys. Lett.* **2014**, *608*, 380–385.

[125] Q. A. T. Le, S. Kim, R. Chang, Y. H. Kim, *J. Phys. Chem. B* **2015**, *119*, 9571–9585.

[126] G. P. Pinto, N. F. Brás, M. A. Perez, P. A. Fernandes, N. Russo, M. J. Ramos, M. Toscano, *J. Chem. Theory Comput.* **2015**, *11*, 2508–2516.

[127] M. Shoji, K. Hanaoka, Y. Ujiie, W. Tanaka, D. Kondo, H. Umeda, Y. Kamoshida, M. Kayanuma, K. Kamiya, K. Shiraishi et al., *J. Am. Chem. Soc.* **2014**, *136*, 4525–4533.

[128] van der Kamp, Marc W, A. J. Mulholland, *Biochemistry* **2013**, *52*, 2708–2728.

[129] T. Vasilevskaya, M. G. Khrenova, A. V. Nemukhin, W. Thiel, *J. Comput. Chem.* **2015**, *36*, 1621–1630.

[130] F. Claeyssens, K. E. Ranaghan, F. R. Manby, J. N. Harvey, A. J. Mulholland, *Chem. Commun.* **2005**, 5068–5070.

[131] M. P. Gleeson, N. A. Burton, I. H. Hillier, *Phys. Chem. Chem. Phys.* **2003**, *5*, 4272–4278.

[132] a) M. Fang, A. Macova, K. L. Hanson, J. Kos, D. R. J. Palmer, *Biochemistry* **2011**, *50*, 8712–8721; b) M. P. Patel, W.-S. Liu, J. West, D. Tew, T. D. Meek, S. H. Thrall, *Biochemistry* **2005**, *44*, 16753–16765.

[133] M. J. S. Dewar, E. F. Healy, J. M. Ruiz, *J. Am. Chem. Soc.* **1988**, *110*, 2666–2667.

[134] V. Guner, K. S. Khuong, A. G. Leach, P. S. Lee, M. D. Bartberger, K. N. Houk, *J. Phys. Chem. A* **2003**, *107*, 11445–11459.

[135] Y. Itou, S. Mori, T. Udagawa, M. Tachikawa, T. Ishimoto, U. Nagashima, *J. Phys. Chem. A* **2007**, *111*, 261–267.

[136] H. Kwart, M. W. Brechbiel, R. M. Acheson, D. C. Ward, *J. Am. Chem. Soc.* **1982**, *104*, 4671–4672.

[137] W. R. Roth, J. Koenig, *J. Liebigs Ann. Chem.* **1966**, 24–32.

[138] S. C. Sharma, J. P. Klinman, *J. Am. Chem. Soc.* **2008**, *130*, 17632–17633.

[139] a) L. Chantranupong, T. A. Wildman, *J. Am. Chem. Soc.* **1990**, *112*, 4151–4154; b) D. Antoniou, S. D. Schwartz, *Proc. Natl. Acad. Sci. U.S.A.* **1997**, *94*, 12360–12365; c) D. Borgis, J. T. Hynes, *J. Chem. Phys.* **1991**, *94*, 3619.

[140] J. L. Abad, F. Camps, G. Fabrias, *Angew. Chem. Int. Ed.* **2000**, *39*, 3279–3281.

[141] J. Basran, S. Patel, M. J. Sutcliffe, N. S. Scrutton, *J. Biol. Chem.* **2001**, *276*, 6234–6242.

[142] J. Basran, M. J. Sutcliffe, N. S. Scrutton, *Biochemistry* **1999**, *38*, 3218–3222.

[143] J. Basran, M. J. Sutcliffe, N. S. Scrutton, *J. Biol. Chem.* **2001**, *276*, 24581–24587.

[144] B. A. Johnson, Y. Hu, K. N. Houk, M. A. Garcia-Garibay, *J. Am. Chem. Soc.* **2001**, *123*, 6941–6942.

[145] A. Kohen, R. Cannio, S. Bartolucci, J. P. Klinman, *Nature* **1999**, *399*, 496–499.

[146] a) J. N. Bandaria, C. M. Cheatum, A. Kohen, *J. Am. Chem. Soc.* **2009**, *131*, 10151–10155; b) R. J. Harris, R. Meskys, M. J. Sutcliffe, N. S. Scrutton, *Biochemistry* **2000**, *39*, 1189–1198; c) A. Kohen, J. P. Klinman, *Acc. Chem. Res.* **1998**, *31*, 397–404.

[147] S. Hu, S. C. Sharma, A. D. Scouras, A. V. Soudackov, C. A. M. Carr, S. Hammes-Schiffer, T. Alber, J. P. Klinman, *J. Am. Chem. Soc.* **2014**, *136*, 8157–8160.

[148] N. S. Scrutton, J. Basran, M. J. Sutcliffe, *Eur. J. Biochem.* **1999**, *264*, 666–671.

[149] C. J. Cramer, *Essentials of Computational Chemistry. Theories and Models*, Wiley, Chichester, **2014**.

[150] C. Adamo, V. Barone, *J. Chem. Phys.* **1998**, *108*, 664.

[151] C. Møller, M. S. Plesset, *Phys. Rev.* **1934**, *46*, 618–622.

[152] M. Leypold, *Studien zur Synthese von mechanistischen Sonden des PhzF-Proteins. MSc Thesis*, TU Graz, **2011**.

[153] J. Tomasi, B. Mennucci, R. Cammi, *Chem. Rev.* **2005**, *105*, 2999–3094.

[154] B. A. Hess, J. E. Baldwin, *J. Org. Chem.* **2002**, *67*, 6025–6033.

[155] N. J. Saettel, O. Wiest, *J. Org. Chem.* **2000**, *65*, 2331–2336.

[156] G. S. Hammond, *J. Am. Chem. Soc.* **1955**, *77*, 334–338.

[157] W. J. Bruno, W. Bialek, *Biophys. J.* **1992**, *63*, 689–699.

[158] Y. Zhang, H. Liu, W. Yang, *J. Chem. Phys.* **2000**, *112*, 3483.

[159] T. Gaich, P. S. Baran, *J. Org. Chem.* **2010**, *75*, 4657–4673.

[160] S. Hanessian, *J. Org. Chem.* **2012**, *77*, 6657–6688.

[161] S. Hanessian, S. Giroux, B. L. Merner, *Design and Strategy in Organic Synthesis. From the Chiron Approach to Catalysis*, Wiley-VCH, Weinheim, **2013**.

[162] C. A. Kuttruff, M. D. Eastgate, P. S. Baran, *Nat. Prod. Rep.* **2014**, *31*, 419–432.

[163] T. Newhouse, P. S. Baran, R. W. Hoffmann, *Chem. Soc. Rev.* **2009**, *38*, 3010–3021.

[164] J. B. Hendrickson, *J. Am. Chem. Soc.* **1975**, *97*, 5784–5800.

[165] B. Trost, *Science* **1991**, *254*, 1471–1477.

[166] B. M. Trost, *Angew. Chem. Int. Ed.* **1995**, *34*, 259–281.

[167] P. A. Wender, M. P. Croatt, B. Witulski, *Tetrahedron* **2006**, *62*, 7505–7511.

[168] P. A. Wender, B. L. Miller, *Nature* **2009**, *460*, 197–201.

[169] P. A. Wender, V. A. Verma, T. J. Paxton, T. H. Pillow, *Acc. Chem. Res.* **2008**, *41*, 40–49.

[170] J. M. Richter, Y. Ishihara, T. Masuda, B. W. Whitefield, T. Llamas, A. Pohjakallio, P. S. Baran, *J. Am. Chem. Soc.* **2008**, *130*, 17938–17954.

[171] N. Z. Burns, P. S. Baran, R. W. Hoffmann, *Angew. Chem. Int. Ed.* **2009**, *48*, 2854–2867.

[172] M. E. Bunnage, T. Ganesh, I. B. Masesane, D. Orton, P. G. Steel, *Org. Lett.* **2003**, *5*, 239–242.

[173]   I. B. Masesane, A. S. Batsanov, J. A. K. Howard, R. Mondal, P. G. Steel, *Beilstein J. Org. Chem.* **2006**, *2*, 1–6.

[174]   I. B. Masesane, P. G. Steel, *Tetrahedron Lett.* **2004**, *45*, 5007–5009.

[175]   R. N. Bwire, R. R. Majinda, I. B. Masesane, P. G. Steel, *Pure Appl. Chem.* **2009**, *81*.

[176]   K. Faber, *Biotransformations in Organic Chemistry. A Textbook*, Springer-Verlag Berlin Heidelberg, Berlin, Heidelberg, **2011**.

[177]   R. Bloch, E. Guibe-Jampel, C. Girard, *Tetrahedron Lett.* **1985**, *26*, 4087–4090.

[178]   C. M. Schueller, D. D. Manning, L. L. Kiessling, *Tetrahedron Lett.* **1996**, *37*, 8853–8856.

[179]   F. Brion, *Tetrahedron Lett.* **1982**, *23*, 5299–5302.

[180]   M.-A. Raheem, J. R. Nagireddy, R. Durham, W. Tam, *Synth. Commun.* **2010**, *40*, 2138–2146.

[181]   J. K. Addo, P. Teesdale-Spittle, J. O. Hoberg, *Synthesis* **2005**, *2005*, 1923–1925.

[182]   a) R. Ballini, D. Fiorini, A. Palmieri, *Tetrahedron Lett.* **2004**, *45*, 7027–7029; b) S. Mukherjee, E. J. Corey, *Org. Lett.* **2010**, *12*, 1024–1027.

[183]   K. Itoh, K. Kitoh, A. Sera, *Heterocycles* **1999**, *51*, 243.

[184]   P. Diehl, E. Fluck, H. Günther, R. Kosfeld, J. Seelig, U. Fleischer, W. Kutzelnigg, H.-H. Limbach, G. J. Martin, M. L. Martin et al., *NMR Basic Principles and Progress*, Springer Berlin Heidelberg, Berlin, Heidelberg, **1991**.

[185]   a) F. Alonso, Y. Moglie, G. Radivoy, C. Vitale, M. Yus, *Appl. Catal., A* **2004**, *271*, 171–176; b) F. Alonso, G. Radivoy, M. Yus, *Tetrahedron* **1999**, *55*, 4441–4444; c) K. S. Chan, C. R. Liu, K. L. Wong, *Tetrahedron Lett.* **2015**, *56*, 2728–2731; d) T. Mutsumi, H. Iwata, K. Maruhashi, Y. Monguchi, H. Sajiki, *Tetrahedron* **2011**, *67*, 1158–1165; e) K. Inoue, A. Sawada, I. Shibata, A. Baba, *J. Am. Chem. Soc.* **2002**, *124*, 906–907.

[186]   F. Alonso, I. P. Beletskaya, M. Yus, *Chem. Rev.* **2002**, *102*, 4009–4092.

[187]   E. Iwasa, Y. Hamashima, S. Fujishiro, D. Hashizume, M. Sodeoka, *Tetrahedron* **2011**, *67*, 6587–6599.

[188]   E. Iwasa, Y. Hamashima, S. Fujishiro, E. Higuchi, A. Ito, M. Yoshida, M. Sodeoka, *J. Am. Chem. Soc.* **2010**, *132*, 4078–4079.

[189]   A. Krief, W. Dumont, A. Kremer, *Tetrahedron Lett.* **2009**, *50*, 2398–2401.

[190]   N. C. Mancey, N. Sandon, A.-L. Auvinet, R. J. Butlin, W. Czechtizky, J. P. A. Harrity, *Chem. Commun.* **2011**, *47*, 9804–9806.

[191]   F. A. Khan, J. Dash, *J. Org. Chem.* **2003**, *68*, 4556–4559.

[192]   J.-F. Brazeau, A.-A. Guilbault, J. Kochuparampil, P. Mochirian, Y. Guindon, *Org. Lett.* **2010**, *12*, 36–39.

[193]   F. Chagnon, I. Guay, M.-A. Bonin, G. Mitchell, K. Bouarab, F. Malouin, É. Marsault, *Eur. J. Med. Chem.* **2014**, *80*, 605–620.

[194]   K. Ravindar, M. S. Reddy, L. Lindqvist, J. Pelletier, P. Deslongchamps, *J. Org. Chem.* **2011**, *76*, 1269–1284.

[195]   A. Attouche, D. Urban, J.-M. Beau, *Angew. Chem. Int. Ed.* **2013**, *52*, 9572–9575.

[196]   S. Guyenne, E. I. León, A. Martín, I. Pérez-Martín, E. Suárez, *J. Org. Chem.* **2012**, *77*, 7371–7391.

[197]   T. Hashimoto, D. Hirose, T. Taniguchi, *Angew. Chem. Int. Ed.* **2014**, *53*, 2730–2734.

[198]   A. Kamimura, T. Kotake, Y. Ishihara, M. So, T. Hayashi, *J. Org. Chem.* **2013**, *78*, 3961–3971.

[199]   I. Kempter, A. Groß, J. Hartung, *Tetrahedron* **2012**, *68*, 10378–10390.

[200]   J. L. Stockdill, A. M. Lopez, A. A. Ibrahim, *Tetrahedron Lett.* **2015**, *56*, 3503–3506.

[201]   a) A. Henglein, J. Langhoff, G. Schmidt, *J. Phys. Chem.* **1959**, *63*, 980; b) I. I. Bilkis, S. M. Shein, *Tetrahedron* **1975**, *31*, 969–971; c) G. R. Chalfont, M. J. Perkins, *J. Am. Chem. Soc.* **1967**, *89*, 3054–3055; d) I. Kraljić, C. N. Trumbore, *J. Am. Chem. Soc.* **1965**, *87*, 2547–2550; e) S. Terabe, R. Konaka, *J. Am. Chem. Soc.* **1969**, *91*, 5655–5657; f) R. Toba, H. Gotoh, K. Sakakibara, *Org. Lett.* **2014**, *16*, 3868–3871; g) L. Grossi, *Chem. Eur. J.* **2005**, *11*, 5419–5425; h) G. Majetich, K. Wheless, *Tetrahedron* **1995**, *51*, 7095–7129.

[202]   a) S. Ciblat, P. Besse, V. Papastergiou, H. Veschambre, J.-L. Canet, Y. Troin, *Tetrahedron: Asymm.* **2000**, *11*, 2221–2229; b) D. J. Dixon, S. V. Ley, D. J. Reynolds, *Chem. Eur. J.* **2002**, *8*, 1621–1636; c) V. S. Enev, W. Felzmann, A. Gromov, S. Marchart, J. Mulzer, *Chem. Eur. J.* **2012**, *18*, 9651–9668; d) B. Hélal, F. Ferreira, C. Botuha, F. Chemla, A. Pérez-Luna, *Synlett* **2009**, 3115–3118; e) P. G. Jones, H. Weinmann, E. Winterfeldt, *Angew. Chem. Int. Ed.* **1995**, *34*, 448–450; f) A. B. Smith, E. G. Nolen, R. Shirai, F. R. Blase, M. Ohta, N. Chida, R. A. Hartz, D. M. Fitch, W. M. Clark, P. A. Sprengeler, *J. Org. Chem.* **1995**, *60*, 7837–7848; g) M.-E. Trân-Huu-Dâu, R. Wartchow, E. Winterfeldt, Y.-S. Wong, *Chem. Eur. J.* **2001**, *7*, 2349–2369.

[203]   L. B. Barkley, M. W. Farrar, W. S. Knowles, H. Raffelson, *J. Am. Chem. Soc.* **1954**, *76*, 5017–5019.

[204]   a) D. J. Burton, P. E. Greenlimb, *J. Fluor. Chem.* **1974**, *3*, 447–449; b) H. W. Geluk, *Synthesis* **1970**, 652–653; c) A. G. Gonzalez, J. Bermejo, J. L. Breton, G. M. Massanet, B. Dominguez, J. M. Amaro, *J. Chem. Soc., Perkin Trans. 1* **1976**, 1663; d) H. M. R. Hoffmann, U. Eggert, A. Walenta, E. Weineck, D. Schomburg, R. Wartchow, F. H. Allen, *J. Org. Chem.* **1989**, *54*, 6096–6100; e) Sarhan, Abd El-Wareth A. O., *Synth. Commun.* **1999**, *29*, 1075–1086; f) S. Sendelbach, R. Schwetzler-Raschke, A. Radl, R. Kaiser, G. H. Henle, H. Korfant, S. Reiner, B. Föhlisch, *J. Org. Chem.* **1999**, *64*, 3398–3408; g) J. G. Vinter, H. M. R. Hoffmann, *J. Am. Chem. Soc.* **1974**, *96*, 5466–5478.

[205]   L.-M. Zhu, M. Catriona Tedford, *Tetrahedron* **1990**, *46*, 6587–6611.

[206]   E. Heymann, W. Junge, *Eur. J. Biochem.* **1979**, *95*, 509–518.

[207]   N. Oehrner, A. Mattson, T. Norin, K. Hult, *Biocatalysis* **1990**, *4*, 81–88.

[208]   L. K. P. Lam, C. M. Brown, B. de Jeso, L. Lym, E. J. Toone, J. B. Jones, *J. Am. Chem. Soc.* **1988**, *110*, 4409–4411.

[209]   S. Sicsic, J. Leroy, C. Wakselman, *Synthesis* **1987**, 155–156.

[210]   M. D. Lilly, *J. Chem. Technol. Biotechnol.* **1982**, *32*, 162–169.

[211]   B. Neises, W. Steglich, *Angew. Chem. Int. Ed.* **1978**, *17*, 522–524.

[212]   B. Neises, W. Steglich, *Org. Synth.* **1985**, *63*, 183.

[213]   J. Åhman, P. Somfai, *Synth. Commun.* **1995**, *25*, 2301–2303.

[214]   R. E. Ireland, R. S. Meissner, *J. Org. Chem.* **1991**, *56*, 4566–4568.

[215]   R. Bhushan, H. Brückner, *Amino Acids* **2004**, *27*, 231–247.

[216]   C. B'Hymer, M. Montes-Bayon, J. A. Caruso, *J. Sep. Sci.* **2003**, *26*, 7–19.

[217] R. Bhushan, H. Brückner, *J. Chromatogr. B: Anal. Technol. Biomed. Life Sci.* **2011**, *879*, 3148–3161.

[218] J. Bongaerts, S. Esser, V. Lorbach, L. Al-Momani, M. A. Müller, D. Franke, C. Grondal, A. Kurutsch, R. Bujnicki, R. Takors et al., *Angew. Chem. Int. Ed.* **2011**, *50*, 7781–7786.

[219] R. Bujnicki, *Schriften des Forschungszentrums Jülich Reihe Lebenswissenschaften*, *Vol. 37*, Forschungszentrum Zentralbibliothek, Jülich, **2007**.

[220] a) H. Yamamoto, E. Carreira, *Comprehensive Chirality*, Elsevier, **2012**; b) H. D. Flack, G. Bernardinelli, *J. Appl. Crystallogr.* **2000**, *33*, 1143–1148; c) H. D. Flack, G. Bernardinelli, *Chirality* **2008**, *20*, 681–690.

[221] a) A. J. Lloyd, T. Huyton, J. Turkenburg, D. I. Roper, *Acta Crystallogr., Sect. D: Biol. Crystallogr.* **2004**, *60*, 397–400; b) J. S. Park, W. C. Lee, J. H. Song, S. I. Kim, J. C. Lee, C. Cheong, H. Y. Kim, *Acta Crystallogr., Sect. F: Struct. Biol. Commun.* **2013**, *69*, 42–44; c) V. Usha, L. G. Dover, D. I. Roper, K. Fütterer, G. S. Besra, *Acta Crystallogr., Sect. D: Biol. Crystallogr.* **2009**, *65*, 383–387.

[222] Y. Chiang, A. J. Kresge, P. Pruszynski, N. P. Schepp, J. Wirz, *Angew. Chem. Int. Ed.* **1990**, *29*, 792–794.

[223] B. Mitra, A. T. Kallarakal, J. W. Kozarich, J. A. Gerlt, J. R. Clifton, G. A. Petsko, G. L. Kenyon, *Biochemistry* **1995**, *34*, 2777–2787.

[224] J. A. Gerlt, J. W. Kozarich, G. L. Kenyon, P. G. Gassman, *J. Am. Chem. Soc.* **1991**, *113*, 9667–9669.

[225] a) G. Alagona, C. Ghio, P. A. Kollman, *J. Mol. Struct.: THEOCHEM* **1997**, *390*, 217–223; b) P. Babbitt, G. Mrachko, M. Hasson, G. Huisman, R. Kolter, D. Ringe, G. Petsko, G. Kenyon, J. Gerlt, *Science* **1995**, *267*, 1159–1161; c) J. A. Gerlt, G. L. Kenyon, J. W. Kozarich, D. J. Neidhart, G. A. Petsko, V. M. Powers, *Curr. Opin. Struct. Biol.* **1992**, *2*, 736–742; d) J. Gu, H. Yu, *J. Biomol. Struct. Dyn.* **2012**, *30*, 585–593; e) A. T. Kallarakal, B. Mitra, J. W. Kozarich, J. A. Gerlt, J. R. Clifton, G. A. Petsko, G. L. Kenyon, *Biochemistry* **1995**, *34*, 2788–2797; f) G. L. Kenyon, J. A. Gerlt, G. A. Petsko, J. W. Kozarich, *Acc. Chem. Res.* **1995**, *28*, 178–186; g) A. Narmandakh, S. L. Bearne, *Protein Expression Purif.* **2010**, *69*, 39–46; h) G. A. Petsko, G. L. Kenyon, J. A. Gerlt, D. Ringe, J. W. Kozarich, *Trends Biochem. Sci.* **1993**, *18*, 372–376; i) V. M. Powers, C. W. Koo, G. L. Kenyon, J. A. Gerlt, J. W. Kozarich, *Biochemistry* **1991**, *30*, 9255–9263; j) S. L. Schafer, W. C. Barrett, A. T. Kallarakal, B. Mitra, J. W. Kozarich, J. A. Gerlt, J. G. Clifton, G. A. Petsko, G. L. Kenyon, *Biochemistry* **1996**, *35*, 5662–5669; k) T. R. Sharp, G. D. Hegeman, G. L. Kenyon, *Biochemistry* **1977**, *16*, 1123–1128; l) M. St Maurice, S. L. Bearne, *Biochemistry* **2004**, *43*, 2524–2532.

[226] J. A. Landro, J. A. Gerlt, J. W. Kozarich, C. W. Koo, V. J. Shah, G. L. Kenyon, D. J. Neidhart, S. Fujita, G. A. Petsko, *Biochemistry* **1994**, *33*, 635–643.

[227] J. A. Landro, A. T. Kallarakal, S. C. Ransom, J. A. Gerlt, J. W. Kozarich, D. J. Neidhart, G. L. Kenyon, *Biochemistry* **1991**, *30*, 9274–9281.

[228] J. A. Gerlt, P. G. Gassman, *J. Am. Chem. Soc.* **1993**, *115*, 11552–11568.

[229] J. A. Gerlt, P. G. Gassman, *Biochemistry* **1993**, *32*, 11943–11952.

[230] L. Onsager, *J. Am. Chem. Soc.* **1936**, *58*, 1486–1493.

[231] V. Leskovac, *Comprehensive Enzyme Kinetics*, Kluwer Academic/Plenum Publ, New York, **2003**.

[232] K. A. Johnson, *FEBS Lett.* **2013**, *587*, 2753–2766.

[233] A. Cornish-Bowden, *FEBS Lett.* **2013**, *587*, 2725–2730.

[234] L. Michaelis, M. L. Menten, *Biochem. Z.* **1913**, *49*, 333–369.

[235] a) A. Dirksen, S. Dirksen, T. M. Hackeng, P. E. Dawson, *J. Am. Chem. Soc.* **2006**, *128*, 15602–15603; b) M. E. Furrow, A. G. Myers, *J. Am. Chem. Soc.* **2004**, *126*, 5436–5445; c) A. Job, C. F. Janeck, W. Bettray, R. Peters, D. Enders, *Tetrahedron* **2002**, *58*, 2253–2329; d) E. T. Kool, D.-H. Park, P. Crisalli, *J. Am. Chem. Soc.* **2013**, *135*, 17663–17666.

[236] a) E. Buncel, I.-H. Um, *Tetrahedron* **2004**, *60,* 7801–7825; b) N. J. Fina, J. O. Edwards, *Int. J. Chem. Kinet.* **1973**, *5*, 1–26; c) W. P. Jencks, J. Carriuolo, *J. Am. Chem. Soc.* **1960**, *82*, 1778–1786; d) Y. Ren, H. Yamataka, *J. Org. Chem.* **2007**, *72*, 5660–5667.

[237] a) M. Dieckmann, M. Kretschmer, P. Li, S. Rudolph, D. Herkommer, D. Menche, *Angew. Chem. Int. Ed.* **2012**, *51*, 5667–5670; b) A. S. Kende, S. Johnson, *J. Org. Chem.* **1985**, *50*, 727–729; c) E. R. Parmee, P. G. Steel, E. J. Thomas, *J. Chem. Soc., Chem. Commun.* **1989**, 1250; d) D. J. Plata, J. Kallmerten, *J. Am. Chem. Soc.* **1988**, *110*, 4041–4042; e) D. F. Taber, J. C. Amedio, K. Raman, *J. Org. Chem.* **1988**, *53*, 2984–2990.

[238] a) A. Bar-Even, E. Noor, Y. Savir, W. Liebermeister, D. Davidi, D. S. Tawfik, R. Milo, *Biochemistry* **2011**, *50*, 4402–4410; b) R. Samson, J. M. Deutch, *J. Chem. Phys.* **1978**, *68*, 285–290; c) J. M. Schurr, K. S. Schmitz, *J. Phys. Chem.* **1976**, *80*, 1934–1936.

[239] R. Muller, M. Breuer, A. Wagener, K. Schmidt, E. Leistner, *Microbiol.* **1996**, *142*, 1005–1012.

[240] D. Franke, G. A. Sprenger, M. Müller, *Angew. Chem. Int. Ed.* **2001**, *40*, 555–557.

[241] a) R. Agudo, G.-D. Roiban, M. T. Reetz, *ChemBioChem* **2012**, *13*, 1465–1473; b) H. M. Sirat, E. J. Thomas, N. D. Tyrrell, *J. Chem. Soc., Chem. Commun.* **1979**, 36.

[242] D. A. Evans, D. M. Barnes, *Tetrahedron Lett.* **1997**, *38*, 57–58.

[243] D. A. Evans, D. M. Barnes, J. S. Johnson, T. Lectka, P. von Matt, S. J. Miller, J. A. Murry, R. D. Norcross, E. A. Shaughnessy, K. R. Campos, *J. Am. Chem. Soc.* **1999**, *121*, 7582–7594.

[244] S.-H. Shin, J.-H. Han, S.-I. Lee, Y.-B. Ha, D.-H. Ryu, *Bull. Korean Chem. Soc.* **2011**, *32*, 2885–2886.

[245] M. K. Ghorai, K. Das, A. Kumar, *Tetrahedron Lett.* **2007**, *48*, 2471–2475.

[246] H. Li, X. Zhang, X. Shi, N. Ji, W. He, S. Zhang, B. Zhang, *Adv. Synth. Catal.* **2012**, *354*, 2264–2274.

[247] X. Shi, W. He, H. Li, X. Zhang, S. Zhang, *Tetrahedron Lett.* **2011**, *52*, 3204–3207.

[248] T.-Y. Tsai, K.-S. Shia, H.-J. Liu, *Synlett* **2003**, 97–101.

[249] A. Cornejo, J. M. Fraile, J. I. García, M. J. Gil, V. Martínez-Merino, J. A. Mayoral, E. Pires, I. Villalba, *Synlett* **2005**, 2321–2324.

[250] D. A. Evans, J. S. Johnson, E. J. Olhava, *J. Am. Chem. Soc.* **2000**, *122*, 1635–1649.

[251] C. K. Andrade, R. O. Rocha, O. E. Vercillo, W. A. Silva, R. A. Matos, *Synlett* **2003**, 2351–2352.

[252]   a) D. Liu, E. Canales, E. J. Corey, *J. Am. Chem. Soc.* **2007**, *129*, 1498–1499; b) E. N. Pitsinos, N. Athinaios, V. P. Vidali, *Org. Lett.* **2012**, *14*, 4666–4669; c) R. S. Singh, S. Adachi, F. Tanaka, T. Yamauchi, C. Inui, T. Harada, *J. Org. Chem.* **2008**, *73*, 212–218.

[253]   a) G. Desimoni, G. Faita, K. A. Jørgensen, *Chem. Rev.* **2006**, *106*, 3561–3651; b) G. Desimoni, G. Faita, K. A. Jørgensen, *Chem. Rev.* **2011**, *111*, PR284-437; c) D. A. Evans, E. J. Olhava, J. S. Johnson, J. M. Janey, *Angew. Chem. Int. Ed.* **1998**, *37*, 3372–3375; d) L.-C. Fang, R. P. Hsung, *Org. Lett.* **2014**, *16*, 1826–1829; e) E. Framery, B. Andrioletti, M. Lemaire, *Tetrahedron: Asymm.* **2010**, *21*, 1110–1124; f) M. Johannsen, K. A. Joergensen, *J. Org. Chem.* **1995**, *60*, 5757–5762; g) M. P. Sibi, H. Matsunaga, *Tetrahedron Lett.* **2004**, *45*, 5925–5929.

[254]   a) M. S. Baker, S. T. Phillips, *J. Am. Chem. Soc.* **2011**, *133*, 5170–5173; b) T. Boisse, B. Rigo, R. Millet, J.-P. Hénichart, *Tetrahedron* **2007**, *63*, 10511–10520; c) K. Lu, M. Huang, Z. Xiang, Y. Liu, J. Chen, Z. Yang, *Org. Lett.* **2006**, *8*, 1193–1196.

[255]   R. M. C. Dawson, D. C. Elliott, *Data for biochemical research*, Clarendon Press, Oxford, **2002**.

[256]   W. R. Taylor, *J. Theor. Biol.* **1986**, *119*, 205–218.

[257]   F. C. Nachod, *Determination of Organic Structures by Physical Methods V4*, Elsevier Science, Oxford, **1971**.

[258]   W. A. Anderson, R. Freeman, *J. Chem. Phys.* **1962**, *37*, 85.

[259]   A. W. Overhauser, *Phys. Rev.* **1953**, *92*, 411–415.

[260]   W. Kutzelnigg, U. Fleischer, M. Schindler, *NMR Basic Principles and Progress* (Eds.: P. Diehl, E. Fluck, H. Günther, R. Kosfeld, J. Seelig, U. Fleischer, W. Kutzelnigg, H.-H. Limbach, G. J. Martin, M. L. Martin et al.), Springer Berlin Heidelberg, Berlin, Heidelberg, **1991**.

[261]   a) M. Ceotto, *Molecular Physics* **2012**, *110*, 547–559; b) Y. Cha, C. Murray, J. Klinman, *Science* **1989**, *243*, 1325–1330.

[262]   M. J. Frisch, G. W. Trucks, H. B. Schlegel, G. E. Scuseria, M. A. Robb, J. R. Cheeseman, G. Scalmani, V. Barone, B. Mennucci, G. A. Petersson et al., *Gaussian 09, Revision D.01*, Gaussian, Inc., Wallingford CT, **2009**.

[263]   A. R. Allouche, *J. Comput. Chem.* **2011**, *32*, 174–182.

9. Abbreviations

9.1. Analytical Methods

APT   attached proton test

COSY   correlation spectroscopy

DI-EI   direct inlet electron impact

EI   electron impact

ESI   electrospray ionization

GC   gas chromatography

GC-MS   gas chromatography mass spectrometry

HPLC   high performance liquid chromatography

HRMS   high resolution mass spectrometry

HSQC   heteronuclear single quantum coherence

LC-MS   liquid chromatography mass spectrometry

NMR   nuclear magnetic resonance

ORTEP   oak ridge thermal ellipsoid plot

TOF   time of flight

bs   broad singlet

d   doublet

dd   doublet of doublet

ddd   doublet of doublet of doublet

dq   doublet of quadruplet

dt   doublet of triplet

h   hexet

m   multiplet

p	pentet
q	quadruplet
s	singlet
t	triplet
td	triplet of doublet
$[\alpha]_D^{20}$	specific optical rotation at 20 °C
BP	basis peak
δ	chemical shift in ppm (parts per million)
d.e.	diastereomeric excess
e.e.	enantiomeric excess
Hz	Hertz
J	coupling constant
λ	wavelength
MHz	Megahertz
min	minute/minutes
M^+	molecule peak
m/z	mass to charge ratio
nm	nanometer
NOE	nuclear OVERHAUSER effect
ppm	parts per million
R_f	retention factor
TLC	thin layer chromatography
t_R	retention time
UV	ultraviolett
v/v	volume per volume

v/v/v	volume per volume per volume
w/w	mass per mass

9.2.   Chemical Abbreviations

A	alanine
Ac	acetyl
ADIC	(5*S*,6*S*)-6-amino-5-hydroxy-1,3-cyclohexadiene-1-carboxylic acid
AIBN	2,2'-azobis(2-methylpropionitrile)
allyl-DHHA	allyl *trans*-2,3-dihydro-3-hydroxyanthranilate
AOCHC	6-amino-5-oxocyclohex-2-ene-1-carboxylic acid
AS	anthranilate synthase
ATP	adenosine triphosphate
2-BuOH	2-butanol
Boc	*tertiary*-butyloxycarbonyl
Boc_2O	di-*tertiary*-butyl dicarbonate
BOX	bis(oxazoline) ligand
brine	saturated aqueous sodium chloride solution
CAM	cerium ammonium molybdate
$CDCl_3$	chloroform-*d*
$CHCl_3$	chloroform
CM	chorismate mutase
D	aspartate
DBU	1,8-diazabicyclo[5.4.0]undec-7-ene
DCC	dicyclohexylcarbodiimide

DCM	dichloromethane
DHHA	*trans*-2,3-dihydro-3-hydroxyanthranilic acid
d-DHHA	*trans*-2,3-dihydro-3-hydroxyanthranilic-3-*d* acid
DHHB	*trans*-2,3-dihydro-3-hydroxybenzoic acid
DHHS	*trans*-2,3-dihydro-3-hydroxysalicylic acid
DHPCA	dihydrophenazine-1-carboxylic acid
DIPEA	*N,N*-diisopropylethylamine
4-DMAP	(4-dimethylamino)pyridine
DMATS	dimethylallyltryptophan synthase
DMF	*N,N*-dimethylformamide
DMSO	dimethyl sulfoxide
DMSO-d$_6$	dimethyl sulfoxide-*d*$_6$
DNA	deoxyribonucleic acid
E	glutamate
EDC.HCl	*N*-(3-dimethylaminopropyl)-*N'*-ethylcarbodiimide hydrochloride
Et	ethyl
Et$_3$B	triethylborane
Et-DHHA	ethyl *trans*-2,3-dihydro-3-hydroxyanthranilate
Et$_3$N	triethylamine
Et$_2$O	diethyl ether
EtOAc	ethylacetate
EtOD	ethanol-*d*
EtOH	ethanol
EtSH	ethanethiol
FMN	flavin mononucleotide

GATase1	type-1 glutamine amidotransferase
Gln	glutamine
Glu	glutamate
H	histidine
HBA	hydrogenobyrinic acid
HCl	hydrochloric acid
H_2-DHHA	(5*S*,6*S*)-6-amino-5-hydroxycyclohex-1-ene-1-carboxylic acid
HHPDC	hexahydrophenazine-1,6-dicarboxylic acid
HLE	horse liver esterase
HMDS	hexamethyldisilazane
IPL	isochorismate pyruvate lyase
K	lysine
KHMDS	potassium bis(trimethylsilyl)amide
Leu	leucine
LHMDS	lithium bis(trimethylsilyl)amide
Me	methyl
MeCN	acetonitrile
Me-DHHA	methyl *trans*-2,3-dihydro-3-hydroxyanthranilate
$MeNO_2$	nitromethane
MeOH	methanol
Me_3SnOH	trimethyltin hydroxide
MR	mandelate racemase
MS	macrophomate synthase
MsCl	methanesulfonyl chloride
MTBE	*tert*-butyl methyl ether

N   asparagine

NADH   nicotinamide adenine dinucleotide

*n*Pr   *n*-propyl

*n*Pr-DHHA   *n*-propyl *trans*-2,3-dihydro-3-hydroxyanthranilate

*n*BuLi   *n*-butyllithium

NBS   *N*-bromosuccinimide

OAc   acetate

PCA   phenazine-1-carboxylic acid

PDC   phenazine-1,6-dicarboxylic acid

Phg   phenylglycine

PLE   pig liver esterase

PPi   pyrophosphate

Q   glutamine

RNA   ribonucleic acid

S   serine

T   threonine

TBTD   tributyltin deuteride

TBTH   tributyltin hydride

TFA   trifluoroacetic acid

THF   tetrahydrofuran

THPDC   tetrahydrophenazine-1,6-dicarboxylic acid

TMS   tetramethylsilane

TRIS   tris(hydroxymethyl)aminomethane

WT   wildtype

9.3.   Miscellaneous

Å	Angstrom
$Å^2$	square Angstrom
$Å^3$	cubic Angstrom
AE	activation energy
aq	aqueous
b_p	boiling point
c	concentration
cm	centimeter
d	day
°	degree
°C	degree Celsius
dest.	distilled
DFT	density functional theory
ΔG	free enthalpy
E	enantioselectivity
EIE	equilibrium isotope effect
elim	elimination
eq	equivalent/equivalents
eV	electron volts
exp.	experimental
g	gram
h	hour/hours
HOMO	highest occupied molecular orbital

iso	isomerization
k_{cat}	turnover number
K_d	dissociation constant
kDa	Kilodaltons
KIE	kinetic isotope effect
1° KIE	primary kinetic isotope effect
2° KIE	secondary kinetic isotope effect
kJ	Kilojoule
K_M	MICHAELIS-MENTEN constant
ln	natural logarithm
LUMO	lowest unoccupied molecular orbital
M	Molar
max	maximum
mbar	millibar
mg	milligram
min	minimum
mL	Milliliter
mM	Millimolar
mmol	millimol
mol. vol.	molecular volume
µL	Microliter
µm	Micrometer
µmol	micromol
m_p	melting point
MS	molecular sieves

nE	neutral educt
nEW	neutral educt water
nm	nanometer
nP	neutral product
nPW	neutral product water
nTS	neutral transition state
nTSW	neutral transition state water
%	percent
pH	pH value
pK_a	logarithm of acid dissociation constant
ppm	parts per million
prod.	product
quant.	quantitative
QM/MM	quantum mechanics/molecular mechanics
rac	racemic
r.d.s.	rate determining step
rpm	rounds per minute
rps	rounds per second
RT	room temperature
s	second/seconds
SET	single electron transfer
tert	*tertiary*
TS	transition state
V	volume
VAT	vibrational assisted tunneling

v_{max} maximum velocity

ZPE   zero point energy